AD-A160 601 INTERACTIVE EFFECTS OF HIGH- AND LOW-FREQUENCY LOADING ON FATIGUE(U) MECHANICAL TECHNOLOGY INC LATHAM N Y A PETROVICH MAY 85 MTI-85TR48 AFWAL-TR-85-4045 1/2

UNCLASSIFIED F33615-82-C-5056 F/G 20/11 NL

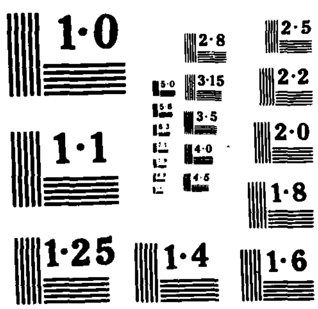
1·0
2·8
2·5
3·15
2·2
3·5
2·0
1·1
4·0
4·5
1·8
1·25
1·4
1·6

12

AFWAL-TR-85-4045

INTERACTIVE EFFECTS OF HIGH- AND LOW-FREQUENCY LOADING ON FATIGUE

MECHANICAL TECHNOLOGY INCORPORATED
968 ALBANY-SHAKER ROAD
LATHAM, NEW YORK 12110

May 1985

Final Report for Period September 1982 - December 1984

Approved for Public Release, Distribution Unlimited

MATERIALS LABORATORY
AF WRIGHT AERONAUTICAL LABORATORIES
AIR FORCE SYSTEMS COMMAND
WRIGHT-PATTERSON AFB, OHIO 45433

NOTICE

When Government drawings, specifications, or other data are used for any purpose other than in connection with a definitely related Government procurement operation, the United States Government thereby incurs no responsibility nor any obligation whatsoever; and the fact that the government may have formulated, furnished, or in any way supplied the said drawings, specifications, or other data, is not to be regarded by implication or otherwise as in any manner licensing the holder or any other person or corporation, or conveying any rights or permission to manufacture use, or sell any patented invention that may in any way be related thereto.

This report has been reviewed by the Office of Public Affairs (ASD/PA) and is releasable to the National Technical Information Service (NTIS). At NTIS, it will be available to the general public, including foreign nations.

This technical report has been reviewed and is approved for publication.

David I.G. Jones

DAVID I.G. JONES, Project Engineer
Metals Behavior Branch
Metals and Ceramics Division

John P. Henderson

JOHN P. HENDERSON, Chief
Metals Behavior Branch
Metals and Ceramics Division

FOR THE COMMANDER

LAWRENCE N. HJELM, Asst Chief
Metals and Ceramics Division
Materials Laboratory

"If your address has changed, if you wish to be removed from our mailing list, or if the addressee is no longer employed by your organization please notify AFWAL/MLLN*, W-PAFB, OH 45433 to help us maintain a current mailing list".*

Copies of this report should not be returned unless return is required by security considerations, contractual obligations, or notice on a specific document.

UNCLASSIFIED
SECURITY CLASSIFICATION OF THIS PAGE

AD-A160601

REPORT DOCUMENTATION PAGE

1a. REPORT SECURITY CLASSIFICATION Unclassified	1b. RESTRICTIVE MARKINGS None
2a. SECURITY CLASSIFICATION AUTHORITY 2b. DECLASSIFICATION/DOWNGRADING SCHEDULE	3. DISTRIBUTION/AVAILABILITY OF REPORT Approved for public release, distribution unlimited
4. PERFORMING ORGANIZATION REPORT NUMBER(S) 85TR48	5. MONITORING ORGANIZATION REPORT NUMBER(S) AFWAL-TR-85-4045
6a. NAME OF PERFORMING ORGANIZATION Mechanical Technology Inc. 6b. OFFICE SYMBOL (If applicable)	7a. NAME OF MONITORING ORGANIZATION Materials Laboratory
6c. ADDRESS (City, State and ZIP Code) 968 Albany-Shaker Road Latham, New York 12110	7b. ADDRESS (City, State and ZIP Code) AFWAL/MLLN WPAFB, Ohio 45433
8a. NAME OF FUNDING/SPONSORING ORGANIZATION Materials Laborotory 8b. OFFICE SYMBOL (If applicable) AFWAL/MLLN	9. PROCUREMENT INSTRUMENT IDENTIFICATION NUMBER Contract F33615-82-C-5056
8c. ADDRESS (City, State and ZIP Code) Wright-Patterson AFB, Ohio 45433	10. SOURCE OF FUNDING NOS.

PROGRAM ELEMENT NO.	PROJECT NO.	TASK NO.	WORK UNIT NO.
62102F	2420	01	24200135

11. TITLE (Include Security Classification)
Interactive Effects of HCF/LCF (U) see cover

12. PERSONAL AUTHOR(S)
A. Petrovich

13a. TYPE OF REPORT	13b. TIME COVERED	14. DATE OF REPORT (Yr., Mo., Day)	15. PAGE COUNT
Technical Final	FROM 1 Sept 82 TO 31 Dec 84	1985 May	148

16. SUPPLEMENTARY NOTATION

17. COSATI CODES		
FIELD	GROUP	SUB. GR.

18. SUBJECT TERMS (Continue on reverse if necessary and identify by block number)

19. ABSTRACT (Continue on reverse if necessary and identify by block number)

This report describes the results of a program to measure and model the controlling mechanisms of fatigue and creep-crack growth behavior of a typical aircraft engine disk material under high frequency/low frequency loading cycles. The goal of the program is to provide a basis for damage-tolerant design of aircraft engine components under combined high and low frequency loading. Cyclic [illegible]; [illegible]; Crack propagation; life expectancy (Service life).

20. DISTRIBUTION/AVAILABILITY OF ABSTRACT UNCLASSIFIED/UNLIMITED ☒ SAME AS RPT. ☐ DTIC USERS ☐	21. ABSTRACT SECURITY CLASSIFICATION Unclassified
22a. NAME OF RESPONSIBLE INDIVIDUAL Dr. D.I.G. Jones	22b. TELEPHONE NUMBER (Include Area Code) (513) 2-5-2689 22c. OFFICE SYMBOL AFWAL/MLLN

DD FORM 1473, 83 APR   EDITION OF 1 JAN 73 IS OBSOLETE.

Unclassified
SECURITY CLASSIFICATION OF THIS PAGE

FOREWORD

This report was prepared by Mechanical Technology Incorporated (MTI), Latham, New York for the Metals Behavior Branch, Metals and Ceramics Division, Materials Laboratory, Air Force Wright Aeronautical Laboratories, (AFWAL/MLLN), Wright-Patterson Air Force Base, under Contract F33615-82-C-5056. The work was administered under the direction of Dr. David I.G. Jones, AFWAL/MLLN. The program effort was conducted at MTI by A. Petrovich, W.F. Bessler and W.H. Ziegler. Additional support was provided by J. Walton, L.A. Peterson and L. Isley. This report describes work conducted from September, 1982 to December, 1984.

TABLE OF CONTENTS

LIST OF TABLES

LIST OF ILLUSTRATIONS

LIST OF ILLUSTRATIONS

LIST OF ILLUSTRATIONS

FIGURE PAGE

LIST OF ILLUSTRATIONS

I. INTRODUCTION

A means of more fully utilizing the useful life of aircraft engine components is provided by the Retirement-for-Cause (RFC) life management concept. Under the RFC philosophy, components are inspected at intervals of operation such that a crack or other service induced defect just below the level of detectability cannot grow to a critical size between inspections. Those components with no observable flaw are returned to service with the assurance that if a fatigue crack develops, it will not grow to a size that will result in catastrophic failure of the component while in service. A cost savings results from the fact that by retiring the components on the condition of an observable flaw, components without flaws that would otherwise be retired by the probabalistic scheme would now be allowed to remain in service until cracking is apparent.

Implementation of the Retirement-for-Cause method requires advances both in non-destructive evaluation and crack growth life prediction. The primary requirement with regard to crack growth life prediction is an improvement in the accuracy of life prediction for the complex loading profile experienced by engine components. Important to the improvement of the accuracy of life prediction is an accounting of the interaction between the various components of the loading profile.

The life limiting loading profile experienced by an engine disk consists basically of a group of low frequency cycles associated with thermal gradients or centrifugal forces and superimposed high frequency loading associated with blade passage. The cycle period associated with the low frequency cycle (low cycle) loading is on the order of seconds to several hundred seconds. A wide range of loading rates and load levels may also be involved in the low cycle loading. The high frequency cycle (high cycle) loading would typically involve frequencies on the order of hundreds to several thousand hertz. Important to accurate life prediction is establishing the manner in which each of these features of the engine disk loading profile contribute to crack growth and how these features interact. The specific aspects of combined cycle loading that must be addressed are the following:

- Establishment of the limits of high cycle loading under which the disk can be safely operated.
- How cumulative damage rules should be applied when combined high cycle/low cycle loading contribute to crack growth.
- The degree to which the high cycle and low cycle loading influence each others contribution to crack growth.

A test system was designed and constructed specifically for the present study to provide adequate load levels up to 2000 Hz and minimize the frequency ranges over which dynamic complications in load application are present. A purely servo-hydraulic system based on an Akashi voice-coil servo-valve was used for all of the testing. The load frame and specimen were designed to minimize the number of system resonances that create undesirable specimen stress patterns and either complicate or invalidate the representation of stresses around the specimen crack. The test system constructed for their study is described in Section 2.

The specimen type used for this study was a center crack panel also described in Section 2. A clevis arrangement with provisions to clamp the specimen ends was used to grip the specimen. By securely clamping the specimen and providing additional lateral support, specimen resonances could be avoided at the selected test frequencies. Both the high frequency and low frequency was sensed by a load cell. It was recognized that resonances in the load frame and specimen could disturb the correlation between the load cell measurement and stresses in the specimen as well as provide significant bending stresses associated with resonant lateral vibration. Modal analyses of a preliminary specimen were performed to determine its natural frequencies and mode shapes over a range of steady load and crack length. These modal analyses indicated the specimen modifications required to make the specimen suitable for testing in bands of frequencies up to 2000 Hz. Test frequencies of 200 and 1825 Hz were chosen for most of this study. The absence of excessive bending stresses and a proper correlation between load cell measurement and specimen stresses was verified at these frequencies with strain gage measurement on the specimen. The precision in the high frequency ΔK measurement required for this study made these specimen dynamic evaluations and detailed verification of specimen stress absolutely essential.

The high/low frequency loading profile used in this study is described in Section 2. The low frequency component was a trapezoidal waveform with a rise time (T_1) and fall time (T_2) of 0.5 seconds and with a hold time (T_o) of between 2 and 180 seconds. The high frequency loading was applied during the low frequency cycle hold period and typically ranged between 220 and 4450 Newtons (50 to 1000 lbs). The low frequency load levels P_1 and P_2 were varied during the tests such that the low frequency stress intensity factors K_1 and K_2 were maintained constant. The high frequency load range (P_o) was either increased during the test or maintained constant which in either case resulted in an increasing high frequency stress intensity factor range (K_o). The low cycle R ratio (P_1/P_2) was 0.1 for all of the testing. All testing was performed at 649°C.

Section 3 presents the results of a series of crack growth tests that were performed on Inconel 718 at 649°C (1200°F). The following aspects of the high/low cycle interaction were investigated in the series of crack growth tests:

- the effect of high cycle frequency up to 2000 Hz on the low cycle/high cycle interaction
- the effect of low cycle stress intensity factor range (ΔK_{LC})
- variation of crack growth rate as a function of high cycle stress intensity factor range (ΔK_{HC}) over a ΔK_{LC} range of 15 to 40 MPa $\sqrt{m}$
- the influence of low cycle hold time between 2 and 180 seconds on the crack growth rate under combined cycle loading

The results of testing are summarized in curves representing crack growth rate versus high frequency ΔK for constant low frequency cycle ΔK range and low cycle hold time. Crack growth rate is reported in terms of growth per unit time at the upper level of the low cycle trapezoidal loading profile. The low cycle ΔK ranges included in the testing were 15, 20, 30 and 40 MPa $\sqrt{m}$. The low cycle hold times included 2, 5, 10 and 180 seconds. Comparisons are made in Section 3 between the results for a high cycle frequency of 200 and 1825 Hz provided by this study and those for 10 Hz provided in Reference 1.

Section 4 also explores possible mechanisms associated with the combined cycle interaction. Correlations are made between the crack growth data and features of the fracture surface. Means of modelling combined cycle crack growth rate are also discussed.

II. SYSTEM CONSTRUCTION, EVALUATION OF SYSTEM DYNAMICS, AND SPECIMEN DESIGN

A. Background on the Selection of Test Equipment

There have been several approaches to providing controllable load levels in the frequency regime above 100 Hz. One system used for high frequency fatigue testing is the electrodynamic shaker. Motion and forces in these systems are generated by interaction of a solenoid generated field with a moveable armature. Standard commercial electrodynamic shakers have force ratings up to 9000 lbs. with up to 100 g's of acceleration available to 3000 Hz.(2) Magnetrostrictive devices have also been used to generate forces and displacements of frequencies up to 1000 Hz. An example of a study of threshold crack growth conducted with magnetostrictive system is that of Reference 3.

The desire to test materials with a loading profile similar to that of an aircraft turbine engine has lead to the development of test systems that can apply low cycle high amplitude loading (on the order of 5000-20,000 lbs.) along with low amplitude high frequency (100 to 2000 lbs.) loading. A novel example of the machines developed for the application of combined cycle loading is the major/minor cycling system constructed by Instron Ltd.(4) The characteristics of this system are summarized in Table 1 and a schematic representation of the system appears in Figure 1. The high frequency loading component is applied by the electrodynamic shaker and the low frequency component by a hydraulic actuator. This is made possible by a specially developed isolation unit between the hydraulic actuator and shaker which allows the simultaneous application of loading by the hydraulic actuator and electrodynamic shaker.

An alternative to a combined servohydraulic/electrodynamic and purely electrodynamic system for the application of a combined high cycle/low cycle loading profile is a purely servohydraulic system based on a voice coil servo-valve.(5) The use of electrohydraulic servo-valves for material testing is widely practiced and is usually performed with a flapper-nozzle valve, which, in spite of its inherent low-frequency limitation, has been totally adequate for the testing of such material properties as creep, ultimate strength, yield strength, and low-frequency cyclic fatigue.

TABLE 1

SPECIFICATION FOR INSTRON COMBINED CYCLE TEST SYSTEM

High Frequency Component:

Waveform:	Sinusoidal
Frequency Range:	50 - 600Hz depending upon the specimen stiffness
Max. Dynamic Load:	±5kN

Low Frequency Component:

Waveform:	Trapezoidal
Minimum rise and fall times:	0.4 sec.
Dwell times:	0.1 - 99.9 secs. or 0.1 - 99.9 min.
Maximum Load Unidirectional tension or compression:	50kN

Load Frame:

Number of Columns:	4
Dynamic Load Rating:	±250kN
Max. Vertical Daylight: (between load cell & shaker)	700mm
Distance between columns:	661 x 305

Load Cell:

Fatigue Rating (Unidirectional):	50kN max. force
Excitation:	5.6 volt DC
Load Measurement Accuracy Static:	±1% of indicated force or ±0.2% of full scale, whichever is the greater
Dynamic:	±3% of indicated force or ±0.2% of full scale, whichever is the greater

Compensation is provided for changes in dynamic load reading caused by the mass of the Grip or Fixture.

NOTE:-

Because of the high operating frequencies, the mass of the moving parts has a significant effect on the performance of the machine. The actual frequency range over which the desired dynamic force can be achieved is dependent upon the stiffness of the specimen. Details of the specimen should be given when ordering.

Patents Pending

PDS 1219

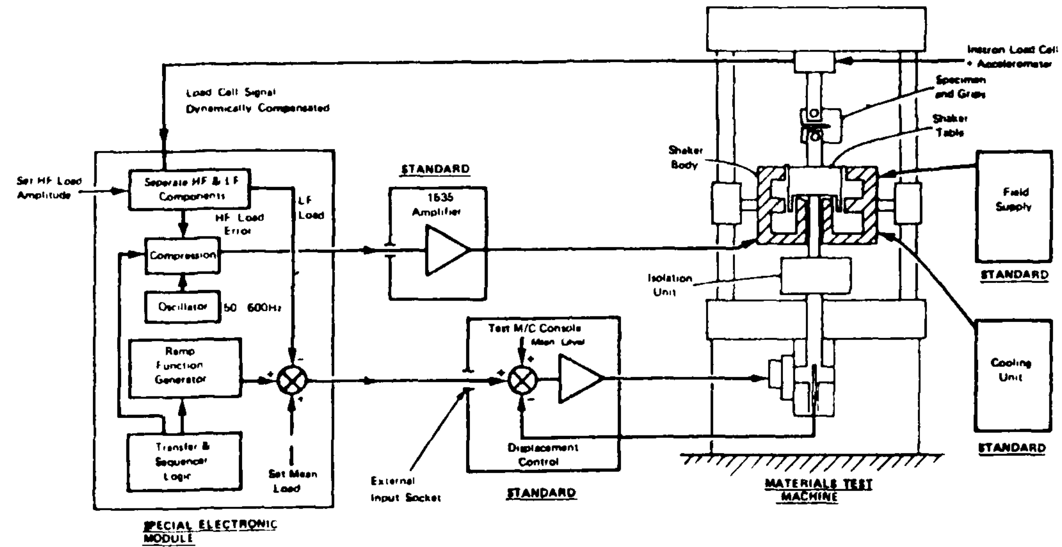

Figure 1 Schematic of Major/Minor Cycling Machine Control System (4)

An example of a high frequency servo-hydraulic system is that developed by Akashi Ltd.[5] The Akashi vibration system employs a servo-valve and actuator with high-frequency capability based on a voice-coil-type servo-valve. In this system, the electrical drive signal directly causes servo-valve spool motion. The voice-coil valve thereby provides a significant advantage in high frequency input flow capability to the actuator. Also the Akashi servo-valve is optimized to reduce the impedance loading associated with high frequency, and its mechanical natural frequency has been established to favor frequencies at the higher end of its useful spectrum. The two types of servo-valves, the flapper-nozzle system and Akashi voice-coil system, are shown in Figures 2 and 3 respectively. Additional high frequency servo-hydraulic systems are manufactured by MTS[6] and Teem.

The ability of a test system to provide adequate displacement at the test frequency is the most important consideration for high frequency testing. It is difficult to accurately estimate the displacement capability of a shaker in specimen fatigue testing application in view of the complexity of the interaction between the actuator and load frame. A means of establishing a rough estimate is to determine the maximum deflection capability of the shaker with a test load of 50 lbs. and without the constraint of a load frame. Such a determination was made for an Akashi test system based on a pilot/slave servo-valve with a 5 gpm/37gpm flow capability and a 1.2 inch stroke actuator. The estimated deflection of this system is shown in Figure 4. This curve provided an adequate estimate of deflection for planning fatigue testing in a test system based on this servo-valve/actuator combination.

Another important consideration for fatigue crack growth testing is ensuring that the stresses around the growing crack are similar to those under quasistatic conditions. Only if this can be assured can results from one frequency be compared to another. Resonance in the load frame and specimen often disturb the patterns of stresses. Investigations of the manner in which specimen stresses can be distorted at high frequency have been carried out with the aid of modal analysis.[7] Figure 5 shows the patterns of standing wave resonant vibration that can occur in a standard center crack panel specimen. Such dynamic complications to crack growth testing can be minimized by proper selection and design of the test system along with proper design of the specimen.

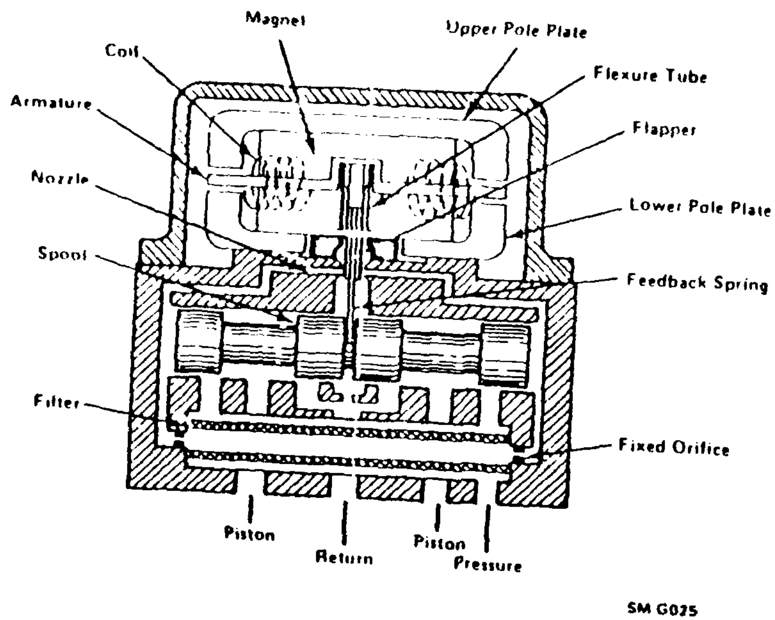

Cross-Sectional View of 252 Servo Valve

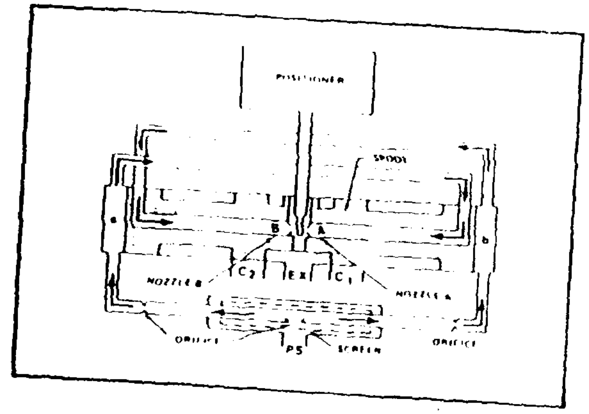

Boost System - Steady State with Spool On Center

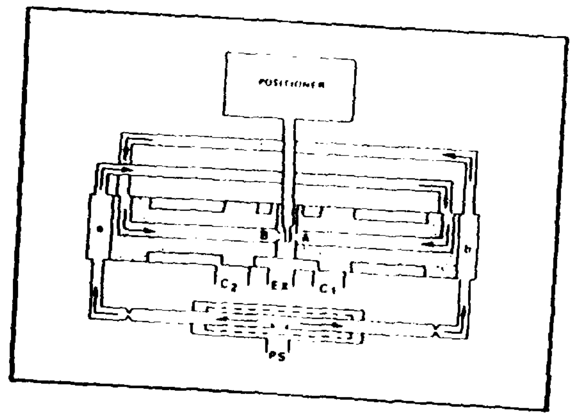

Boost System - Steady State with Spool Off Center

84144

Figure 2 Standard Flapper-Nozzle Servo-Hydraulic Valve

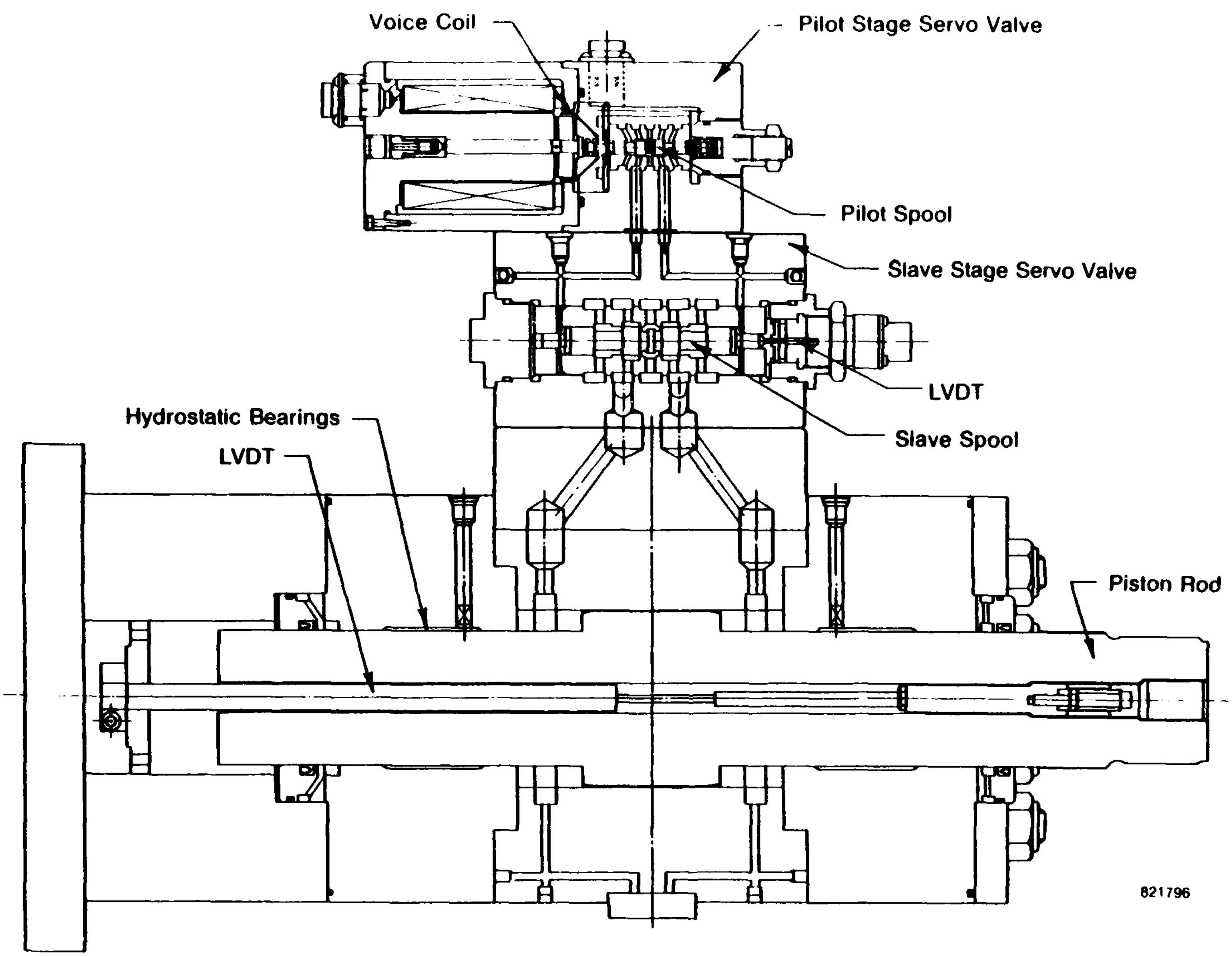

Figure 3 Hydraulic Actuator and Servo Valve (5)

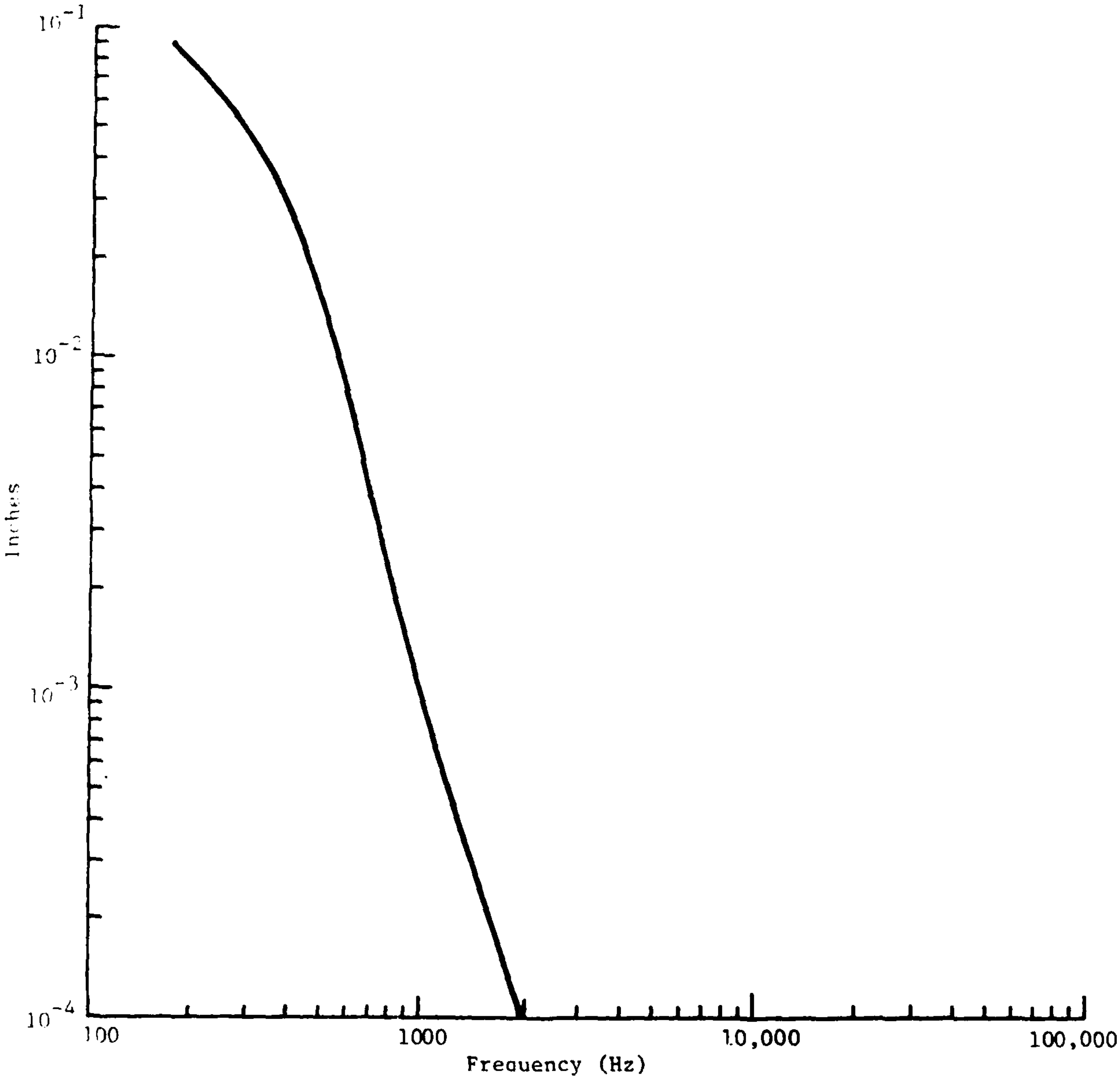

Figure 4 **Estimated Maximum Displacement versus Frequency for the Akashi Servo-valve servo-actuator combination HV 10.0-1.2-37/5.**

821644

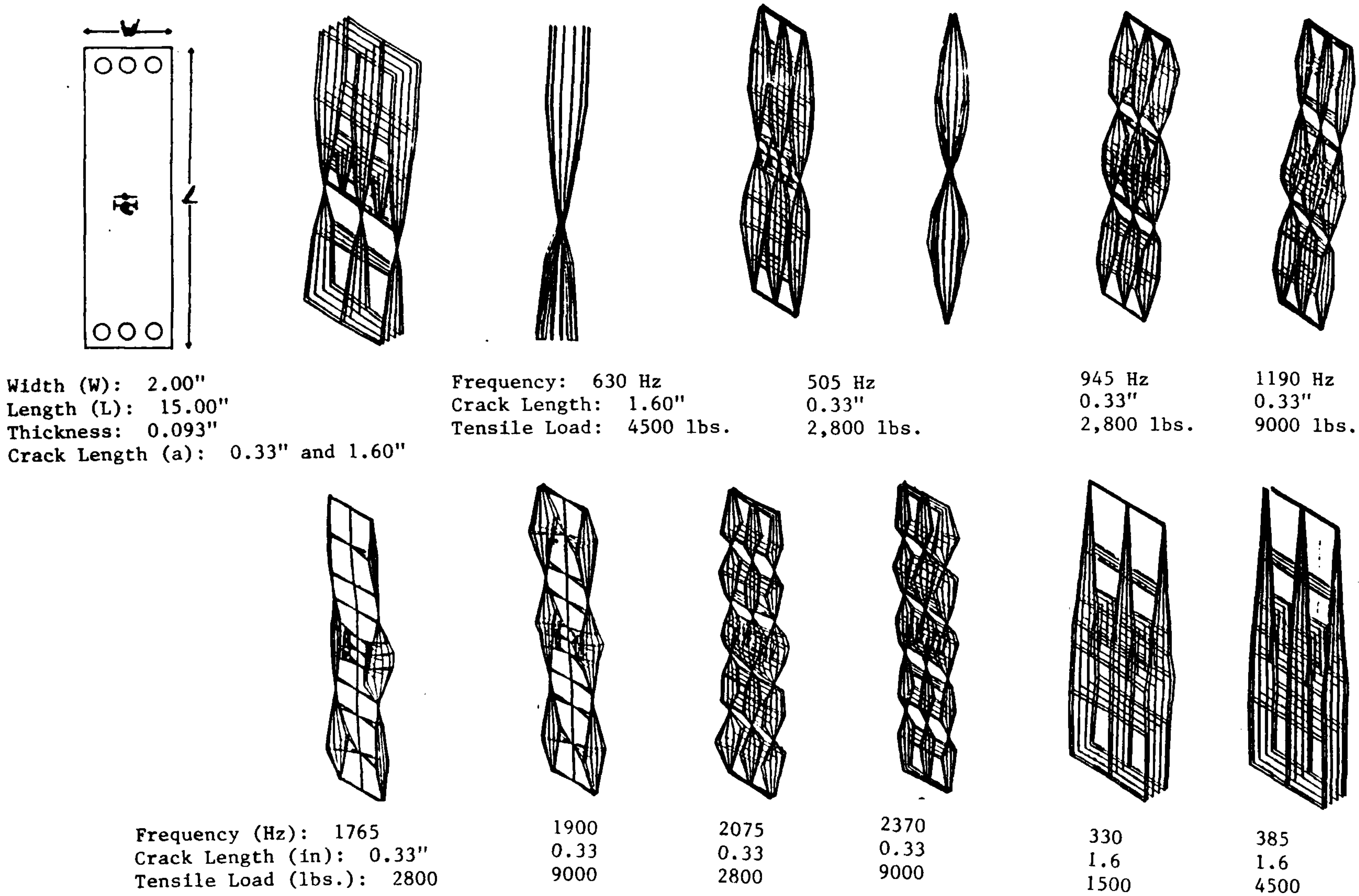

Figure 5 Vibration patterns for a center panel specimen (7)

B. System Selection and Construction

The study of the phenomenon of high-frequency/low frequency load interaction in fatigue and creep crack growth required the construction of a test system that could provide adequate levels of load up to a frequency of 2000 Hz that could provide low cycle load levels up to 10,000 lbs., and allow precise control of both low-frequency and high-frequency loading during fatigue crack growth testing. The following options were available.

- A purely electrodynamic system with a maximum force rating on the order of 10,000 lb.
- A combined high-frequency electrodynamic/low-frequency servo-hydraulic system with some type of isolation system to remove large preloads from the electrodynamic system during high-frequency vibration.
- A purely servo-hydraulic system based on a voice-coil servo-valve.

A preliminary evaluation indicated that the purely electrodynamic and purely servo-hydraulic options would permit a load frame sufficiently rigid to preclude dynamic complications at the higher frequencies. It was also determined that a servo-hydraulic system was less expensive for the load ranges required for this program. It was feared that the combined servo-hydrualic and electrodynamic system with its isolation system had such an extended load frame that a large number of resonances would make testing and verification of loading extremely difficult particularly at higher frequencies. Therefore, because of compatibility with existing MTI equipment, relatively low cost, and ability to construct compact frames and fixturing around the specimens and actuator, the purely servo-hydraulic option was chosen.

The purely servo-hydraulic test system constructed for this program is based on an Akashi voice-coil servo-valve with a frequency capability that far exceeds the more conventional flapper-nozzle servo-valve. The Akashi servo-actuator incorporates all the features of the fatigue-rated actuators currently used today, as well as several key design improvements. The piston-to-cylinder clearance is manufactured to allow operation without a piston seal, thereby eliminating a wear item and, more importantly in high-frequency operation, removing the cause of waveform distortion associated with seal motion during pressure reversal. Hydrostatic bearings are employed to provide high side load capability and to eliminate any metal-to-metal contact at the bearings. Piston rod seals are not used, thus eliminating the largest factor of friction in the system and also removing an element that must be periodically serviced, i.e., replacing the seal and refinishing the piston rod.

The high-frequency servo-hydraulic equipment purchased by MTI for this program includes the following:

- Akashi Servo-Actuator Model HV 10.0-1.2-37/5 (10,000 lb. maximum status load
- Akashi Servo-Valve (pilot/slave) Model SV 5/SV 37
- Akashi Servo-Controller Model SC-1
- Akashi Servo-Amplifier Model SA-400
- Akashi Manifold Model HM-40

The Akashi servo-actuator (Model HV 10.0-1.2-37/5) was installed in a load frame already in operation at MTI. Figure 6 shows the servo-hydraulic testing system with specimen, induction heating coil, and crack-length-measuring telemicroscope in place. Figure 7 shows, in greater detail, the specimen, induction heating coil and specimen gripping arrangement. A standard clevis was used to provide loading to the specimen. To reduce unnecessary deflection, the 2-in.-wide center cracked panels are reinforced at the ends gripped by the clevis.

During the high-frequency experiments, noise levels reached 135 db, and it was necessary to construct a sound-deadening enclosure around the system. The noise reduction provided by this enclosure was sufficient to reduce the noise to an acceptable level in surrounding offices and work areas.

The high-frequency servo-valve receives signals from the servo-controller and servo-amplifier. The command signal applied to the servo-controller is the sum of a high- and low-frequency signals which are controlled independently by the PDP-11/04 computer that interfaces the servo-hydraulic system. A schematic diagram of the control and data acquisition system is shown in Figure 8. The high- and low-frequency signals must be controlled independently becasue the system gain (i.e., the load range per unit input signal) is different for the high- and low-frequency portions of the command signal. Figure 9 schematically

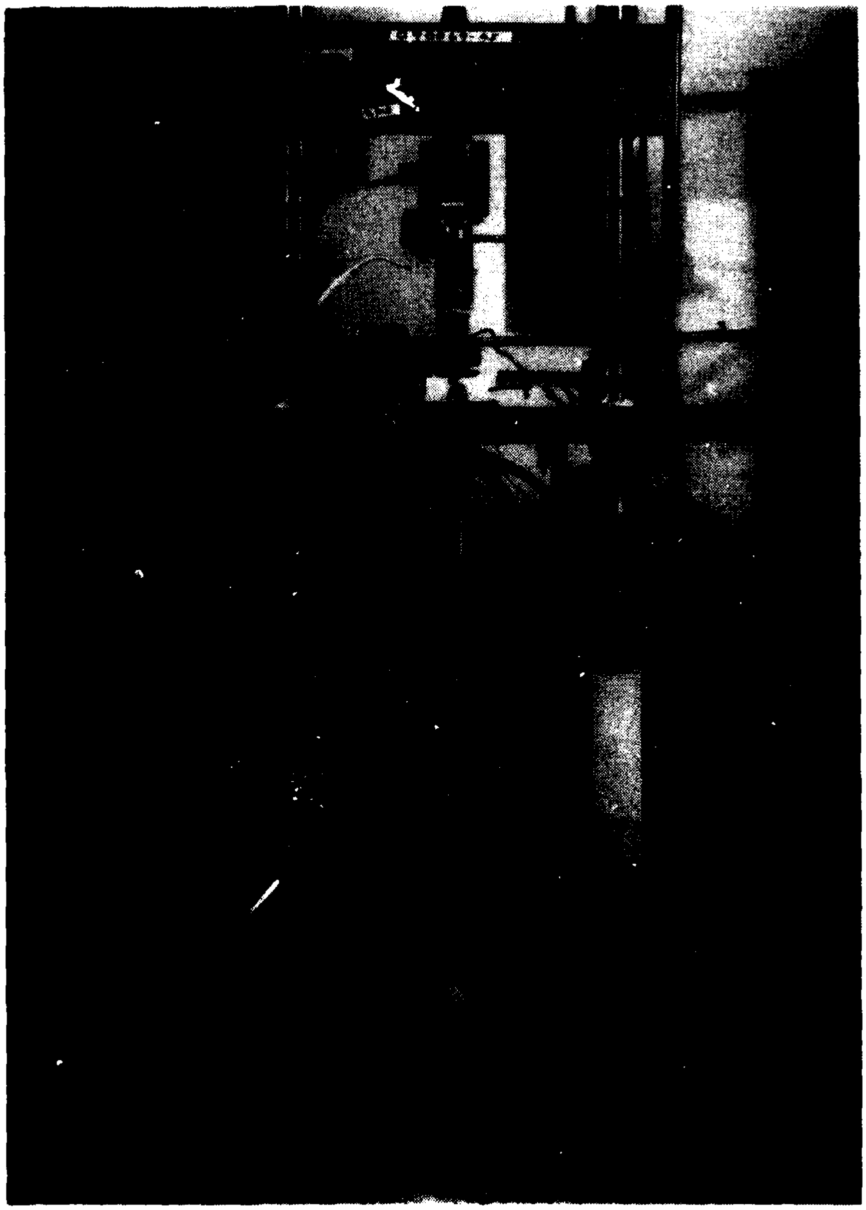

Figure 6 High Frequency Servohydraulic Test System with 2" Width Center Cracked Panel Specimen Installed

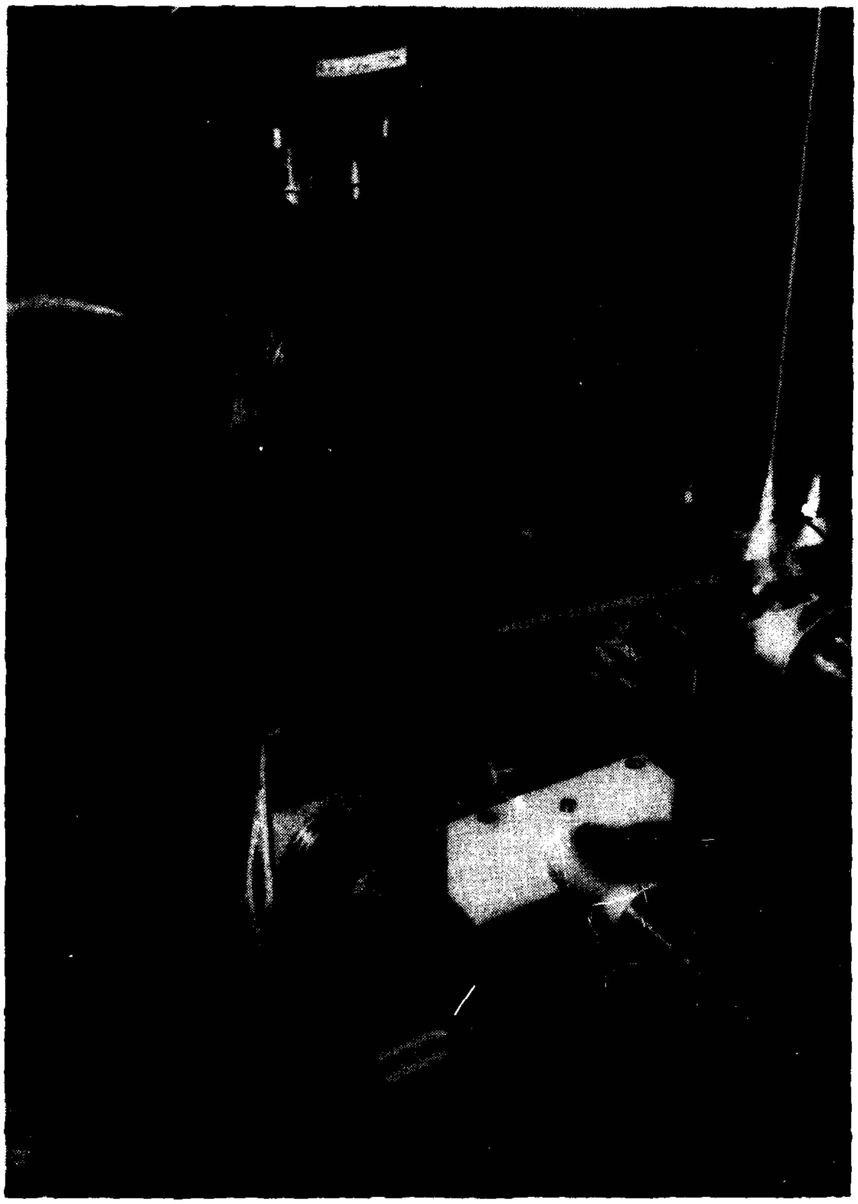

Figure 7 Center-Cracked Panel Specimen in High-Frequency Test System (The specimen is heated inductively, and the crack length is monitored by both a 20X telemicroscope and an AC direct potential crack-measurement system.)

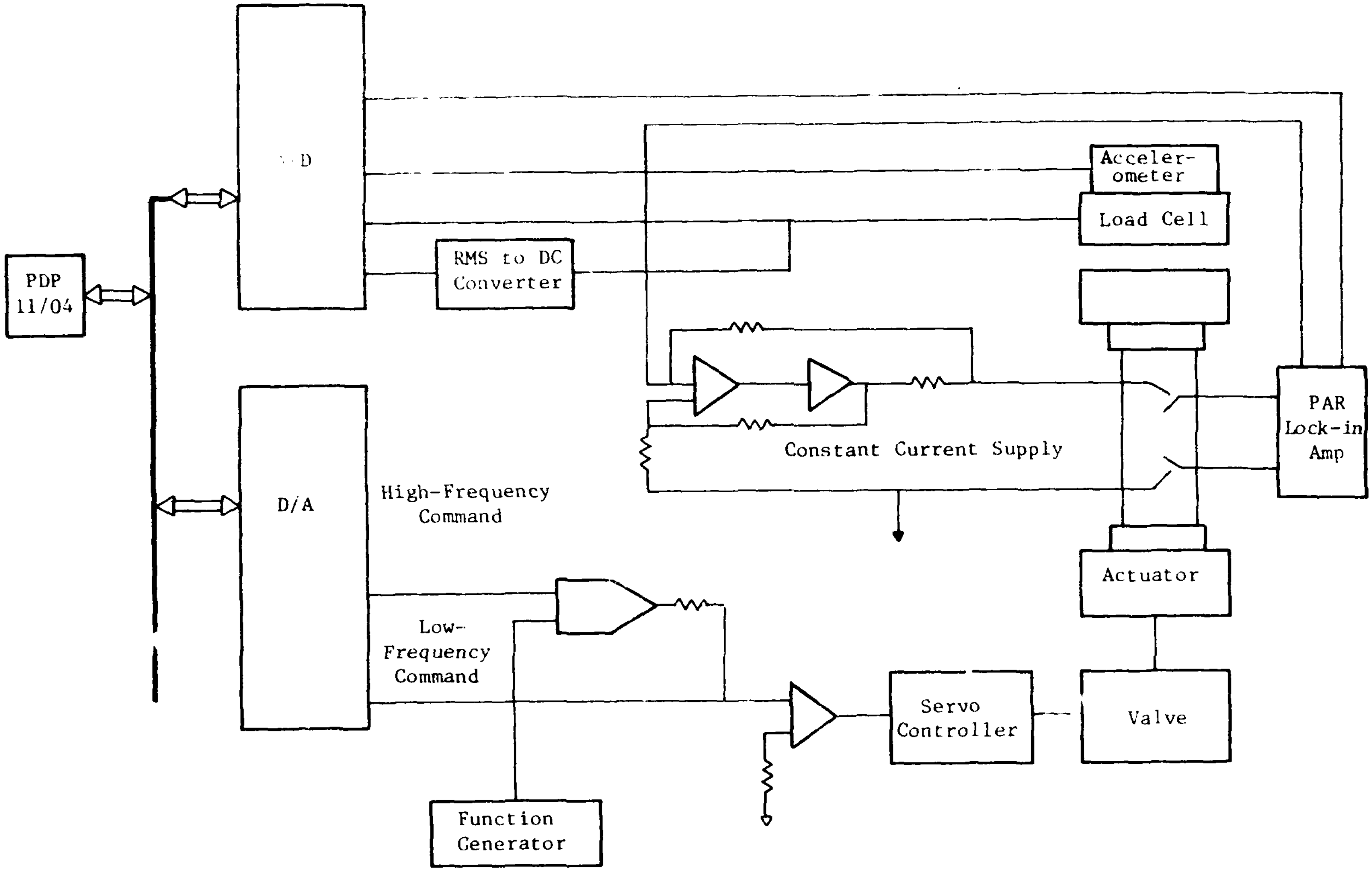

Figure 8 Crack Length Measurement and Servo Control System for High-Frequency Servo Hydraulic System (Based on the Akashi Servo Controller and Actuator with Latest Modification)

84056

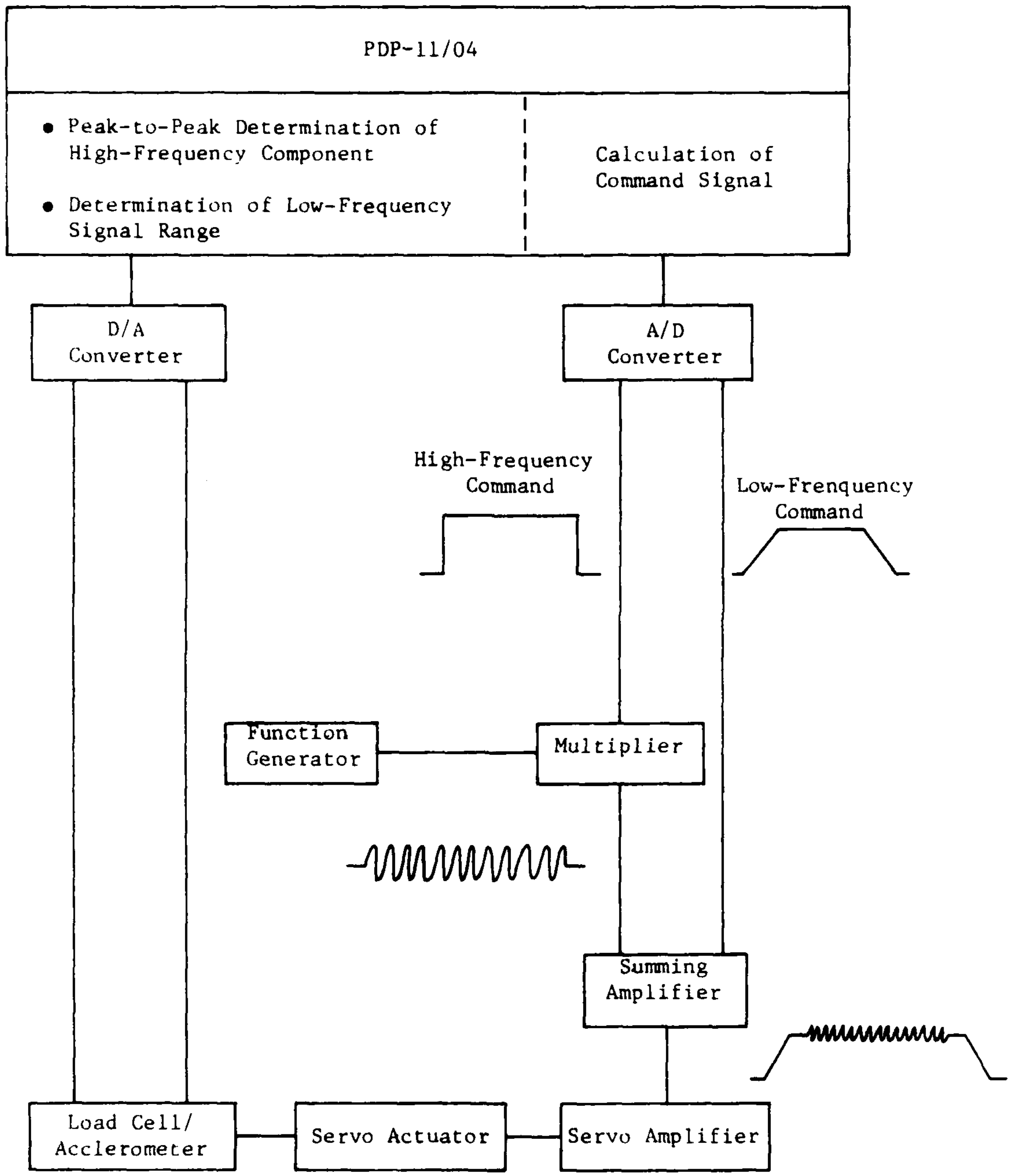

Figure 9 Closed-Loop Control System for High- and Low-Frequency Components of Loading Profile

illustrates the control of the high- and low-frequency signals. The loading profile resulting from the summation of the high- and low-frequency components is shown in Figure 10a which corresponds to the load response of the system with the 2-in.-wide center-cracked panel and a high-frequency component of 460 Hz. The high-frequency segment of the load cell signal is shown in greater detail in Figure 10b.

A servo-hydraulic vibration system test report for the Akashi servo-valve and servo-actuator is included in Appendix A. The first chart in this report shows the maximum performance in terms of acceleration for the Akashi servo-actuator used in this test program. This chart provides the acceleration as a function of frequency for a 60.75 and 108.7 kg payload. The second and third charts in this report show the acceleration as a function of frequency for a specific signal level input to the servo-amplifier for a 60.75 kg and 108.7 kg payload respectively. Such charts are useful in estimating the actuator displacement capability in a materials testing load frame.

The basic types of specimens used in crack growth testing are the compact tensile specimen, the edge-cracked-panels, the center-cracked panel and bend-type specimens, plus many variations on these basic types. For high-frequency testing, several important dynamic considerations have to be addressed if the desired loading conditions are to be achieved at the crack. The most important consideration is the compliance (extension per unit load) for the range of ΔK (K = stress intensity factor) to be covered in the test program. The specimen has to provide as low a compliance as possible consistent with accurate measurement of crack length and of crack growth rate. (Minimizing compliance is important because, as frequency increases, the possible deflection of both servo-hydraulic and electrodynamic systems rapidly decrease). Therefore, the center-cracked-panel type was chosen for use in this program because of it relatively low compliance for a given ΔK range.

In the planning of the test program, frequency ranges for the high and low-frequency ΔK were selected. frequencies. A specimen and loading system were then selected to accomplish testing in these ranges. The dynamic limitations of the system had to be considered. For example, in the frequency regime of 1000 Hz and above, the maximum displacement that a servo-hydraulic system can provide is critically dependent on the design of the servo-valve and servo-actuator. Simi-

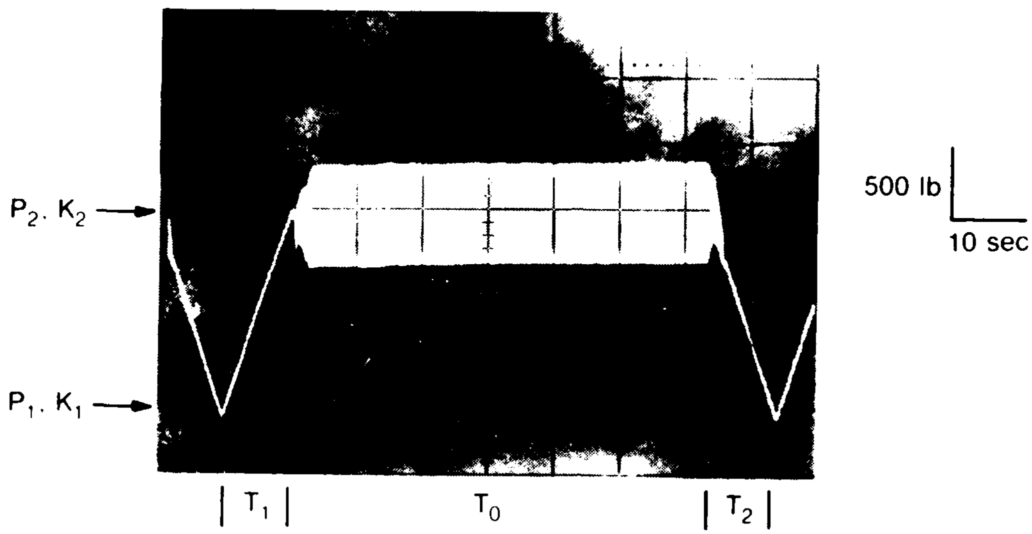

Figure 10a Combined high/low frequency loading profile.

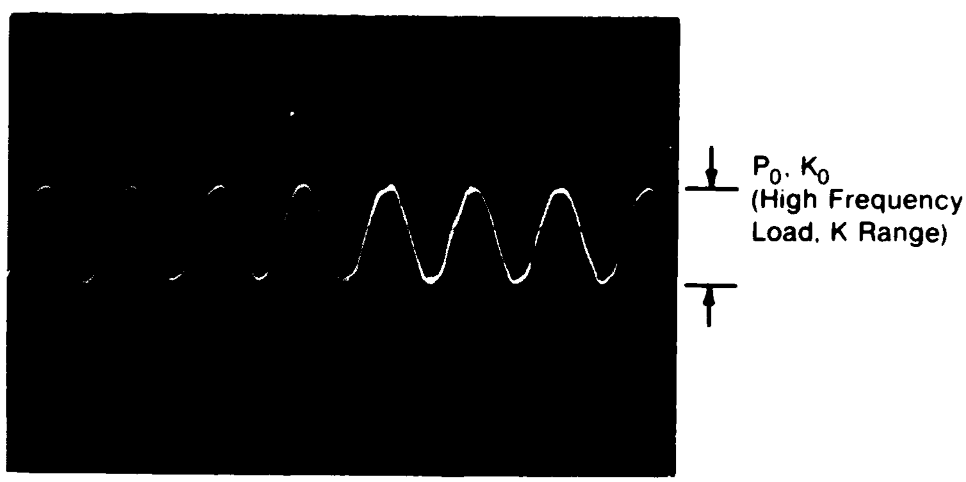

Figure 10b High frequency component with expanded time scale.

lar considerations apply to purely electrodynamic and combined servo-hydraulic/electrodynamic systems. The specimen dimensions and starting crack length (a) were, therefore, chosen based on system displacement limitations and desired high-frequency ΔK range.

C. Dynamic Evaluation of Test Specimens

Strain gage measurements on a preliminary center crack specimen (Figure 11 and 12) used in the test program showed that while it was adequate for 200 Hz testing it was inadequate for frequencies above 500 Hz. A series of system resonances resulted in substantial bending stresses and a generally poor correlation between load cell measurements and strain gage measurements of stress in the crack region. A modal analysis was performed on this preliminary specimen to determine how it should be modified to reduce the density of resonances in the frequency regime beyond 500 Hz. The resulting modifications on the specimens were successful in providing several frequency bands above 500 Hz in which undesirable dynamic stresses were eliminated.

An important objective of the present work is to compare the fatigue crack growth behavior of the material at several frequencies. It is, therefore, extremely important to ensure that the loading pattern is the same at these frequencies. A series of specimen designs were evaluated with strain gages and a successful design evolved. The criteria established for the specimen were as follows:

- Bending stresses and out of phase components of stress at the specimen crack line must be less than 5% of the high cycle amplitude (this is a requirement of ASTM standard E647 extended to cover all dynamic disturbances of stress uniformity).
- The load measurement must have an appropriate relationship to the stresses in the crack region throughout the test.
- Stresses at several locations in the crack stress field must have an appropriate relationship to each other.

In view of the fact that resonant frequencies shift as the crack grows, the following condition must also be fulfilled by the specimen:

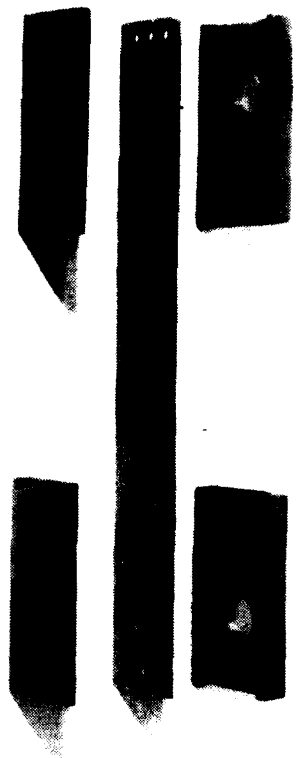

Figure 11 Photographs of the Preliminary Specimen used for 200 Hz Assembled and Disassembled

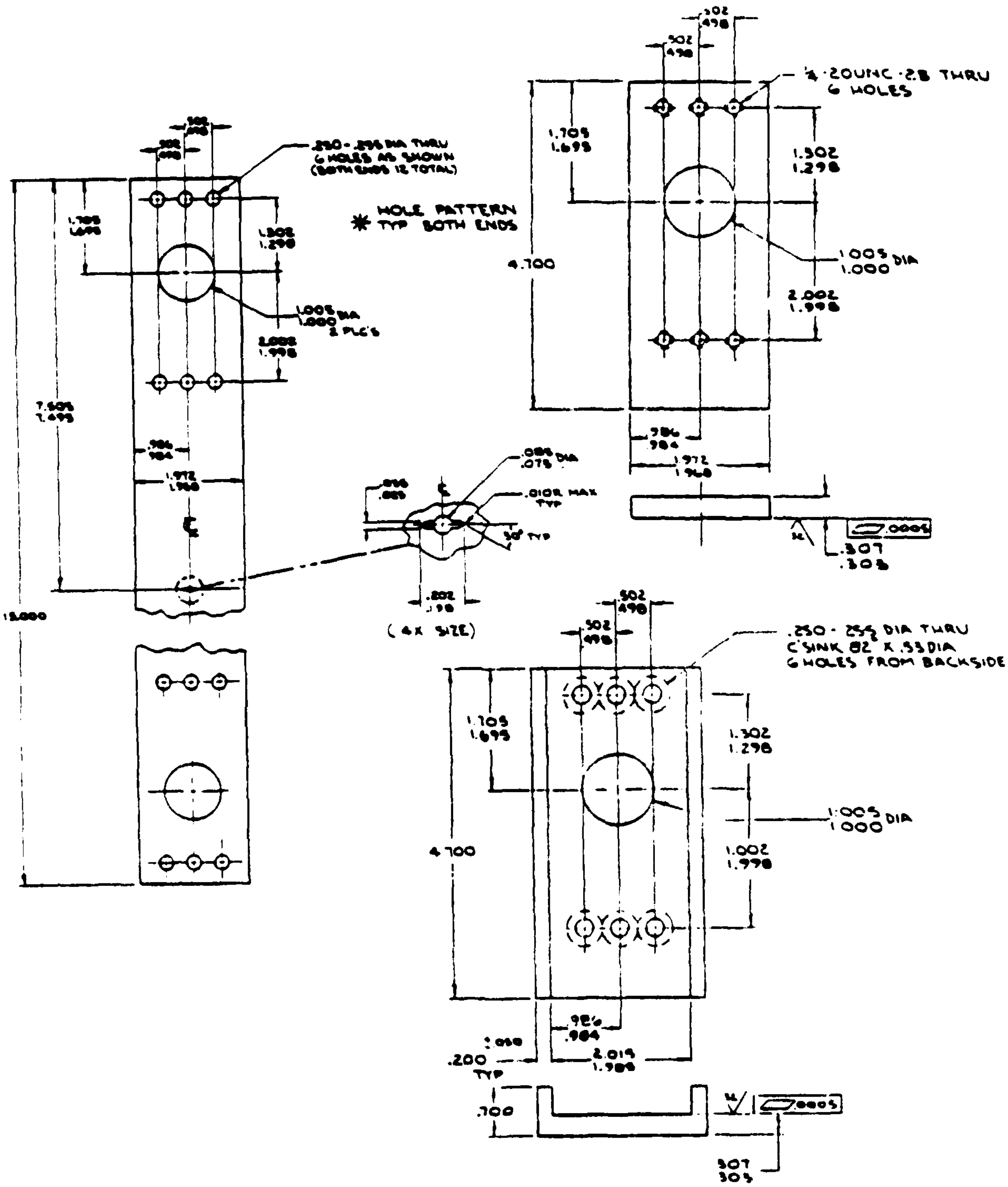

Figure 12 Drawings Showing the Dimensions of the Preliminary Specimen Used for 200 Hz Testing

- The above conditions must apply over a range of at least 200 Hz in the frequency regime of interest over the entire range of loading and crack length experienced during a test.

The interval of 200 Hz was chosen based on the expected variation in resonant frequency resulting from specimen material modulus variation as the specimen is brought to the test temperature. This can be demonstrated by considering the expression for the ringing frequency of an undamped plate:

$$\nu_n = \frac{1}{2\pi} \kappa_n^2 \left(\frac{EIg}{\gamma S} \right)^{1/2} \qquad (2.1)$$

where κ_n is determined by the boundary conditions,

and where

S = specimen cross-sectional area
γ = density
E = elastic modulus
I = moment of inertia
g = accelerometer of gravity
ℓ = length of specimen

With the average 10% reduction in elastic modulus over the specimen region participating in the vibration mode, a 5% change is expected in resonant frequency or about 100 Hz at a resonant frequency of 2000 Hz.

In Sections C.1 and C.2, the results and conclusions of the modal analysis are presented along with a description of the specimen adopted for testing around 2000 Hz and a summary of the strain gage dynamic evaluation of this specimen at 1825 and 2000 Hz.

C.1 Modal Analysis of the Preliminary Specimen

After the evaluation of the preliminary specimen (shown in Figures 11 and 12) with strain gages, it was apparent that some modification of the specimen would be required to make it suitable for testing near 2000 Hz. Comparison of strain gage response from opposite surfaces indicated that bending stresses well beyond that permitted by ASTM standard E647 existed over most of the frequency range from 1000 to 2000 Hz. It was felt that a modal analysis should be performed on the specimen to determine the resonant frequencies and mode shapes of these resonances. The information gained from this modal analysis was subsequently used to determine modifications that would be necessary to make the specimen suitable for 2000 Hz testing.

The preliminary specimen with the clamping fixtures extended (Figure 13) was placed in the load frame in the usual manner and a static load was applied. An accelerometer was attached to the specimen or load frame at one of 43 locations. The specimen was then excited with a random signal having the spectrum shown in Figure 14. The signal was provided with a Scientific Atlanta Vibration Controller which has the capability of open loop or closed loop vibration control. The modal analysis was conducted with open loop excitation. The accelerometer was moved successively to the locations on the specimen shown in Figure 15 and the random vibration was applied. Additional locations on the load frame were included but the levels of vibration were considerably less than those on the specimen. The accelerometer response and shaker excitation were simultaneously recorded. The data was processed using a Hewlett Packard 5451C Fourier Analyzer System which calculates the transfer function between the input and response at points on the specimen and load frame. An analytical model was curve fitted to the transfer function data and modal parameters such as natural frequency, damping factor, and mode shape were identified. The system software also has the capability of providing animated representations of the mode shapes. Modal parameters for the following mean load and crack length (2a) cases were evaluated:

- Mean load = 2000 lbs., crack length (2a) = 0.20"
- Mean load = 4500 lbs., crack length (2a) = 0.20"
- Mean load = 2000 lbs., crack length (2a) = 0.95"

Table 2 lists the natural frequencies and damping factors for the resonant modes for each of these cases. The mode shapes for the three cases are shown in Figure 16 through 18.

The modal analysis on this specimen demonstrated the following:

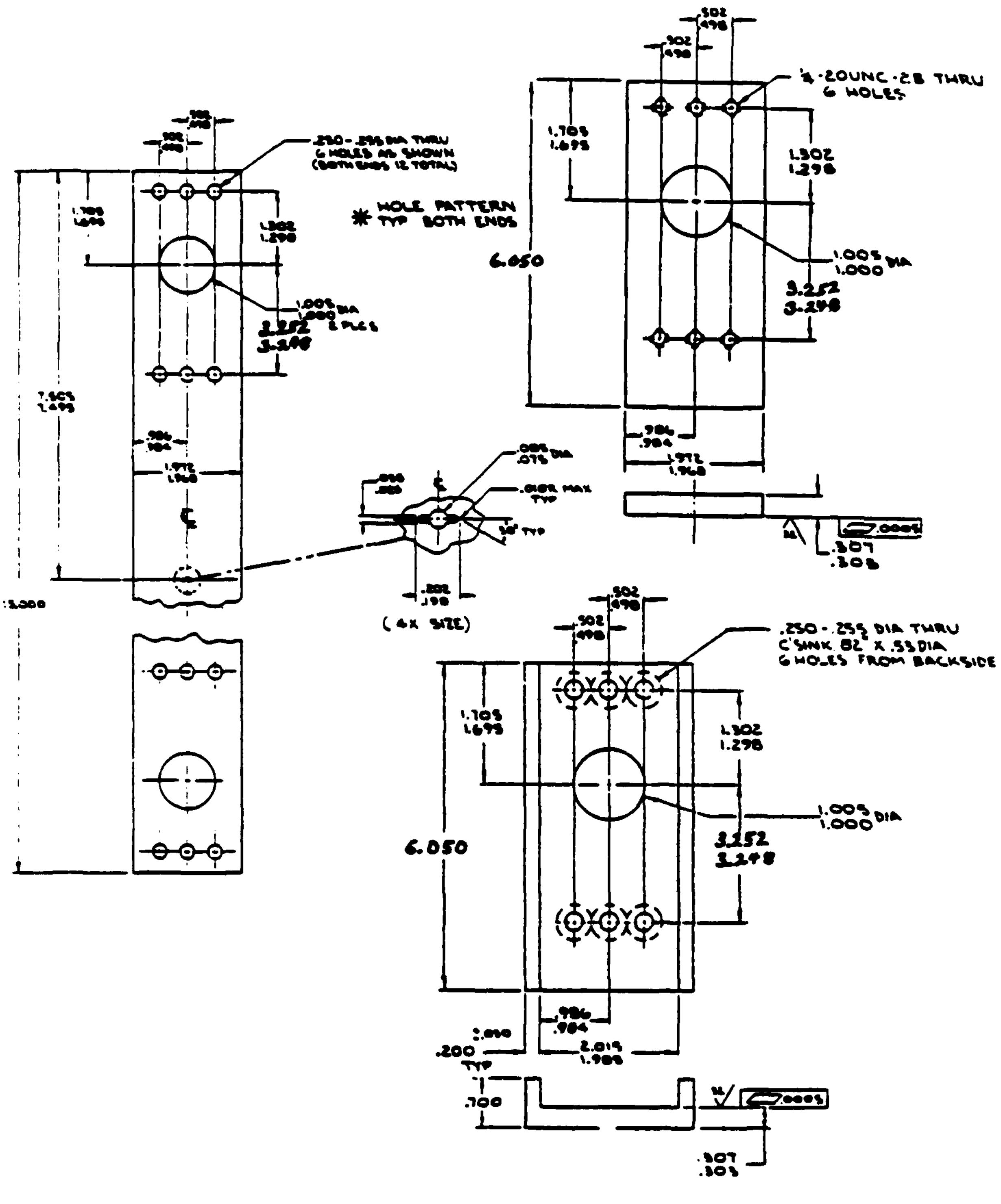

Figure 13 Drawings Showing the Dimensions of the Preliminary Specimen Subjected to Modal Analysis

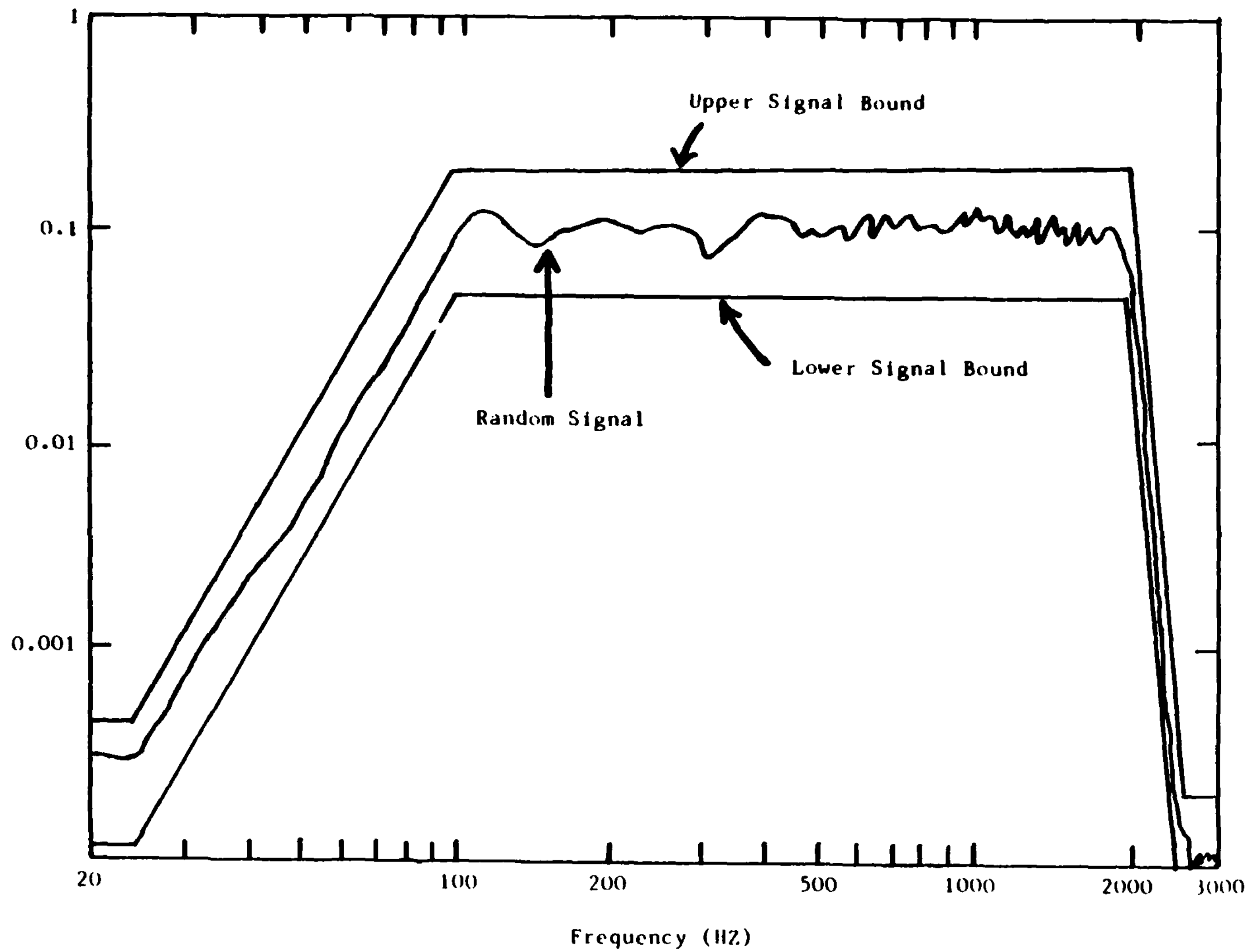

Figure 14 Relative input power spectrum used in the modal analysis

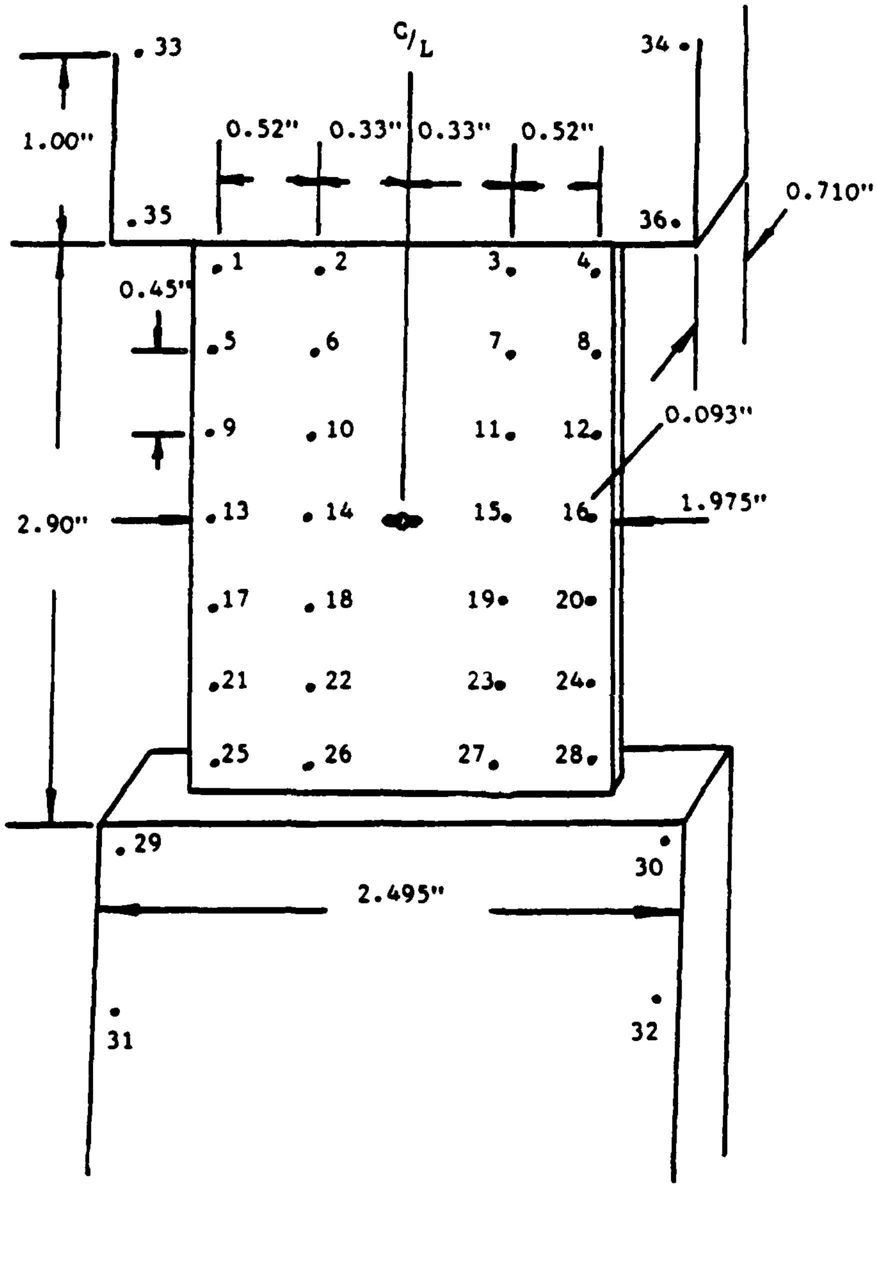

Figure 15 Accelerometer locations used in the modal analysis

TABLE 2 NATURAL FREQUENCIES AND DAMPING FACTORS FOR RESONANT MODES

CASE I: Mean load = 2000 lbs, total crack length (2a) = 0.20"

MODE	NAT. FREQ. (HZ)	DAMP. FACT. (%)	DAMP. COEFF. (RAD/SEC)
1	765.0115	.8677	41.7089
2	1439.8879	3.0185	273.2087
3	1709.9106	1.4115	151.6672
4	1861.4131	1.5402	180.1682
5	1955.4885	.4472	54.9416

CASE II: Mean load = 4500 lbs, total crack length = 0.20"

MODE	NAT. FREQ. (HZ)	DAMP. FACT. (%)	DAMP. COEFF. (RAD/SEC)
1	827.7138	3.6762	191.3148
2	1483.2148	1.0132	94.4276
3	1673.6045	.9470	99.5824
4	1806.6233	2.1325	242.1211
5	1953.5444	.3507	43.0522

CASE III: Mean load = 2000 lbs, total crack length = 0.95 "

MODE	NAT. FREQ. (HZ)	DAMP. FACT. (%)	DAMP. COEFF. (RAD/SEC)
1	646.3500	.3708	15.0568
2	795.7371	2.7693	138.5117
3	1381.7729	3.9457	342.8291
4	1690.2246	1.4620	155.2824
5	1883.5137	1.4233	168.4624

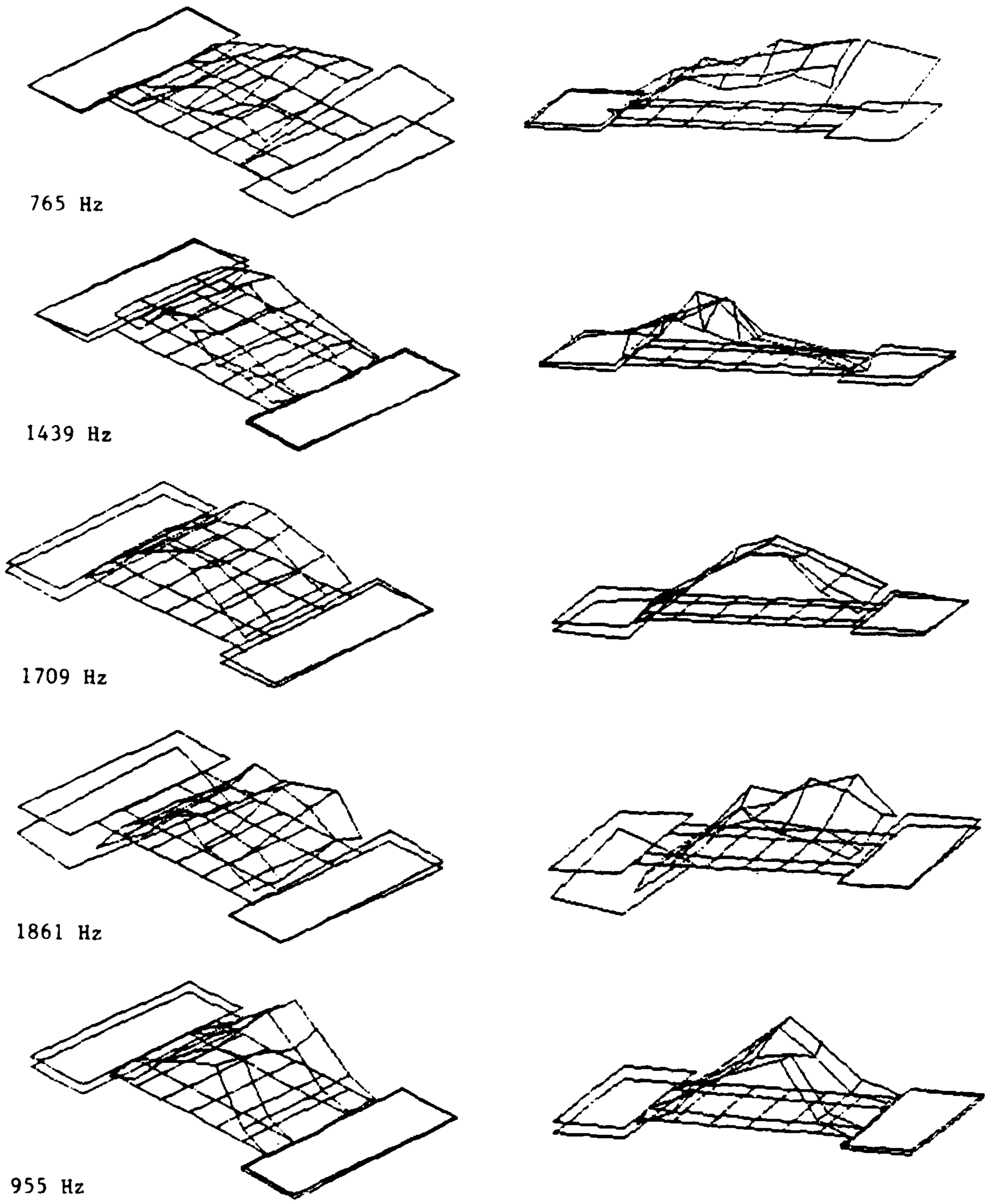

Figure 16 Mode Shapes for Case I: Mean Load 2000 Lbs,
Crack Total Length (2a) of 0.20"

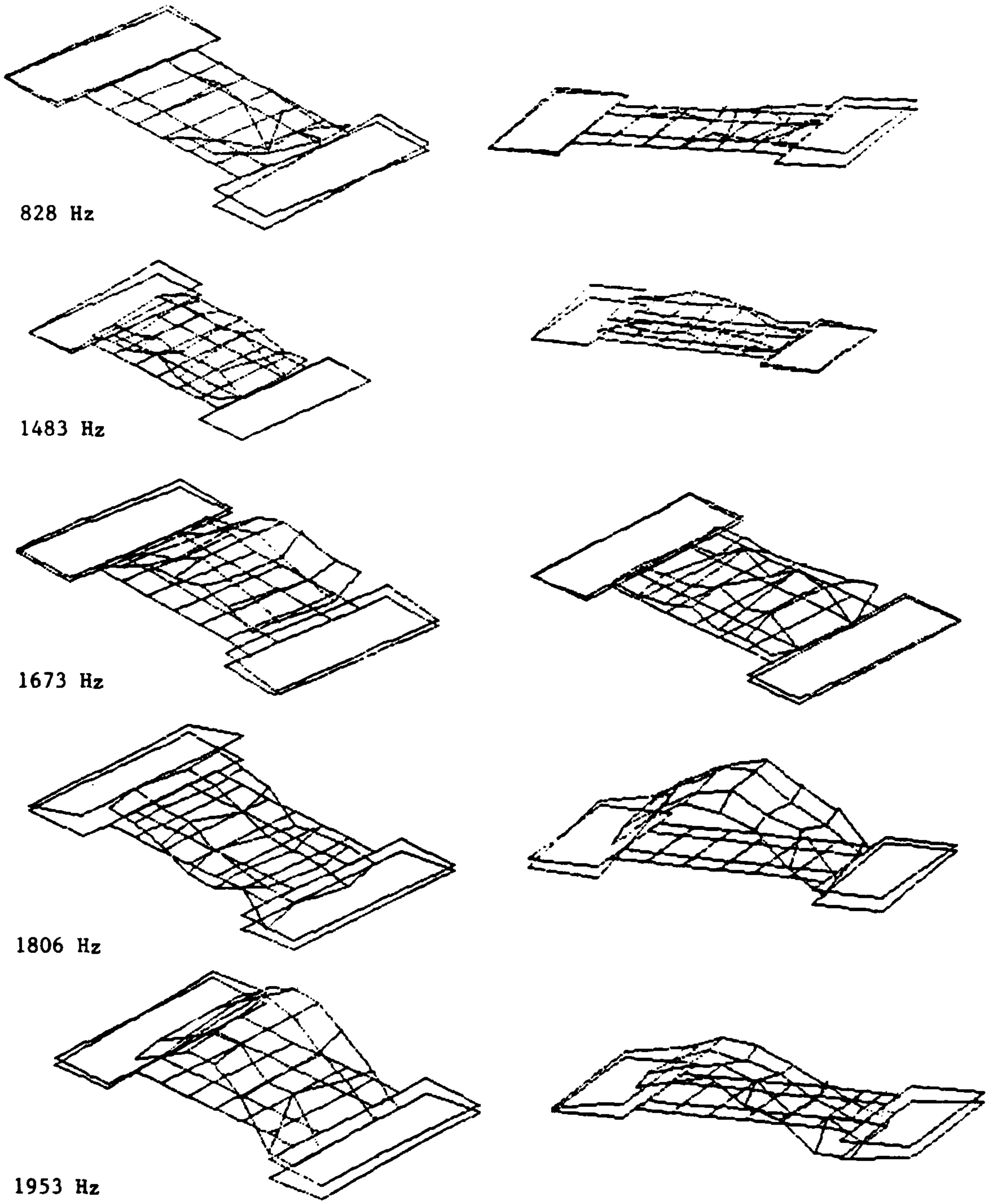

Figure 17 Mode Shapes for Case II: Mean Load 4500 Lbs, Crack Total Length (2a) of 0.20"

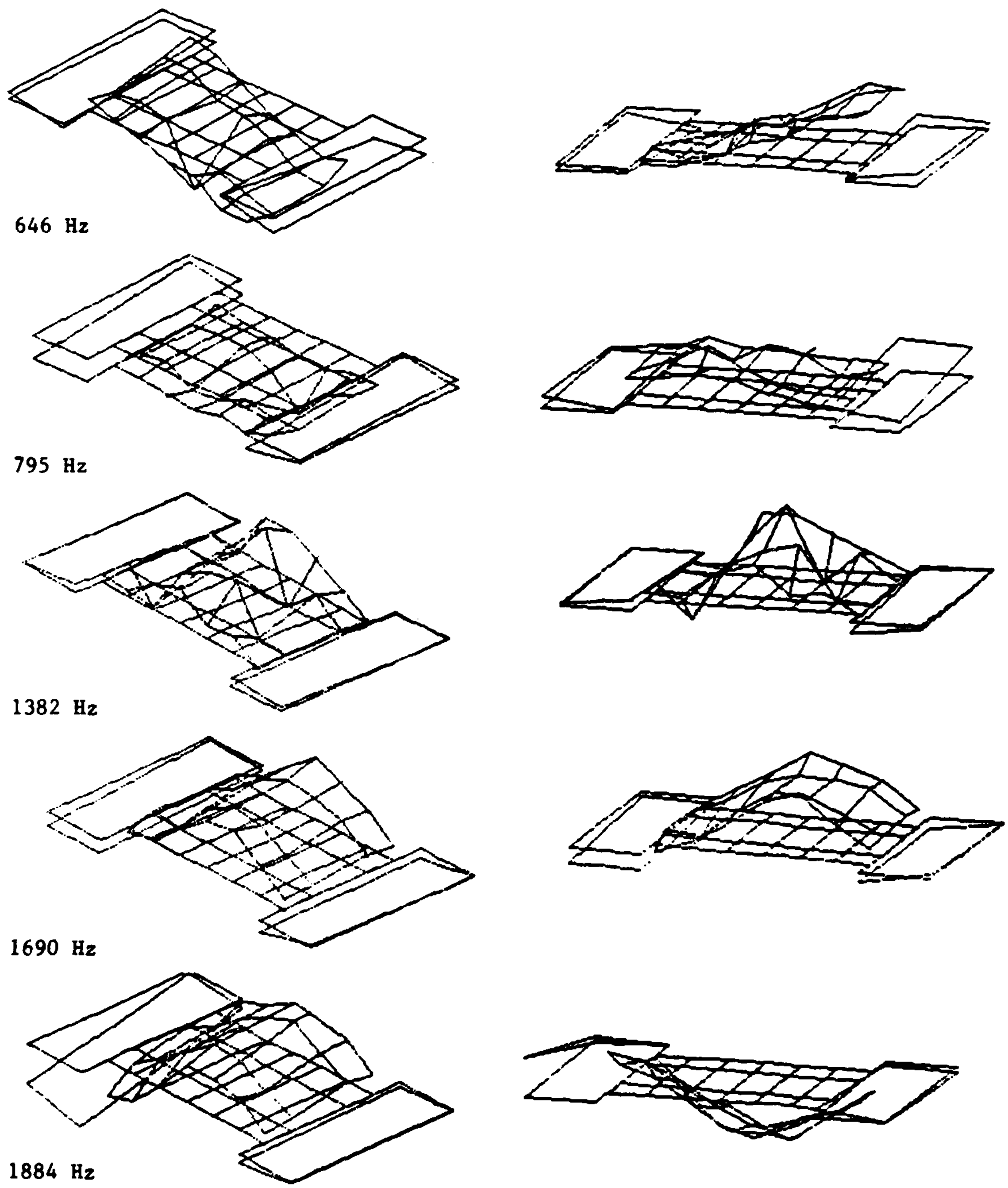

Figure 18 Mode Shapes for Case III: Mean Load 2000 Lbs, Crack Total Length of 0.95"

- The load level and crack length changes expected during a test can shift resonant frequencies substantially, in some cases as much as 200 Hz.
- While these resonances involve the entire load train and possibly the frame as well, the most severe lateral deflection is in the specimen.
- There was a cluster of resonances from 1400 to 2000 Hz with an average of 200 Hz spacing between them.
- There was a rather clear field between 750 Hz to 1200 Hz where no resonances developed for any of the cases.

The behavior shown in the modal analysis corresponds well to that shown by strain gage response of this preliminary specimen. Strain measurements confirmed that there is a regime between approximately 800 to 1200 Hz in which there are no complications from dynamic bending stresses. In the regime between 1200 to 2000 Hz, strain measurements likewise confirmed the series of resonances that result in significant bending strains that cannot be tolerated in a test. In several of the mode shapes the greatest deflection is in the thin part of the specimen. It was felt that if these deflections can be reduced significantly by lateral support and damping, the specimen may provide a satisfactory stress distribution at the crack region.

C.2 Strain Gage Evaluation of a Specimen with Lateral Reinforcement and Damping

The strain gage evaluation of the preliminary specimen showed that bending strains were excessive over most of the frequency between 500 and 2000 Hz with the possible exception of the range 1000 to 2000 Hz. The ranges of frequency over which the strains on either side of the specimen are in phase and of equal magnitude was extremely limited and certainly less than the 200 Hz that is required due to shifting resonances during a test.

Recognizing that the preliminary specimen with the clamping arrangement extended as much as possible was still unsuitable for testing above 1200 Hz, several experiments were performed to determine the effectiveness of various approaches to spreading out or damping resonant vibrations. The modal analyses showed that the most extreme deflection is in the unclamped portion of the specimen. It appears that since this region is the most compliant it acts somewhat as a hinge between the load train elements above and below it. Three additional modifications were, therefore, made to the specimen and system:

- the construction of lateral buttressing that would reinforce the specimen in the unclamped region with respect to out of plane motion yet have minimal effect on tensile stress distribution
- removal of elements in the load train which may add to unwanted deflections
- increasing the size of the clamping fixture to improve stiffness in the lateral direction

Figure 19 shows the lateral reinforcements applied to the specimen. A schematic diagram of the central region of the specimen indicating the elements of the lateral support are shown in Figure 20. Parallel elements were loaded against the unclamped surfaces of the specimen near the crack. By applying this load through several layers of glass cloth, the support still had substantial compliance in shear and would not significantly affect the distribution of tensile stresses in the specimen. The glass cloth was also expected to provide damping of lateral vibration. Specific dimensions of the lateral support and clamping fixtures are shown in Figure 21.

A series of experiments were conducted on this specimen to establish its suitability and also to establish a set of procedures for verifying an appropriate stress distribution on each specimen prior to each experiment. The set of experiments involved strain gage measurements in the locations shown in Figure 22.

The first group of experiments involved the amplitude measurement of two strain gages on opposite surfaces when a 2500 lb. preload and a high cycle amplitude were applied. Figure 23, for example, shows the output of strain gage 1 and 2 as a function of frequency. Over most of the frequency range the correlation is acceptable indicating a satisfactorily low level of bending stresses at the crack line over most of this frequency range. There are, however, several frequency ranges in which large discrepancies occur. The stress amplitudes as shown by strain gages 1 and 7 on the same side of the specimen (Figure 24) likewise show a good correlation for this uncracked specimen over most of the

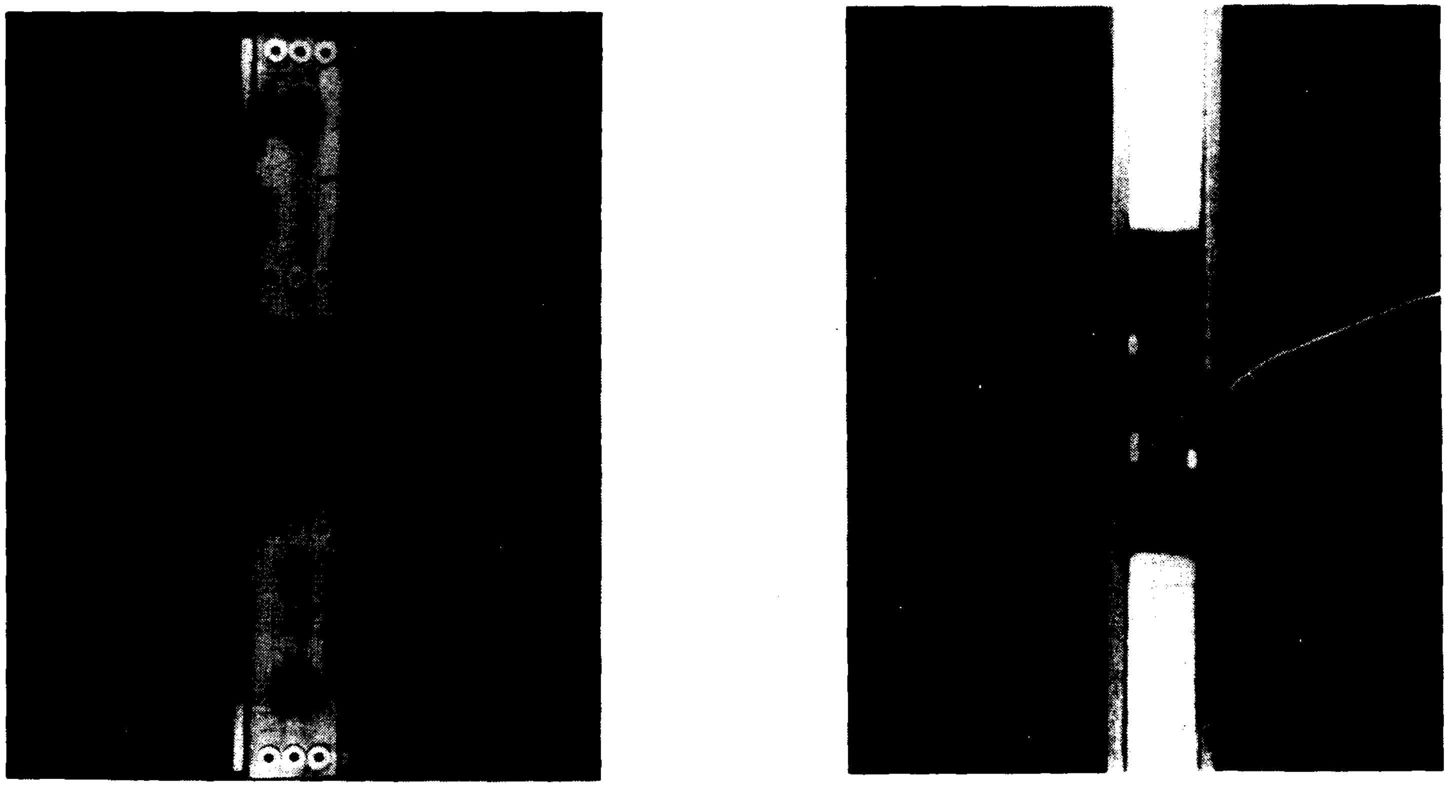

Figure 19 Specimen with End Reinforcement and with Lateral Constraints Applied to the Crack Region

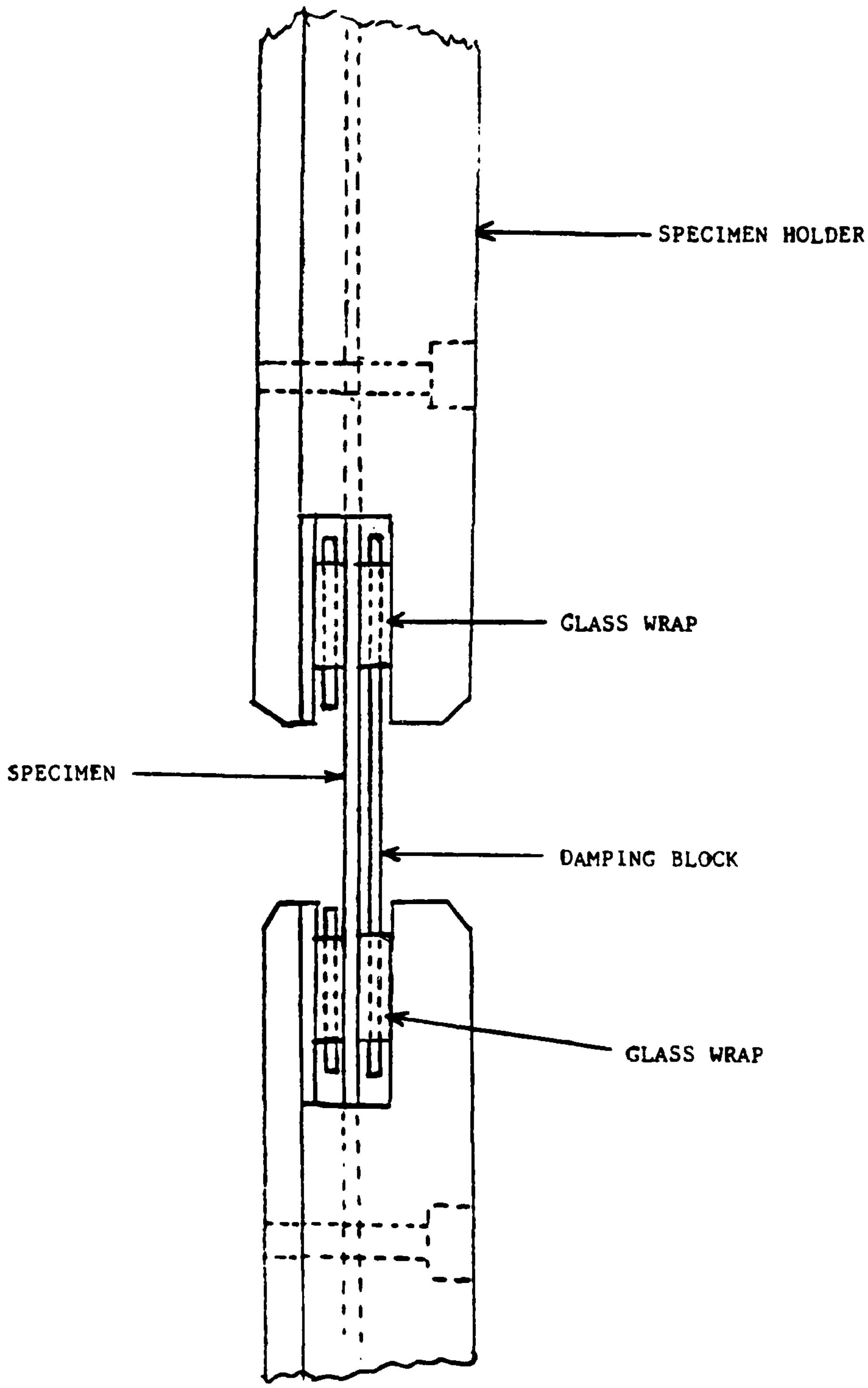

Figure 20 Diagram Showing Location of Damping Blocks and Glass Insulating Material

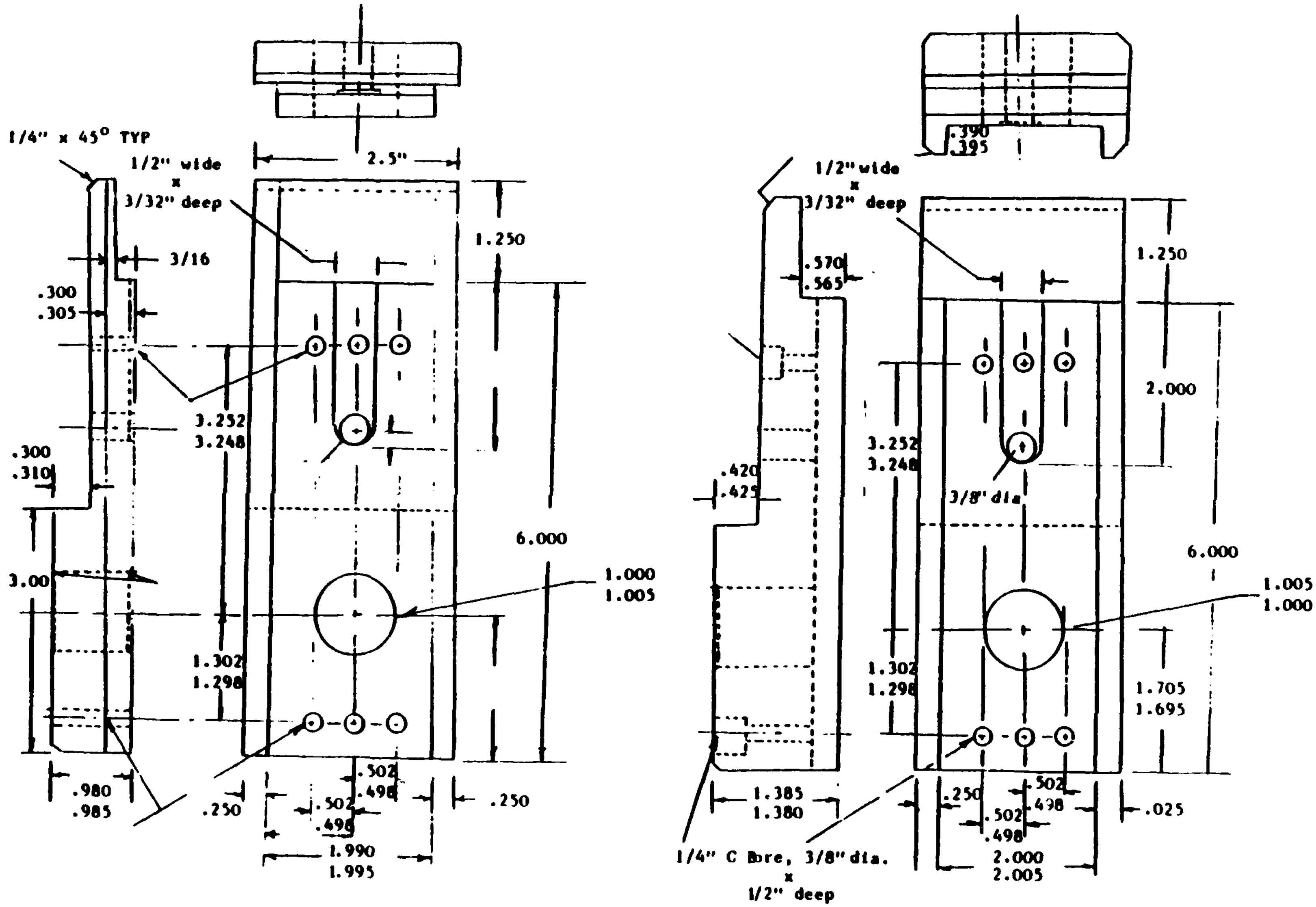

Figure 21 Dimensions of Specimen End Clamps

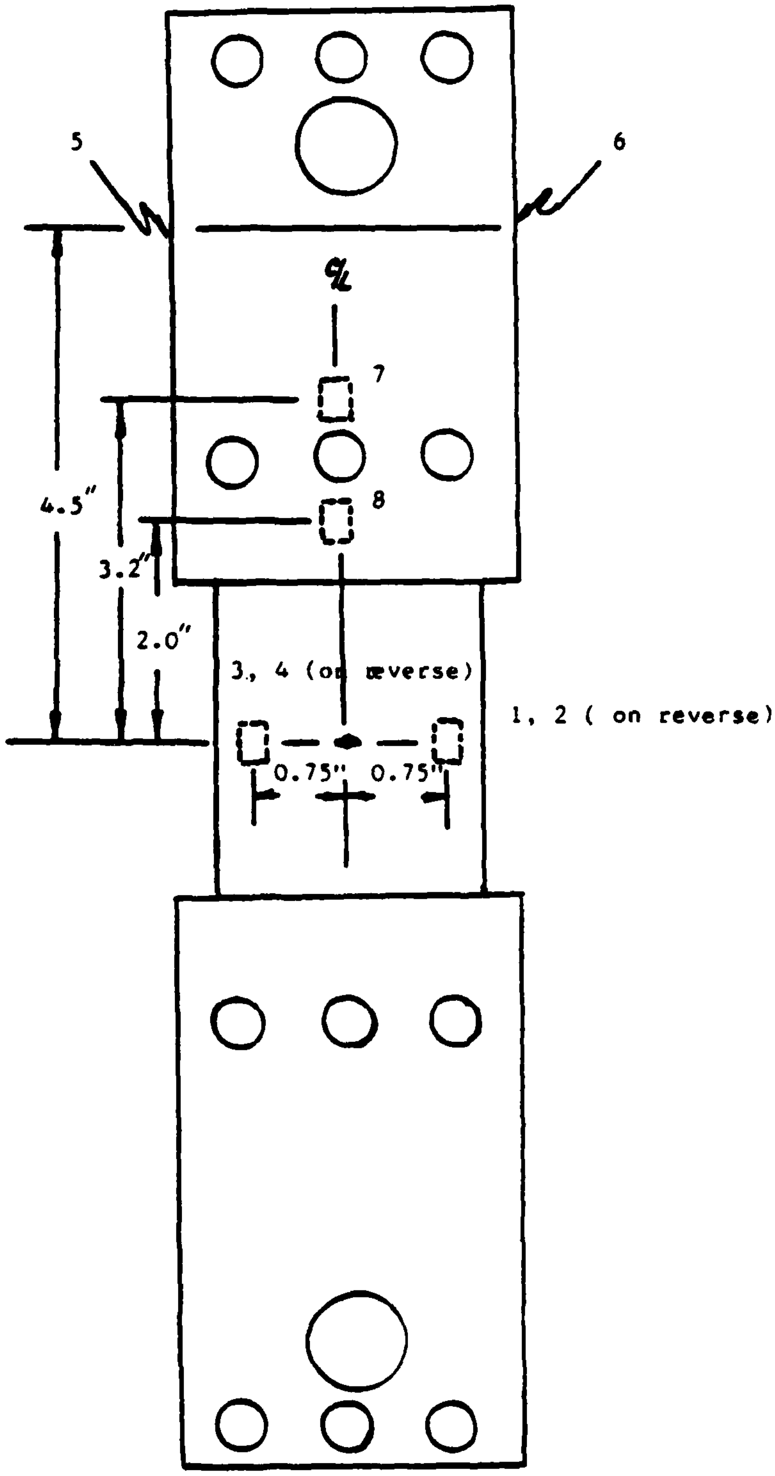

Figure 22 Diagram Showing Location of Strain Gages

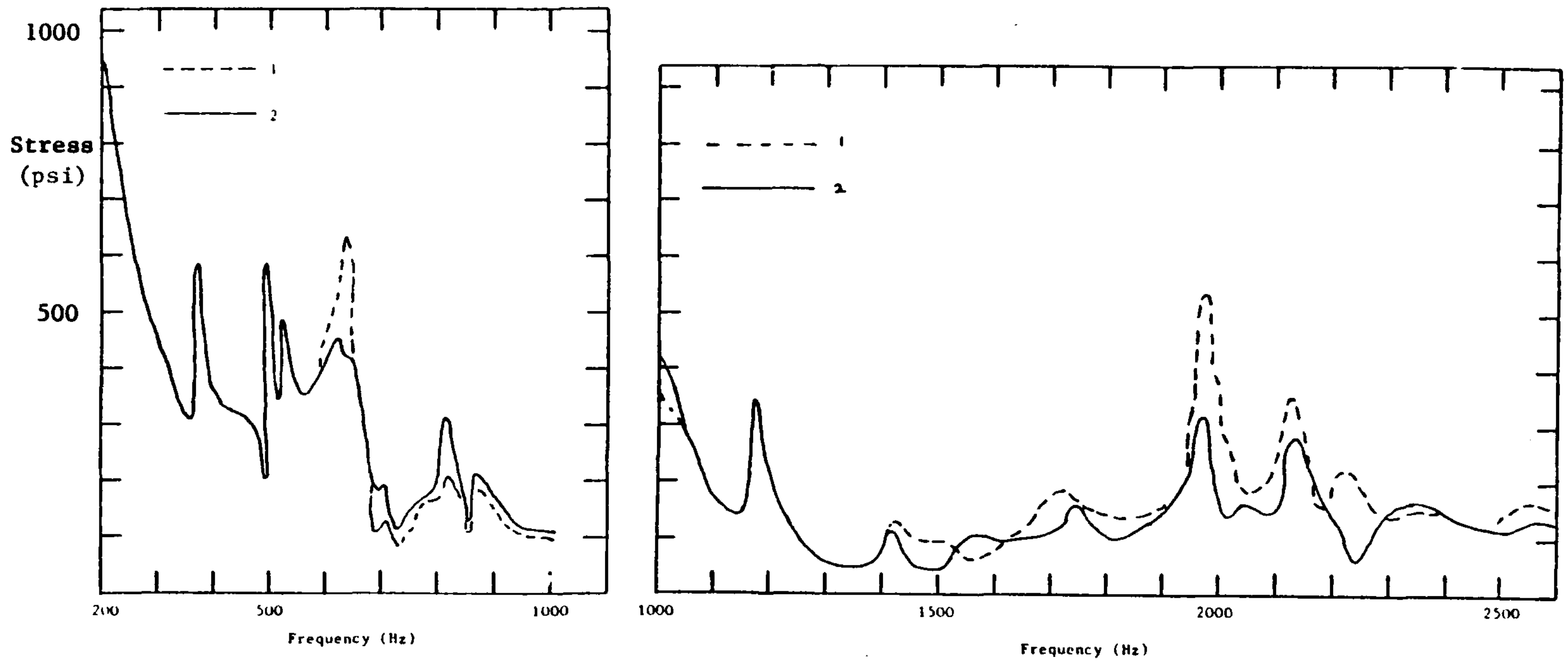

Figure 23 Magnitude of Stress Versus Frequency in Locations
1 and 2 for Laterally Damped and Reinforced Specimens

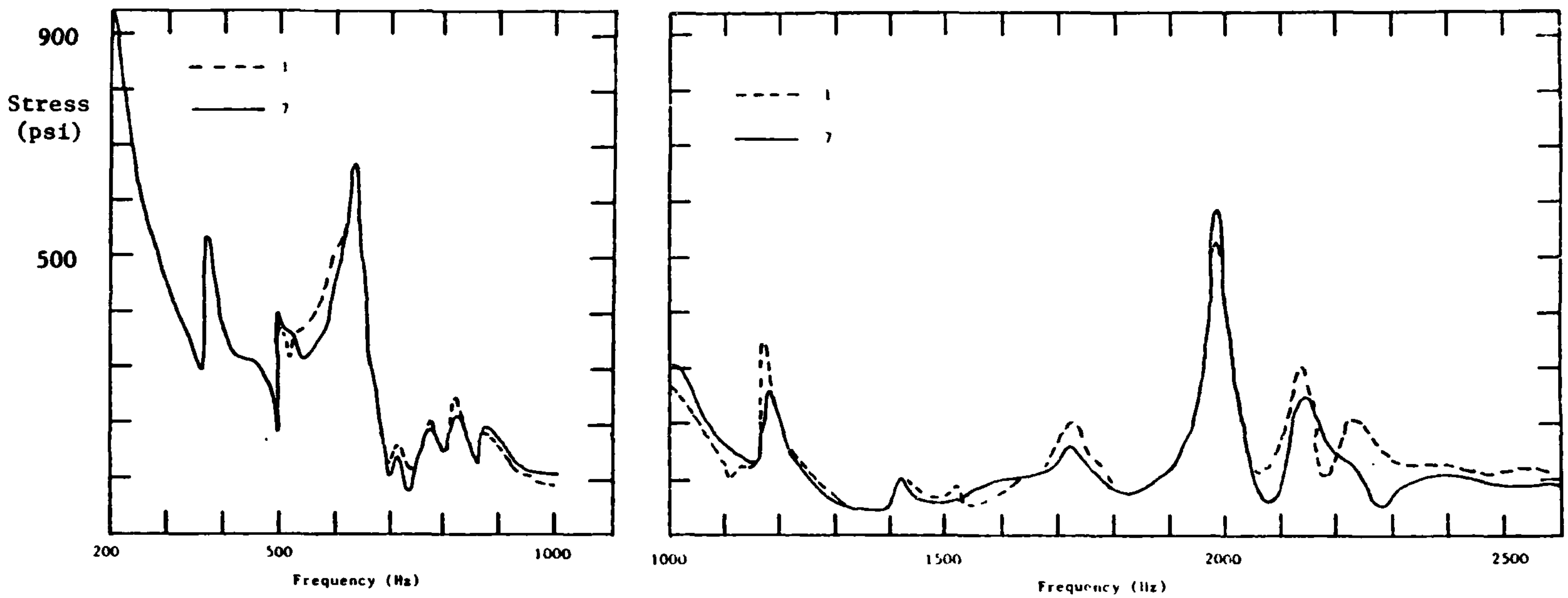

Figure 24 Magnitude of Stress Versus Frequency in Locations 1 and 7 for Laterally Damped and Reinforced Specimens

frequency range investigated but with significant discrepancies in certain narrow ranges of frequency.

The effect of reducing the length of the load train by removing the load cell and compression rings was evaluated. As shown in Figure 25, the effect of eliminating these objects was to modify the ranges over which differences in amplitude between strain gages 1 and 2 occurred. While the correlation between these outputs is improved in the frequency range between 1900 and 2200 Hz, in other ranges the correlation showed little change and in some cases deterioration. It was found in subsequent tests that removing the compression rings alone can improve the correlation of strain gage measurements in the frequency range between 1900 and 2200 Hz.

This series of experiments, involving the measurement of stresses at various locations on the specimen, demonstrated that there are frequency ranges above 1000 Hz in which dynamic stresses do not disturb the stress pattern associated with tensile loading. Satisfied that the specimen with lateral damping could provide satisfactory test results in some frequency band near 2000 Hz experimentation was carried further to identify frequency bands in which testing could be carried out and also establish procedures that could be used to verify the appropriateness of the stress distribution prior to each test. The verification on each specimen is necessary because there is a possibility that the effectiveness of the lateral support may depend on the procedures of assembly.

The verification procedures adopted involved the measurement and comparison of both phase and amplitude on opposite surfaces of the specimen. An initial experiment was carried out over a range of frequencies near 2000 Hz to determine how the relative magnitude and phase vary with changing load and crack length. The strain measurements were along the crack line at locations 1 and 2 of Figure 22. Measurement of the output of strain gages 1 and 2 were made and displayed on an oscilloscope as 1 versus 2. In the absence of bending stresses the resultant would be a line at 45° from the x or y axis, i.e. the stresses would be in phase and of equal magnitude. Resonant vibrations are apparent as a deviation from this pattern. An appropriate stress distribution would have a maximum peak to peak deviation of 5% from the ideal 45° trace. This condition would also be required over a 200 Hz interval around the chosen test frequency in order to ensure that resonances are not "swept in" by increasing the specimen temper-

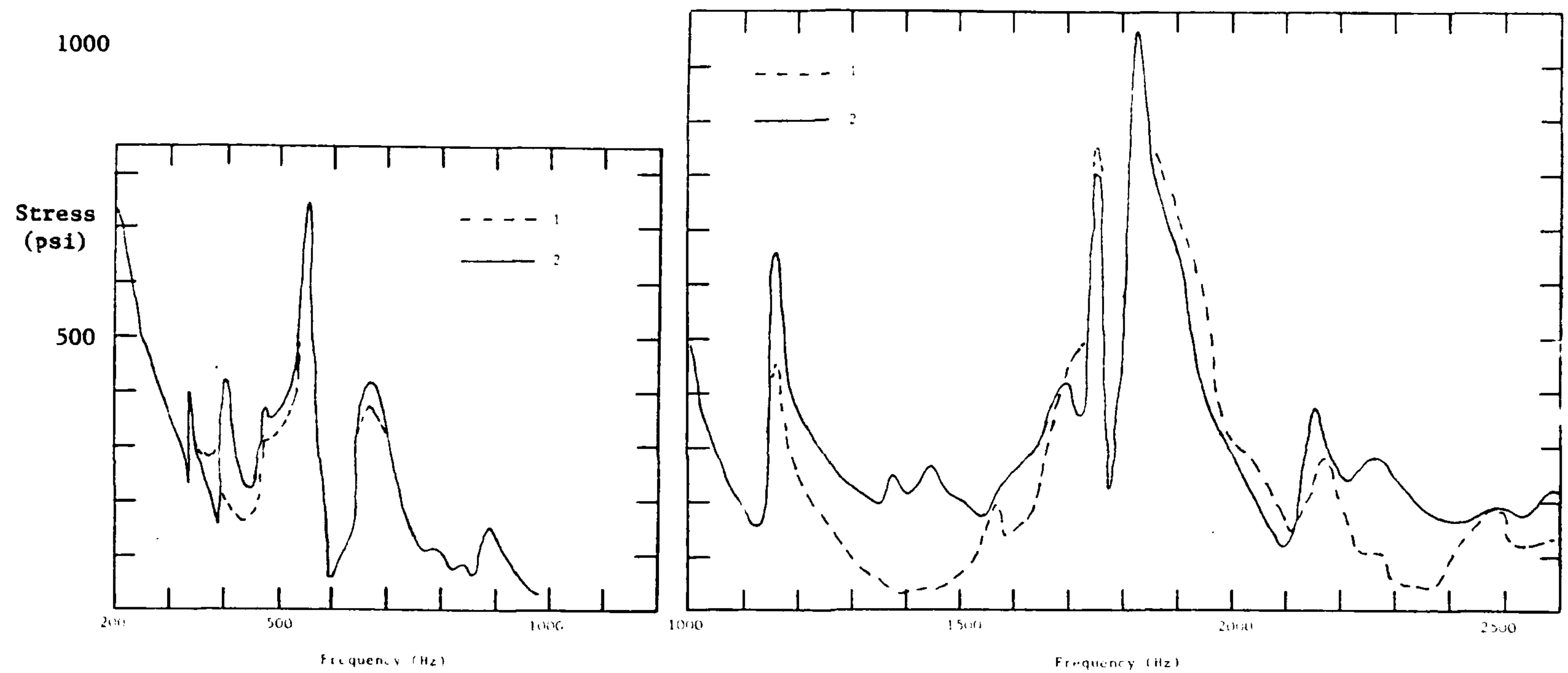

Figure 25 Magnitude of Stress Versus Frequency in Locations 1 and 2 for Laterally Damped Specimens with Compression Rings and Load Cell Removed from System.

[illegible]. It was also required over the load range and crack length experienced in a typical experiment. Figures 26 through 28 show the results of measurements over a range of frequency, crack length and mean load. These measurements were made on several specimens to ensure that bending stresses were consistently below the acceptable level from specimen to specimen.

Prior to each crack growth, test strain gage measurements were made in this manner over a 200 Hz frequency interval to ensure that the specimen was properly assembled. This procedure was adopted to ensure that errors in assembly that might reduce the effectiveness of the lateral support had not occurred.

The load sensing for the high frequency load range was performed with the remote load cell. For frequencies near 2000 Hz it was required to apply a correction factor to the measured load in order to properly represent the stresses in the vicinity of the specimen crack. Load cell output for a given crack length and applied load was measured as a function of strain gage output at 20 and 200 Hz. The proportionality at these two frequencies was consistently the same. The proportionality between load cell output and strain gage output was then measured at 1825 and 2000 Hz. The correction factor that must be applied to load cell measurement in order to provide the same proportionality as at the lower frequencies was established for the range of load and crack length measurement experienced in a typical experiment. The correction factor variation was 12% over a typical range of test conditions.

Sensing load directly on the specimen at locations 7 or 8 shown in Figure 22 was considered. However, in view of the fact that elevated temperature strain gages would be required and that strain gages on the specimen are frequently destroyed near 2000 Hz, it was decided to perform tests with remote load sensing. With remote sensing a much higher testing productivity was achieved with perhaps a small sacrifice of absolute high frequency load measurement accuracy.

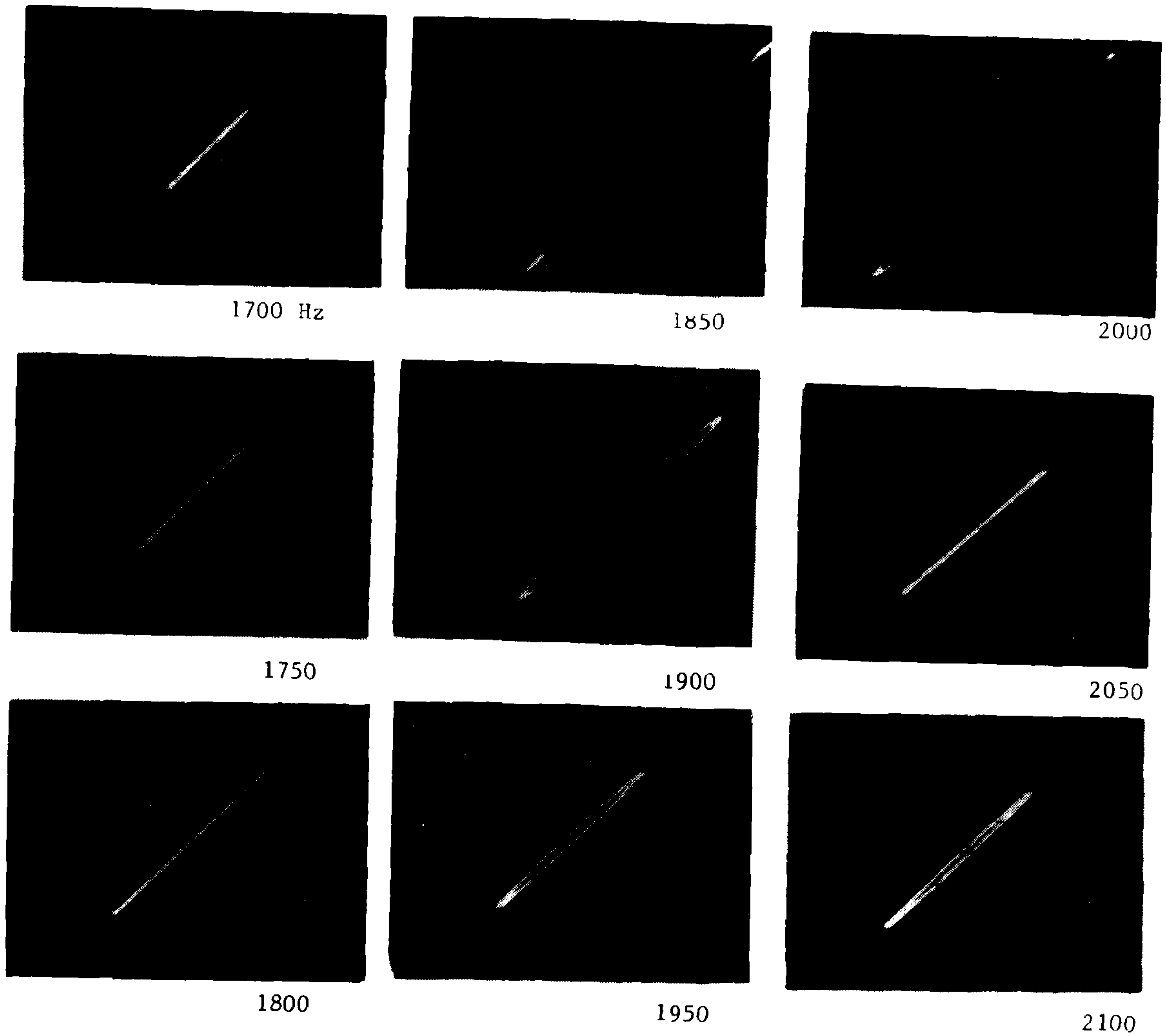

FIGURE 26 Series of Osciloscope Representations of Strain Gage Output #1, versus #2 Showing the Degree of Bending and Out of Phase Vibration on the Specimen Crack Centerline for a Mean Load of 4000 lbs. and a Crack Length of .200".

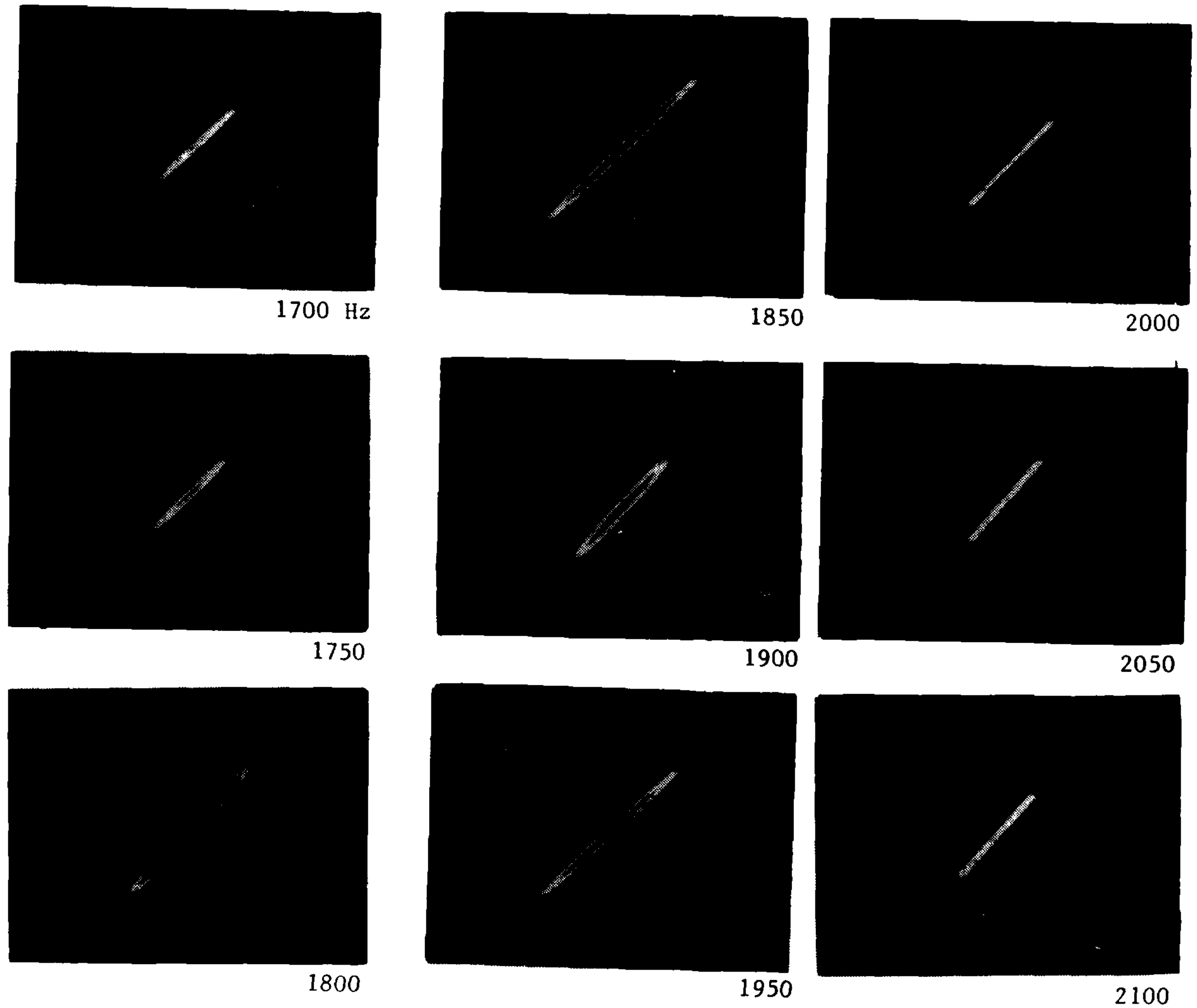

FIGURE 27 Series of Oscilloscope Representations of Strain Gage Output #1 Versus #2 Showing the Degree of Bending and Out of Phase Vibration on the Specimen Crack Centerline for a Mean Load of 2000 lbs. and a Crack Length of 0.200".

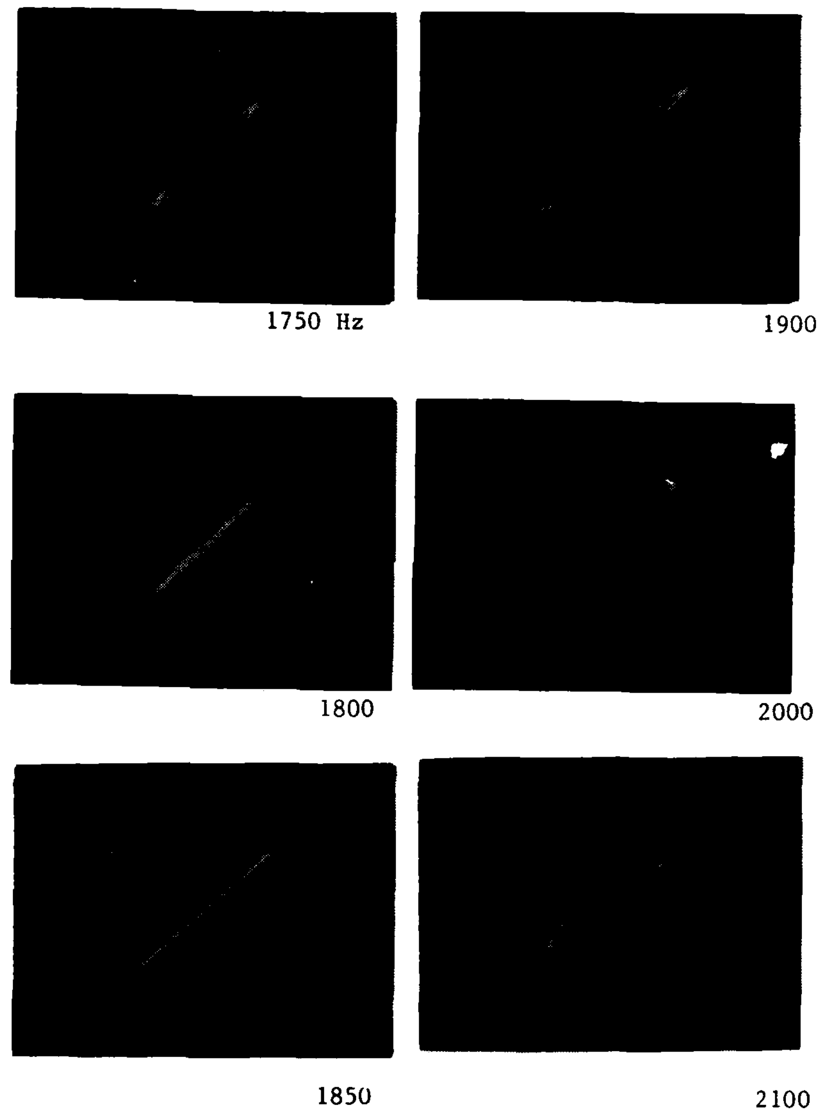

FIGURE 28 Series of Oscilloscope Representations of Strain Gage Output #1 versus #2 Showing the Degree of Bending and Out of Phase Vibration on the Specimen Crack Centerline for a Mean Load of 2000 lbs. and a Crack Length of 0.700".

III. EXPERIMENTAL TEST PROGRAM

The test program objective was the establishment of the relationship between crack growth rate in an aircraft engine disk material and those parameters associated with the high- and low-frequency loading experienced in the engine first- and second-stage disks. The information provided by this testing program was to be applicable to life prediction of flawed engine components and provide guidance to the implementation of the retirement-for-cause engine maintenance and design concept. Consequently, the test parameters selected for this program were based on the loading conditions experienced by aircraft engine disks.

Considering the nature of the loading and the requirements of aircraft engine design, the following were included in the experimental program:

- Determination of the nature of the transition from low cycle to high cycle dominated behavior over ranges of both low cycle and high cycle stress intensity factor range (ΔK).
- Establishment of the high-cycle transition ΔK over as wide a frequency range as possible.
- Major cycle (low cycle) hold times in the regimes in which both fatigue and creep crack growth dominate. Cycle times from a few seconds to several hundred seconds were included.
- A temperature typical of those experienced by the aircraft engine disk. For the Inconel 718 specimens used in this study, 1200°F was chosen.
- A sufficient level of replication to eliminate the influence of material variability on the test results and indicate the level of consistency of the experimental system.
- The influence (if any) of the high-cycle loading on crack growth below the high-cycle transition.

The test program summarized in Table 3 was designed to address these aspects of high- and low-frequency interaction in crack growth. The low cycle waveform used throughout the testing program was a trapezoidal loading profile with ramp times of 0.5 seconds and hold times ranging from a second to essentially infinity (steady mean load). The high-frequency loading was applied during the hold period only.

TABLE 3
TEST PROGRAM OUTLINE
(ALL TESTING AT 1200°F)

Objective	Conditions of Test
Evaluate high-cycle threshold ΔK and crack growth rate versus high frequency ΔK in the creep crack growth regime.	Selected low-frequency ΔK values with long hold times (60 seconds or greater) maintained throughout the test and with varying high-frequencyΔK values.
Evaluate high-cycle threshold ΔK and crack growth rate versus high-frequency ΔK in the fatigue crack growth regime.	Selected low-frequency ΔK values with the shortest practical hold times (probably on the order of 1 to 10 seconds) maintained throughout the test and with varying high-frequency ΔK values.
Evaluate the effect of high-frequency loading on low-cycle crack growth in the regime of transition between creep and fatigue-dominated crack propagation.	Selected low-frequency hold times with specific low-frequency ΔK levels maintained throughout the test and with varying high-frequency ΔK levels.
Evaluate the effect of high-frequency loading at several low-frequency cycle R ratios in the creep and fatigue crack growth regimes.	Varying high-frequency ΔK values emphasizing the high-cycle transition regime with specific low cycle hold times maintained throughout the test.
Evaluate the effect of temperature on the high-cycle transition.	Varying high-frequency ΔK values emphasizing the transition high-cycle regime with specific low-frequency ΔK and hold times and selected temperatures.

A. Fatigue Crack Growth Studies Conducted at 200 Hz

Combined cycle tests with a high cycle frequency of 200 Hz were conducted for low cycle parameters in a test matrix. All testing in this matrix was carried out with a low cycle R ratio of 0.1 and a test temperature of 1200°F. This matrix included low cycle maximum K values ranging from 15 to 40 ksi $\sqrt{in}$ (corresponds to a ΔK of 15 to 40 MPa $\sqrt{m}$ since the R ratio was 0.1) and low cycle hold times ranging from 2 to 180 seconds. Table 4 shows the conditions of tests completed and the number identifying the test. All conditions in the test matrix were applied in at least one test. In several cases replicated tests were conducted. Data plots for all of these tests may be found in Appendix A, with corresponding listings in Appendix B.

The low cycle ΔK ranges included in the testing were 15, 20, 30 and 40 MPa $\sqrt{m}$. The low cycle hold times that included 2, 5, 10 and 180 seconds were expected to cover the regimes in low frequency loading in which the low cycle crack growth is time dominated (creep crack growth) and the regime in which the number of low frequency cycle influences crack growth rate (combination of creep and fatigue crack growth). The lower end of the low cycle hold period range (i.e., 2 and 5 seconds) was expected to show the effect of accumulated low frequency cycles on the low cycle crack growth rate. The series of data plots representing crack growth rates versus high cycle ΔK for constant low cycle ΔK and low cycle hold time obtained in this study show several interesting trends.

In the curves of crack growth versus high frequency ΔK distinct regimes can be seen. As shown in Figure 29, three types of behavior were observed over the range of low frequency ΔK and hold times investigated. In type 1, the crack growth rate versus high cycle ΔK remained relatively constant in the low cycle dominated regime prior to the rapid increase in crack growth rate in the high cycle dominated regime. Type 2 behavior was characterized by retardation of crack growth rate by the high frequency cycle in the low cycle dominated regime. Type 3 behavior was typical of the lowest low cycle ΔK studied, in which the low cycle ΔK was below the crack growth threshold and no crack growth could be measured in the low cycle dominated regime. In all these cases distinct low cycle and high cycle dominated regimes could be observed. However, the transition between these two regimes was not always distinct due to the retardation effect.

TABLE 4: COMBINED CYCLE TEST INCLUDING A 200 HZ HIGH CYCLE FREQUENCY

(All testing was conducted at 649°C (1200°F) and with a low cycle R ratio of 0.1)

LOW CYCLE HOLD TIME (sec)

Low Cycle Maximum K (MPa $\sqrt{m}$)	2	5	10	180
	TEST #'s			
15	24, 25	21, 23	20	42, 43
20	35, 37	30, 28	26, 27	39, 40
30	46	31, 32	47	41
40	36, 38	33, 34	48	44

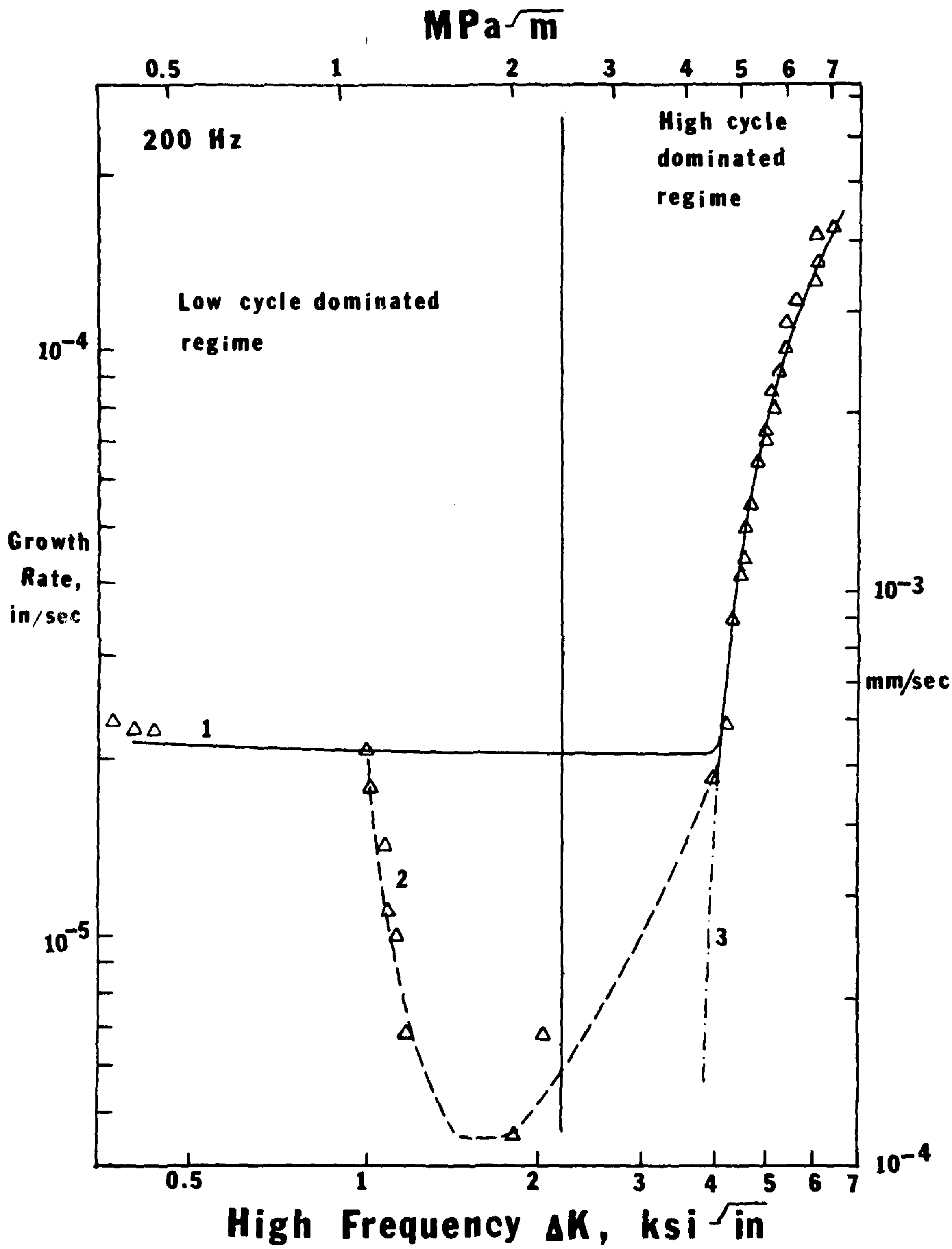

FIGURE 29 Characteristics of the High/Low Frequency Interaction Showing the Three Types of Behavior Observed in This Study. The Points Correspond to testing with a Low Frequency ΔK of 20 MPa $\sqrt{m}$, a Low Cycle Time of 10 Seconds and a High Cycle Frequency of 200 Hz.

Figure 30 shows a curve corresponding to a low cycle ΔK of 15 MPa $\sqrt{m}$ and a hold time of 5 seconds. The data in this representation corresponds to a test with increasing high frequency ΔK. Prior to data acquisition in the increasing high cycle ΔK mode, the crack was allowed to grow with a systematically decreasing ΔK until a crack growth rate on the order of 5×10^{-4}mm/sec (2×10^{-6} inches/sec) was achieved. This precaution was taken to eliminate the effects on crack growth of the prior precycling. The data presented in Figure 30 is characteristic of threshold fatigue crack growth data which generally exhibits increasing growth rate and decreasing slope with increasing ΔK when crack growth versus ΔK is plotted on log-log axes. The lower level of this curve corresponds to a growth rate of 1.3×10^{-8} inches per high frequency cycle (3.30×10^{-7} mm/cycle) which would definitely be in the threshold regime for Inconel 718.

Figure 31 shows the results of a test conducted with a low frequency ΔK of 20 MPa $\sqrt{m}$ and a hold time of 5 seconds. It was carried out with a sequence of loads intended to illustrate an important aspect of the retardation effect that is very pronounced at a low frequency ΔK of 20 MPa $\sqrt{m}$. The line drawn through the experimental points has arrows drawn to show the sequence of points as they occurred during the test. The initial loading up to point A seems to give rise to a measurable retardation, and changing the high frequency load range to that at point B rapidly accelerates the retardation. This results in a more severe retardation in the 0.762mm (0.030) inches of growth beyond point B than was accomplished in the 2.79mm (0.110 inches) of growth with the high cycle ΔK range around point A. (Each point represents 0.010 inches, 0.254mm, of crack growth). Beyond point B the crack growth rate decreases rapidly, reaches a minimum value and then starts to increase. At point C just beyond the minimum value of crack growth, a lower high frequency load range was applied (the new level of high cycle ΔK is represented by point D). The crack growth rate increases from point D to E showing a gradual elimination of the retardation effect. At point E the load range was again increased to point F and crack growth continued in the high cycle dominated regime.

As the low frequency ΔK increases, the retardation effect generally becomes less pronounced. The data for a low cycle ΔK of 30 MPa $\sqrt{m}$ and a low cycle hold time of 5 seconds appears in Figure 32. While the high frequency load results in a factor of four reduction in crack growth rate for a low cycle ΔK of 20 MPa $\sqrt{m}$, at a low cycle ΔK of 30 MPa $\sqrt{m}$ the reduction in crack growth rate is only a factor

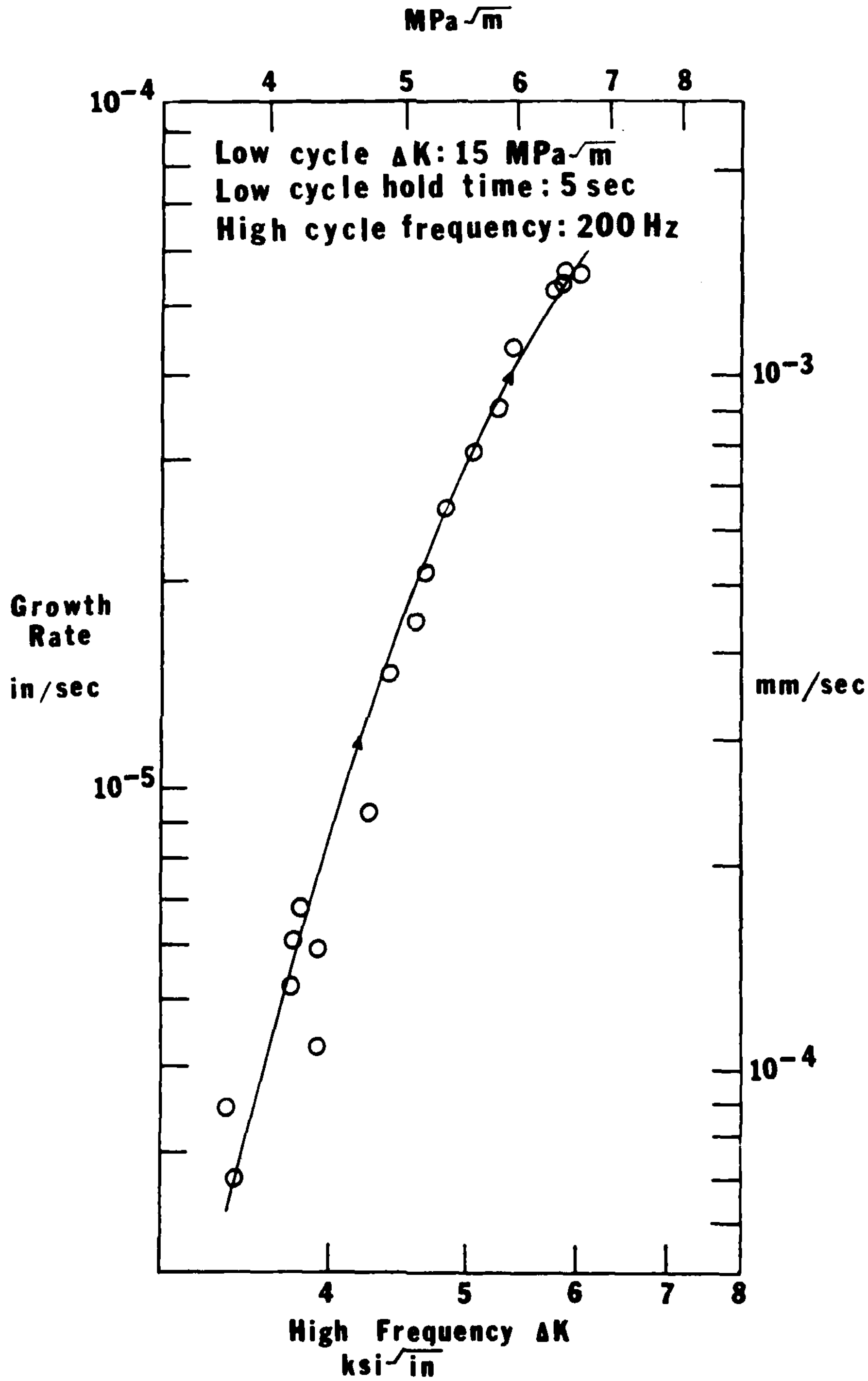

FIGURE 30 Results of Combined High/Low Frequency Test With a Low Cycle ΔK of 15 MPa $\sqrt{m}$ and a Low Cycle Hold Time of 5 seconds.

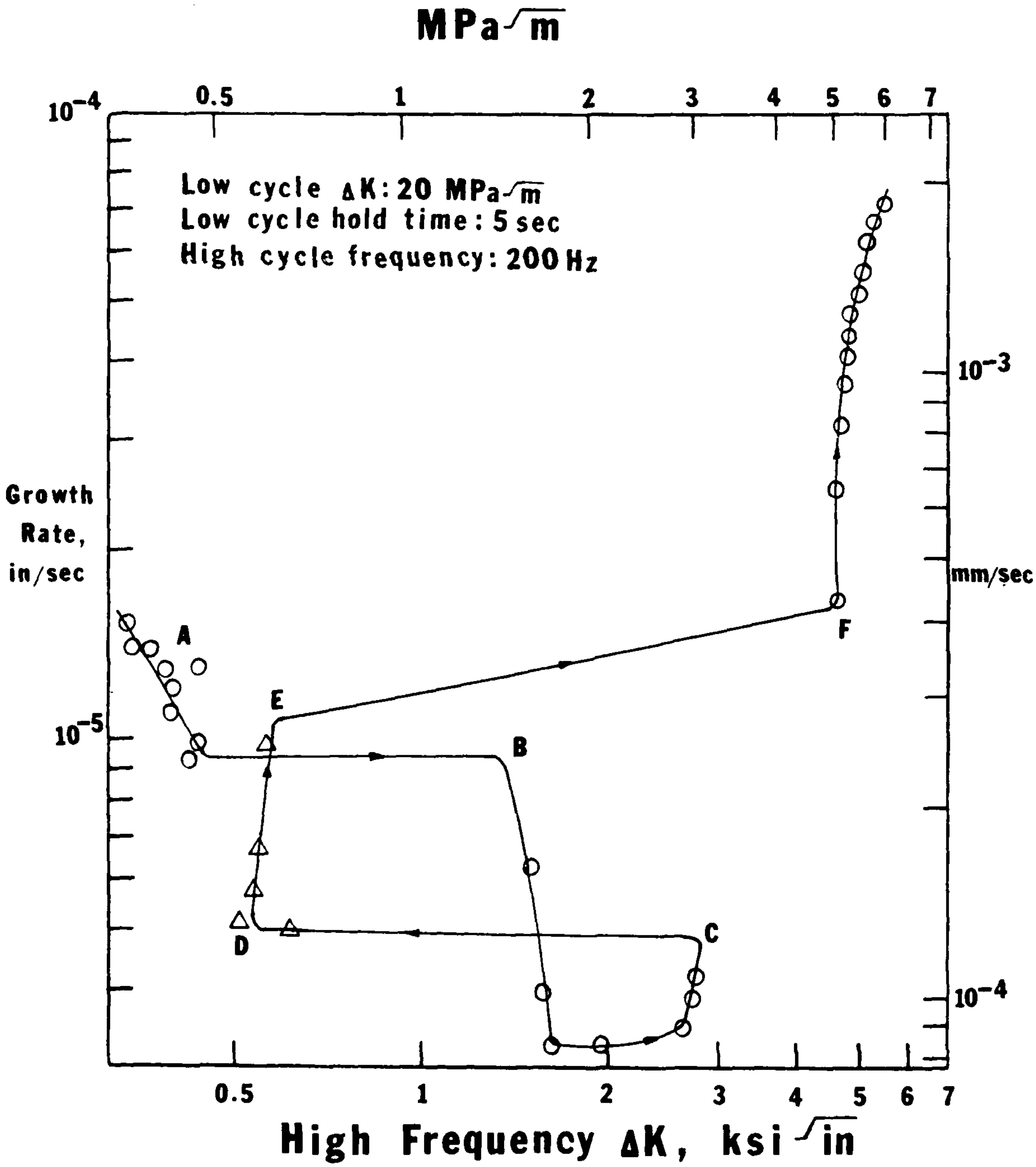

FIGURE 31 Results of Combined Cycle Test With a Low Frequency ΔK of 20 MPa $\sqrt{m}$ and a Hold Time of 5 Seconds. The Line is Shown to Show the Sequency of Points.

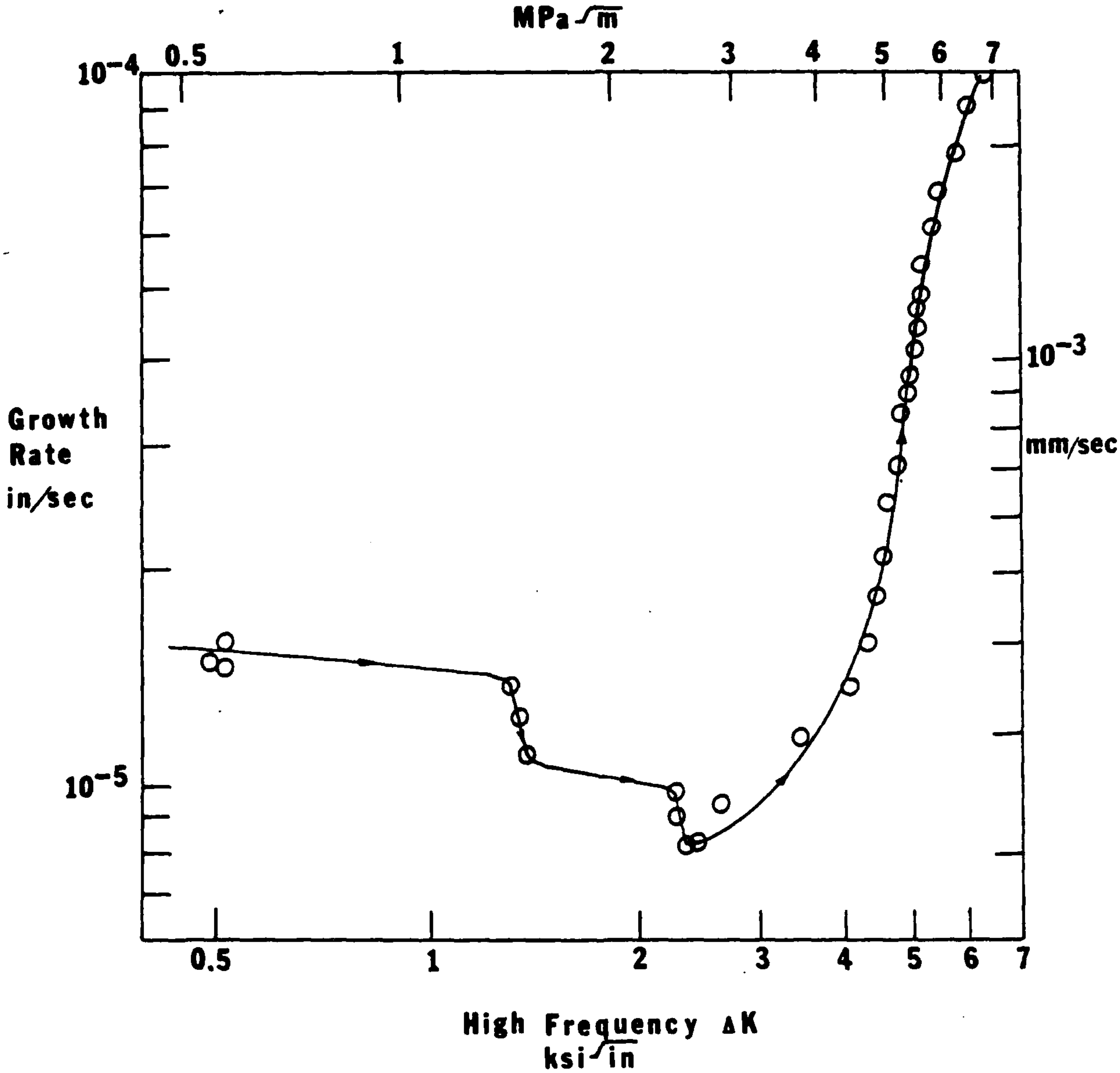

FIGURE 32 Results of a Combined Cycle Test With a Low Frequency ΔK of 30 MPa $\sqrt{m}$ and a Hold Time of 5 Seconds.

of 2. As shown in Figure 33, a low cycle ΔK of 40 MPa $\sqrt{m}$ shows no measurable retardation associated with high frequency loading.

Figure 34 shows the effect of varying cycle time on the crack growth behavior with a low cycle ΔK of 15 MPa $\sqrt{m}$. No distinct trend is apparent and there is little deviation between these curves. Figure 35 shows the effect of cycle time ranging from 2 seconds to 180 seconds on the crack growth behavior with a low cycle ΔK of 20 MPa $\sqrt{m}$. The only significant feature in this group of tests is that with a 180 seconds hold time there appears to be a more severe retardation.

A comparison of crack growth rate versus high cycle ΔK for a hold time of 5 seconds and several values of low cycle ΔK appears in Figure 36. As expected the crack growth rate in the low cycle dominated regime increases as ΔK increases. A similar comparison is made in Figure 37 but with a low cycle hold time of 180 seconds and roughly the same behavior can be observed.

B. Results of Combined Cycle Tests with an 1800 to 2000 Hz High Cycle Component and Comparison with Lower Frequency Results

The parameters covered by the 1800 to 2000 Hz combined cycle testing are indicated in Table 5. Tests 60 through 66 were performed on specimens from a second heat of material. The crack growth rate in the low cycle dominated regime was quite different from the previous batch of material. The newer material has crack growth rates lower by a factor of 6 to 8 at some low cycle ΔK levels. Since, it is desirable to evaluate the effect of frequency without the complication of lot to lot material variation, fatigue crack growth testing near 2000 Hz was also performed on material from the older lot of material. Tests 67 through 75 represent tests from the same lot used for the 200 Hz tests. The complete set of data plots and listings for the 1800 to 2000 Hz combined cycle tests may be found in Appendices B and C respectively.

The dynamic tests performed on the laterally supported and damped specimen indicated that there is greater consistency in dynamic behavior at 1825 Hz than at 2000 Hz. There is also a greater high frequency load capability at 1825 Hz.

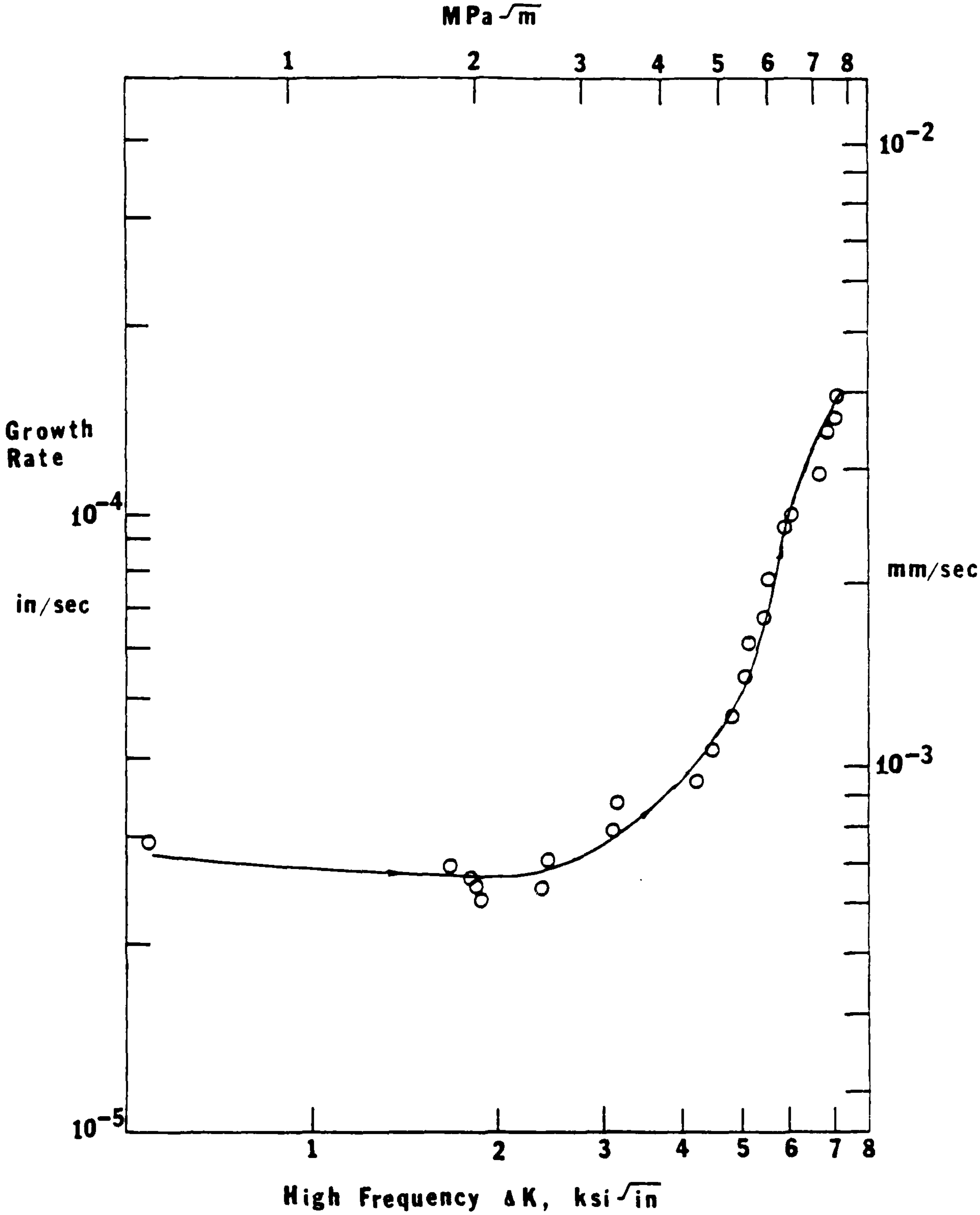

FIGURE 33 Results of a Combined Cycle Test with a Low Cycle ΔK of 40 MPa $\sqrt{m}$ and a Hold Time of 5 Seconds.

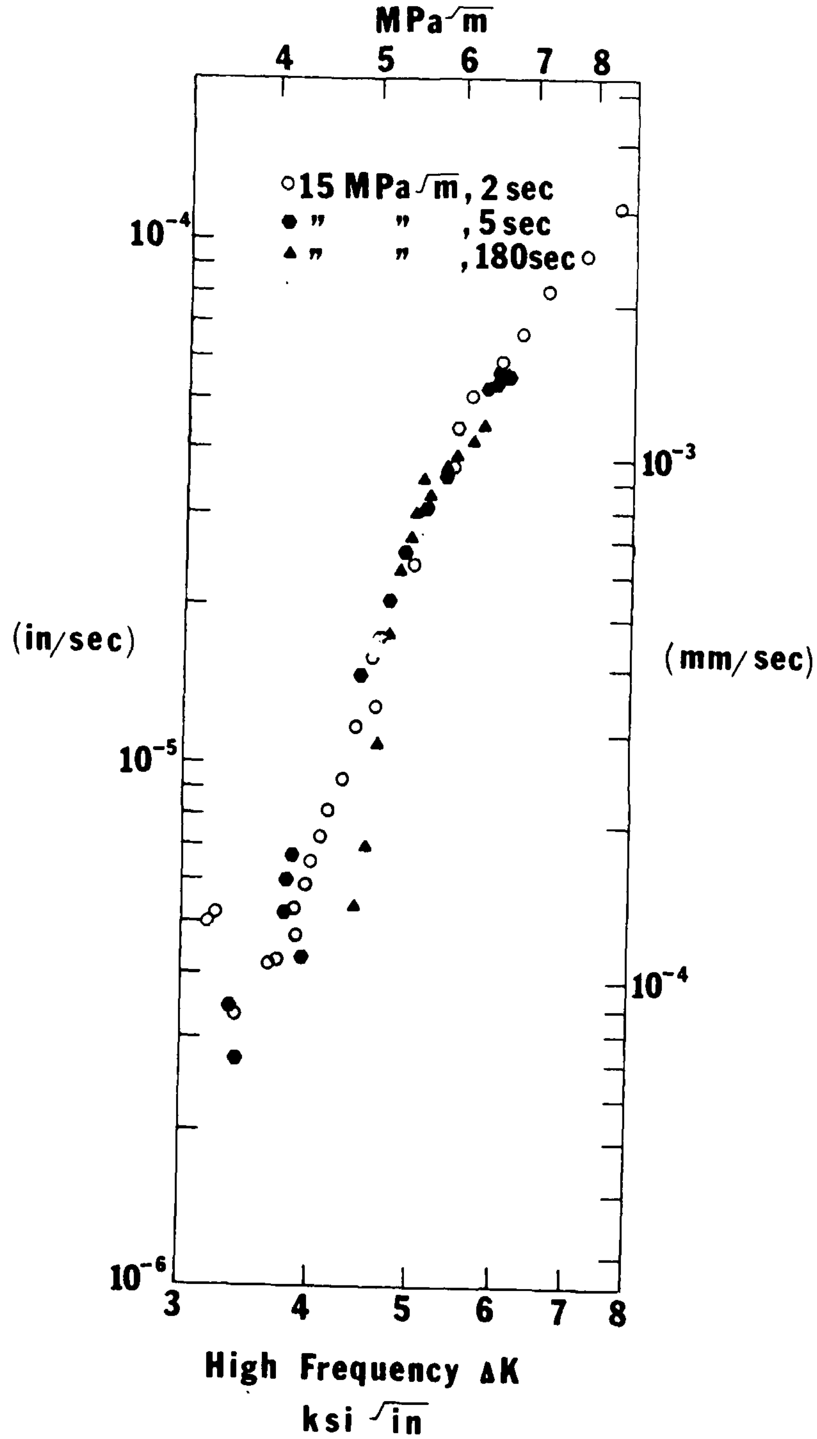

FIGURE 34 Comparison of Crack Growth Rate Versus High Cycle ΔK for several Hold TImes With a Low Cycle ΔK of 15 MPa √m.

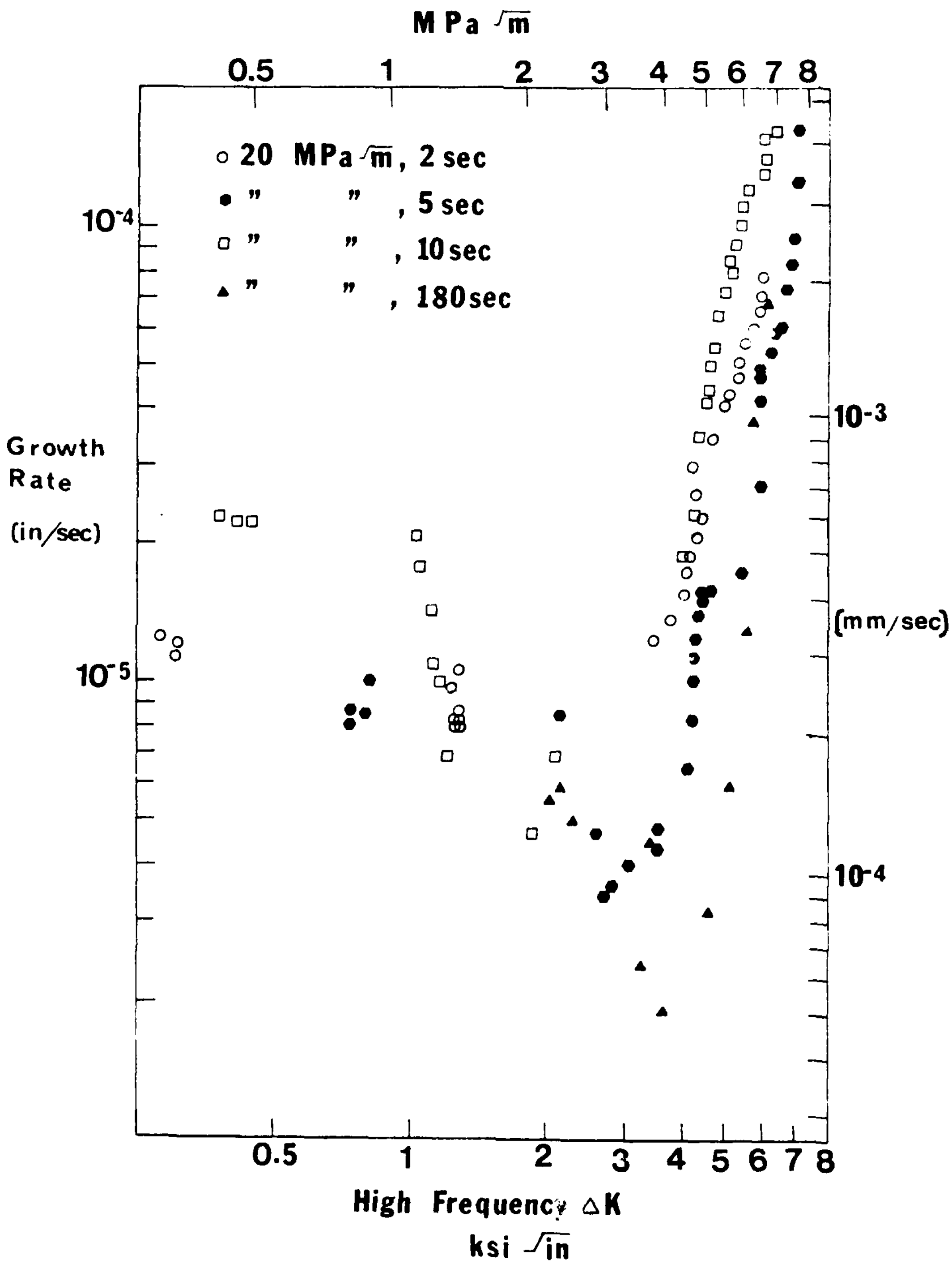

FIGURE 35 Comparison of Crack Growth Rate Versus High Cycle ΔK for Several Hold Times and a Low Cycle ΔK of 20 MPa $\sqrt{m}$.

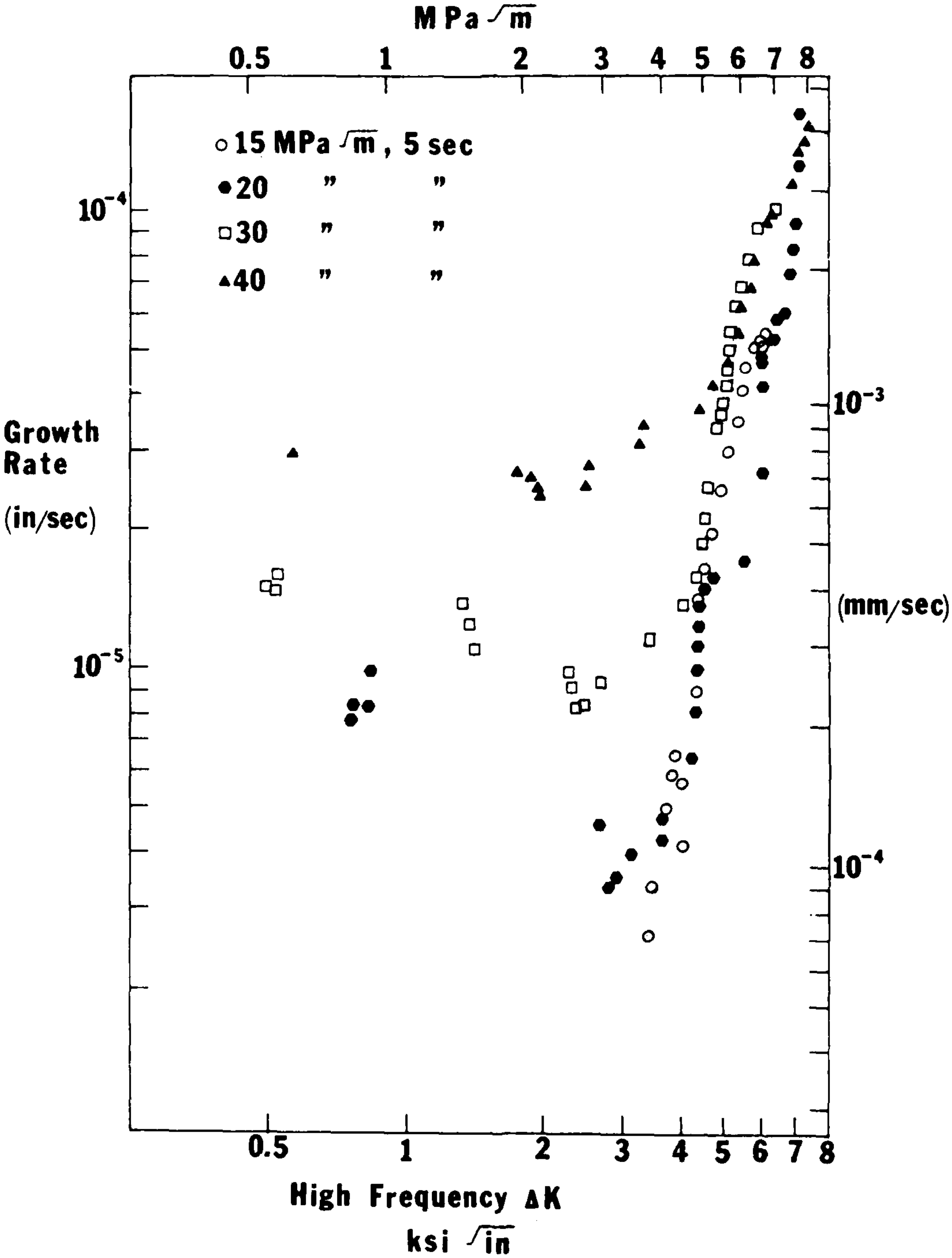

FIGURE 36 Comparison of Crack Growth Rate Versus High Cycle ΔK for Several Low Cycle ΔK ranging From 15 to 40 MPa $\sqrt{m}$ With a Low Cycle Hold Time of 5 Seconds.

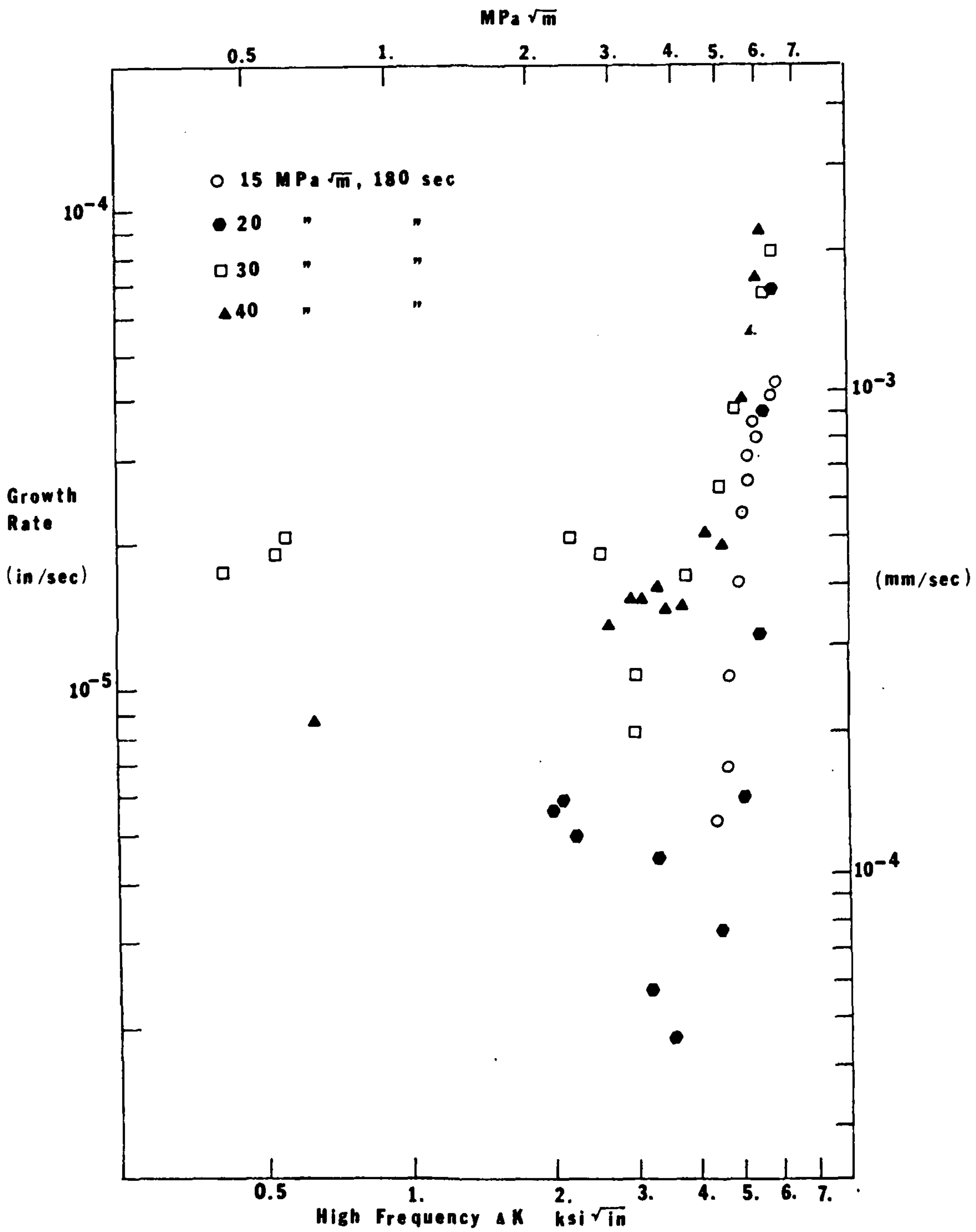

FIGURE 37 Comparison of Crack Growth Rate Versus HTgh Cycle ΔK for Several Low Cycle ΔK Ranging From 5 to 40 MPa √m With a Low Cycle Hold Time of 180 Seconds.

TABLE 5: COMBINED CYCLE TEST INCLUDING AN 1800 to 2000 Hz HIGH FREQUENCY LOAD COMPLETED TO DATE

LOW CYCLE HOLD TIME (sec)

Low Cycle Maximum K (ksi $\sqrt{in}$)	2	5	10	180
	TEST #'s			
20		67	60	
25		63		
30		64, 68	61, 62	
40		66, 65		

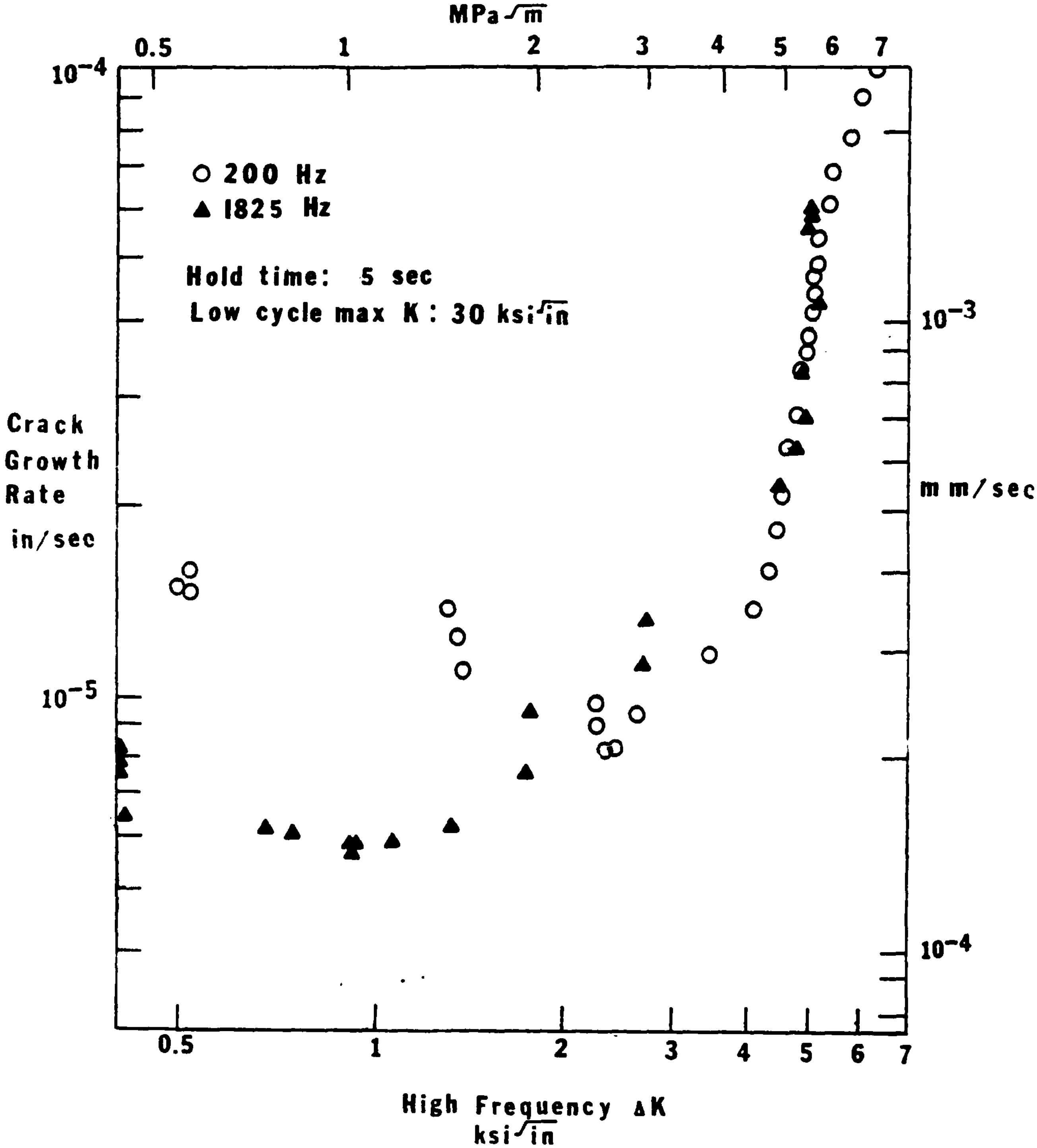

FIGURE 38 Comparison of Results for 200 and 1825 Hz for a Hold Time of 5 Seconds and a Low Cycle ΔK of 30 MPa $\sqrt{m}$.

Tests 60 through 66 in this higher frequency series were conducted with several high cycle frequencies in the range of 1800 to 2000 Hz. The advantages of testing at 1825 Hz became apparent and, therefore, beyond test 66, 1825 Hz was used as the high cycle frequency. Comparison of results for 200 Hz and 1825 Hz tests may be found in Figures 38 and 39 which present data for a 5 second hold time and for a ΔK of 30 MPa $\sqrt{m}$ and 20 MPa $\sqrt{m}$ respectively. A feature that the 1825 Hz tests show in these figures is a less pronounced retardation than at 200 Hz. Other tests performed near 2000 Hz show similar results. In Figure 39 for a low cycle ΔK of 20 MPa $\sqrt{m}$, on the onset of high cycle activity appears to occur at a lower high frequency ΔK at 1825 Hz than at 200 Hz. A distinct low cycle dominated range of high frequency ΔK is apparent at both frequencies.

A comparison between combined cycle loading with a high frequency component of 200 Hz and 10 Hz is presented in Figure 40. The 10 Hz data is from Reference 1. The apparent onset of high cycle behavior is about the same. The initial slopes of the high cycle dominated regime are significantly different with the 200 Hz data having a larger slope. This behavior would be expected in the high cycle dominated regime in which the number of high frequency cycles determines the rate of crack growth.

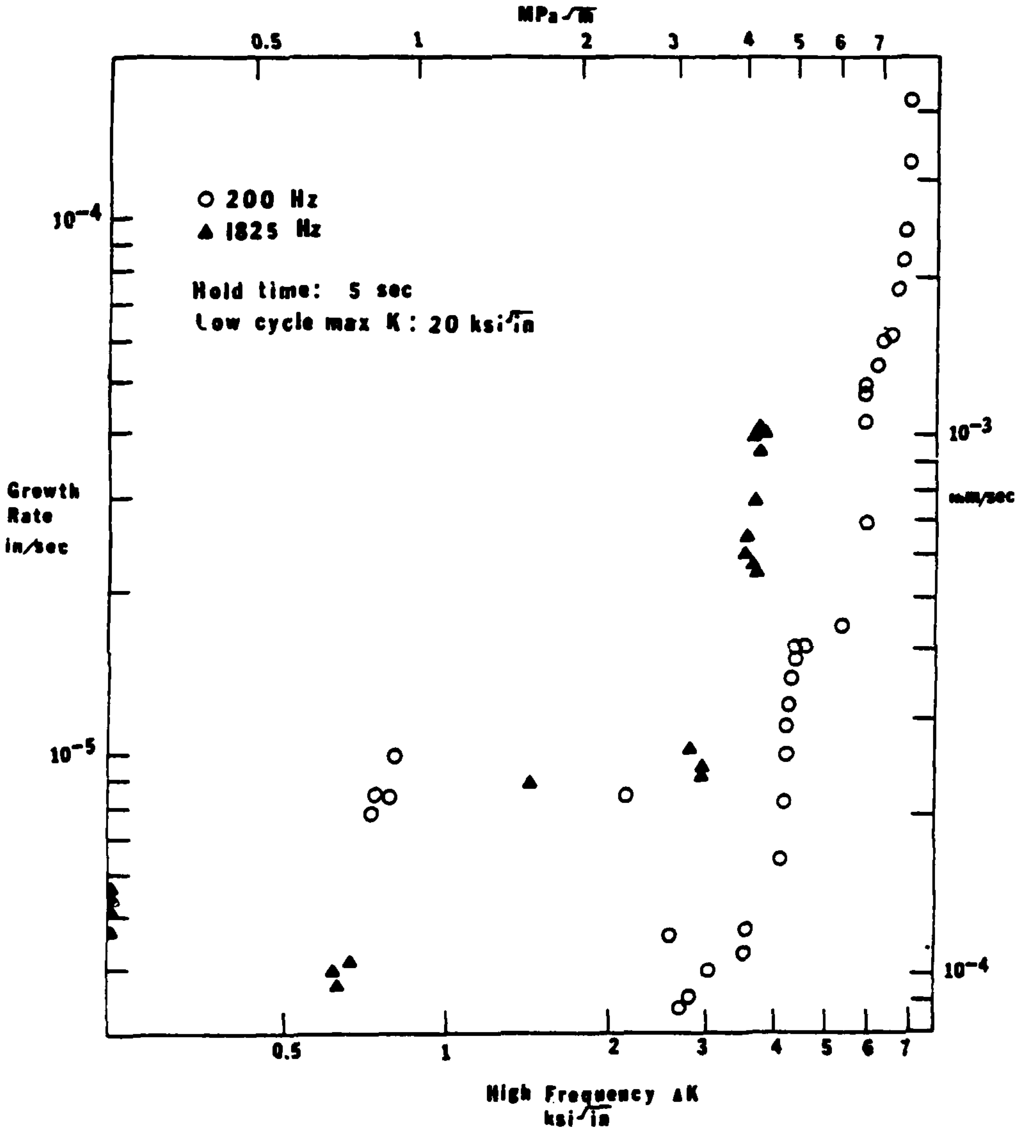

FIGURE 39 Comparison of Results for 200 and 1825 Hz for a Hold Time of 5 Seconds and a Low Cycle ΔK of 20 MPa $\sqrt{m}$.

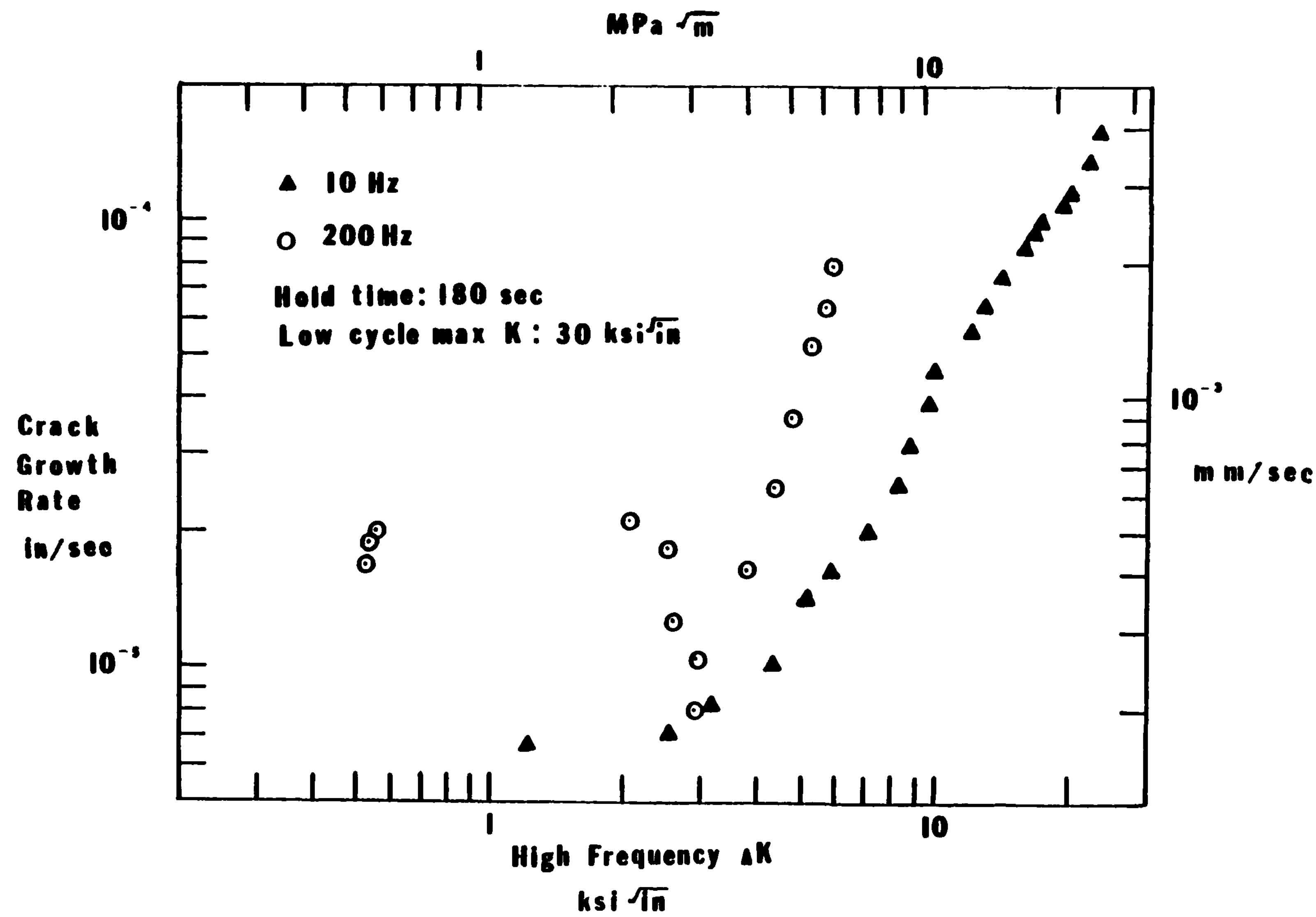

FIGURE 40 Comparison of Results for 10 and 200 Hz for a Hold Time of 180 Seconds and a Low Cycle ΔK of 30 MPa √m.

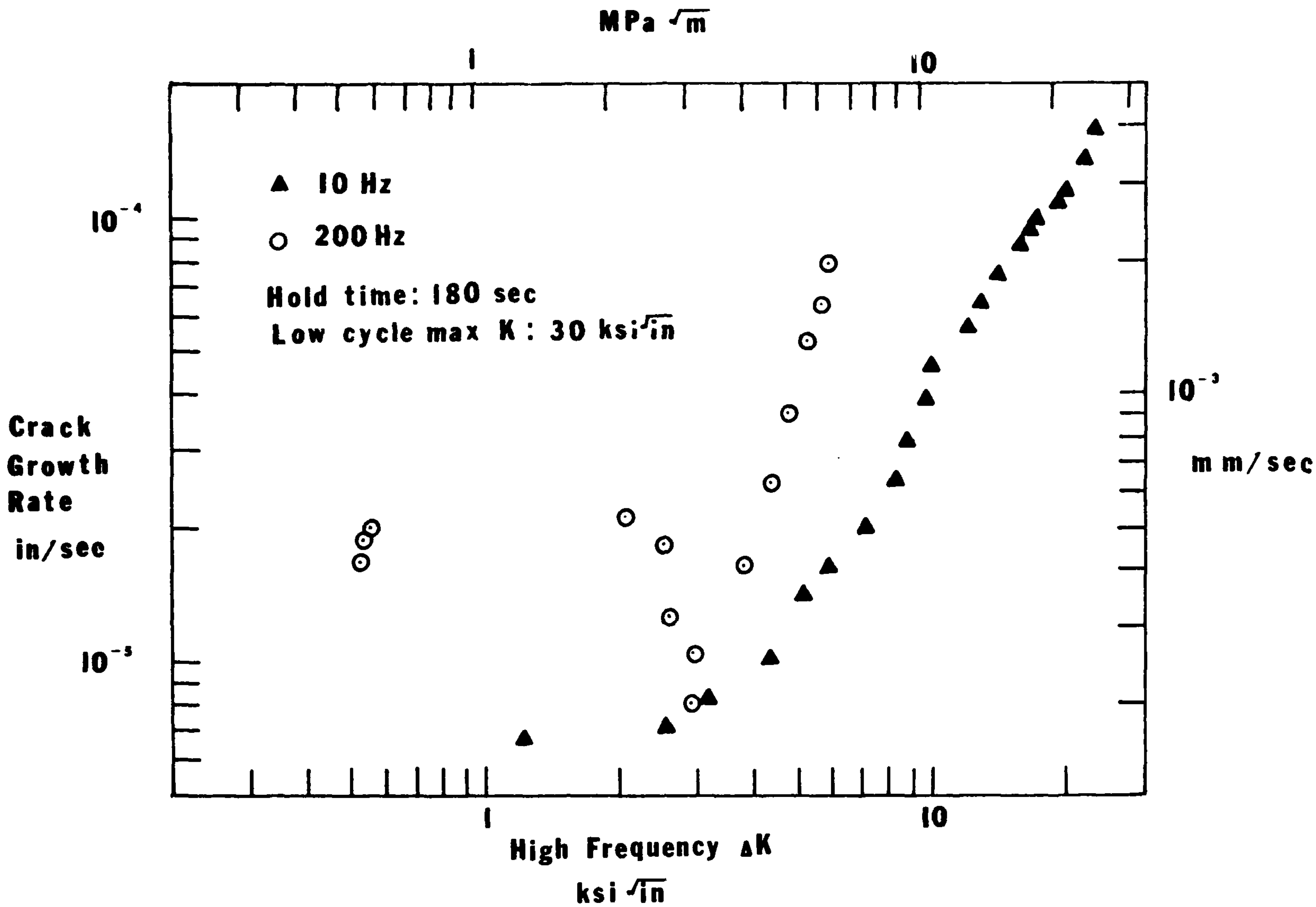

MPa √m
1
10
▲ 10 Hz
○ 200 Hz
Hold time: 180 sec
Low cycle max K : 30 ksi√in
Crack Growth Rate in/sec
10⁻⁴
10⁻⁵
10⁻³
mm/sec
1
10
High Frequency ΔK
ksi √in

IV EVALUATION OF MECHANISMS AND MODELLING ASSOCIATED WITH FREQUENCY EFFECTS AND COMBINED HIGH/LOW CYCLE INTERACTION

There have been several studies of frequency effects in nickel base and other alloys up to frequencies of 20,000 Hz. Investigation of combined high and low frequency interactions in fatigue have also been performed. In this section the important observations and conclusions from these studies will be summarized. The test results from this program will then be discussed in the context of these previous studies.

A. Background

References 8-11 provide a review of mechanisms that apply to fatigue crack growth of nickel base alloys at elevated temperatures. These papers deal with both the initiation and propagation of fatigue cracks and the influence of frequency on these processes. Frequency effects are evaluated in terms of the effect of frequency on "slip character", which is the degree to which dislocations disperse during plastic deformation. The two extremes in slip character that nickel base alloys have exhibited are planar slip and wavy or homogeneous slip. Planar slip is characterised by the concentration of dislocations in planar arrays with planar shear offsets produced on polished surfaces transverse to the crack plane and parallel to the direction of propagation. This type of slip and its associated deformation is favored by low stacking fault energy, ordering, the presence of coherent precipitates, low temperatures, and small strains. Austenitic stainless steel and nickel base alloys both exhibit planar slip at ambient temperatures. Wavy or homogeneous slip on the other hand, is characterized by uniformly distributed, nonplanar dislocation arrangements with an associated rumpling of the surface transverse to the crack plane and parallel to the growth direction. Wavy slip is favored by high stacking fault energies, incoherent precipitates or particles, large strains, and elevated temperatures. Most metals including stainless including stainless steels and nickel base alloys exhibit wavy slip at temperatures greater than $0.4T_M$ (T_M = melting temperature) because a thermally activated process allows dislocations to cross slip and climb out of their original slip planes. Wavy slip can occur in both transgranular and intergranular fracture modes. The fact that wavy slip occurs by a time dependent, thermally activated process in iron and nickel base alloys at elevated temperatures has significant impact on the frequency dependence of fatigue. As the frequency or strain rate increases the degree of slip dispersal decreases, i.e., when the characteristic time constant associated with slip dispersal becomes larger in relation to the cycle time associated with deformation, slip becomes more concentrated on certain planes. It has in fact been observed that as cycling frequency increases, slip becomes similar to that observed at ambient temperatures in nickel base alloys. At higher frequencies as with lower temperatures, planar slip tends to dominate.

Fatigue life over the broad range of frequency from .033 Hz to 1000 Hz for Udimet 700 at 1400°F (760°C) is presented in References 8 and 9 and shown in Figure 41. From .033 Hz to 10 Hz, fatigue life at the given strain range increases by a factor of 100. Over this frequency range there are changes in the site of crack initiation. At the lowest frequency initiation occurs at surface connected grain boundaries and the initial mode of fracture in intergranular. As frequency increases in this range of frequency, intergranular cracking generally associated with creep and oxidation become less dominant giving way to transgranular fracture. At a frequency of 3 Hz, the fracture is almost entirely transgranular. With an increase in frequency from 10 to 1000 Hz, fatigue life is reduced by a factor of seven because of the concentration of deformation in fewer slip bands and the resulting accelerated crack initiation and propagation. Reference 9 suggests that the main reason for the reduced fatigue life beyond a frequency of 10 Hz may be associated primarily with the number of cycles required for crack initiation.

The nature of crack initiation has been shown to change with changing frequency. Stage I and Stage II are two classifications of fatigue crack initiation. Stage I crack initiation is favored by low temperatures and high frequencies, i.e., the same conditions that lead to planar slip. Low frequencies and high temperature on the other hand, favor Stage II crack initiation. Additional observations regarding the influence of frequency on crack initiation in nickel base alloys is given in Reference 10. Fatigue cracks in Udimet 700 at 1400°F (760°C) are shown to initiate in an intergranular mode from a surface intitation site at frequencies of 0.033 to 0.33 Hz. The crack then extends intergranularly along the surface to a depth of 1 to 3 grain diameters below the surface and then changes to a transgranular Stage II mode. At frequencies in the range 3 to 1000 Hz, crack propagation began in the Stage I transgranular mode and changed to a Stage II mode. It was also observed over the many specimens examined that low

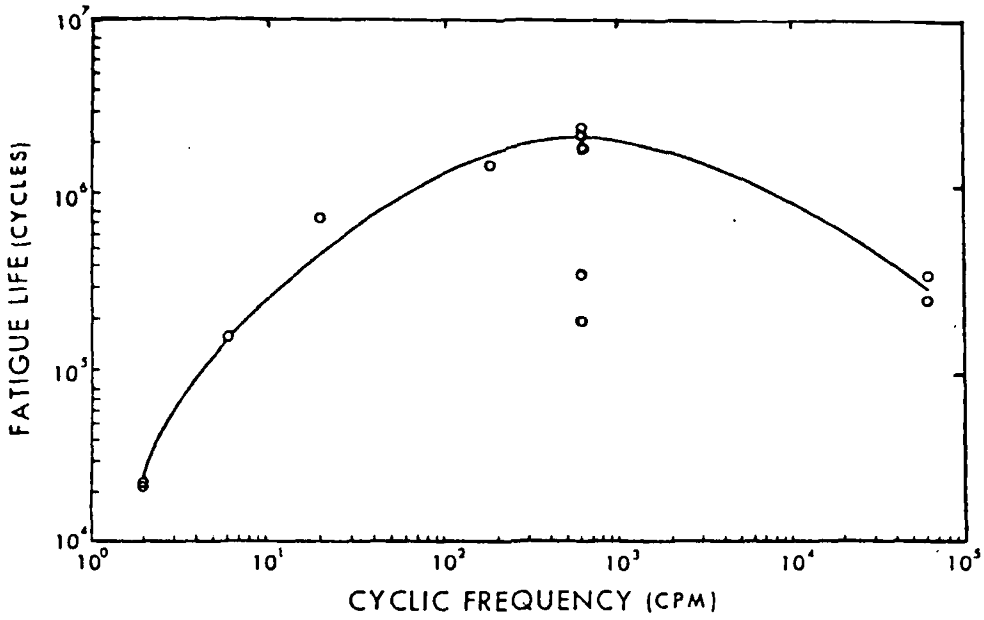

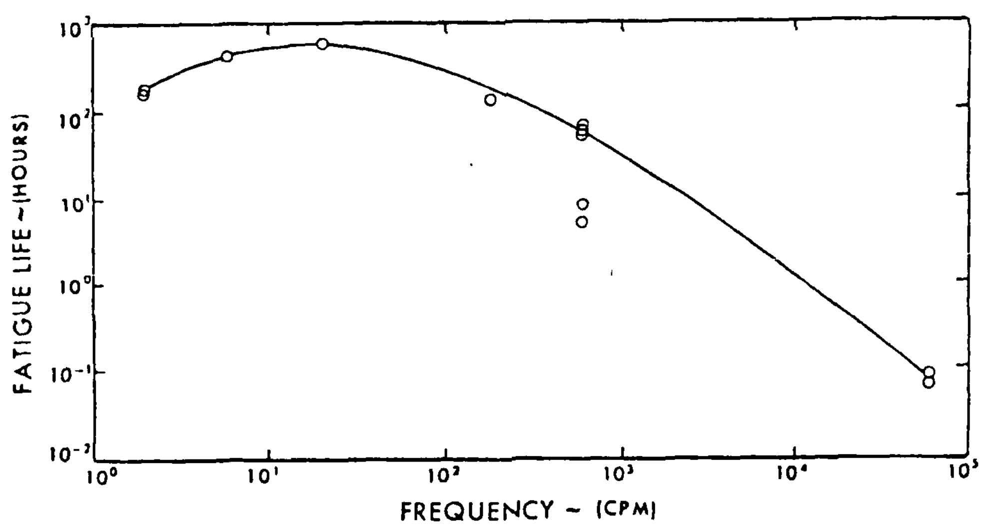

Figure 41 The Effect of Frequency on the Number of cycles and Time to Failure of U-700 at 1400°F (760°C) and a Stress Range of 85 Ksi. (9)

frequencies favor surface intergranular crack initiation and intergranular crack propagation. High frequencies on the other hand favor subsurface initiation at grain boundaries or twin boundary intersections and transgranular crack propagation.

A study of the influence of cyclic frequency on the fatigue properties of single crystal MAR-M-200(11) showed results similar to those for Udimet 700. Testing was performed on MAR-M-200 at frequencies from 0.033 Hz to 1030 Hz over the temperature range 1400°F (760°C) to 1800°F (982°C). The number of cycles to failure at 1400°F (760°C) and 1550°F (787°C) reached a peak in the range of 1 to 10 Hz. Stage I crack initiation was favored at the lower temperatures and higher frequencies and Stage II crack initiation at the higher temperatures and lower frequencies. At 1030 Hz crack initiation and propagation occurred entirely in the Stage I mode with facets corresponding to 110 slip planes. Generally, the amount of Stage I fracture varied according to temperature and frequency as shown in Figure 42. The nature of the fracture was attributed to degree of slip homogeneity. Stage I is favored by inhomegeous planar slip and Stage II is favored by homogeneous slip. In almost all specimens of MAR-M~200 cracks initiated at subsurface micropores.

Clavel and Pineau(12) studied the effects of frequency and wave form on the fatigue crack growth of Alloy 718 (a nickel base superalloy) in the frequency range between 5×10^{-3} Hz and 20 Hz at 298°K and 823°K. The variation in fatigue crack growth rate with frequency that they observed at 823°K is summarized in Figure 43. Consistent with the observations on Udimet 700, Nimonic 90, and MAR-M-200 single crystals, the fatigue crack growth rate decreases with increasing frequency in the regime in which environmental and time dependent material deformation processes creep effects can operate. Fractography revealed that this decrease in fatigue crack growth rate (FCGR) is accompanied by a change in fracture mode from intergranular to transgranular. Suprisingly, they observed through TEM examination of the substructure that higher strain rates promoted more homogeneous plastic deformation while low strain rates favor inhomogeneous deformation and the formation of twins. The crystallographic aspects of the fracture surface observed at room temperature in the threshold regime is attributed to the decohesion along the twin deformation bands.

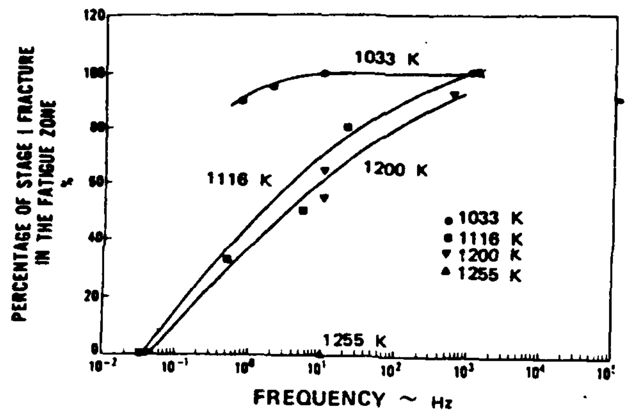

FIGURE 42 The Percentage of Stage I Fracture in the Fatigue Zone as a Function of Cyclic Frequency at Temperatures of 1033, 1116, 1200, and 1255 K. (9)

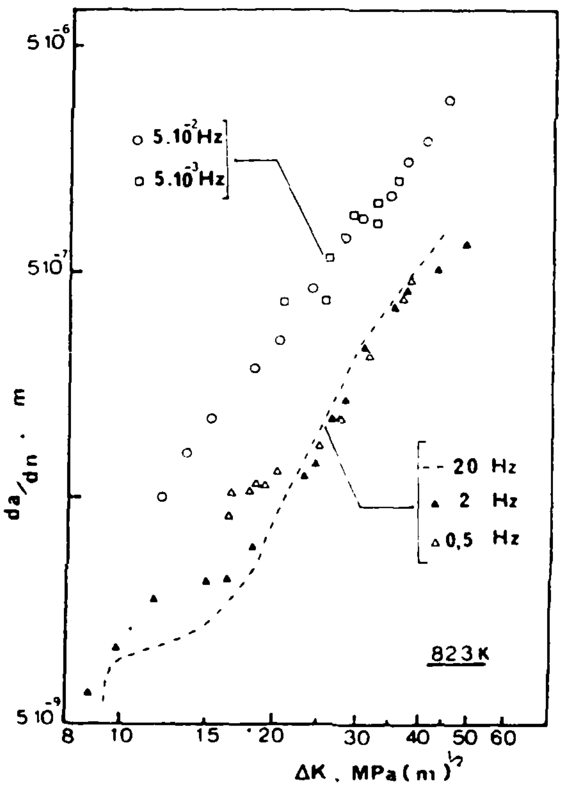

FIGURE 43 Variation of FCG Rate (da/dN) With Stress Intensity Factor (ΔK) and Frequency ($\sqrt{}$) at 823 K (Sinusoidal Load) for Inconel 718. (12)

A paper by Sullivan et. al.[13] discusses the effect of cycling frequency in the very low frequency regime for the nickel base superalloys Udimet 700 and MAR-M-200. Creep tests were performed on these materials at 955°C in air with periodic unloading. The time intervals between unloadings were on the order of 15 minutes to 5 hours. The main observation made regarding the effects of unloading is that it produced accelerated creep rate in both Udimet 700 and directionally solitied MAR-M-200.

Scarlin[14] also studied the effect of frequency in the range 10^{-4} to 10^{2} Hz on the fatigue crack growth of two nickel base superalloys: Nimonic 105 at 750°C and IN 738 LC at 850°C. The results show the expected decreasing crack growth rate with increasing frequency.

The influence of environment on the frequency dependence of fatigue has also been investigated. For example, in the lower frequency regime (up to 1.7 Hz) Solomon and Coffin[15] studied the effect of frequency on the fatigue crack growth of A286 at 1100°F in both air and vacuum. They observed generally that the crack growth mode and frequency dependence of crack growth rate varied with frequency in the manner shown in Figure 44. This representation of the crack growth data shows that specimens tested in air and vacuum both have frequency regimes of intergranular and transgranular fracture but with different behavior in the lower cycle regime. Likewise, both air and vacuum tested specimens have a frequency above which the crack growth rate is independent of frequency. This study also shows that the dependence of crack growth rate (in growth per cycle) may be represented as follows.

$$\frac{dC}{dN} = \phi C(\Delta\varepsilon_{\rho})^{\alpha}\nu^{k-1} \qquad (1)$$

where $\Delta\varepsilon_{\rho}$ is the plastic strain range for the specimen used in their experiments, C is the measured crack length, dC/dN is the crack growth rate and ϕ, α, and k are constants. Each regime shown in Figure 44 is characterized by a different value of k; the pure cycle dependent regime has a k value of 1.0.

The tests performed in vacuum generally have a lower growth rate than in air. The difference in fatigue crack growth rate, however, decreases with increasing frequency and the results converge at high frequency. These results suggest

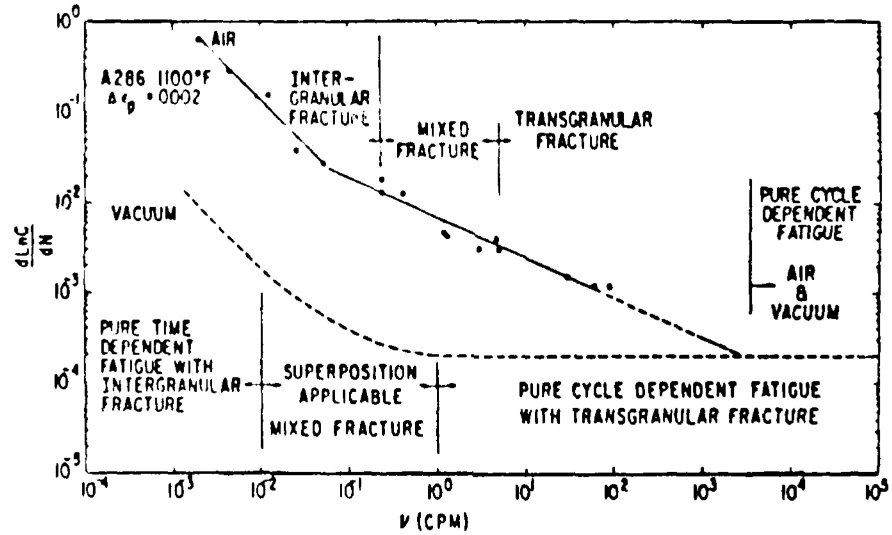

FIGURE 44 Schematic Comparison of the Air and Vacuum Crack Growth Behavior.

that as frequency increase the effect of environment reduces, or in effect the crack at higher frequencies out runs the processes of oxidation that degrade the fatigue crack growth properties.

Another study demonstrating the influence of environment on frequency effects in the fatigue crack growth involves 200 Maraging steel in a salt water environment and is reported in Reference 16. A significant frequency effect on the crack growth of this alloy in salt water in the frequency range 0.17 Hz and 3.3 Hz. At 3.3 Hz, it was found that the salt water solution had little effect on the crack growth rate as compared to the results in air. There was a factor of ten increase in crack growth rate when the frequency was reduced to 0.017 Hz. This along with the comparisons for different gaseous environments demonstrates that environment may be responsible for much of the frequency effect.

An important aspect of frequency effects in component life prediction is the effect of frequency on the threshold stress intensity factor range (ΔK_{th}). There are reports on the aspect for several materials. Mautz and Weiss[17] reported the effects of frequency on ΔK_{th} for D6ac steel at room temperature for both air and argon environments. No frequency effects on threshold behavior were observed for an air environment between frequencies of 100 and 375 Hz. In dry argon, however, the results for 100 Hz were slightly higher than those at 375 Hz.

A very extensive study of fatigue crack growth properties of titanium alloys used in aircraft engine compressors was performed by Beyer, Sims and Wallace[3]. Frequency effects up to 1000 Hz on the fatigue crack growth properties of Ti-6Al-2Sn-4Zr-6Mo, Ti-8Aℓ-1Mo-1v, and Ti- 6Al-2Sn-4Zr-2Mo were investigated at room, 600°F, 800°F, 900°F and 1000°F for several R ratios for crack growth rates down to the threshold regime. For the higher R ratios such as 0.5 and 0.7 there is a considerable reduction for all three alloys when the frequency is increased to 1000 Hz from 0.17 Hz at elevated temperatures. The threshold stress intensity factor likewise reduced on increasing the frequency to 1000 Hz. The variation in crack growth in the frequency range 0.017 Hz to 30 Hz was much less than that between 30 and 1000 Hz.

The highest test frequency in fatigue testing that we were able to find in the literature was that used by St. Stanzl and Mitsche[18] who performed crack growth tests on 0.04%C steel, chromium steel 20A13 (0.29.C, 13%a), and pure molybdenum at 20 kHz. They conclude that their results in terms of crack growth rate versus ΔK are similar to those for 10 Hz provided by another investigation.

Combined high cycle/low cycle loading has been investigated for several materials. The frequencies for the high cycle and low cycle components represented in these studies cover a very broad range in both loading components. At the lowest extreme in low cycle loading there is the low cycle frequency of zero with the high cycle frequency in the range that will with sufficient amplitude cause fatigue crack growth. This combined cycle interaction is often referred to as creep-fatigue interaction.[19-24] Another group of papers and reports [1, 25-28] deal with high cycle/low cycle interaction where the high and low cycle components correspond to those that are encountered in rotating machinery. The low cycle component has a cycle period on the order of seconds to several hundred seconds and the high cycle frequency ranges from 10 Hz to several thousand Hz.

Several studies have shown that load cycling can have an effect on the creep rate. Both increases and decrease. in creep rate have been observed when cycling is applied. The softening has been attributed to and increased mobility of piled up dislocations as a result of the fatigue cycling assisting the dislocations to overcome obstacles and "friction" stress fields in the slip plane. The hardening effect has been explained in terms of migration of solute atoms or dispersed point defects towards free dislocations. Venkiteswaran et. al.[19] who studied the precipitation hardened alloy Inconel Alloy X-750 attributed the reduction in creep rate due to an applied fatigue cycle to the formation of complex dislocation tangles and vacancy condensation along dislocation lines. A change in fracture mode from intergranular to transgranular was also observed with the application of the 555 to 910 Hz fatigue loading.

Atanmo and McEvily[24] reported on the creep-fatigue interaction during crack growth of aluminum alloy 5052 at 400°F. Conducting tests with ramped loading and hold times ranging from 30 to 65 seconds, as well as with steady load, they-observed that cyclic-creep lifetimes can exceed creep lifetimes, perhaps as a result of the reversal of the creep process at the crack tip during the off-load period of the test.

There are several investigations of high cycle/low cycle interaction motivated by design considerations in rotating machinery such as generating plants, gas turbines and compressors. These studies all involve a low cycle loading component consisting of a trapezoidal waveform with a high frequency component applied during the upper level hold time as shown in Figure 45. Included in these studies are those performed at Portsmouth Polytechnic Institute on Ti-6Al-4V.[25-27] The dwell period for this test was 6.8 seconds. Testing was performed at room temperature with a high cycle frequency of 150 Hz. Fatigue crack propagation experiments with increasing load and high cycle load levels were undertaken using minor to major amplitude ratios (Q) of 0, 0.1, 0.2 and 0.3. Figure 46 shows the effect of amplitude ratio (Q) on the measured FCG rates.

A series of tests were conducted to determine the value of high frequency ΔK under major-minor cycling corresponding to measureable influence of the high cycle component on crack growth. A step down procedure was used to determine the threshold for high cycle activity. Table 6 lists the conditions for the onset of minor cycle damage and onset of fast fracture. The authors also evaluated the appropriate manner of predicting crack growth rate under combined cycle loading. The two approaches to crack growth prediction evaluated by the authors are the linear summation of the major and minor cycle crack growth rates measured individually and the representation of the complex loading in terms of its RMS value. A comparison of the experimental results with the predicted results are shown in Figures 47 and 48. In these cases, the crack growth is dominated by the high cycle (minor cycle) loading and the prediction of both the linear summation and RMS representation are satisfactory.

Goodman and Brown[1] report on several combined cycle tests on alloy 718 at 649°C with a high cycld frequency of 10 Hz and the same loading profile as used in the studies of References 25 and the present study. Features similar to those found in the present study at 200 and 1825 Hz were observed including retardation in the low cycle dominated regime and the existence distinct high and low cycle dominated regimes. Also included in the program conducted by Goodman and Brown, tests with a high cycle frequency of 100 and 200 Hz.

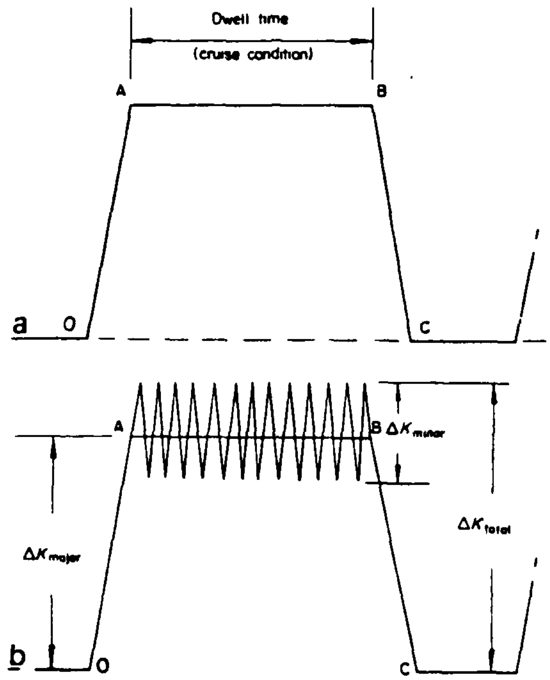

FIGURE 45 a - Major Cycles Only; b - Major and Minor Cycles (Minor/Major Amplitude Ratio $Q = \Delta K_{minor}/\Delta K_{major}$)

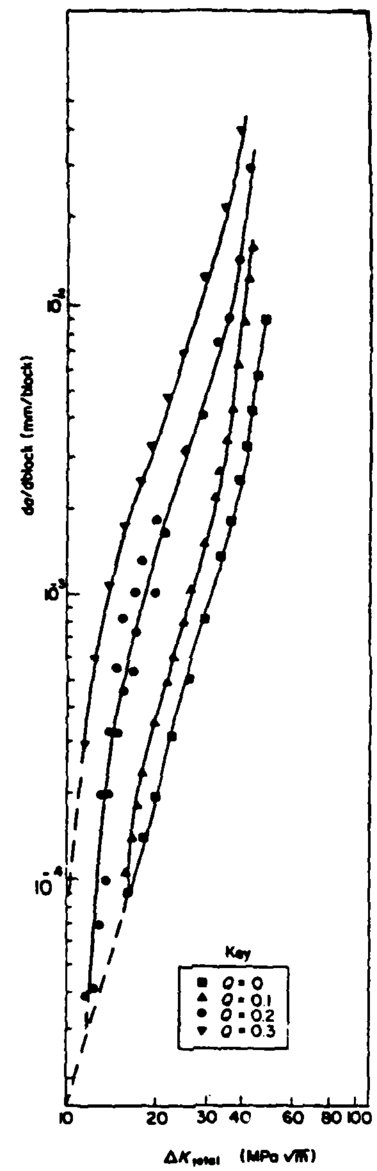

FIGURE 46 Effect of Amplitude Ratio on FCG Rates for Major and Minor Cycles. (25)

TABLE 6 Conditions for the Onset of Minor Cycle Damage and Onset of Fast Fracture (ΔK Values in MPa $\sqrt{m}$).

Amplitude ratio	R	Onset of minor cycle activity			Onset of fast fracture	
		ΔK_{minor}	ΔK_{major}	ΔK_{total}	ΔK_{minor}	ΔK_{total}
0.02	0.982	1.5	75.0	75.8	1.3	63.1
0.04	0.965	1.6	40.0	40.8	2.5	63.1
0.1	0.914	1.7	17.0	17.9	6.0	63.3
0.2	0.835	2.1	10.5	11.6	11.6	63.6
0.3	0.762	2.3	7.7	8.8	16.7	63.9

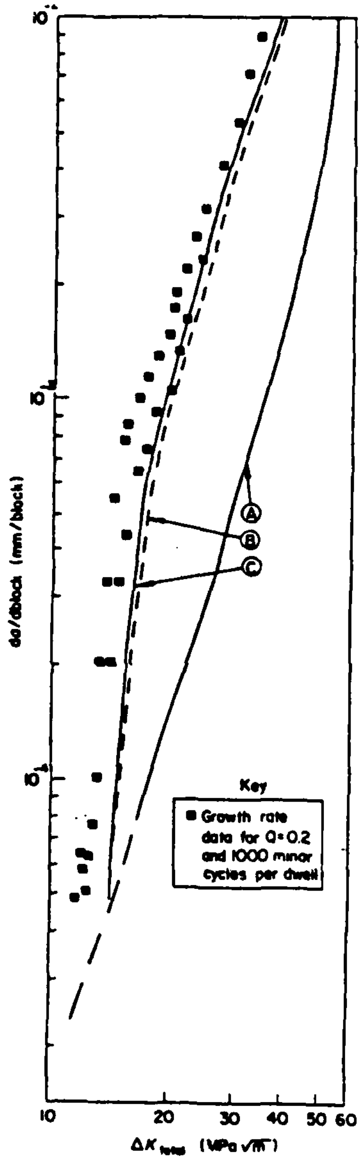

FIGURE 47 Linear Summation of FCG Rates (Damage: A-Associated With Applied Major Cycle: B-Associated With Applied Minor Cycles: C-Given by Summation of Major and Minor Cycle Damage). (25)

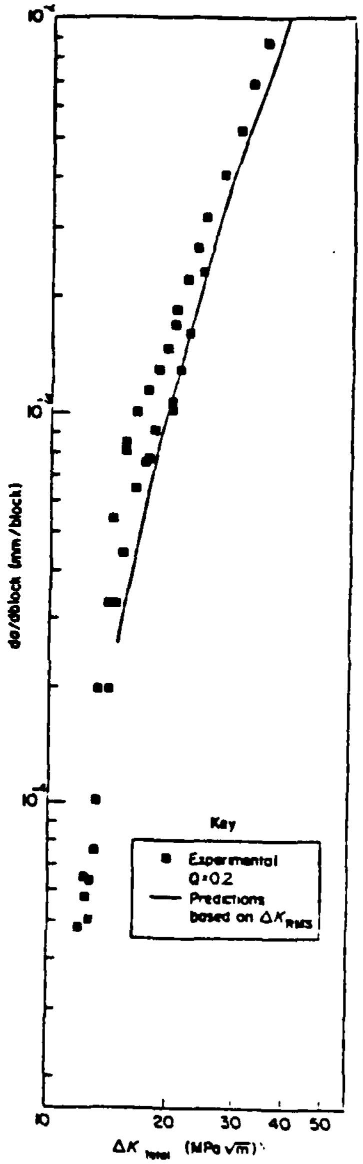

FIGURE 48 Analysis of Major-Minor Fatigue Crack Growth Rates in Terms of ΔK_{RMS} (25)

B. Evaluation of Fatigue Crack Growth Mechanisms Under Combined Cycle Loading

The study of Venkiteswaran et. al.,[19] reports the results of creep testing with a superimposed small vibratory stress on the axial creep behavior of a high temperature nickel base alloy, Inconel X-750. This work demonstrated that the creep rate was lower and rupture life higher by an order of magnitude when a 500 to 900 Hz vibratory stress was applied transverse to the axial creep load. This effect was attributed to the formation of complex dislocation tangles, vacancy condensation along dislocation lines and crack tips and also a change in fracture mode from purely intergranular fracture to a mixture of intergranular, fatigue and cleavage modes. It was suggested that the application of the high frequency loading, therefore, made creep crack propagation more difficult along the matrix containing γ' precipitates. Since the heat treated Inconel 718 used in this study likewise contains γ' (Ni_3 $A\ell$-Ti) as well as γ''(Ni_3Cb) precipitates, this mechanism could apply in the present study. The changing mode of fracture observed by them is consistent with the fractographic features of the combined cycle crack growth specimen that we investigated.

Fractographic examination was performed on specimens subjected to 200 Hz cyclic load in order to obtain information regarding fracture mechanisms. Areas on a 200 Hz specimen were examined by Scanning Electron Microscopy (SEM) and Scanning Transmission Electron Microscopy (STEM). All of these photographs correspond to specimen 28. The fracture surface includes areas corresponding to creep crack growth with no high frequency loading and areas corresponding to combined high/low cycle loading with crack growth both in the low and high cycle dominated regimes. The fracture surfaces of these regions show distinct differences. Figures 49 and 50 show SEM photomicrographs of the purely low cycle and combined cycle regions respectively. The purely low cycle region shows intergranular fracture typical of creep crack growth. With the application of a high frequency load range at a level that maintained the low cycle dominated behavior, the fracture becomes predominantly transgranular with the appearance of fatigue striations.

Replicas were taken of the fracture surface and subsequently shadowed with chromium and coated with a film of carbon. These replicas were then examined in an SEM with a transmitted beam. The resulting photomicrographs for a region of low cycle loading only, are shown in Figure 51. The intergranular nature of the

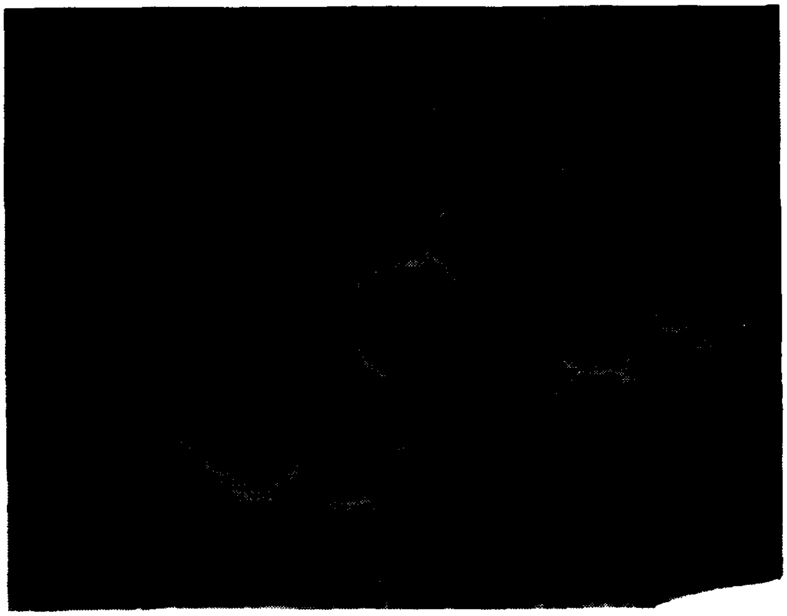

1000x E5631

FIGURE 49: Scanning Electron Microscope (SEM) photomicrograph of a region in which only low cycle loading was applied. (Specimen #28)

1000x E5636

FIGURE 50: Scanning Electron Microscope (SEM) photomicrograph of a region in which combined cycle loading (with 200 Hz high cycle load) was applied.

fracture is clearly shown in these photomicrographs. In Figure 52 are shown the STEM photomicrographs for a region which had experienced combined cycle loading. The striation pattern is this predominantly transgranular fracture seems to show grouping of striations. At the higher magnification of 10,000x the pattern appears to be obscured, probably by oxidation at the test temperature of 649°C.

Additional STEM photomicrographs were made on a specimen tested with a high cycle frequency of 1825 Hz (specimen 67). Without high frequency cycles applied, the fracture surface showed the expected intergranular fracture. Figure 53 shows the fracture surface in the low cycle dominated regime where the high cycle ΔK is large enough to cause retardation. A striation pattern is apparent. Figure 54 shows the fracture surface well into the high cycle dominated regime. The striation pattern in this region is more pronounced and shows a greater spacing corresponding to the increased crack growth.

The relationship between fatigue crack growth and high cycle ΔK for constant low cycle ΔK show three regimes. At the lower limit of ΔK_{HC} the low cycle loading dominates the rate of fatigue crack growth. In an intermediate range of ΔK_{HC}, the high cycle loading causes a retardation of the crack growth rate. At the highest values of ΔK_{HC}, crack growth rate is dominated by the high cycle loading with crack growth determined by the number of high frequency cycles. The low and high cycle dominated regimes are distinct but the transition between the two regimes is obscured by the retardation effect. The behavior of alloy 718 at 649°C revealed by this study is similar to that shown by Goodman and Brown[1] who studied the interactive effect of this alloy at 649°C with a high cycle frequency of 10 Hz. In their investigation, distinct low and high cycle dominated regimes as well as a regime of ΔK_{HC} where retardation occurred were also apparent. The investigation of Powell et. al.,[25] on Ti-6-4 showed regimes of ΔK_{HC} where the high cycle loading was either active or inactive, but a retardation effect was not apparent.

The retardation effect was unexpected and an experiment was carried to gain insight into its origin and characteristics. The experiment summarized in Figure 31 shows the rate (with respect to crack length) at which the retardation effect develops and also the rate at which it relaxes. There seems to be a crack growth interval of about 1mm (0.0394 inches) required for the retardation effect

1000x A E5665

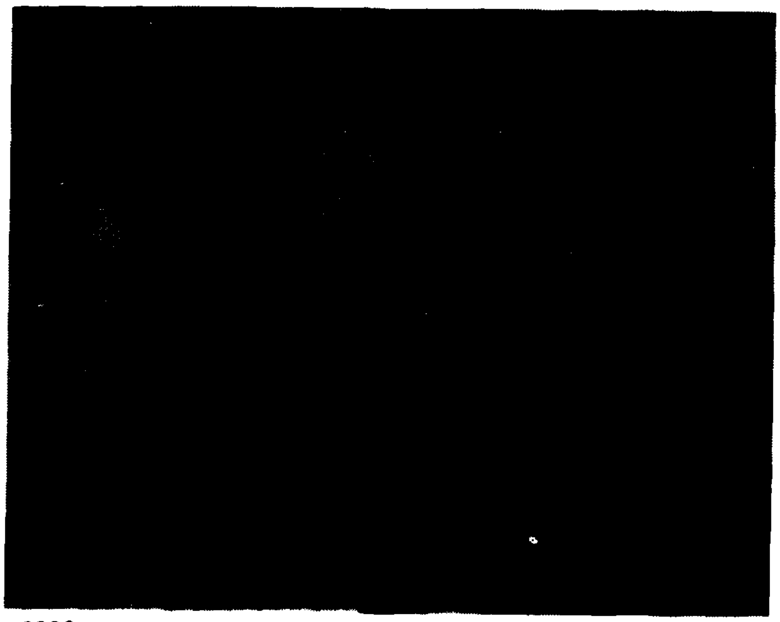

3000x B E5663

FIGURE 51: Scanning Transmission Electron Microscope (STEM) photomicrographs of a region in which only low cycle loading was applied.

6000x C E5664

Figure 51 (Cont'd) Scanning Transmission Electron Microscope (STEM) photomicrographs of a region in which only low cycle loading was applied.

AD-A160 601 INTERACTIVE EFFECTS OF HIGH- AND LOW-FREQUENCY LOADING ON FATIGUE(U) MECHANICAL TECHNOLOGY INC LATHAM N Y A PETROVICH MAY 85 MTI-85TR48 AFWAL-TR-85-4045 2/2

UNCLASSIFIED F33615-82-C-5056 F/G 20/11 NL

END
DATE
FILMED
12-85
DTIC

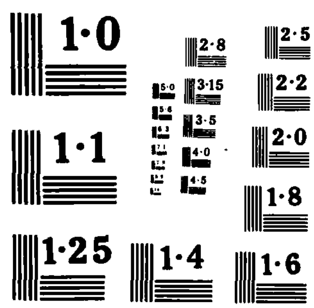
1·0
2·8
2·5
5·0
3·15
2·2
3·5
1·1
4·0
2·0
4·5
1·8
1·25
1·4
1·6

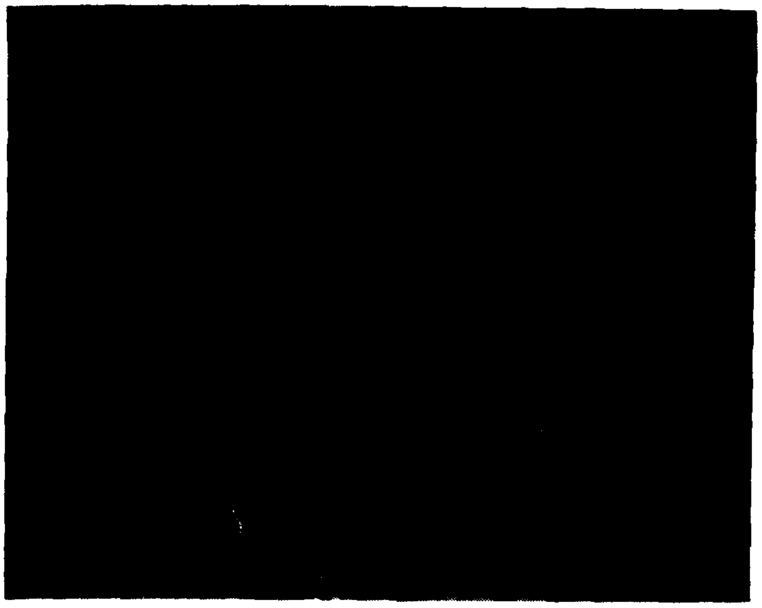

1000x A E5662

2000x B E5651

FIGURE 52: Scanning Transmission Electron Microscope (STEM) photomicrographs of a region in which combined cycle loading (with 200 Hz high cycle load) was applied.

6000x C E5648

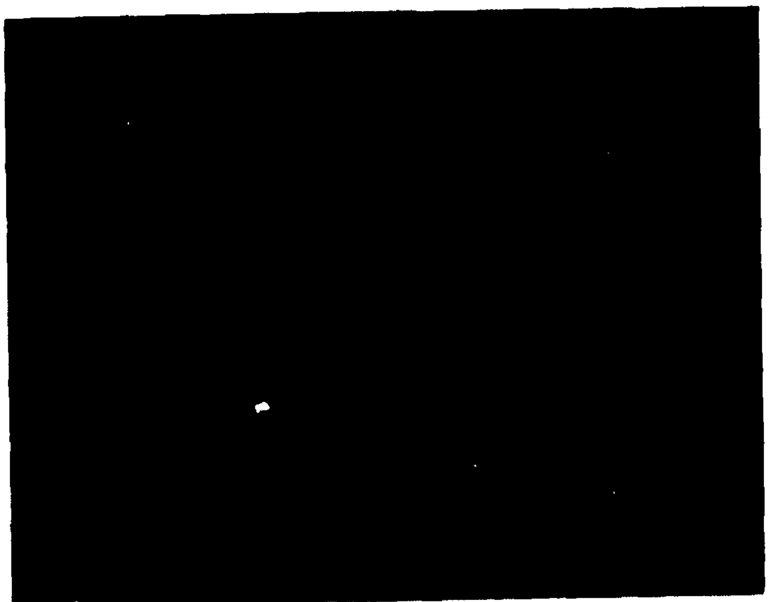

10,000x D E5654

Figure 52 (Cont'd) Scanning Transmission Electron Microscope (STEM) photomicrographs of a region in combined cycle loading (with 200 Hz high cycle load) was applied.

A.

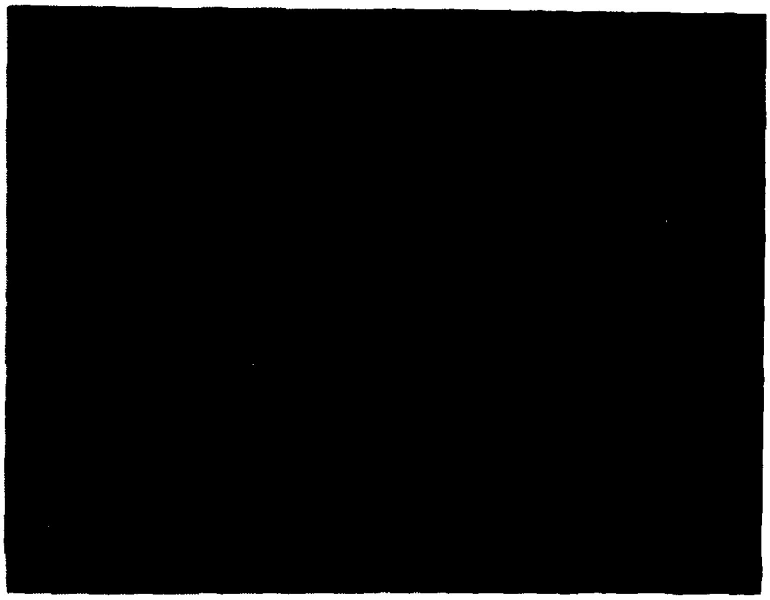

E5894 x3000

B.

E5893 x10,000

Figure 53 STEM Photomicrographs of a Region on the Fracture Surface of Specimen #67 Corresponding to the Low Cycle Dominated Regime where the High Cycle K is Large Enough to Cause Retardation

A.

E5785 x3000

B.

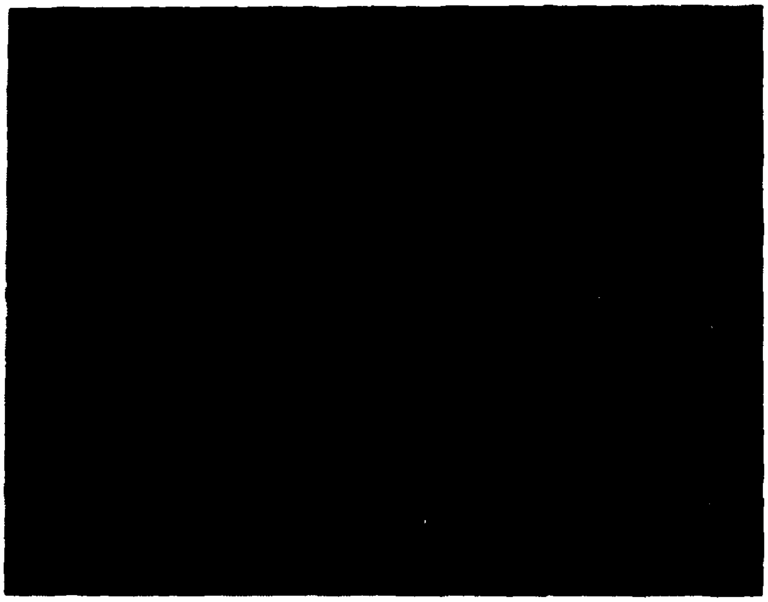

E5786 x10,000

Figure 54 STEM Photomicrograph of a Region on the Specimen #67 Fracture Surface Where the High Cycle Component Dominates Crack Growth.

to subside. The plastic zone size associated with the crack, however, is a small function of this length.

The size of the plastically deformed region (R) ahead of the crack as given by the Dugdale model[28] neglecting the effects of creep is:

$$R = \left\{\sec[1/2\pi(\sigma/\sigma y)]-1\right\} a$$

where σ is the applied stress, σy is the yield strength and a is the half crack length.

As calculated using this expression at the crack length corresponding to the retardation relaxation in Figure 31 and assuming a yield strength 980 MN/m^2 (140 ksi) the plastic zone size is 0.20mm (0.008 inches). A possible explanation of the fact that the affected region is considerably larger than the calculated plastic zone length is that creep stress relaxation results in a larger characteristic zone where structural changes important to retardation effects occur. Reference 29 demonstrates that crack tip stresses can be modified significantly by creep. The most significant influence of creep relaxation as shown by Reference 29 is the reduction of the stress gradient beyond the crack tip, i.e., the development of a more uniform distribution of stress in a region that includes the above calculated "plastic zone" and an area further from the crack tip. However, it is unlikely that creep can have such a pronounced influence on the crack stress distribution.

An alternative explanation of the long relaxation interval is suggested by the study of Venkiteswaran[19] that showed that the high frequency loading affects the creep rate versus stress constitutive properties. The modification of the creep rupture processes may in turn modify the residual plastic deformation remaining in the wake of the advancing crack (crack closure).[30] Such a concept would allow the possibility of the effect persisting well beyond the above calculated plastic zone without postulating a significant modification in the crack tip stresses due to creep relaxation effects. The crack growth interval of four or five times the plastic zone size is in fact characteristic of the development of closure effects.

cycle frequency is applied. However, when the retardation effect occurs with this lower high cycle frequency, a longer time period is required to reach the minimum crack growth rate. This would be expected if the retardation effect is related to the accumulated number of high frequency cycles.

A feature of the high cycle loading revealed by this and other studies is that there is a sharply defined value of transition ΔK (ΔK_{tr}) associated with the dominance of ΔK_{HC} for crack growth under combined cycle loading. For the range of conditions investigated, the influence of high cycle loading on crack growth below ΔK_{tr} can essentially be ignored. This is consistent with the observations of Powell et. al.[25] who performed combined cycle crack growth experiments on Titanium - 6 - 4 at ambient temperatures with a high cycle frequency of 150 Hz and with all of the combined cycle testing results of Goodman and Brown[1] performed on Inconel 718 at 649°C for a high cycle frequency of 10 Hz. Furthermore, there is little variation of this transition ΔK with frequency distinguishable beyond the ΔK_{tr} variation intrinsic to the material.

Considering the various features of the crack growth rate beyond ΔK_{tr}, i.e., that growth rate depends on number of cycles, that it is sharply defined by a threshold value, and that is shows a relationship between growth rate and ΔK_{HC} similar to that for stage I crack growth leads to the conclusion that it could be represented by a relationship of the form:

$$\frac{da}{dN} = C\ (\Delta K_{HC} - \Delta K_{tr})^{m}$$

where C is a constant and da/dN is crack growth rate in terms of crack extension per high frequency cycle. This relationship has been used to describe crack growth in the threshold regime (stage I) with a constant R ratio (K_{min}/K_{max}). The R ratio in the high cycle dominated regimes in the experiment conducted in this study, varies a small amount since they correspond to increasing ΔK_{HC} and constant ΔK_{LC} tests. The ΔK_{tr} is the above expression is expected to vary with low cycle ΔK and perhaps hold time but as shown by the present investigation it is essentially invariant with respect to frequency. This feature is helpful to the design since an acceptable level of high cycle loading can be established without concern for the frequency of the superimposed high frequency load.

is essentially invariant with respect to frequency. This feature is helpful to the design since an acceptable level of high cycle loading can be established without concern for the frequency of the superimposed high frequency load.

The investigation of Gell and Leverant[8] showed a pronounced influence of frequency on fatigue life of nickel base alloys in the frquency range of 10 to 1000 Hz. In this range they observed that fatigue life decreases with increasing frequency. Comparing the results of the present investigation with those of Goodman and Brown,[1] there is little variation in ΔK_{tr} over the frequency range to 2000 Hz. This fact and the fact that the crack growth rate per cycle versus ΔK_{HC} beyond ΔK_{tr} does not increase with increasing frequency leads to the conclusion that the decreasing fatigue life with increasing frequency observed by Gell and Leverant[8] is associated primarily with crack initiation.

C. Consideration of High/Low Cycle Interactions in Crack Growth Life Prediction of Engine Systems

Attention has been devoted recently to the effects of gas turbine engine load spectra on crack propagation. This is a result of increased performance requirements for U.S. Air Force gas turbines and the resulting high operating stresses and severe service environments experienced by gas turbine components. Many of the investigations are associated with the development of the advanced life management concept and focus on engine disks.

An important aspect of life prediction under engine loading spectra is the interaction of the low and high cycle components in crack growth of turbine disks. The cycle period associated with the low frequency cycle (low cycle) loading is on the order of seconds to several hundred seconds. A wide range of loading rates and load levels may also be involved in the low cycle loading. The high frequency cycle (high cycle) loading would typically involve frequencies on the order of hundreds to several thousand hertz. Important to accurate life prediction is establishing the manner in which each of these features of the engine disk loading profile contribute to crack growth and how these features interact. The specific aspects of combined cycle loading that must be addressed are the following:

- Establishment of the limits of high cycle loading under which the disk can be safely operated.
- How cumulative damage rules should be applied when combined high cycle/low cycle loading contribute to crack growth.
- The degree to which the high cycle and low cycle loading influence each others contribution to crack growth.

There are previous studies of load spectrum interaction in crack growth of aircraft engine components that deal with periodic overloads, overload/underload combinations and periods of sustained load interspersed with relatively constant amplitude loading. An example of such a study in that of Macha et. al.[31] which considered these effects on IN-100 and evaluates the applicability of crack growth rate models for engine complex loading spectra. Another study that addresses the effects of flight loading in military gas turbine operation on the fatiuge crack growth of IN-100 and Waspaloy is summarized in References 32 and 33. This study addresses the effect of overload ratio and the effect of the number of cycles between overloads.

The simplest approach to crack growth prediction is a linear summation of crack growth on a cycle by cycle basis for the given loading profile. However, this approach has been shown to be inadequate for many situations of variable amplitude loading where retardation or acceleration can result from certain sequences of loading. Various approaches have been established to account for these effects including models based on crack closure[34] and the interactions in the crack yield zone[35].

In the present study, the applicability of a linear summation of high and low cycle crack growth contribution in predicting combined high/low cycle crack growth was investigated for Alloy 718 with a high cycle component of 200 and 1825 Hz. Figures 55 and 56 show a comparison between a combined cycle test result and a linear summation of crack growth rate calculated from crack growth data for the low and high cycle contributions measured individually. The manner of summing the individual high and low cycle components is shown schematically in these figures. The individual contributions were measured in an experiment with increasing ΔK_{HC} superimposed on steady (not cycled) ΔK_{LC} and in an experiment wit' pure low cycle loading with a triangular waveform and an R ratio of

0.1. For a high cycle frequency of 200 Hz, a low cycle ΔK of 30 MPa $\sqrt{m}$ and a hold time of 180 seconds, Figure 55 shows a reasonable correspondence between actual results and those predicted from a linear summation in the high cycle dominated regime only. For the case of a high cycle frequency of 1825 Hz on the other hand there appears to be deviation in the high cycle dominated regime associated with a difference in ΔK_{tr} and a fair correspondence of crack growth rate in the low cycle dominated regime. These trends, however, are not necessarily representative. In this study, as well as that of Goodman and and Brown[1] a substantial variation in low cycle crack growth rate was apparent for tests carried out under identical conditions. Likewise, for given values of ΔK_{LC} hold time and frequency, a variation in ΔK_{tr} of 20% was apparent. The results of linear summation show a deviation from the combined cycle data that is in the range of variation in crack growth rate behavior for a given set of combined cycle parameters.

With some qualifications, a linear summation provides an adequate representation of combined cycle crack growth rate. In applying the linear summation approach to design, one must be aware of the fact that the low cycle crack growth rate, the retardation behavior and ΔK_{tr} can vary. An appropriate design curve to account for combined crack growth rate is the dashed line construction of Figure 55. The upper bound on low cycle crack growth is the horizontal dashed line. The upper bound on high cycle dominated crack growth is represented by the dashed line on the right side of the diagram. Together, the two curves define an upper bound on crack growth rate in the low cycle dominated, the retardation, and the high cycle dominated regimes. The crack growth rate predicted in the retardation regime would be a significant over estimate. However, this is necessary because the extent of retardation is not easily predicted and its benefit should, therefore, be ignored. Another important factor that must be kept in mind in applying a linear summation rule is that the relationship between crack growth rate and high cycle loading with a high level of mean load (i.e., large enough to cause creep crack growth) is not necessarily unique. For nickel base alloys, crack growth resulting from steady loads has been shown to exhibit non equilibrium behavior. In the present study, this effect was apparent when a small high cycle component was superimposed on a large steady load.

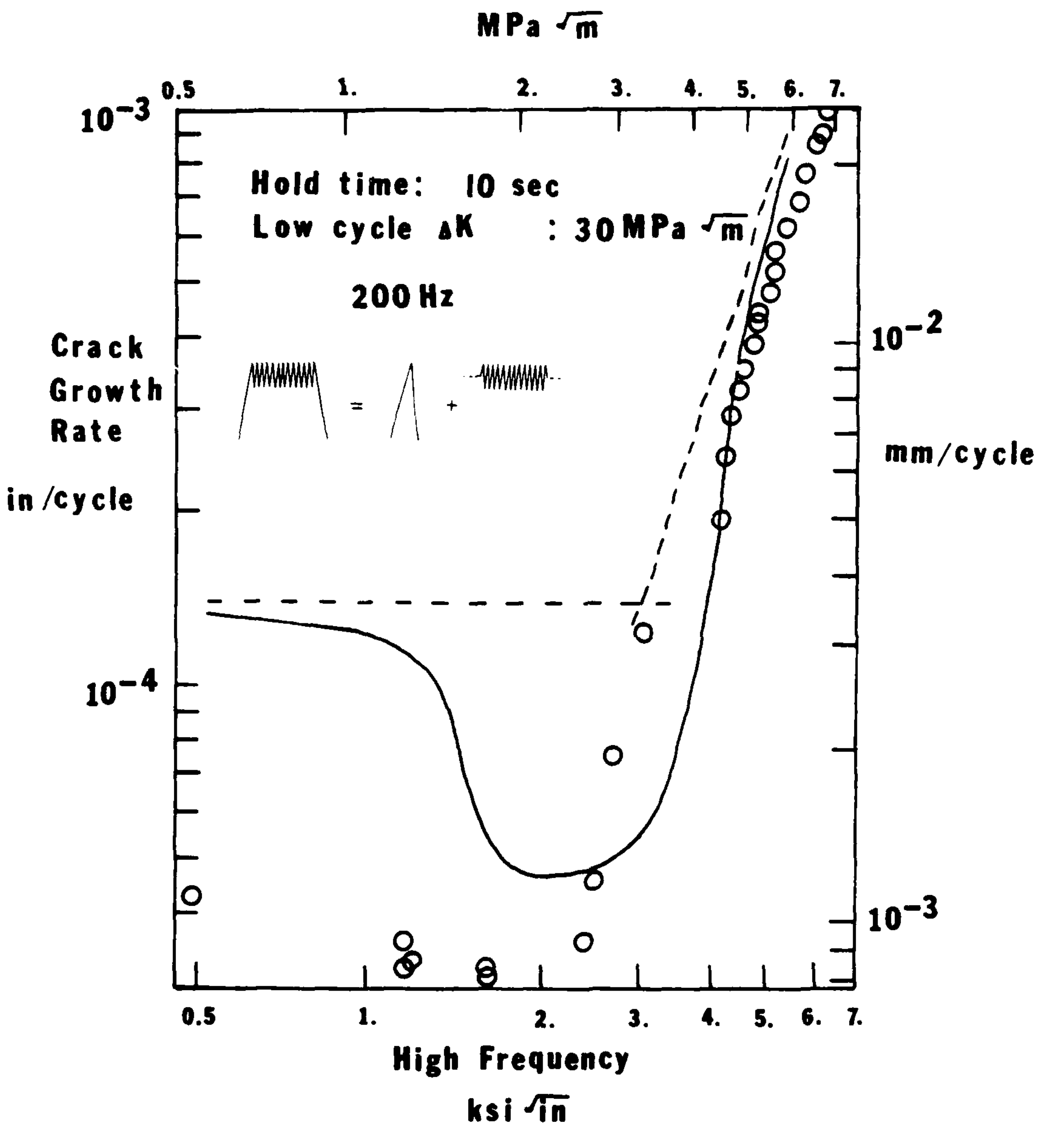

Figure 55 Comparison of Data (Points) with Growth Rate Predicted (Line) From a Linear Summation of Uncycled 1825 Hz High Cycle Data and Pure Low Cycle Data

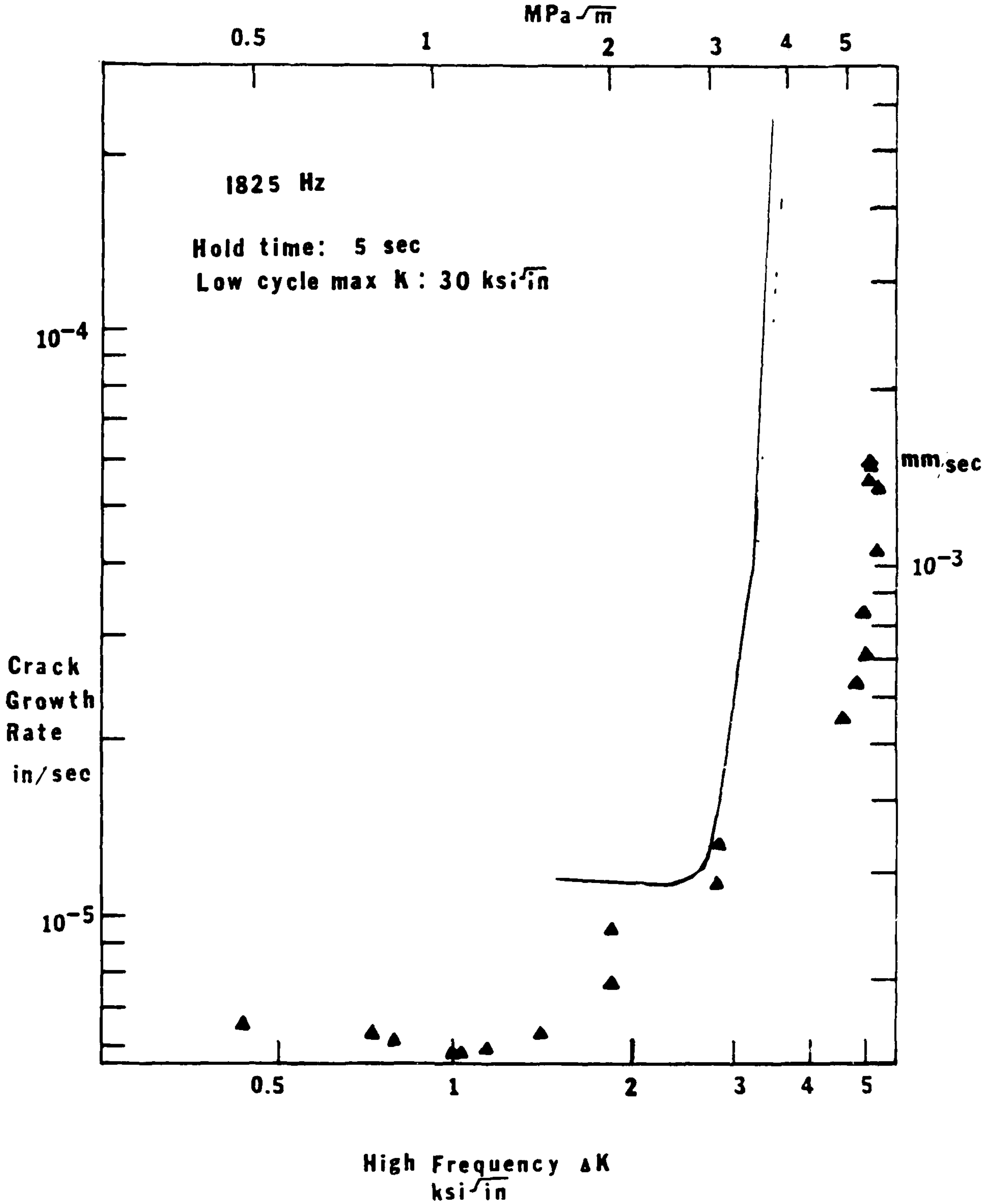

Figure 56 Comparison of Data (Points) With Growth Rate Predicted (Line) From a Linear Summation of Uncycled 1825 Hz High Cycle Data and Pure Low Cycle Data

V CONCLUSIONS

The crack growth rate for Alloy 718 at 649°C was measured for combined cycle loading over ranges of low cycle ΔK, high cycle ΔK, low cycle hold time, and high cycle frequency. Several interesting trends in combined cycle crack growth were revealed. Generally, at lower values of high cycle ΔK, crack growth is dominated by the low cycle components of the load spectrum and with a sufficient level of high cycle loading, crack growth is determined predominantly by the accumulated number of high frequency cycles. These two features of combined loading crack growth behavior were consistent and straight forward. The nature of the transition from the low cycle to high cycle regime, however, depends significantly on the value of low cycle ΔK and to a lesser extent on high cycle frequency and low cycle hold time. The transition from low to high cycle dominated crack growth is obscured by a retardation effect.

This interactive effect is apparent under combined cycle loading generally at low values of ΔK and values of ΔK_{HC} in a range between the purely low and high cycle dominated regimes. Fractographic examination reveals that it is associated with a change in crack growth mechanism from one characterized by intergranular fracture for pure low cycle loading to transgranular fracture for combined cycle loading. The degree of crack growth retardation appears to decrease with increasing low cycle ΔK and also decreases with increasing high cycle frequency. Another interesting featrue associated with the retardation effect is that a crack growth interval of several plastic zone sizes is required for its development or relaxation. Considering this fact and the fact that it becomes increasingly less pronounced with increasing ΔK_{LC}, leads to the conclusion that the retardation effect is associated with a change in the extent of plastically deformed material left in the wake of the advancing crack when high cycle loading is applied.

The slope of the log (crack growth rate per unit time) versus log ΔK_{HC} curve beyond ΔK_{tr} increases with increasing frequency as one would expect for a situation where crack growth rate in the high cycle regime is dependent on the number of cycles. The shape of the curve in the high cycle dominated regime is similar to that experienced for near threshold behavior (Stage I) observed in constant R ratio tests. (The R ratio of the high cycle loading in these studies varies with ΔK_{HC}).

A crack growth rate prediction based on the linearly summed contributions for the high and low cycle components of loading correlate well in the case of a high cycle frequency of 200 Hz with some deviation in the low cycle dominated regime. For the case of 1825 Hz some deviation was observed for the high cycle dominated regime. This may be associated with the intrinsic variation in ΔK_{tr}.

BIBLIOGRAPHY

1. Goodman, R.C. and Brown, A.M., "High-Frequency Fatigue of Turbine Blade Materials", Report #AFWAL-TR-82-4151 (Materials Laboratory, Air Force Wright Aeronautical Laboratories), Contract No. F33615-79-C-5108, October 1982.

2. Ling descriptive brochures of electrodynamic shakers, Ling Electronics Inc. 1525 South Manchester Ave. Anaheim, California 92803.

3. Beyer, J.R., Sims, D.L., Wallace, R.M., "Titanium Damage Tolerant Design Data for Propulsion Systems", Air Force Materials Laboratory Report, AFML-TR-77-101.

4. Instron Limited, "Major/Minor Cycling System", Instron Limited, Coronation Rd, High Wycombe, Bucks HP123SY.

5. Ling - Akashi brochure on 2000 Hz hydraulic system.

6. MTS Systems Corporation, "Dynamic High Frequency Test System", Application note, MTS Systems Corporation, Box 24102, Minniapolis, Minnesota 55424.

7. Thomas Lagnese, private communication.

8. Gell, M., Leverant, G.R. "Mechanisms of High-Temperature Fatigue," ASTM, STP 520, 1973, p.37.

9. Gell, M. and Organ, F.E., "The Effect of Frequency on the Elevated Temperature Fatigue of a Nickel-Base Superalloy, "Metall. Trans., Vol.2, April 1971, p.943.

10. Gell, M., Leverant, G.R. and Wells, C.H., "The Fatigue Strength of Nickel-Base Superalloys," Achievement of High Fatigue Resistance in Metals and Alloys, ASTM STP 467, American Society for Testing and Materials, 1970, pp.113-153.

11. Leverant, G.R. and Gell, M. "The Influence of Temperature and Cycle Frequency on the Fatigue Fracture of Cube Oriented Nickel-Base Superalloy Single Crystals" Metallurgical Transaction A, Vol.6A, p.367, Feb. 1975.

12. Clavel, M. and Pineau, A., "Frequency and Wave Form Effects on the Fatigue Crack Growth Behavior of Alloy 718 at 298°K and 823°K", Metallurgical Transactions A, Vol.9A, p.471 (1978).

13. Sullivan, C.P., Webster, G.A., and Piearcey, B.J., "The Effect of Stress Cycling on the Creep Behavior of a Wrought Nickel-Base Alloy at 955°C", Journal of the Institute of Metals, Vol.96, p.274, (1968).

14. Scarlin, R.B., "Effects of Loading Frequency and Environment on High Temperature Fatigue Crack Growth in Nickel-Base Alloys", Fracture 1977, Vol.2, p.849, Proceedings of ICF4, Waterloo, Canada, June, 1977.

15. Solomon, H.D., and Coffin, L.F., Jr., "Effects of Frequency and Environment on Fatigue Crack Growth in A-286 at 1100°F", ASTM STP 520, 1973, p.112.

16. Eisenstadt, R. and Smail, D.L. "The Effect of Frequency on Cyclic Crack Growth in 200 Managing Steel in a Salt Water Environment", Fracture 1977, Vol.2, p.911, Proceedings of ICF4, Waterloo, Canada, June, 1977.

17. Mautz, and Weiss, "Mean Stress and Environmental Effects on Near Threshold Fatigue Crack Growth, "Cracks and Fracture, ASTM STP601, American Society for Testing and Materials, 1976, pp.154-168.

18. St. Stanzl, and Mische, R., "High Frequency Fatigue of Metals, Crack Initiation and Propagation", Fracture, 1977, Vol.2. p.249, ICF4, Waterloo, Canada, June, 1977.

19. Venkiteswaran, P.K., Ferguson, D.C. and Taplin, D.M.R., "Combined Creep-Fatigue Behavior of Inconel Alloy X-750", Fatigue at Elevated Temperatures, ASTM STP520, American Society for Testing and Materials, 1973, pp.462-472.

20. Davies, P.W. and Wilshire, B., "Some Observations on the Creep and Fracture of Nimonic 80A Under Combined Creep/Fatigue Conditions", Journal of the Institute of Metals, Vol.97, p.15, (1969).

21. Price, A.T. "Creep-Fatigue Behavior of Polycrystaline Zinc", Journal of the Institute of Metals, Vol. 95, p.87, (1967).

22. Melika, A.H. and Evershed, A.V., "The Dependence of Creep Behavior on the Duration of a Superimposed Fatigue Stress", Journal of the Institute of Metals, Vol.88, p.411.

23. Kamel, R. and Bessa, F.A., "Effect of Superimposed Small Vibrations on the Static Creep Behavior of Polycrystalline Zinc", Acta Metallurgical, Vol.13, p.19, (1985).

24. Atommo, P.N. and McEvily, A.J., Jr., "Creep-Fatigue Interaction During Crack Growth", Fatigue at Elevated Temperatures, ASTM STP 520, American Society for Testing and Materials, 1973, pp.157-165.

25. Powell, B.E. Duggan, T.V., and Jeal, R.H., "The Influence of Minor Cycles on Low Cycle Fatigue Crack Propagation", International Journal of Fatigue, Vol.4, No.1, (1982).

26. Powell, B.E., "The Onset of Minor Cycle Activity", Interim report on Contract "AFOSR-82-0077 (Air Force Office of Scientific Research), Portsmouth Polytechnic, Portsmouth, U.K., March, 1982

27. Powell, B.E., and Henderson I., "Predicting Fatigue Crack Growth Rates", Interim report on contract #AFOSR-82-0077, (Air Force Office of Scientific Research), Portsmouth Polytechnic, Portsmouth, U.K., June, 1982.

28. Dugdale, D.S., "Yielding of Steel Sheets Containing Slits", J. Mech. Phys. Solids, (1960) p.100.

29. To, K.C., "A Phenomenological Theory of Subcritical Creep Crack Growth Under Constant Loadng in an Inert Environment", "International Journal of Fracture", Vol.11, No.4, August 1975, p.641.

30. Elber, W., "Fatigue Crack Closure Under Cyclic Tention". "Engineering Fracture Mechanics, Vol.2, 1970, pp.37-45.

31. Macha, D.E., Grandt, A.F., Jr., and Wicks, C.J., "Effects of Gas Turbine Engine Load Spectrum Variables on Crack Propagation, "Effects of Load Spectrum Variables on Fatigue Crack Initiation and Propagation, ASTM STP 714. D.F. Bryan and J.M. Potter, Eds., American Society for Testing and Materials, 1980, pp.108-127.

32. Larsen, J.M. and Annis, C.G., Jr., "Observation of Crack Retardation Resulting from Load Sequencing Characteristic of Military Gas Turbine Operation", Effect of Load Spectrum Variables on Fatigue Crack Initiation and Propagation. ASTM STP 714, D.F. Bryan and J.M. Potter, Eds., American Society for Testing and Materials, 1980, pp.91-107.

33. Larsen, J.M., Schwartz, B.J., and Annis, C.G., "Cumulative Damage Fracture Mechanics Under Engine Spectra", Air Force Materiasl Laboratory Report II AFML-TR-79-4159, January, 1980.

34. Newman, J.C., Jr., "A Crack-Closure Model for Predicting Fatigue Crack Growth Under Aircraft Spectrum Loading", J.B. Chang and C.M. Hudson, eds., ASTM STP748, 1981, pp.52-84.

35. Johnson, W.S., "Multi-Parameter Yield Zone Model for Predicting Spectrum Crack Growth, "Methods and Models for Predicting Fatigue Crack Growth Under Random Loading, J.B. Chang and C.M. Hudson, eds., ASTM STP748, 1981, pp.85-102.

APPENDIX A

PERFORMANCE OF HIGH FREQUENCY SERVO-HYDRAULIC SYSTEM

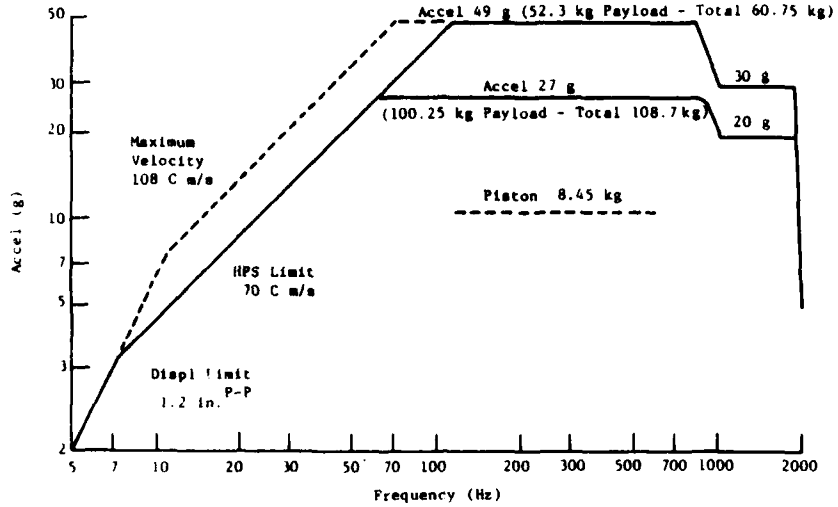

Figure A-1 HVIO-1.2-37/5 Test Data (Vertical) Maximum Performance (ront Mount Type)

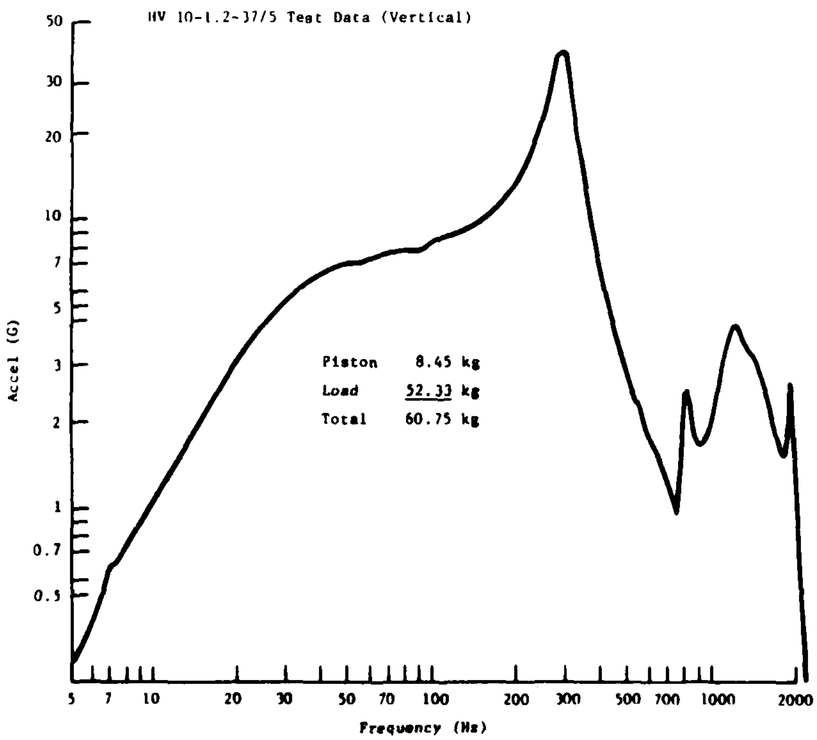

Figure A-2 Front Mount Type Constant Input-Frequency Response

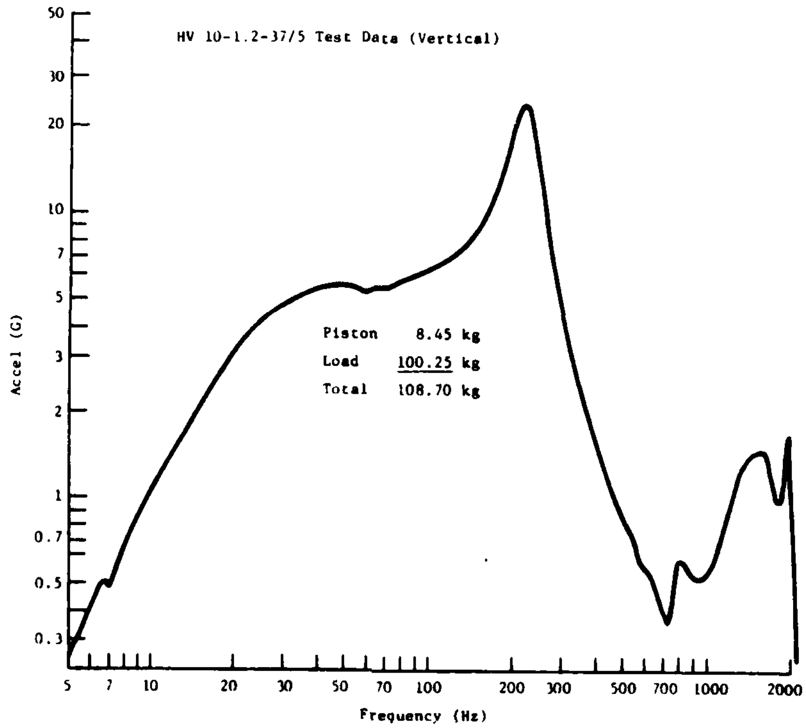

Figure A-3 Front Mount Type Constant Input-Frequency Response

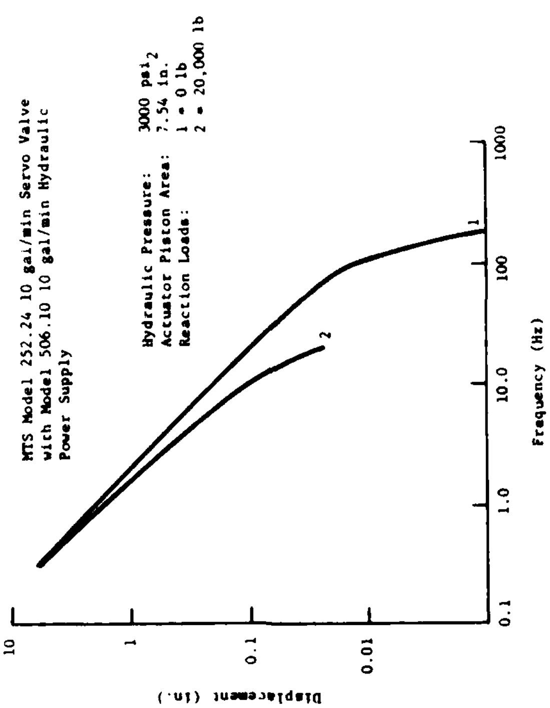

Figure A-4 MTS System Fatigue Performance

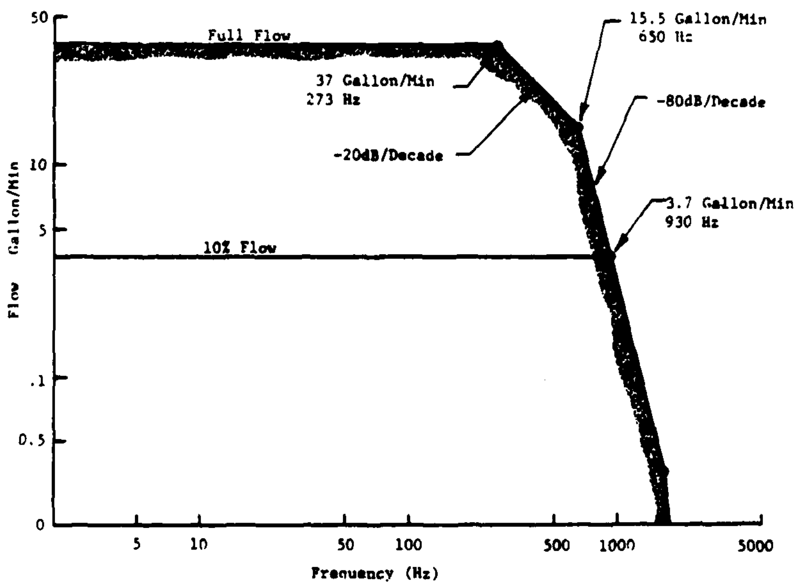

Figure A-5 Flow Versus Frequency for Akashi 37 gpm servo-valve

APPENDIX B

DATA PLOTS FOR ALL TESTS

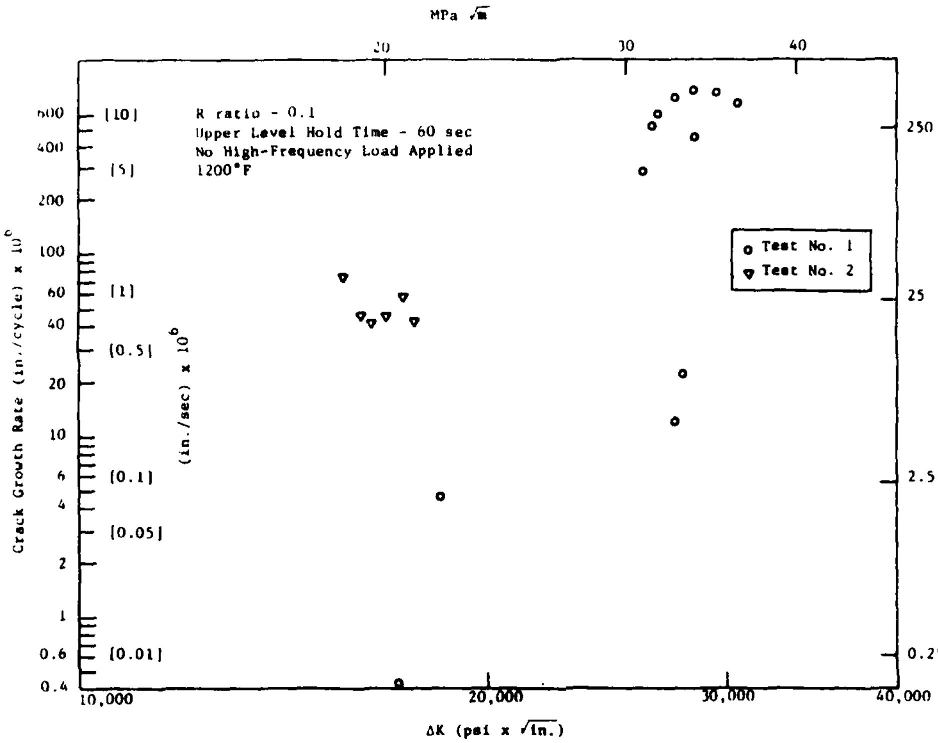

Figure B-1 Test No. 1 and No. 2

84058

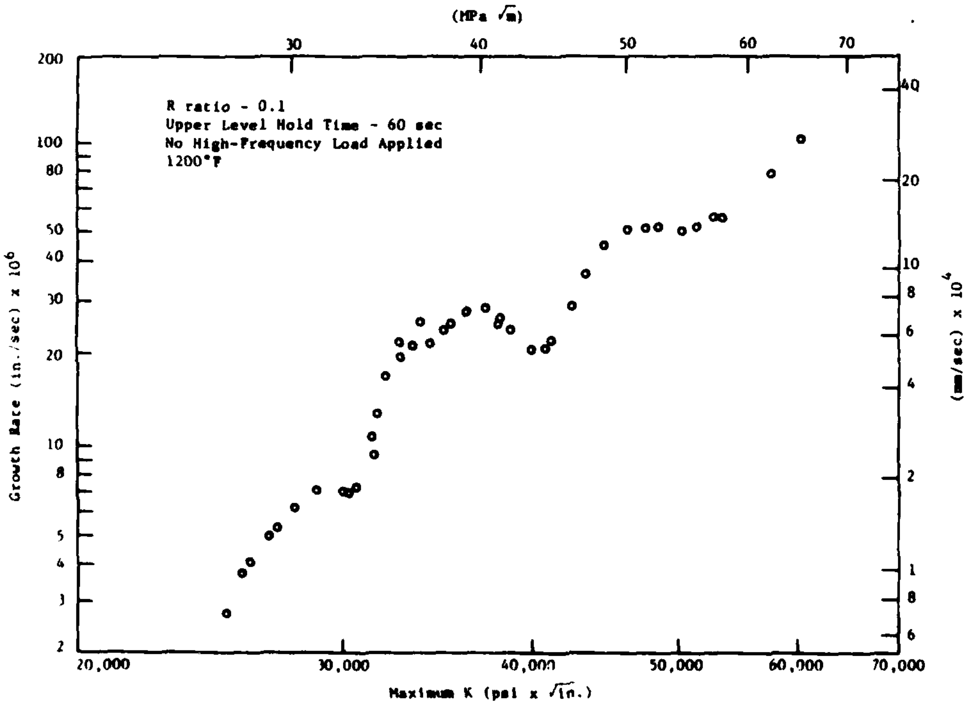

Figure B-2 Test No. 3

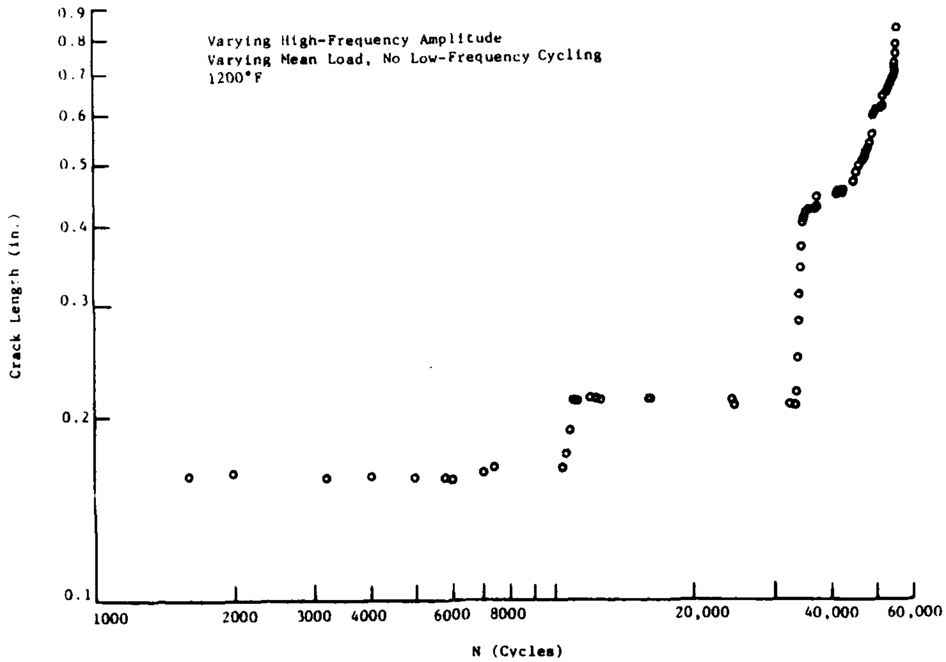

Figure B-3 Test No. 4

84080

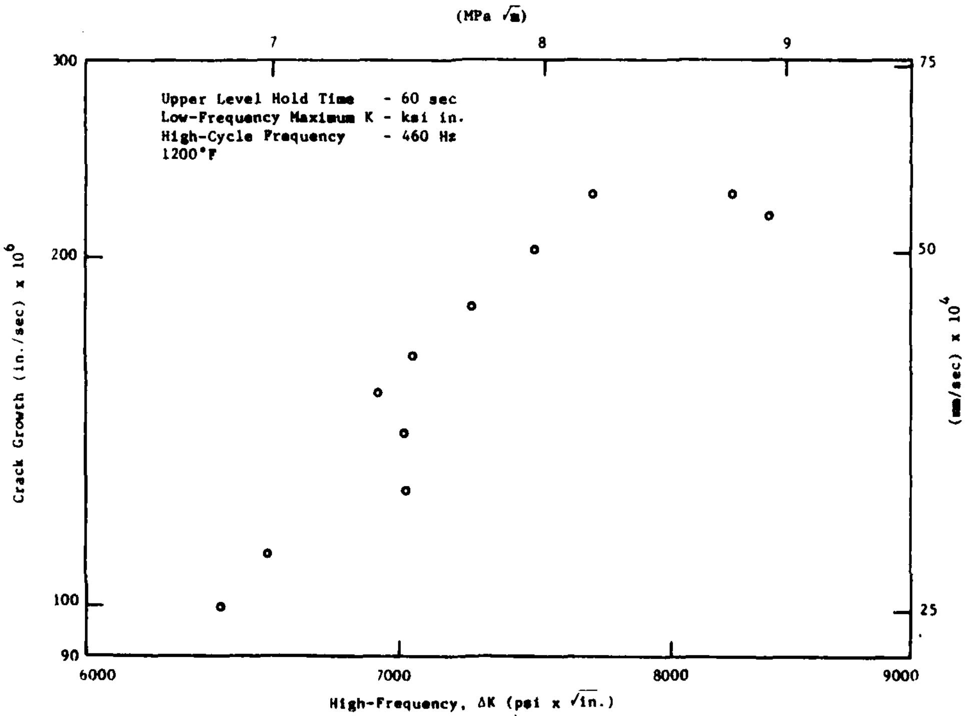

Figure B-4 Test No. 6

84081

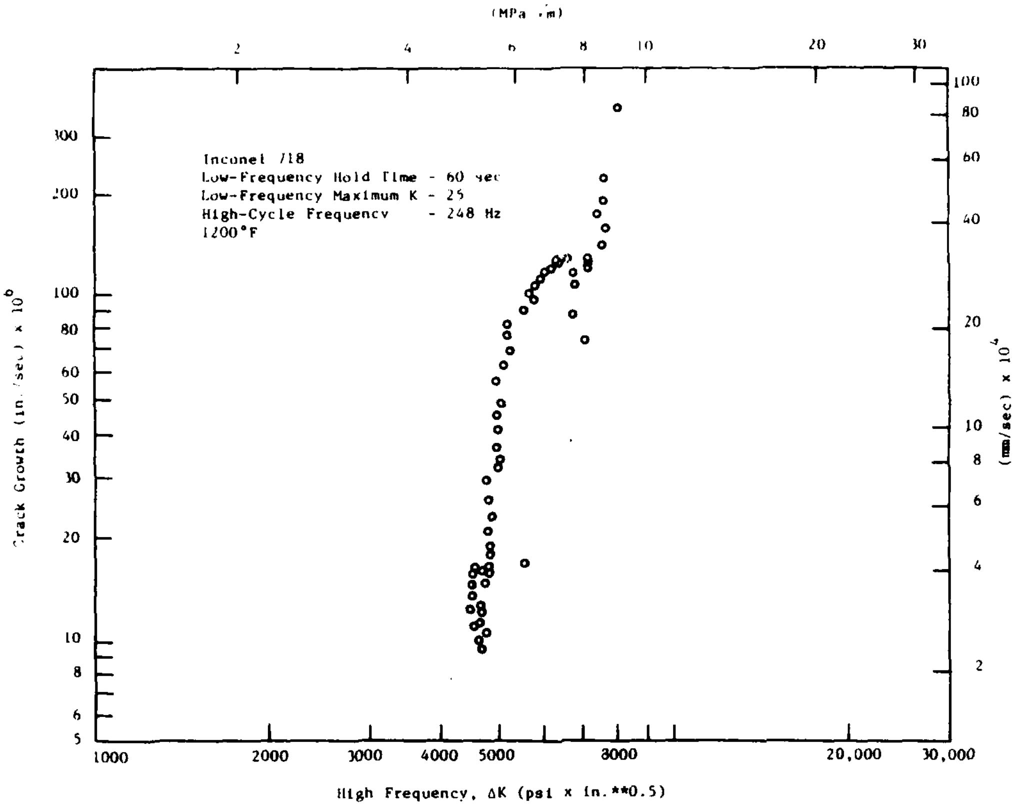

Figure B-5 Test No. 7

84067

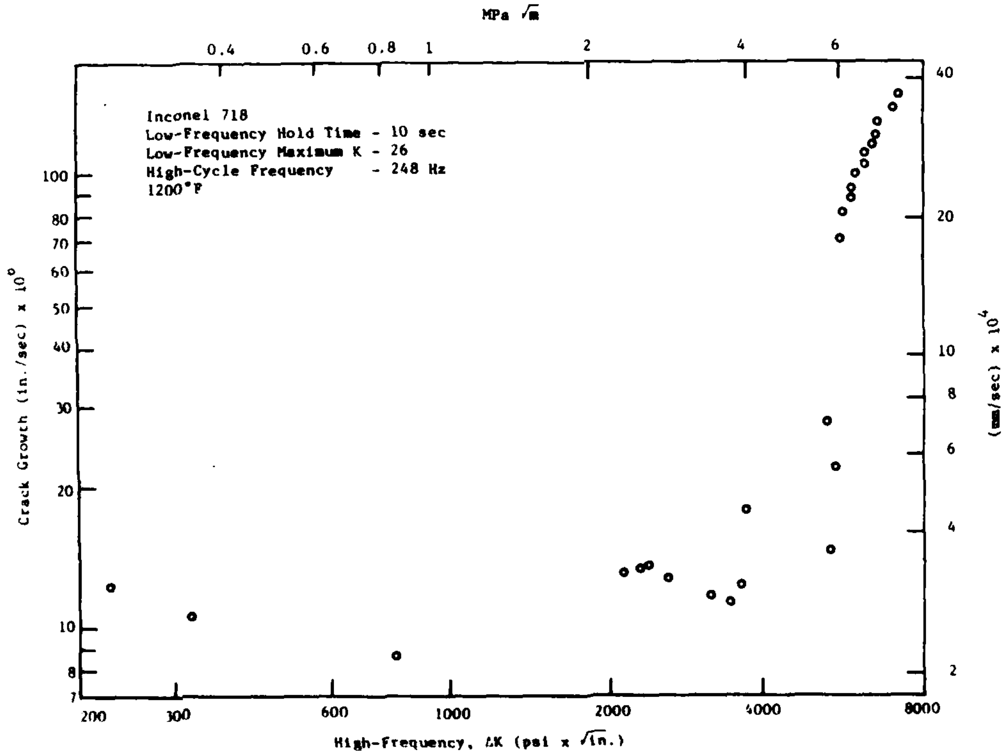

Figure B-6 Test No. 8

84411

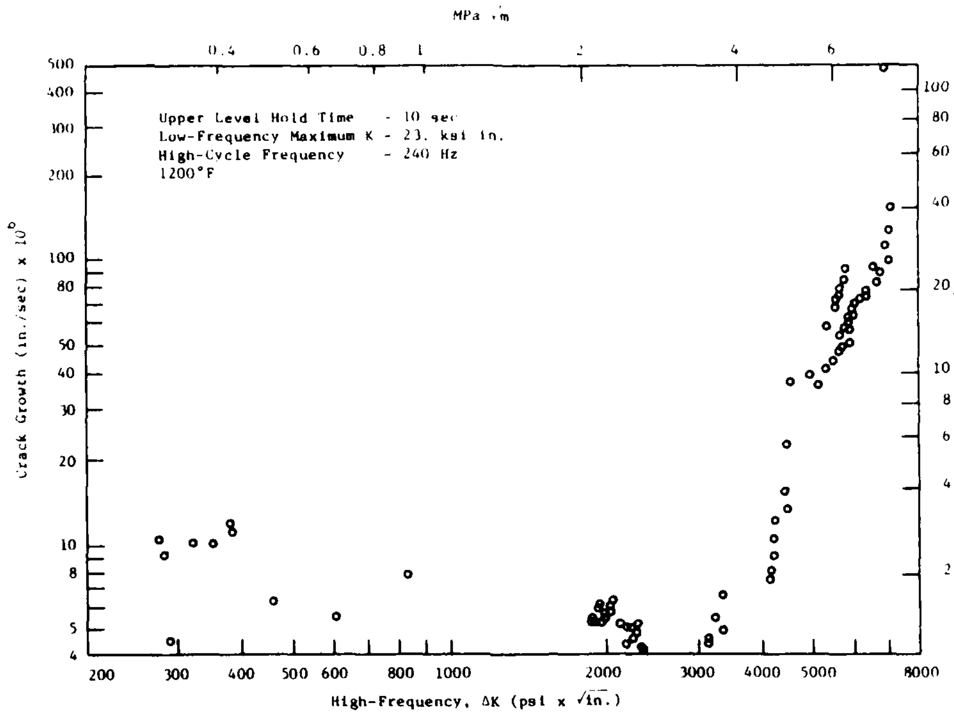

Figure B-7 Test No. 9

84082

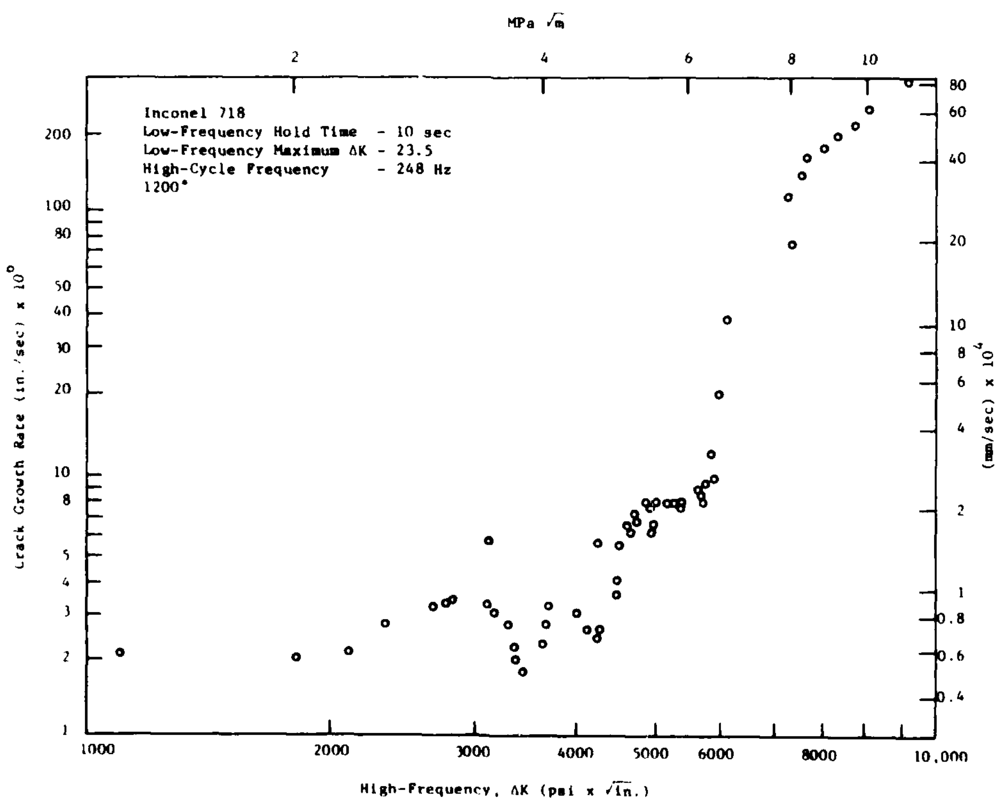

Figure B-8 Test No. 10

84083

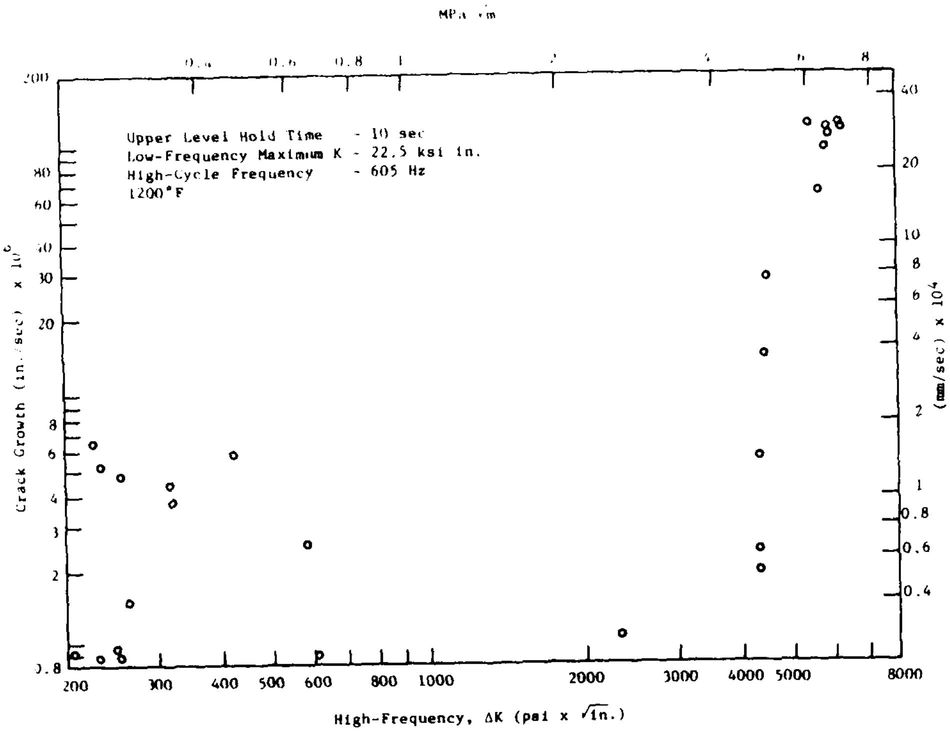

Figure B-9 Test No. 11

84106

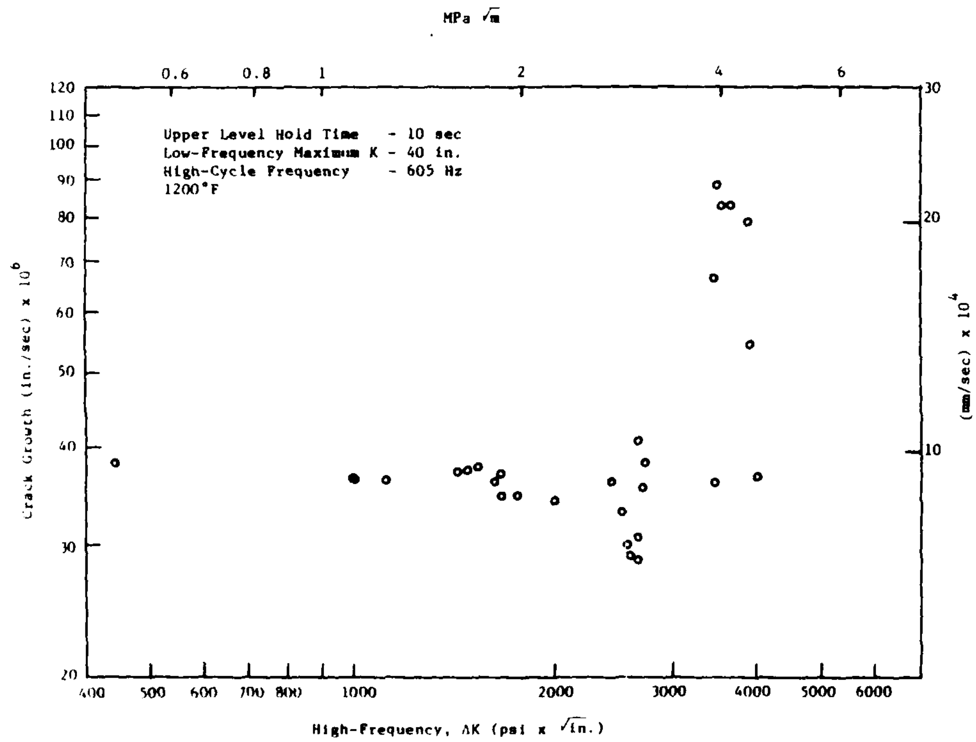

Figure B-10 Test No. 12

84107

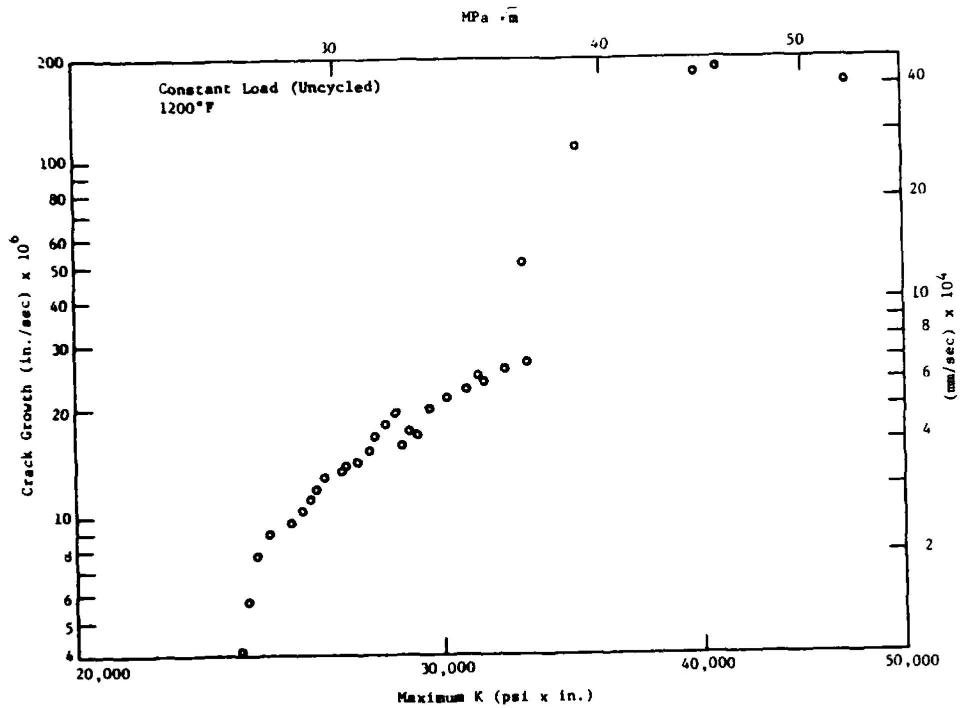

Figure B.11 Test No. 13

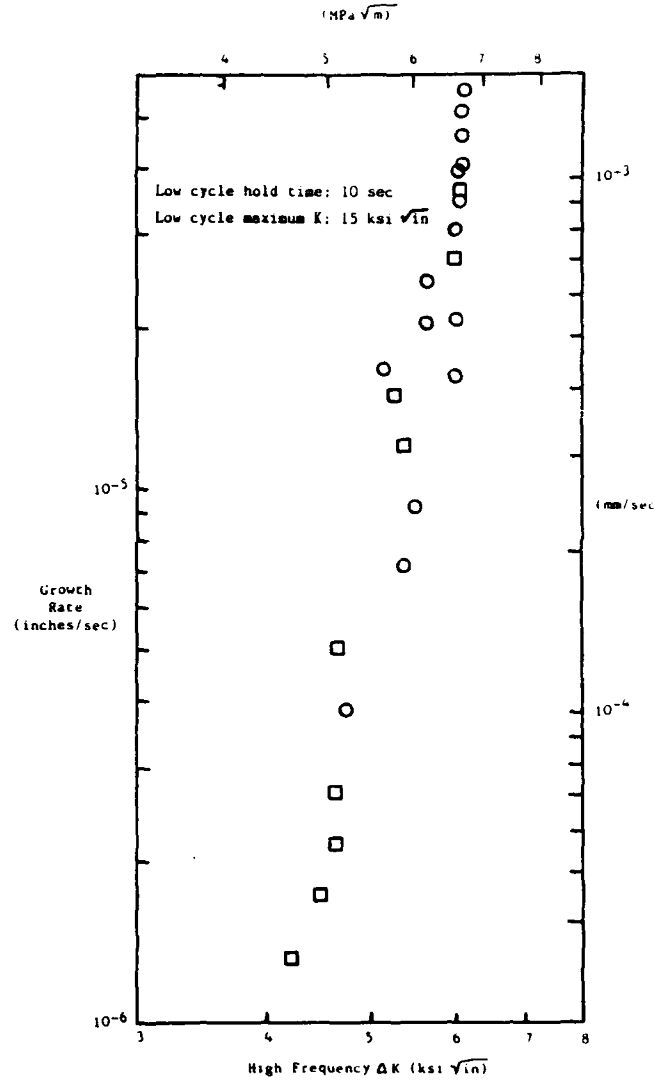

Figure B.12 Test No. 20

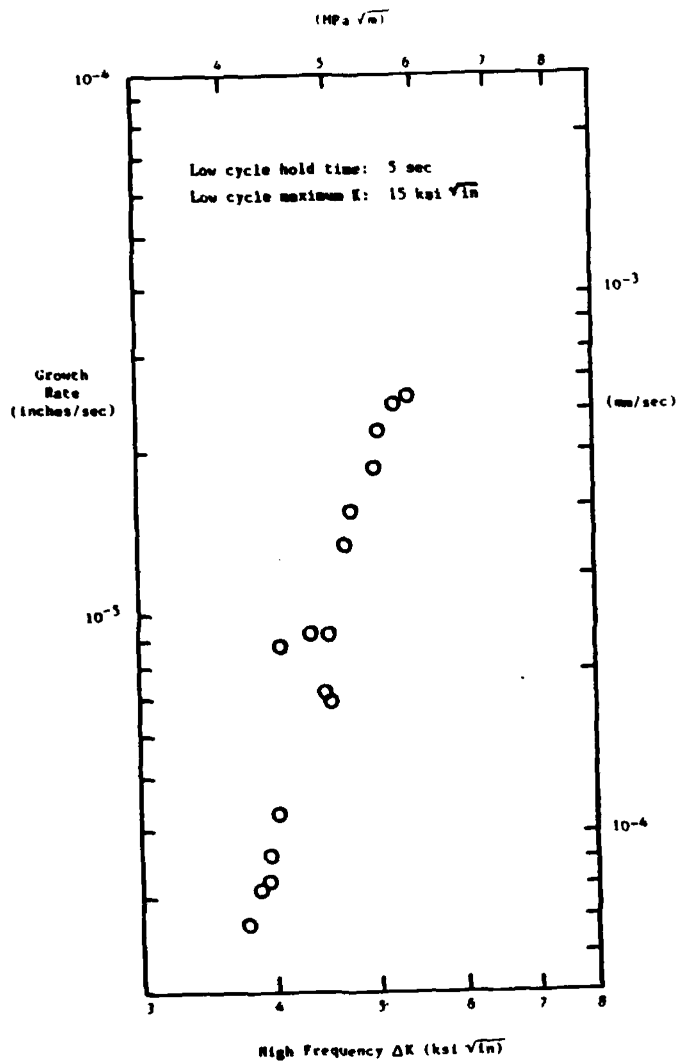

Figure B.13 Test No. 21

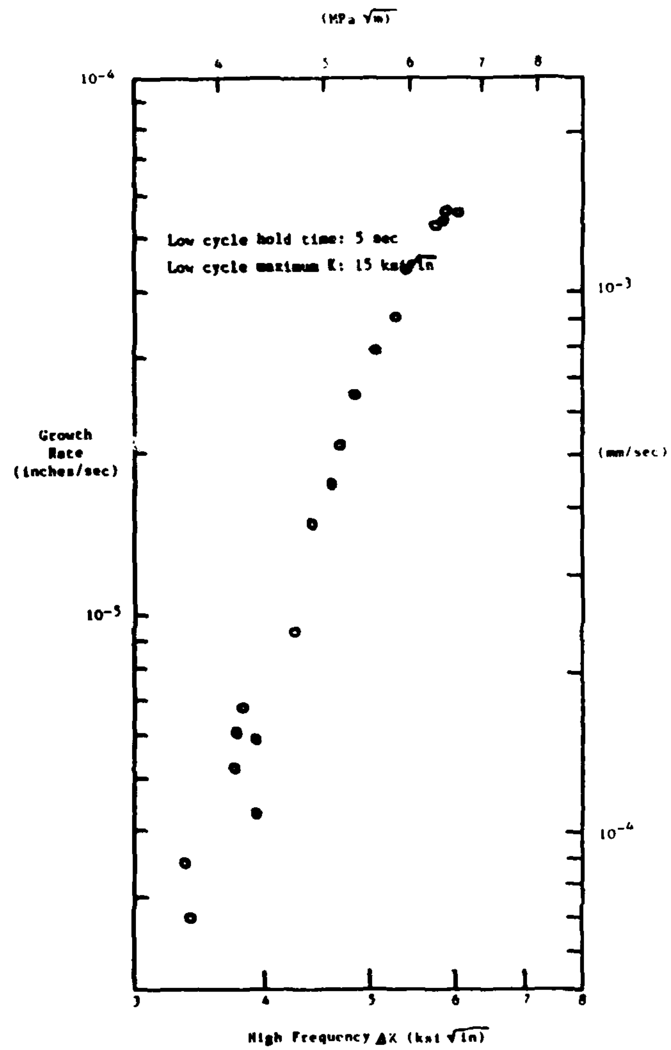

Figure B.14 Test No. 23

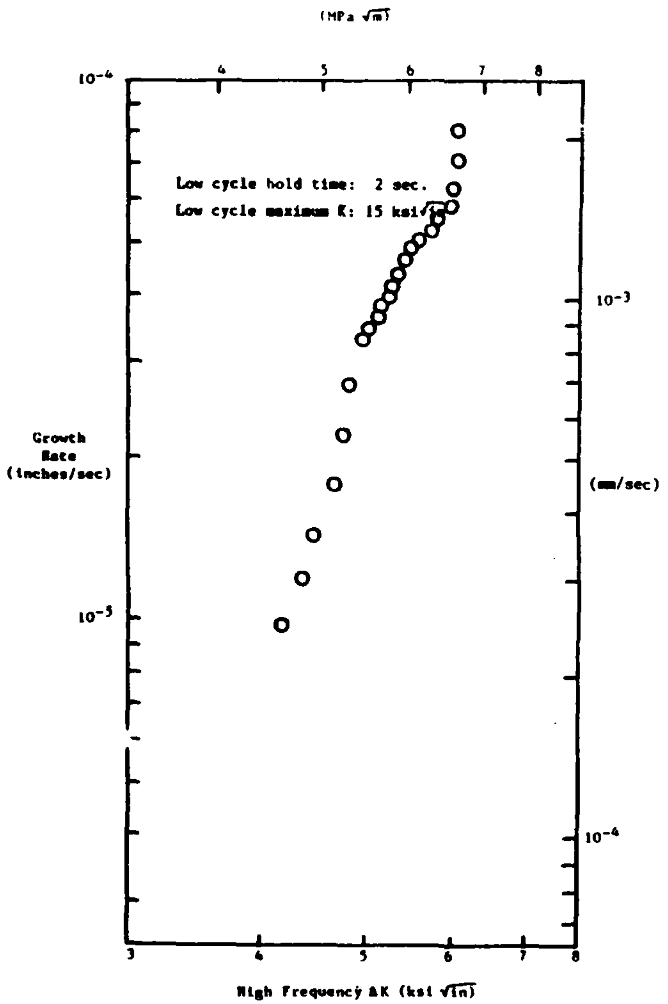

Figure B.15 Test No. 25

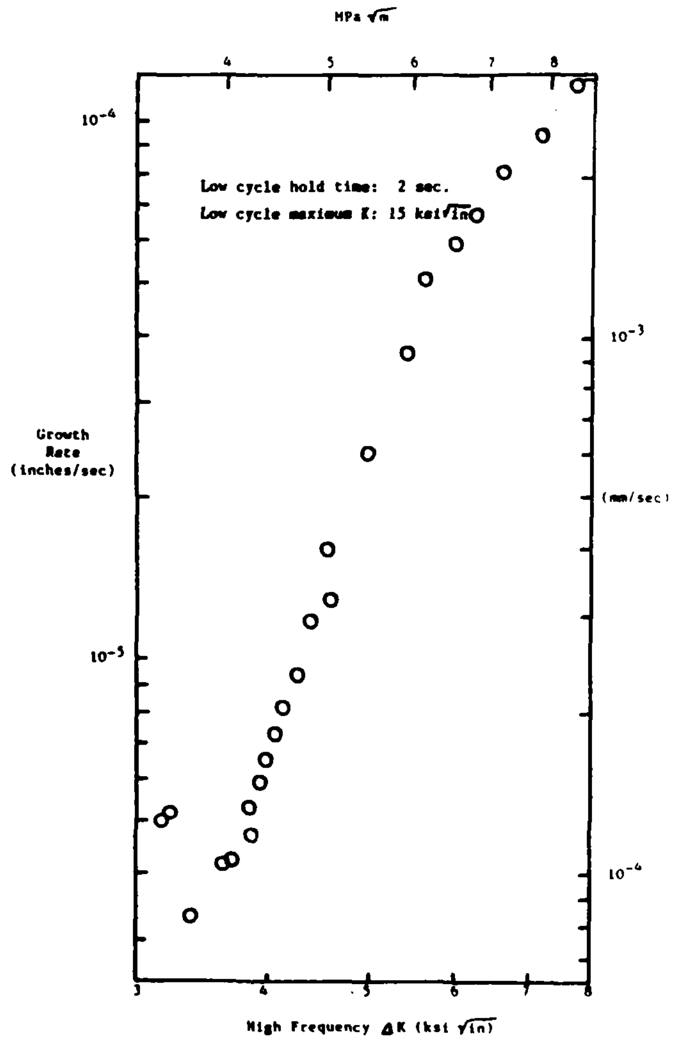

Figure B.16 Test No. 24

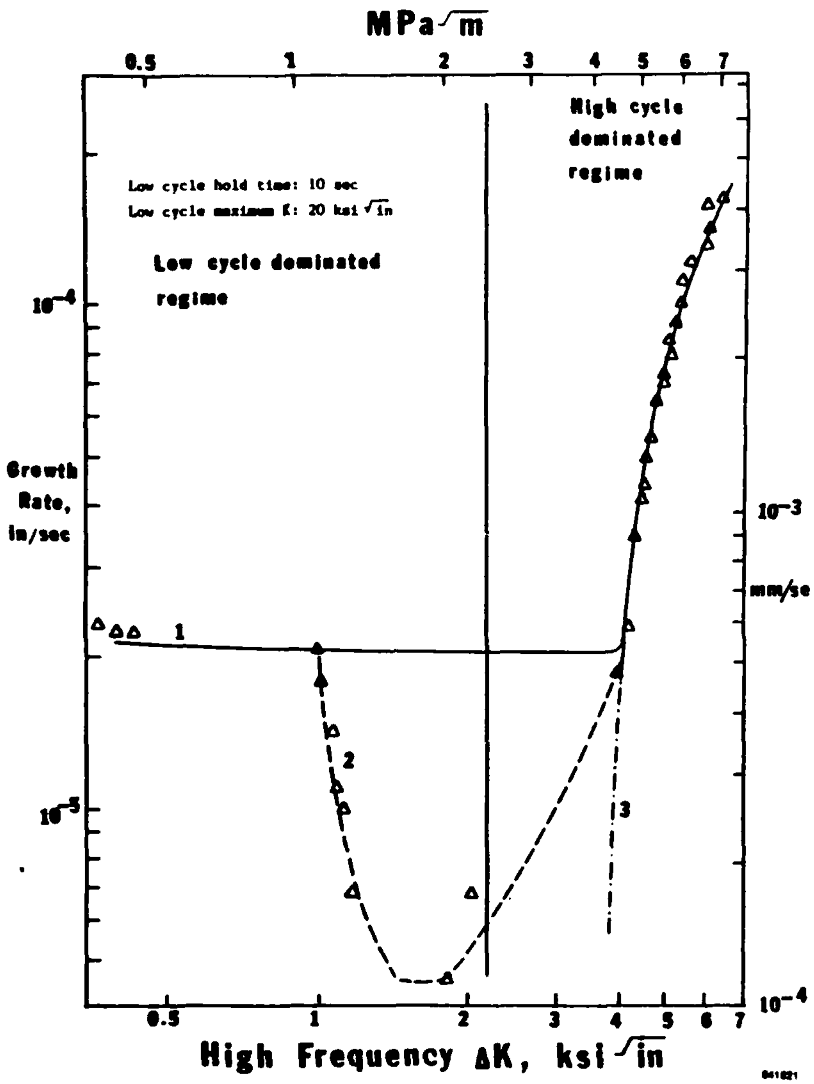

Figure B.17 Test No. 26

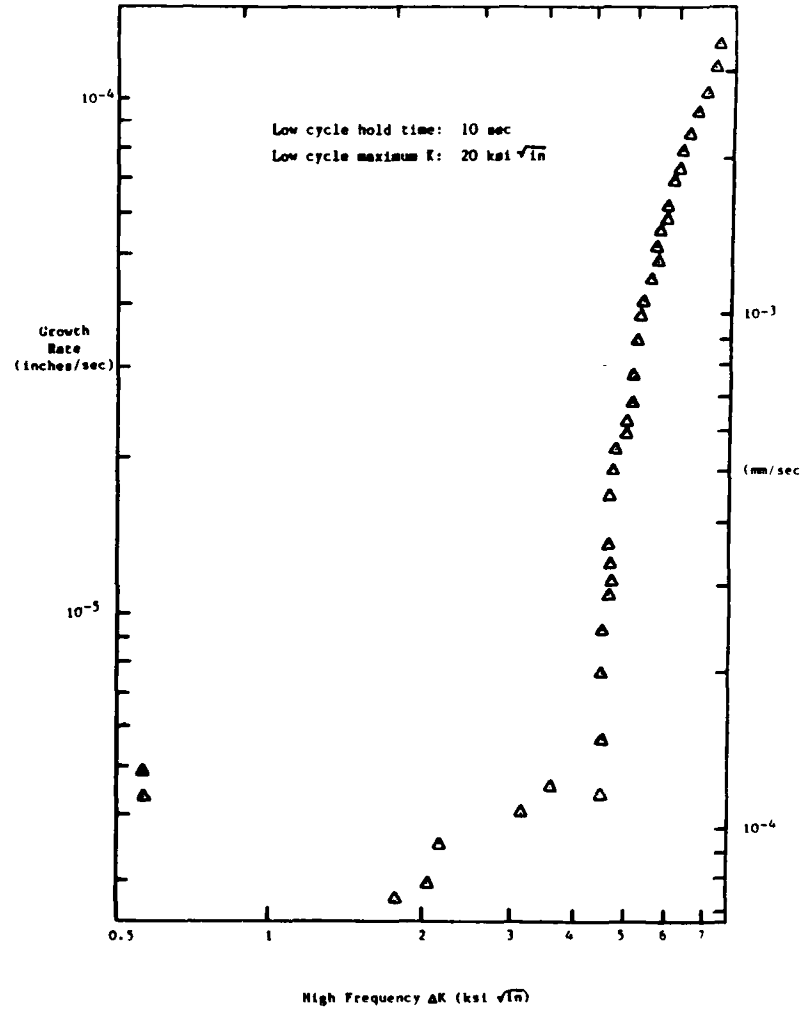

Figure B.18 Test NO. 27

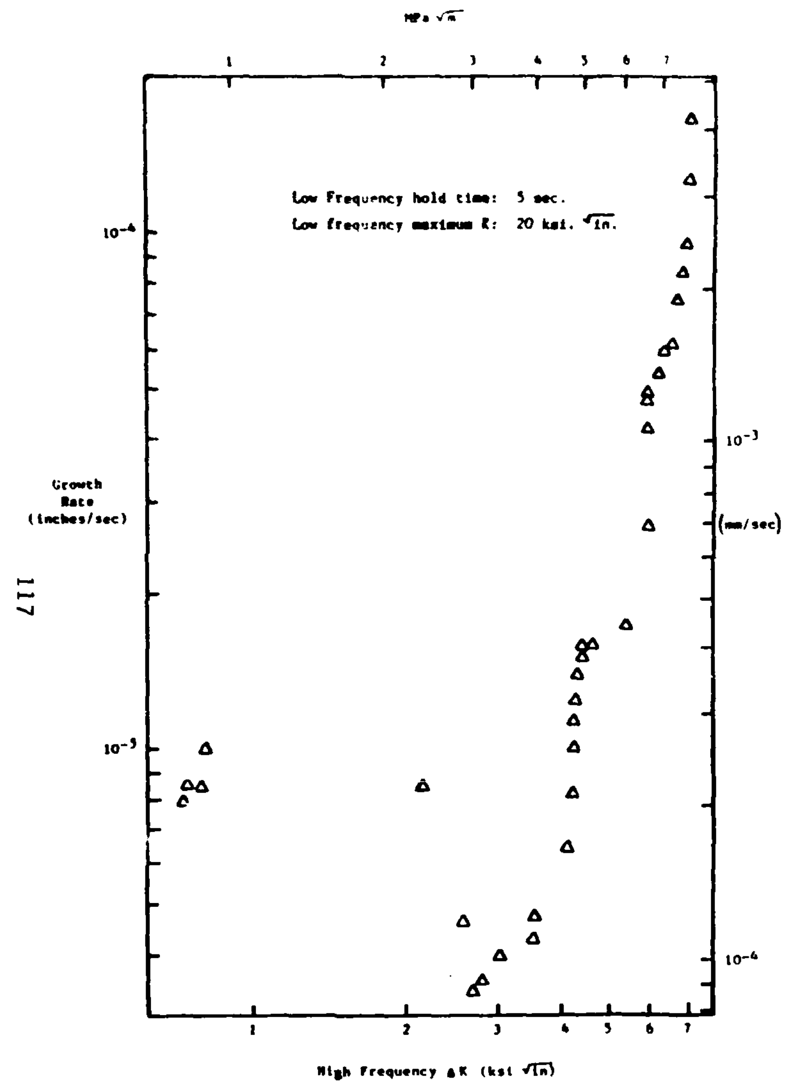

Figure B.19 Test No. 28

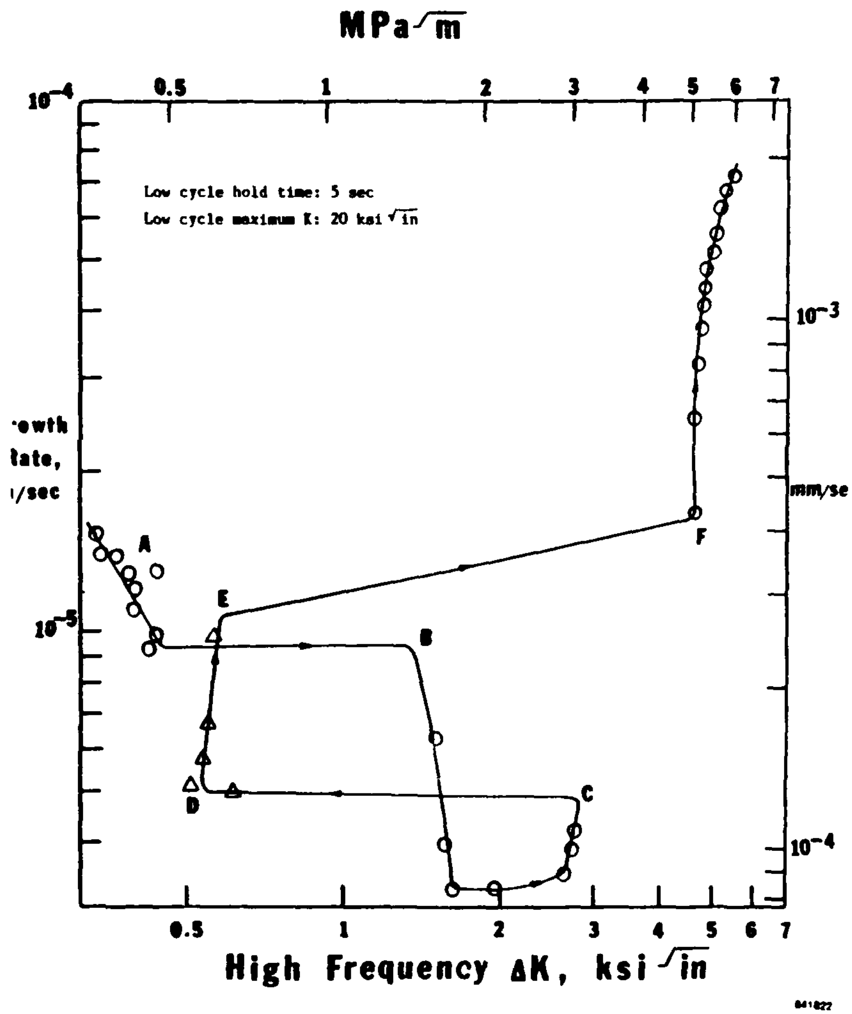

Figure B. 20 Test No. 30

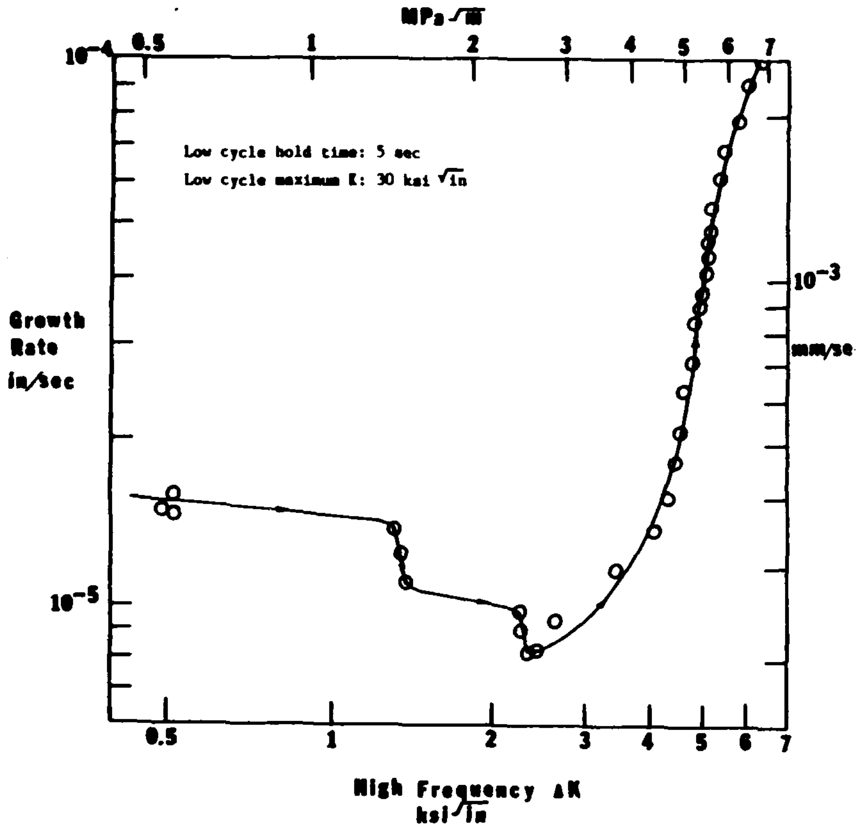

Figure B.21 Test No. 31

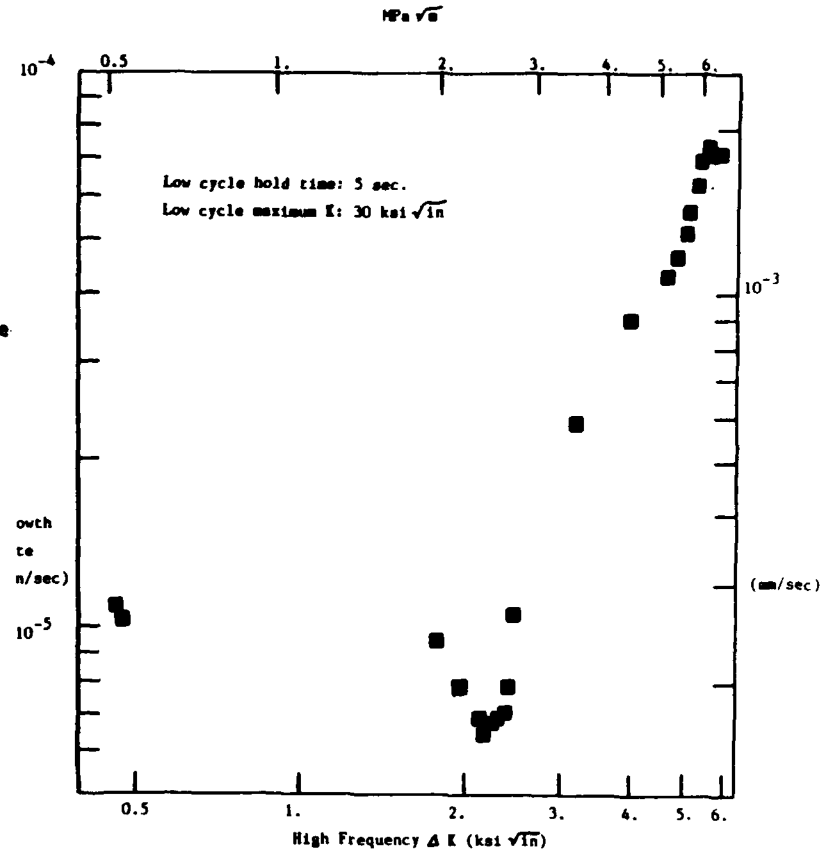

Figure B.22 Test No. 32

841823

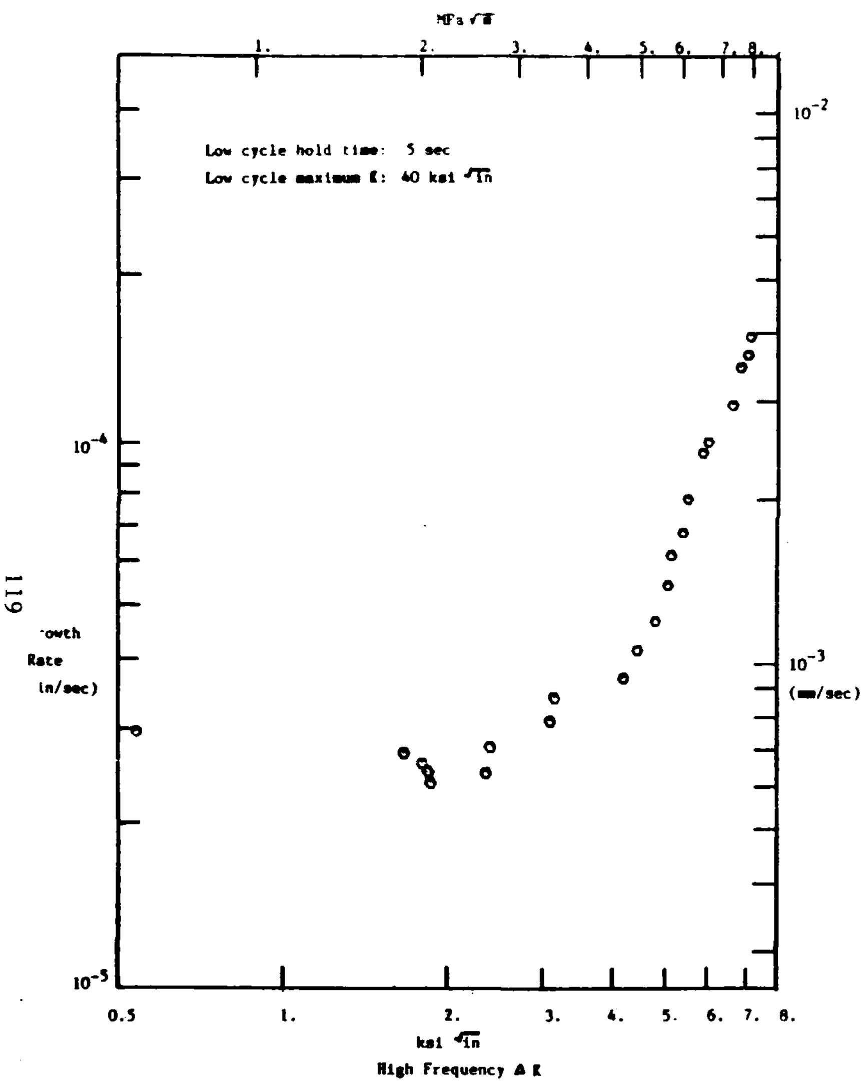

Figure B.23 Test No. 33

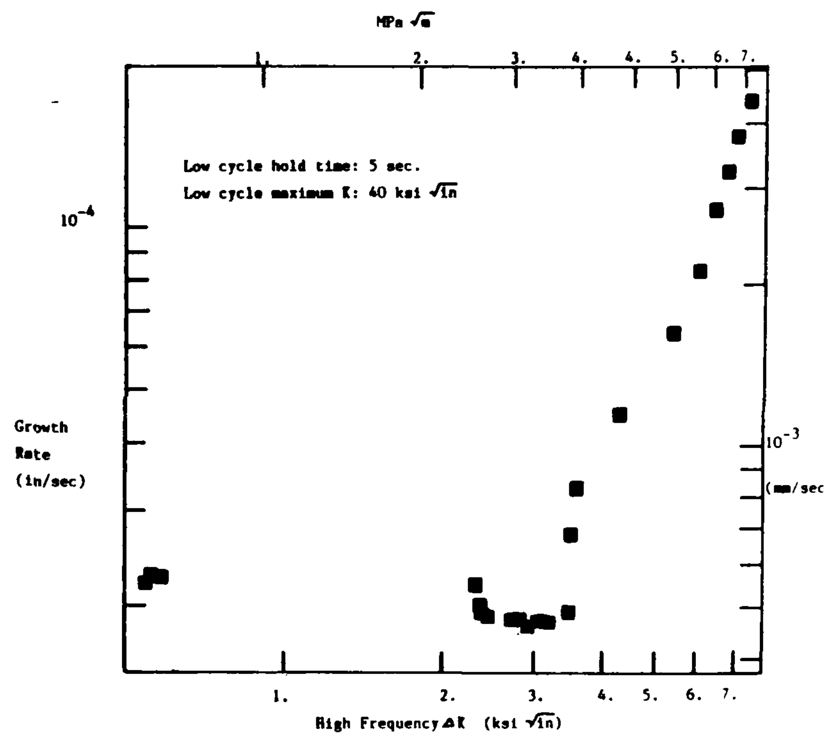

Figure B.24 Test No. 34

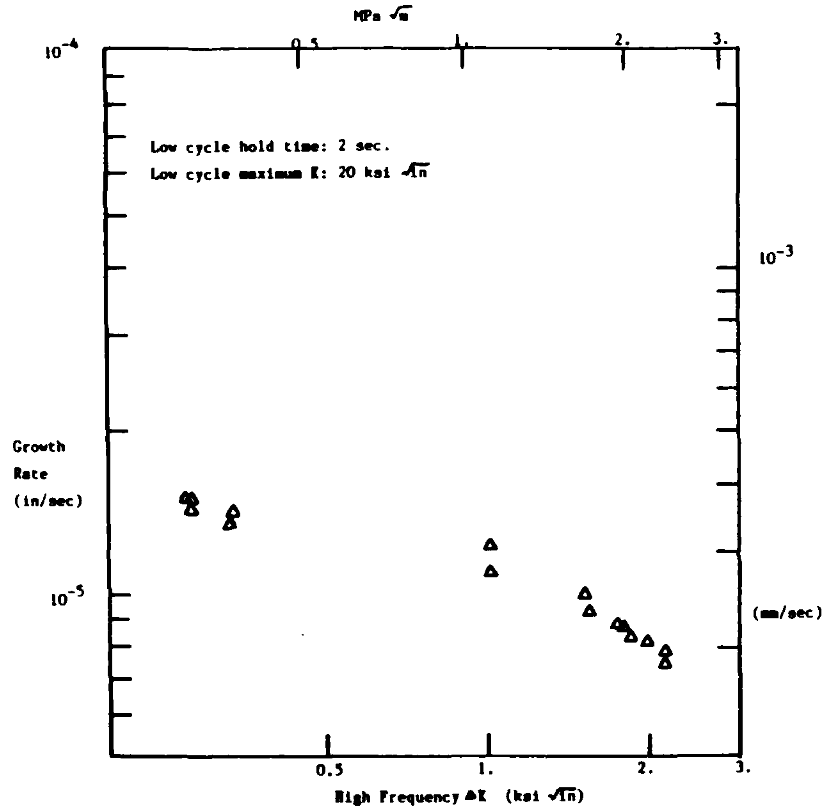

Figure B.25 Test No. 35

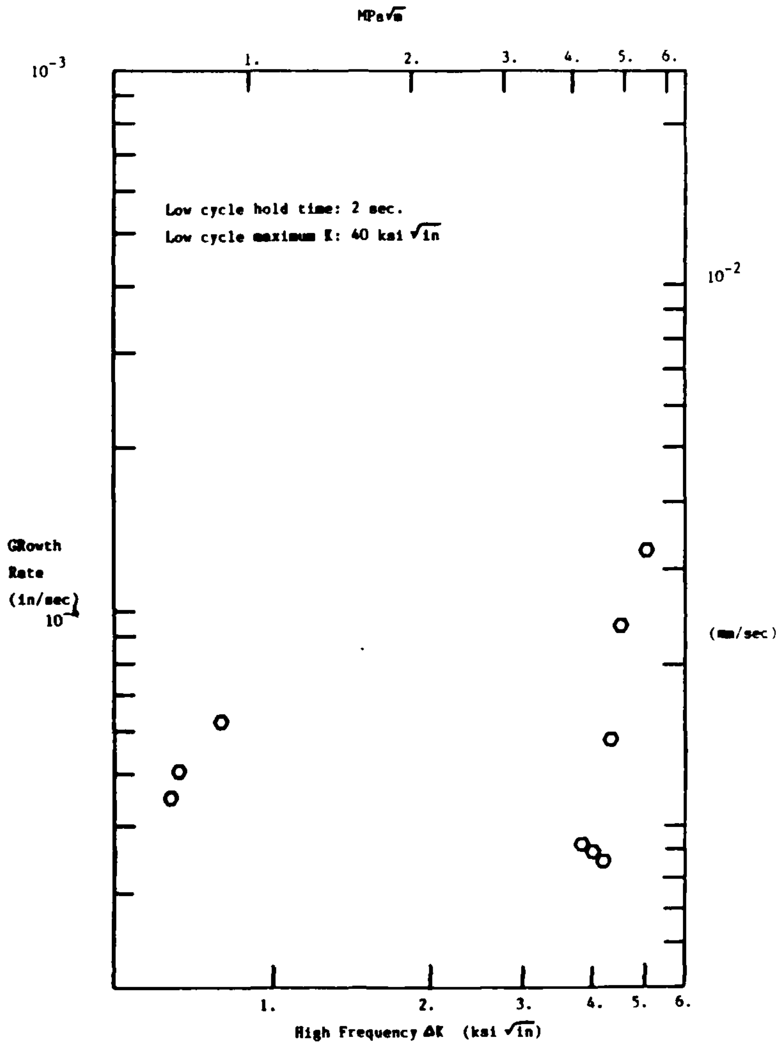

Figure B.26 Test No. 36

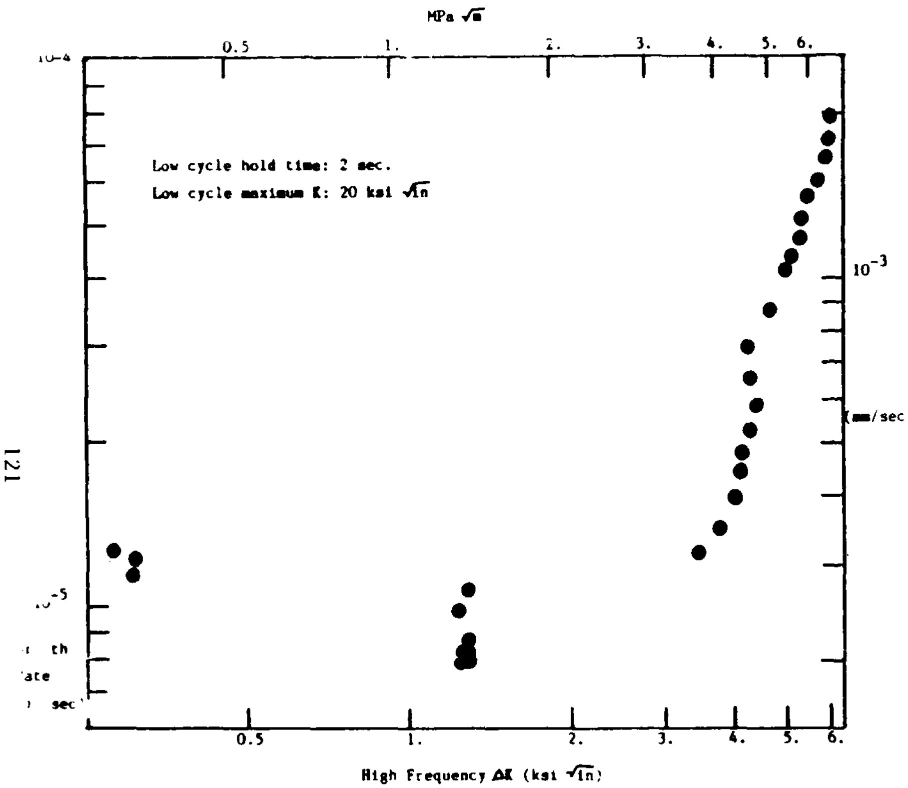

Figure B.27 Test No. 37

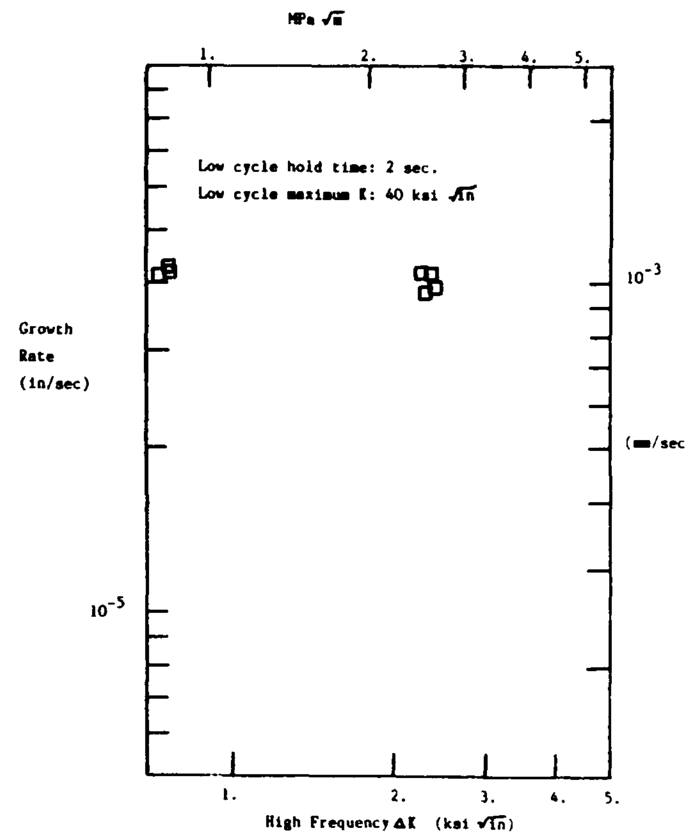

Figure B.28 Test No. 38

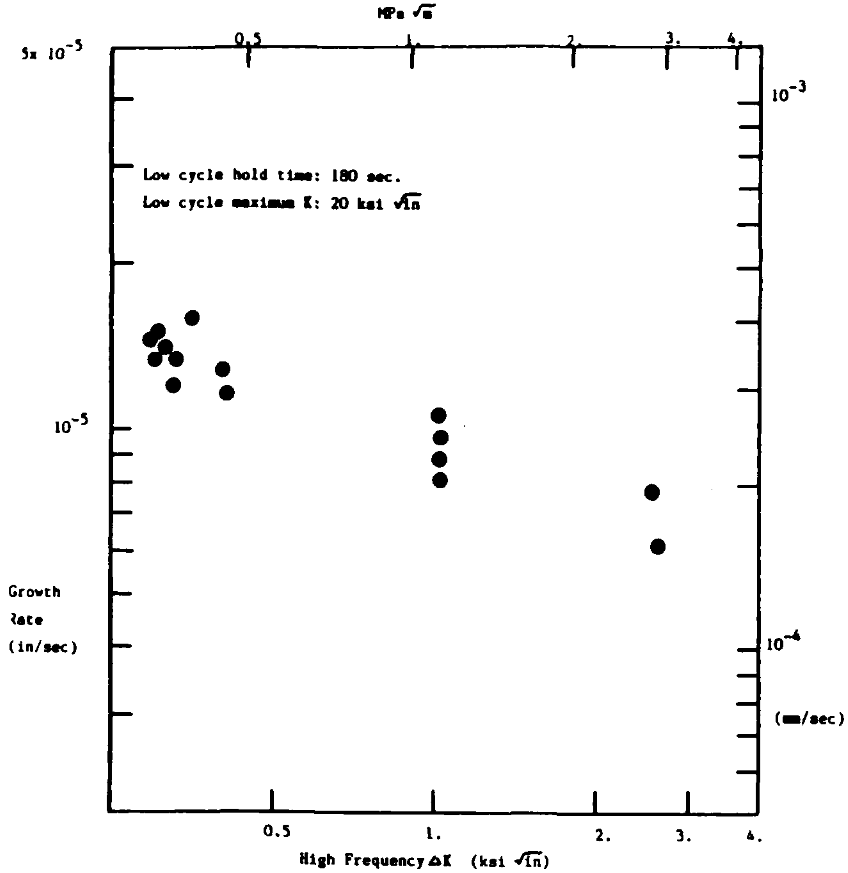

Figure B.29 Test No. 39

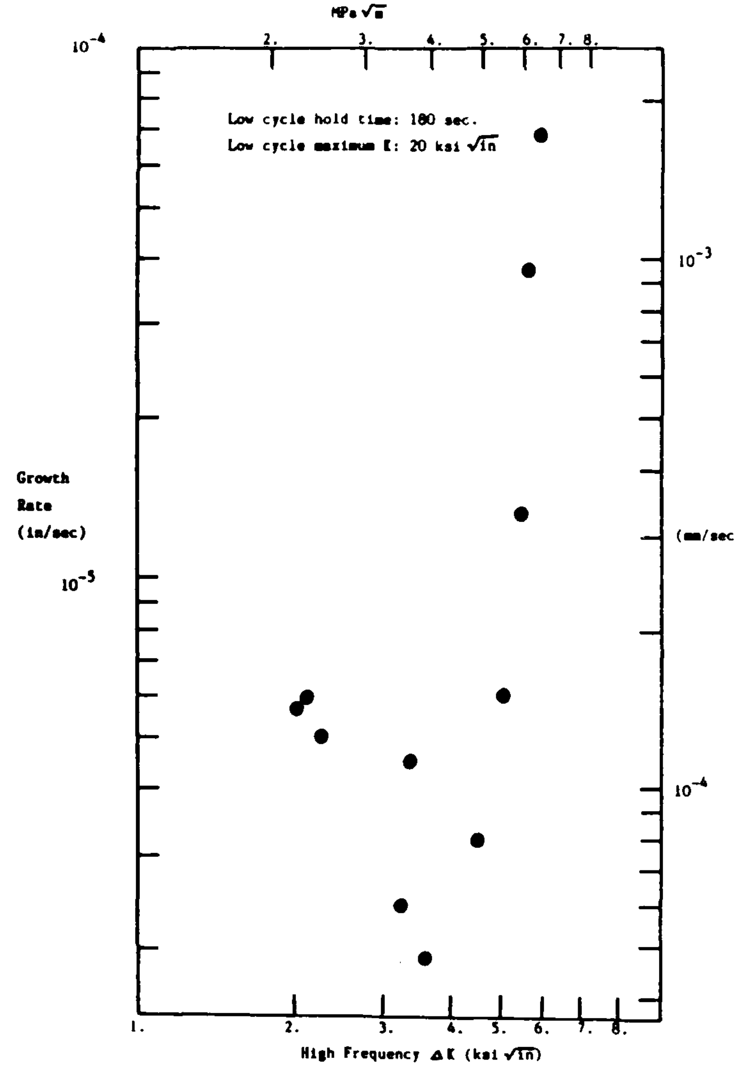

Figure B.30 Test No. 40

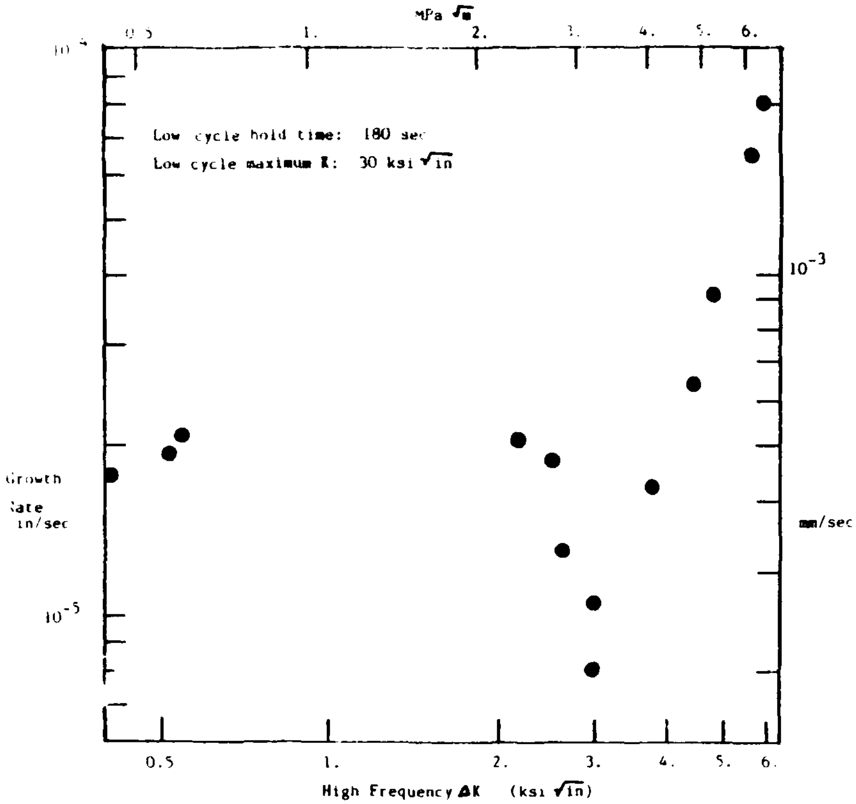

Figure B.31 Test No. 41

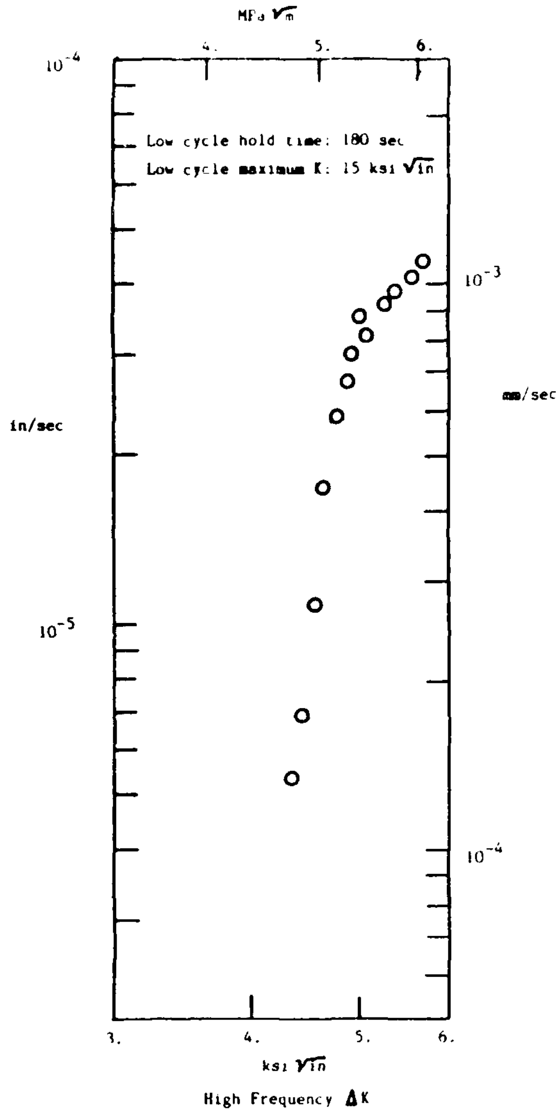

Figure B.32 Test No. 42

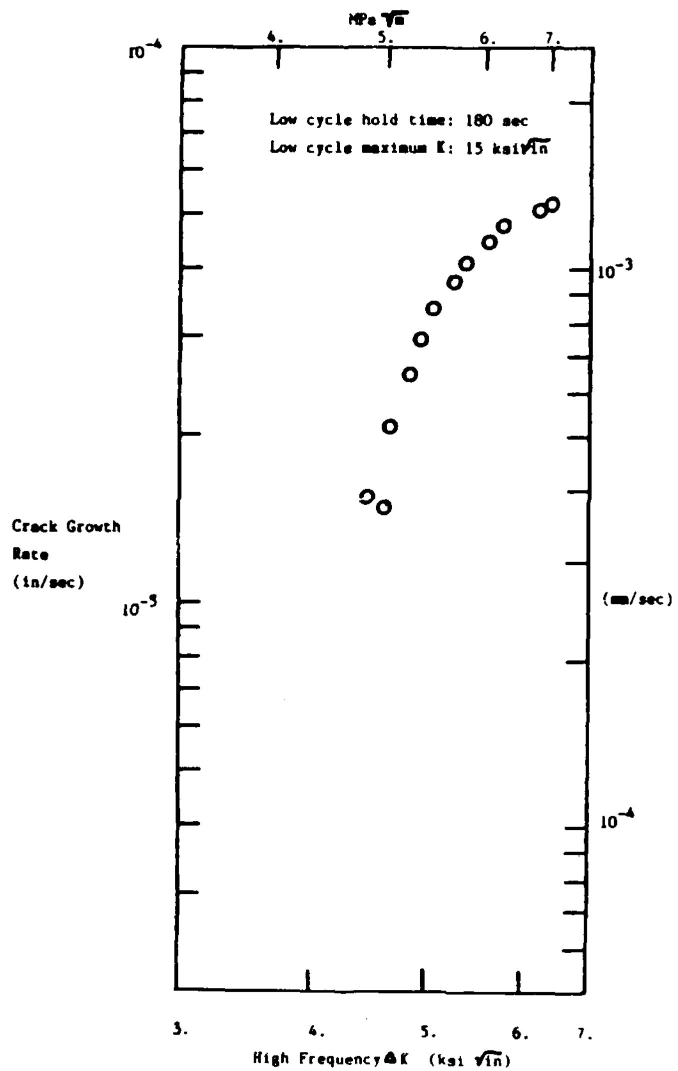

Figure B.33 Test No. 43

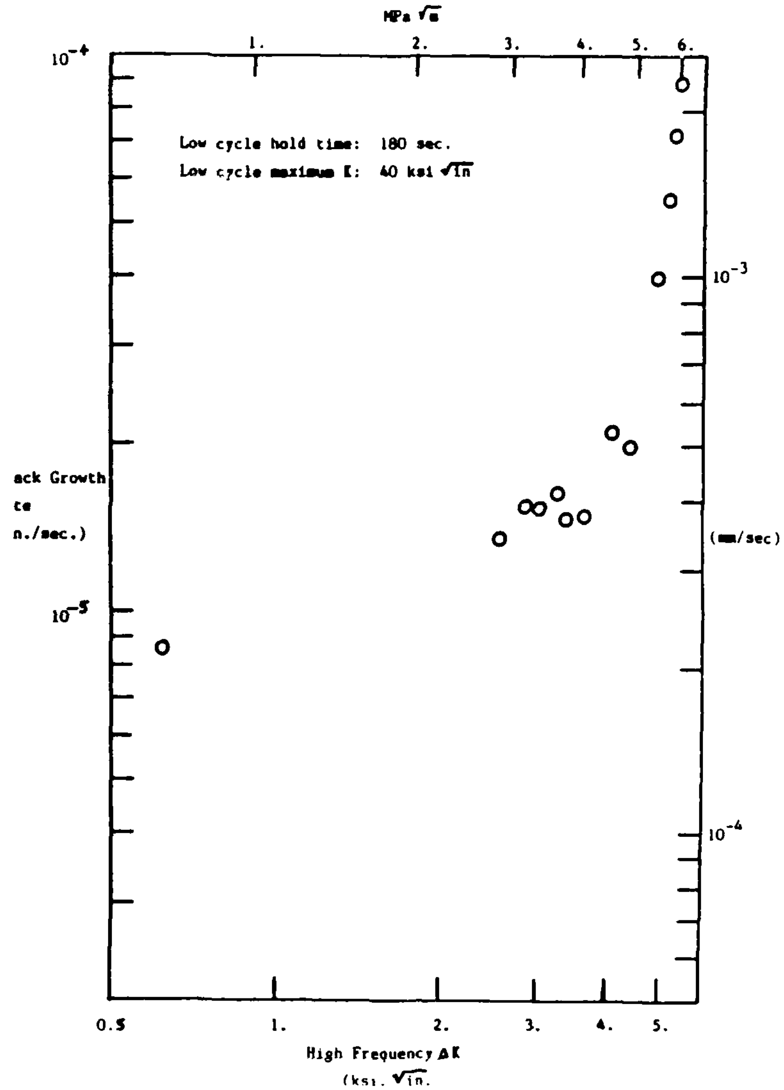

Figure B.34 Test No. 44

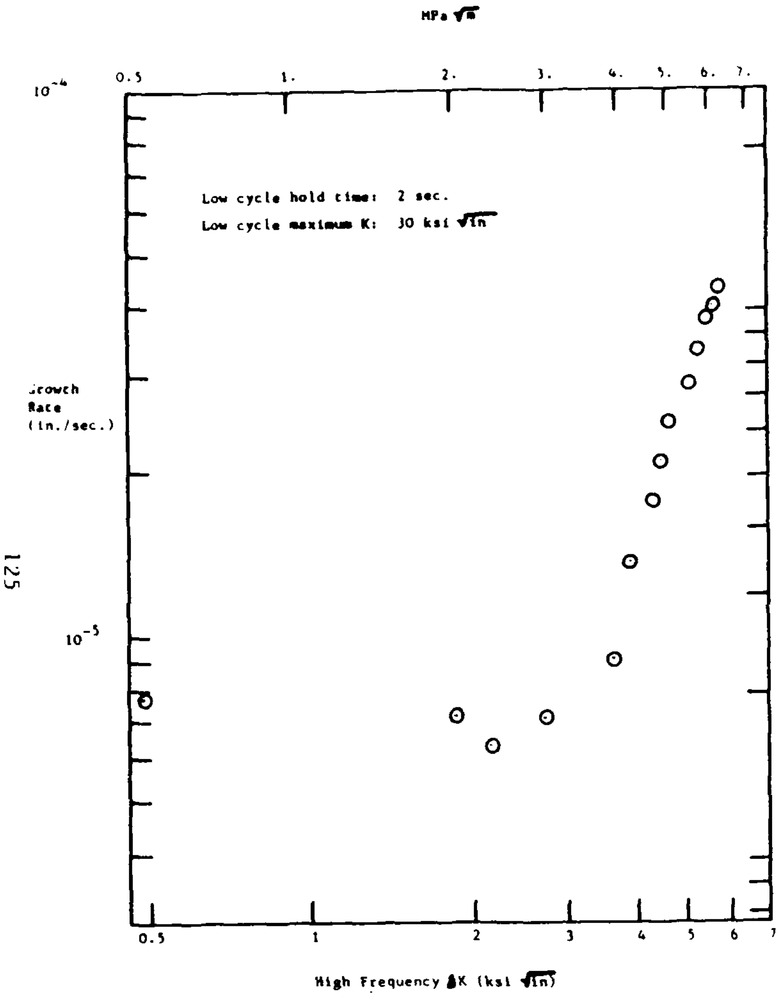

Figure B.35 Test No. 46

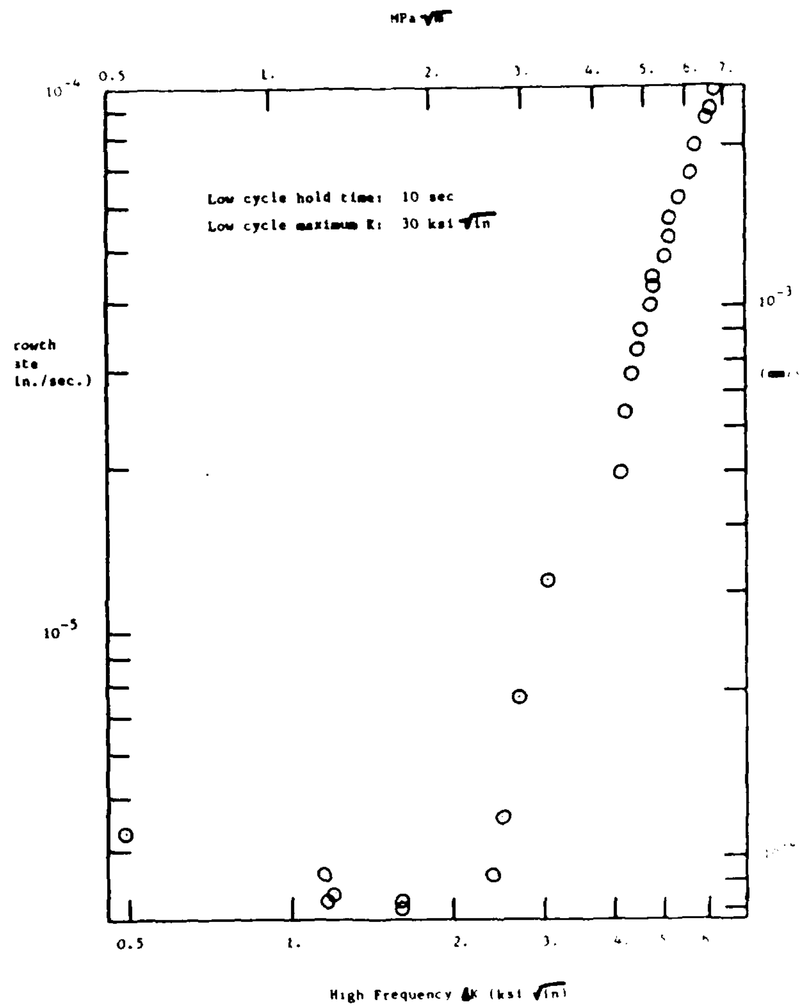

Figure B.36 Test No. 47

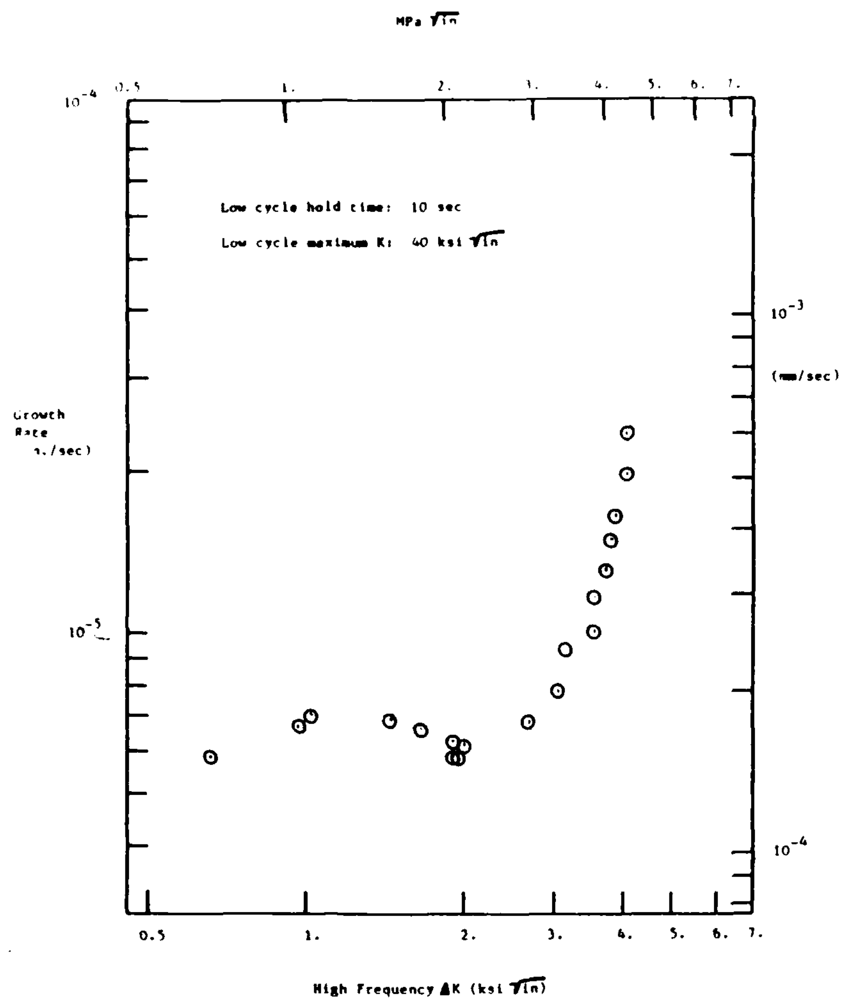

Figure B.37 Test No. 48

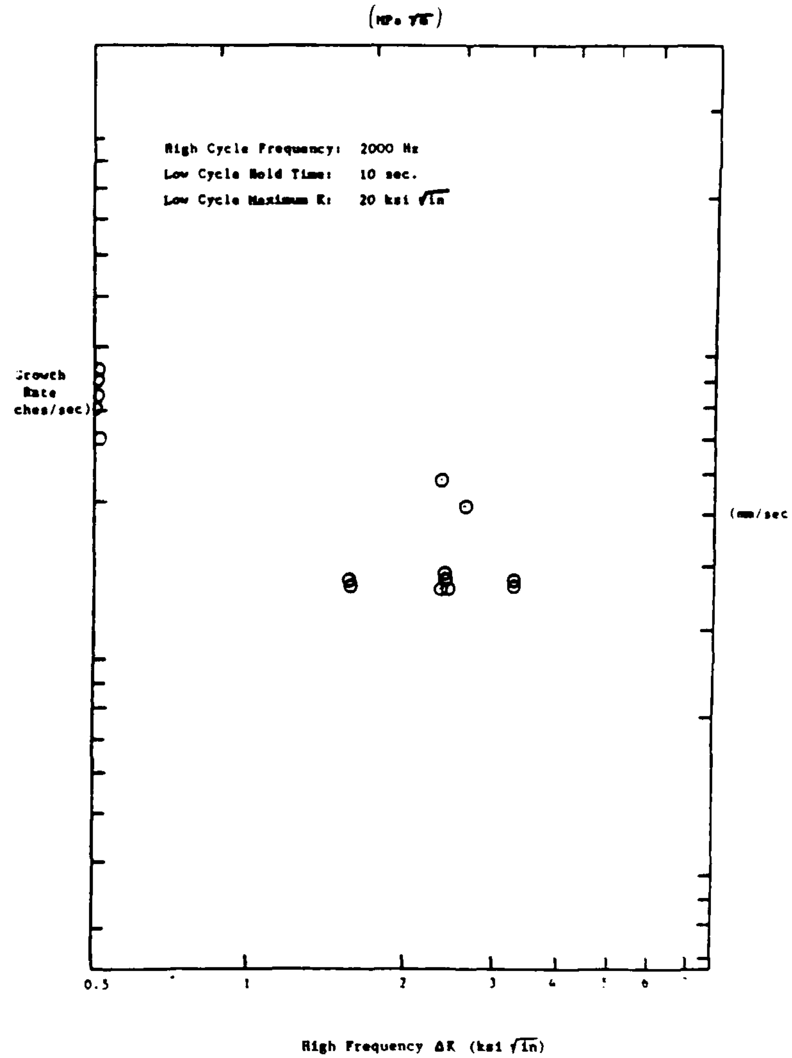

Figure B.38 Test No. 60

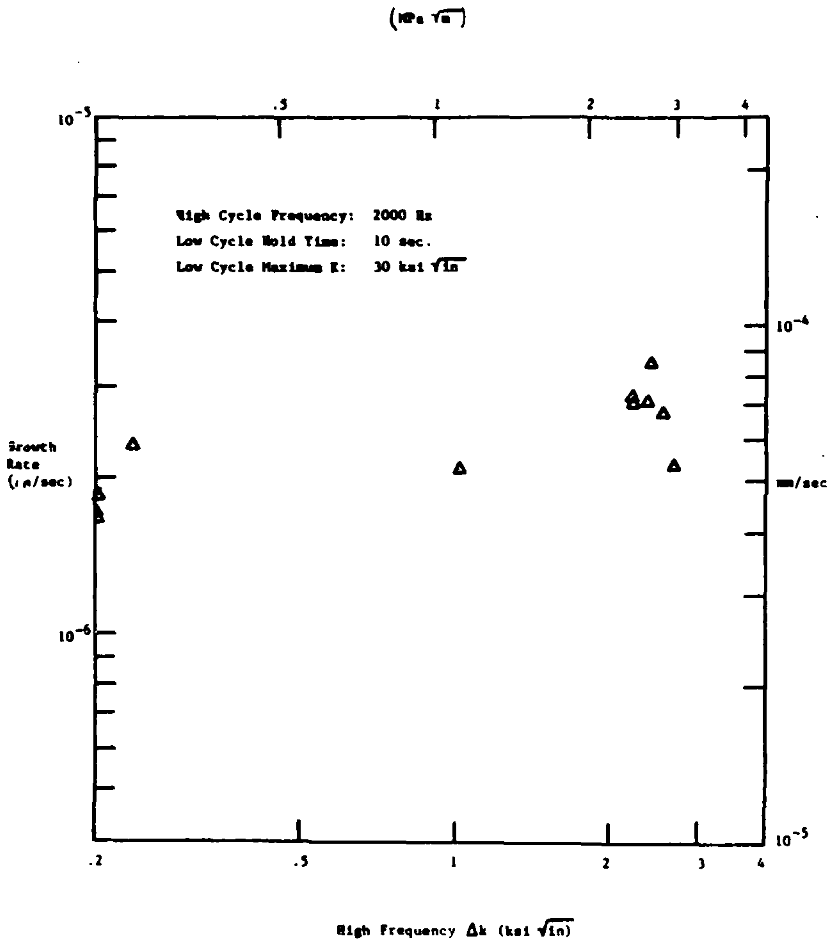

Figure B.39 Test No. 60

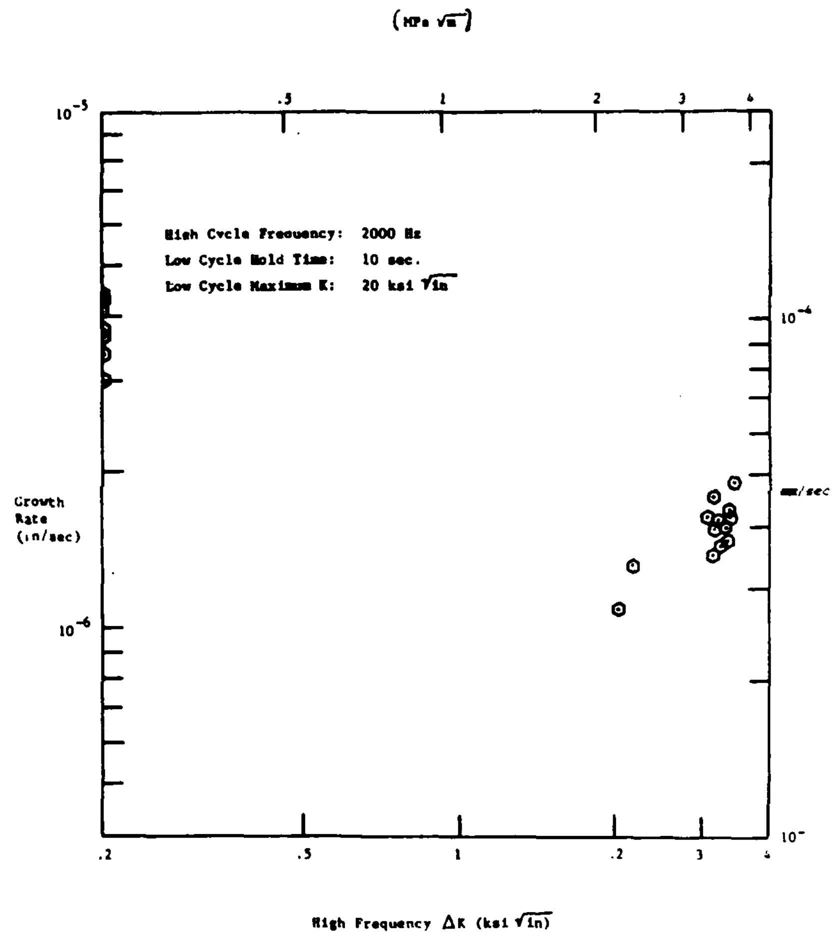

Figure B.40 Test No. 62

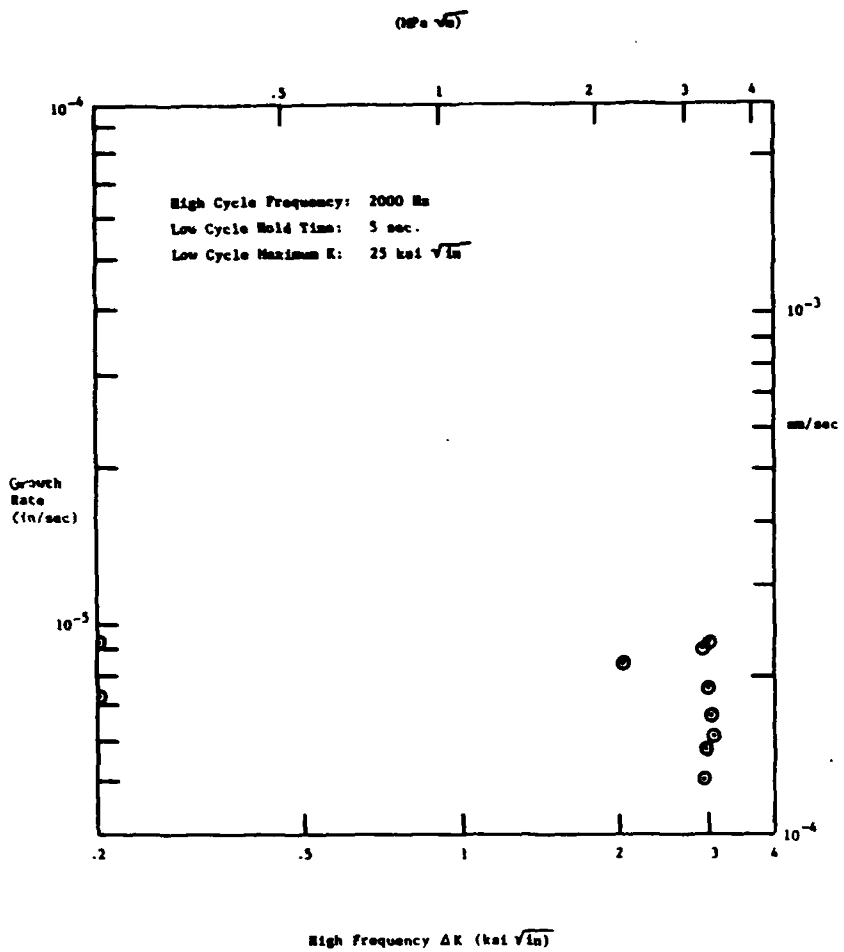

Figure B.41 Test No. 63

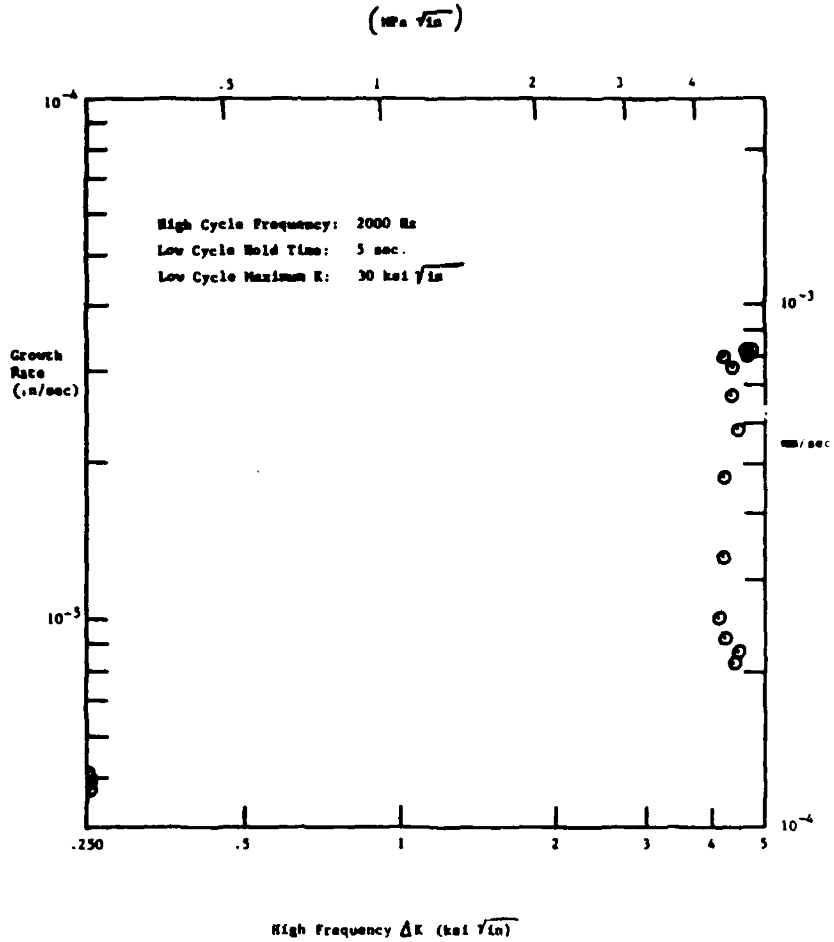

Figure B.42 Test No. 64

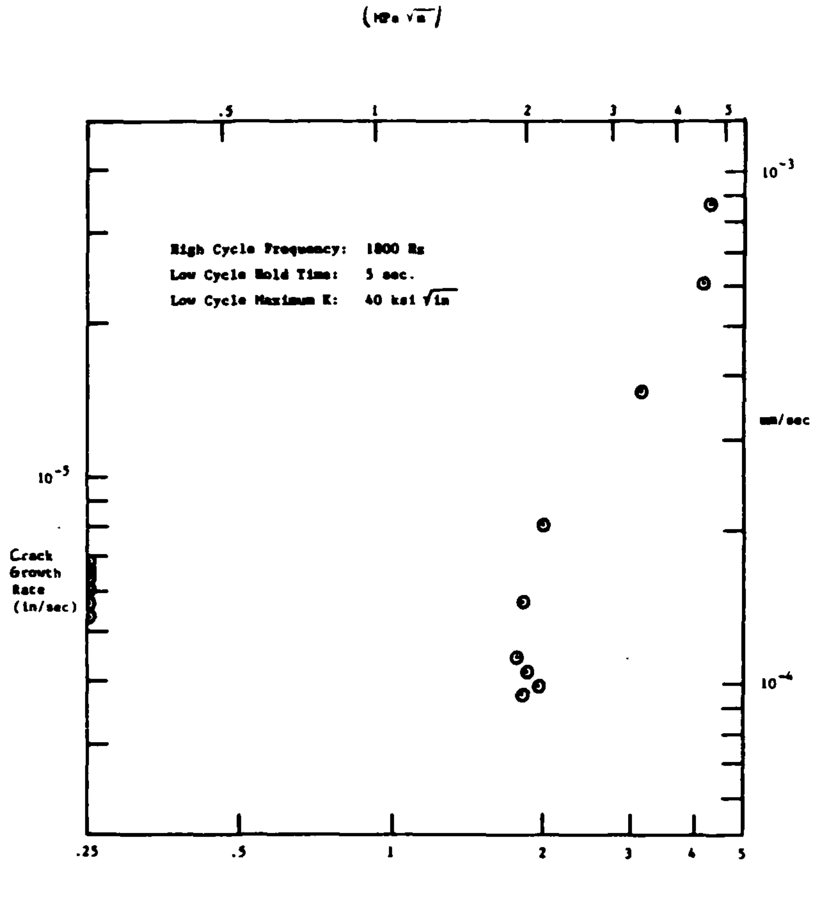

Figure B.43 Test No. 65

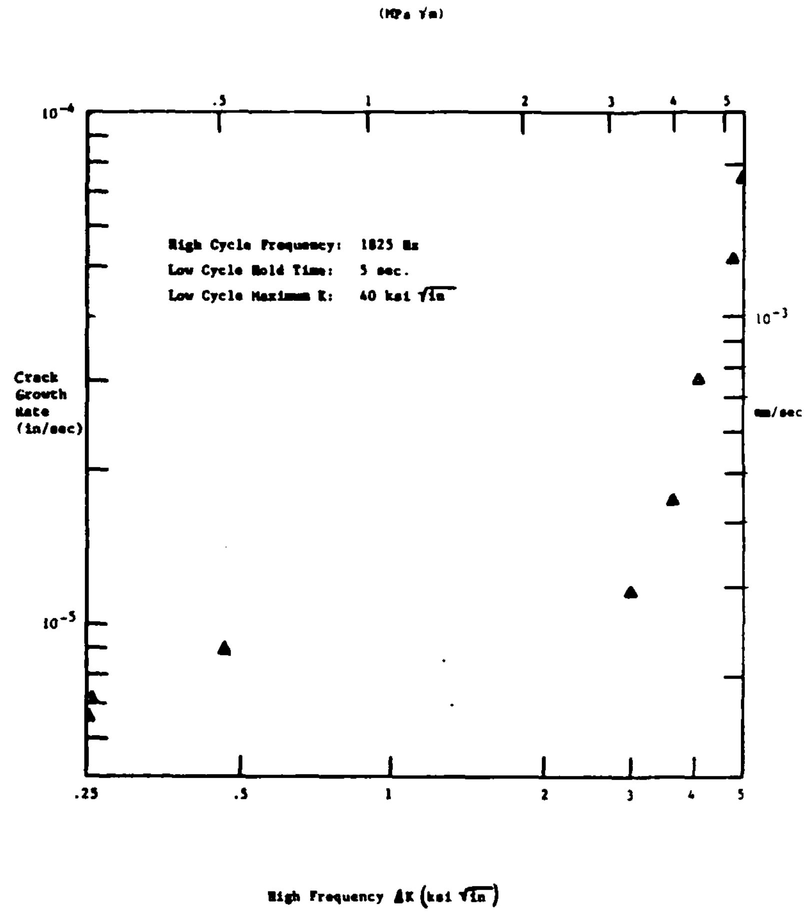

Figure B.44 Test No. 66

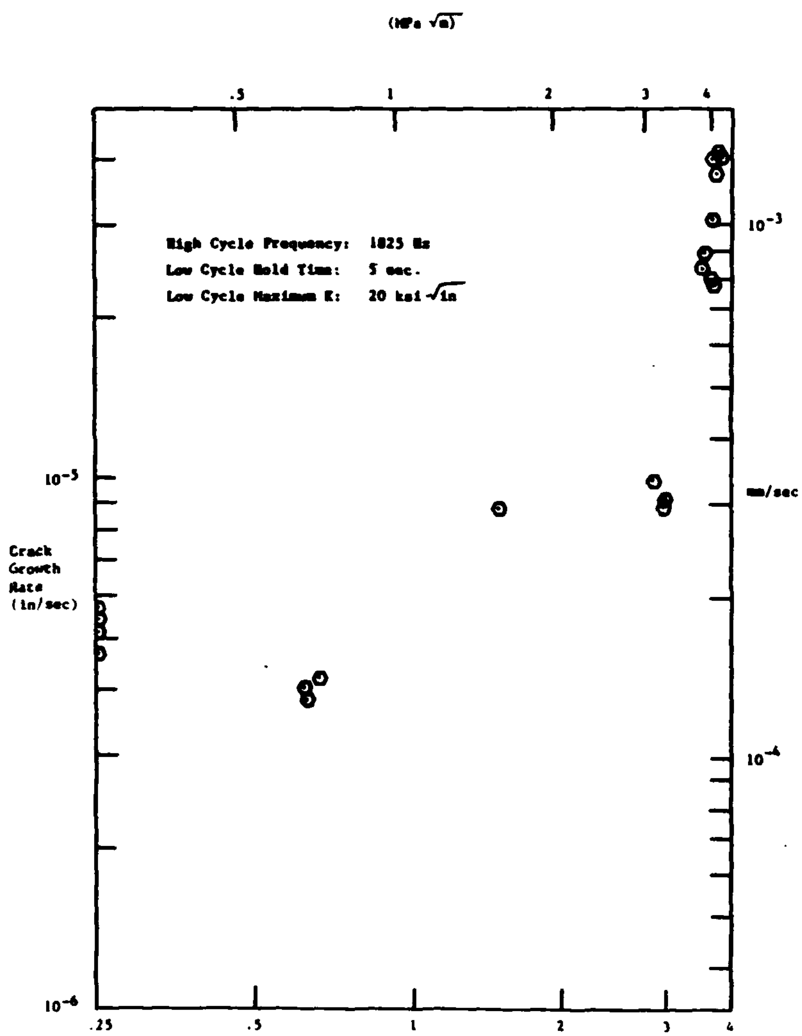

Figure B.45 Test No. 67

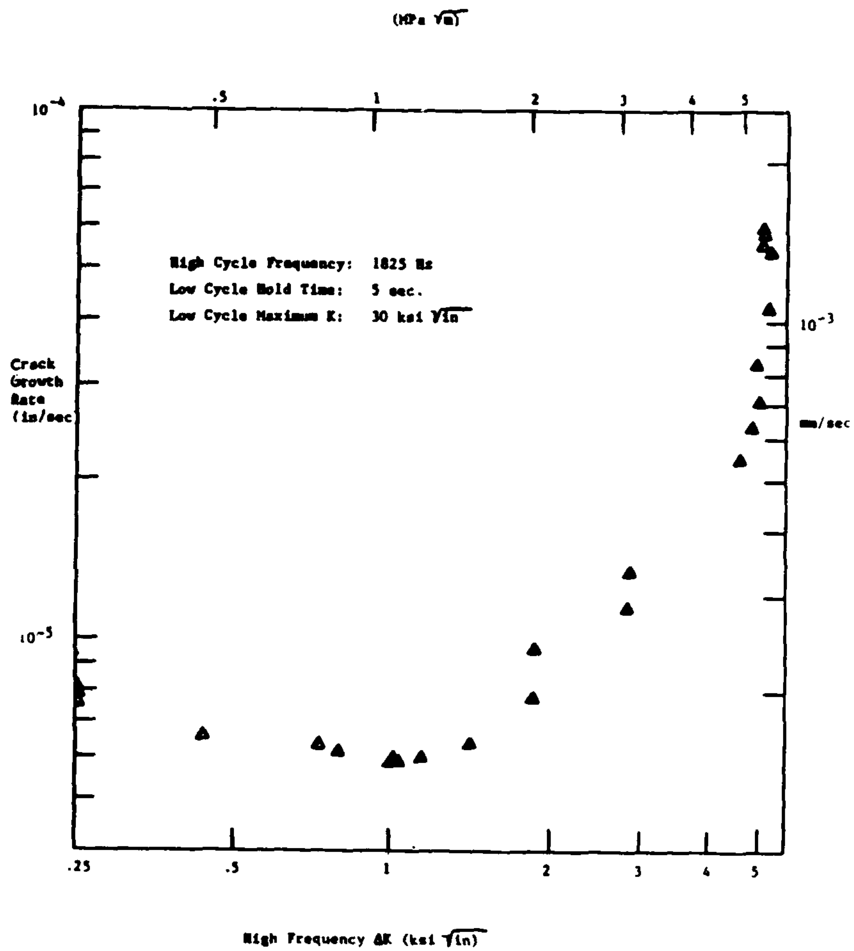

Figure B.46 Test No. 68

APPENDIX C

DATA LISTINGS FOR ALL EXPERIMENTS

TABLE C.1

RESULTS OF TEST NO. 1

Constant load test with a trapezoidal waveform having a 60 second hold time, no high cycle loading, R = 0.1

Time (Sec x 10^{-5})	Crack Length (in.)	Low Frequency (psi $\sqrt{in.}$)	Growth Rate (in./sec x 10^{6})
1.321	0.1946	17220.6094	0.00715
2.699	0.1990	18519.7266	0.0794
3.947	0.2183	27527.7383	0.1986
3.955	0.2229	27853.1562	0.3624
4.012	0.2320	26116.6055	4.687
4.028	0.2387	26547.0898	8.404
4.034	0.2429	26813.5547	9.927
4.045	0.2545	27549.0000	12.37
4.054	0.2679	28394.6094	13.58
4.066	0.2875	29625.5273	13.20
4.078	0.3045	30696.8203	11.57
4.089	0.3168	28607.9453	7.285

TABLE C.2

RESULTS OF TEST NO. 2

Constant load test with a trapezoidal waveform having a 60 second hold time, no high cycle loading, R = 0.1

Time (sec)	Crack Length (in.)	Low Freuquency ΔK (psi $\sqrt{in.}$)	Growth Rate (in./sec)
2340.0000	0.1945	16136.2617	0.00000125385
7500.0000	0.2000	16387.5547	0.00000092738
11880.0000	0.2032	16529.8945	0.00000075387
19740.0000	0.2080	16300.0469	0.00000068074
20640.0000	0.2086	16324.1562	0.00000066424
22380.0000	0.2097	16375.2969	0.00000067260

TABLE C.3

RESULTS OF TEST NO. 3

Crack growth testing with low frequency loading only, 60 sec hold time, and R = 0.1

Time (sec)	Crack Length (in.)	ΔK (psi in. 1/2)	Crack Growth Rate (in./sec)
50691	0.3502	25046	0.2738E-05
55311	0.3631	25661	0.3763E-05
56931	0.3696	25979	0.4100E-05
60531	0.3859	26775	0.4963E-05
62031	0.3932	27134	0.5314E-05
64671	0.4081	27882	0.6227E-05
67491	0.4265	28819	0.7154E-05
70491	0.4490	30004	0.7060E-05
71031	0.4537	30259	0.7010E-05
71991	0.4611	30661	0.7309E-05
73791	0.4745	31397	0.1070E-04
74031	0.4764	31502	0.9375E-05
74331	0.4795	31679	0.1275E-04
74751	0.4857	32028	0.1691E-04
75471	0.4986	32776	0.2179E-04
75471	0.4988	32785	0.1961E-04
75951	0.5092	33399	0.2134E-04
76191	0.5163	33826	0.2533E-04
76611	0.5253	34380	0.2177E-04
77091	0.5359	35044	0.2383E-04
77331	0.5423	35457	0.2504E-04
77811	0.5550	36285	0.2731E-04
78351	0.5703	37326	0.2819E-04
78711	0.5805	38047	0.2519E-04
78771	0.5825	38192	0.2615E-04
79131	0.5910	38809	0.2388E-04
79856	0.6071	40018	0.2070E-04
80121	0.6116	40865	0.2090E-04
80421	0.6171	41301	0.2228E-04
81137	0.6330	42618	0.2854E-04
81511	0.6437	43545	0.3631E-04
81861	0.6570	44753	0.4475E-04
82192	0.6735	46336	0.5109E-04
82432	0.6865	47656	0.5146E-04
82576	0.6950	48559	0.5207E-04
82871	0.7113	50398	0.5052E-04
83091	0.7203	51473	0.5214E-04
83311	0.7316	52877	0.5584E-04
83421	0.7369	53574	0.5590E-04
83876	0.7659	57730	0.7868E-04
84081	0.7827	60487	0.1036E-03

TABLE C.4

RESULTS OF TEST NO. 4

Constant uncycled load, high cycle load of various frequencies

Crack Length (in.)	Mean Load (lb)	HF Load (lb)	Freq.	DADN (in./sec)	K Mean (psi $\sqrt{in.}$)	HF K (psi $\sqrt{in.}$)
0.16	3450	821	110	0	13362.1	3179.78
0.165	3450	1120	110	7.59600E-07	13583.1	4409.6
0.19	3400	1450	110	7.85000E-05	14445.6	6160.63
0.213	3420	500	460	0	15476.3	2262.61
0.213	3450	650	460	0	15612	2941.4
0.211	3600	1035	460	0	16205.3	4659.04
0.214	3600	1350	460	5.50000E-05	16333.5	6125.05
0.233	3600	1250	460	1.35000E-04	17136.6	5950.19
0.264	3600	1250	460	1.79000E-04	18424.7	6397.45
0.296	3600	1090	460	1.40000E-04	19741.5	5977.29
0.326	3600	1090	460	1.60000E-04	20978.9	6351.96
0.356	3600	1090	460	1.35000E-04	22231.8	6731.3
0.386	3600	1090	460	1.70000E-04	23512	7118.92
0.415	3600	660	460	8.85000E-06	24786.8	4544.25
0.435	3500	0	460	4.66000E-06	24979.6	0
0.455	3550	400	460	6.13000E-06	26256.8	2958.52
0.49	3550	510	460	1.92000E-05	27944	4014.49
0.522	3650	500	460	1.70000E-05	30424.1	4167.69
0.542	3620	575	460	4.00000E-05	31285.6	4969.39
0.575	3620	575	460	1.02500E-04	33245.1	5280.64
0.616	3550	360	460	1.61500E-05	35252.3	3574.88
0.649	3440	200	460	1.83300E-05	36487.6	2121.37
0.671	3405	0	460	1.77000E-05	37812.7	0
0.695	3405	0	460	4.50000E-05	39841.4	0
0.732	3430	0	460	1.17500E-04	43746	0

TABLE C.5

RESULTS OF TEST NO. 6

High Cycle Frequency: 460 Hz
Low Cycle Hold Time: 60 sec
Low Cycle Maximum K: 25 ksi $\sqrt{in}$

Time (sec)	Crack Length (in.)	Max LF K (psi $\sqrt{in.}$)	HF K Range (psi $\sqrt{in.}$)	Growth Rate (in./sec)
3311.9458	0.6205	27476.0000	6412.0000	0.00009967999
3370.7698	0.6284	27637.0000	6563.0000	0.00011073000
3429.5937	0.6369	26262.0000	7028.0000	0.00012606000
3489.1919	0.6475	26560.0000	7021.0000	0.00014138001
3548.7898	0.6594	26475.0000	6935.0000	0.00015327999
3608.3879	0.6713	25879.0000	7056.0000	0.00016482000
3668.7598	0.6845	24541.0000	7260.0000	0.00018151999
3729.1318	0.6986	24092.0000	7490.0000	0.00020299001
3788.7297	0.7144	23358.0000	7705.0000	0.00022772000
3849.1018	0.7396	23643.0000	8251.0000	0.00022777000
3910.2478	0.7560	21938.0000	8400.0000	0.00021758000
3972.9419	0.7555	19520.0000	8321.0000	0.00009875000

TABLE C.6

RESULTS OF TEST NO. 7

High Cycle Frequency: 248 Hz
Low Cycle Hold Time: 60 sec
Low Cycle Maximum K: 25 ksi $\sqrt{in}$

Time (sec)	Crack Length (in.)	Max LF K (psi $\sqrt{in.}$)	HF K Range (psi $\sqrt{in.}$)	Growth Rate (in./sec)
235.9407	0.3488	26050.1055	4641.8477	0.00001485884
294.7646	0.3496	26180.7734	4619.1836	0.00001456062
353.6274	0.3503	26096.9609	4536.2344	0.00001352035
412.5032	0.3511	26094.1445	4692.4609	0.00001273368
471.3792	0.3519	26220.4687	4699.5312	0.00001222918
530.2542	0.3526	26130.7539	4676.3711	0.00001134939
589.1299	0.3533	26031.0469	4801.8828	0.00001064065
648.5212	0.3537	26128.5039	4716.1523	0.00000965623
707.4358	0.3543	26118.2617	4660.9531	0.00001008975
766.3374	0.3549	26097.4492	4575.9453	0.00001107305
825.2773	0.3555	26050.8672	4491.2266	0.00001245337
884.2173	0.3563	26152.9297	4498.0156	0.00001386796
943.1343	0.3572	26032.5469	4505.3750	0.00001459003
1002.0745	0.3581	26010.4258	4513.0781	0.00001596280
1061.0146	0.3591	25930.0977	4551.9258	0.00001669205
1119.9624	0.3601	25894.3047	4712.9687	0.00001626340
1178.9023	0.3611	26044.4453	4690.9336	0.00001595949
1238.4231	0.3620	25969.8164	4699.2500	0.00001599903
1297.4019	0.3630	25894.2305	4738.0430	0.00001586429
1356.3806	0.3639	25941.2773	4776.5820	0.00001504465
1415.3750	0.3647	25890.8359	4845.7852	0.00001571118
1474.3770	0.3657	25889.5586	4823.7812	0.00001679330
1533.3943	0.3667	25922.3984	4802.0977	0.00001643198
1592.4043	0.3677	25929.0977	4810.9414	0.00001639908
1651.4294	0.3686	25330.3164	5561.1875	0.00001713847
1710.4778	0.3697	25169.4687	4859.8945	0.00001801133
1769.5186	0.3706	24908.0820	4868.6133	0.00001906550
1828.5750	0.3718	25210.2891	4847.9258	0.00002092373
1887.9792	0.3732	25079.3047	4922.8750	0.00002321890
1947.0200	0.3746	25178.6992	4873.1836	0.00002580561
2006.0764	0.3761	25086.8164	4792.9062	0.00002911617
2065.1711	0.3779	25178.6328	5029.3516	0.00003200150
2124.2661	0.3800	25106.1836	5080.1484	0.00003330523
2183.3997	0.3820	25275.6289	5004.3242	0.00003640015
2242.5642	0.3842	25184.8789	5024.1953	0.00004052975
2301.7212	0.3865	25182.9961	5013.7969	0.00004469036
2360.9089	0.3892	25301.0586	5103.1992	0.00004939397
2420.0889	0.3924	25343.1797	5035.8086	0.00005693898
2479.8726	0.3961	25279.8359	5168.0312	0.00006370625
2539.1223	0.4000	25405.6094	5302.6328	0.00006922033
2598.4185	0.4042	25569.5586	5277.6445	0.00007534429
2657.7378	0.4090	25305.2305	5190.6367	0.00008002591
2717.1113	0.4141	25441.1562	5305.6836	0.00008314816
2776.5081	0.4191	25400.4102	5353.8477	0.00008421815
2835.9514	0.4242	25242.5508	5368.6641	0.00008648771
2895.4563	0.4292	25242.9961	5555.3789	0.00008798379
2955.0002	0.4344	25281.3555	5502.6719	0.00009084668
3014.6138	0.4400	25036.0352	5592.9492	0.00009541119
3074.8464	0.4459	24978.6758	5723.4236	0.00009973258
3134.3605	0.4520	25143.6094	5965.7109	0.00010364498
3194.3130	0.4582	25232.8320	5850.9609	0.00010745380
3254.1438	0.4648	24869.8516	5772.6367	0.00011143394
3314.0349	0.4717	24969.2734	5880.7109	0.00011377316
3374.0049	0.4786	24853.3633	5916.5117	0.00011540043

TABLE C.6 (Cont'd)

Time (sec)	Crack Length (in.)	Max LF K (psi $\sqrt{in.}$)	HF K Range (psi $\sqrt{in.}$)	Growth Rate (in./sec)
3434.0444	0.4857	24775.5117	6143.3750	0.00011676035
3494.1987	0.4927	24727.0937	6104.7031	0.00011801535
3554.3772	0.4997	24777.2227	6221.4023	0.00011853676
3614.6404	0.5069	24565.5859	6261.2969	0.00012063261
3675.3782	0.5143	24692.2109	6345.1562	0.00012372177
3735.8499	0.5219	24673.5234	6391.3633	0.00012608935
3796.4094	0.5295	24587.4453	6604.2812	0.00012877809
3857.0596	0.5377	24693.5117	6660.4961	0.00012703062
3917.8093	0.5463	24741.9375	6807.7109	0.00011206591
3978.6863	0.5533	24271.8594	6810.2422	0.00008711699
4038.9282	0.5580	24813.1836	1521.6460	0.00005887295
4098.6562	0.5602	25037.1406	1309.5159	0.00003027947
4158.3398	0.5600	24864.1562	1396.2622	0.00000974585
4218.0273	0.5590	24890.7734	1480.7656	0.00000763518
4337.3789	0.5606	27021.7930	1703.5078	0.00004808255
4397.1328	0.5643	27786.2773	7168.7266	0.00007431422
4456.9375	0.5698	27709.9531	6886.9102	0.00010690858
4516.7930	0.5781	27659.7031	7220.5000	0.00011901073
4576.7930	0.5862	27859.9844	7285.3516	0.00012386656
4637.4453	0.5938	27568.5273	7204.9531	0.00012535922
4697.6523	0.6012	27221.5977	7307.0391	0.00012802753
4758.0078	0.6084	27061.8008	7313.0977	0.00013088530
4818.5273	0.6156	26763.2344	7659.3750	0.00013706277
4879.1953	0.6252	26335.9062	7854.3320	0.00015658276
4940.0430	0.6348	26240.7578	7552.2773	0.00017108484
5001.0977	0.6453	26035.8125	7714.1992	0.00019060491
5062.3750	0.6572	25432.2539	7799.1172	0.00021805093
5123.9727	0.6669	24977.2227	8066.3203	0.00032618269

*Crack growth rate was not based on a sufficient range of crack length.

TABLE C.7

RESULTS OF TEST NO. 8

High Cycle Frequency: 248 Hz
Low Cycle Hold Time: 10 sec

Time (sec)	Crack Length (in.)	Max LF K (psi $\sqrt{in.}$)	HF K Range (psi $\sqrt{in.}$)	Growth Rate (in./sec)
7984.6875	0.2884	21420.8984	787.9695	0.00000941813
9383.9336	0.3034	25230.0312	322.9622	0.00001158264
11084.0156	0.3252	25599.7070	226.9065	0.00001351392
12386.5664	0.3436	26294.6680	2122.8723	0.00001455599
13183.5195	0.3553	26434.4062	2349.8621	0.00001497631
14080.9570	0.3707	26770.3984	2298.0520	0.00001488024
14978.3984	0.3842	27066.2187	2610.2822	0.00001415124
15875.2070	0.3963	27487.7969	3088.2178	0.00001307475
16971.7266	0.4095	25899.5234	3429.1816	0.00001222489
18166.2070	0.4219	26296.1211	3541.4712	0.00001361158
19361.3203	0.4383	25894.9062	3646.9678	0.00001984589
20157.6406	0.4558	26672.8047	5140.4961	0.00003097781
20555.8008	0.4675	27050.7266	5286.1211	0.00001640414
20754.8789	0.4750	27109.5391	5388.1836	0.00002467167
20854.1016	0.4815	26361.7422	2574.1467	0.00004010730
23646.2773	0.5050	25651.9141	5529.7539	0.00007742233
23745.5039	0.5127	25658.5820	5607.1758	0.00008925261
23844.0937	0.5218	25790.3672	5824.7070	0.00009586086
23943.3203	0.5312	25939.6523	5838.7500	0.00010083221
24042.5430	0.5420	25779.1484	5867.9297	0.00010941603
24141.1367	0.5532	25608.0781	6121.9414	0.00011525118
24240.3594	0.5649	25686.8867	6164.8516	0.00012083116
24338.9492	0.5770	25452.4258	6397.6758	0.00012737671
24438.1758	0.5897	25350.6016	6505.2383	0.00013430661
24536.7656	0.6032	25332.5664	6529.3125	0.00014346938
24635.9922	0.6177	25388.5117	6964.9023	0.00015487349
24735.2148	0.6336	24974.6055	7135.6016	0.00016758432

TABLE C.8

RESULTS OF TEST No. [illegible]

High Cycle Frequency: [illegible]48 Hz
Low Cycle Hold Time: 10 sec

Time (sec)	Crack Length (in.)	Max LF K (psi √in.)	HF K Range (psi √in.)	Growth Rate (in./sec)
1297.6589	0.2170	23661.3945	379.6965	0.00001193026 *
1596.4446	0.2217	23475.0703	384.3052	0.00001112623
1995.1733	0.2257	23330.4062	319.7415	0.00001019931
2295.4114	0.2283	23165.2422	275.8506	0.00001054148
2795.3040	0.2340	23343.9687	349.6875	0.00001015593
3195.5178	0.2383	23484.0547	252.6753	0.00000919912
3695.0818	0.2428	23015.2344	833.2820	0.00000785337
4094.7725	0.2462	22994.7344	456.0718	0.00000626598
4594.4180	0.2487	23056.7305	603.5396	0.00000557428
4494.0820	0.2486	23763.4336	289.6609	0.00000451123
4893.9727	0.2497	23646.6445	1863.3027	0.00000533309
5692.3750	0.2538	23806.5547	1881.1353	0.00000527830
6390.5273	0.2575	23722.8008	1872.4729	0.00000555178
7089.2773	0.2615	23730.6758	1914.4634	0.00000594603
7687.7852	0.2652	23679.9727	1930.4856	0.00000613035
8286.3828	0.2692	23600.2578	1972.8279	0.00000569293
8885.1445	0.2728	23479.3633	1937.4783	0.00000536517
9483.6328	0.2757	23261.8047	1975.7278	0.00000544718
9882.4453	0.2776	24077.3320	2009.4587	0.00000573105
10281.5430	0.2798	23941.7852	1993.0725	0.00000572622
10780.3203	0.2832	23786.5625	2033.8948	0.00000609858
11379.1406	0.2874	23739.9102	2052.1628	0.00000640959
11977.9570	0.2908	23790.7578	2040.3015	0.00000581068
12775.5508	0.2948	23693.6914	2110.9604	0.00000531340
13673.1094	0.2993	23290.4023	2184.7642	0.00000508978
14271.4297	0.3023	23320.2422	2225.3672	0.00000507647
15069.1406	0.3064	23111.6016	2107.4619	0.00000522172
15866.2812	0.3108	23348.2891	2292.0698	0.00000521949
16563.7070	0.3144	23436.2812	2281.2092	0.00000488244
17361.2305	0.3183	23285.8359	2242.9773	0.00000462104
18158.6211	0.3218	23195.1484	2173.9397	0.00000442329
19254.8281	0.3261	23165.9844	2334.8945	0.00000417723
20351.1562	0.3303	23674.4258	2325.7239	0.00000429527
21148.4883	0.3338	23679.1172	3122.1267	0.00000443624
21945.2500	0.3376	23527.7852	3144.9368	0.00000462211
22742.2656	0.3414	23583.3750	3344.2373	0.00000492933
23638.9453	0.3456	23617.0547	3224.0215	0.00000553705
24436.0898	0.3500	23783.2578	3340.6040	0.00000637227
25033.8359	0.3540	23743.0586	4147.8242	0.00000755576
25431.[illegible]961	0.3572	23887.7461	4172.7227	0.00000814868
25830.[illegible]312	0.3607	23525.2734	4200.5391	0.00000917626
26328.0469	0.3654	23281.5078	4206.9492	0.00001053531
26726.2656	0.3695	23158.6328	4239.4687	0.00001226367
27025.0156	0.3732	24189.5625	4456.1328	0.00001333111
27224.4727	0.3761	23981.6953	4417.2656	0.00001538843
27523.0312	0.3810	24041.9727	4457.5859	0.00002236864
27722.1719	0.3854	23994.3086	4557.1250	0.00003695786
27821.6523	0.3888	23510.2031	5708.0898	0.00004877275
27920.4961	0.3934	23284.8125	5336.7148	0.00005742149
28020.5430	0.4007	23254.0078	5538.9648	0.00006690418
28120.3320	0.4079	23189.2734	5578.5000	0.00007164774
28219.8125	0.4151	23152.2305	5651.8242	0.00007403755
28319.2227	0.4225	23056.8945	5659.2812	0.00007786212
28418.5742	0.4301	22915.8672	3771.8008	0.00008352491

TABLE C.8 (Cont'd)

Time (sec)	Crack Length (in.)	Max LF K (psi √in.)	HF K Range (psi √in.)	Growth Rate (in./sec)
28517.8008	0.4385	22791.0039	5789.0703	0.00009162258
28617.1484	0.4500	24008.7461	6553.1680	0.00009264356
28716.4336	0.4498	23373.3711	6551.1367	0.00001536791
33973.8359	0.4836	25795.6094	5132.2422	0.00003636177
34073.0000	0.4876	24674.6523	4939.6250	0.00003904545
34172.1641	0.4915	24768.9023	5319.1445	0.00004091009
34271.2305	0.4955	23836.7578	5513.8203	0.00004369611
34370.4023	0.5001	23596.6914	5638.1250	0.00004751662
34469.5352	0.5049	23527.7773	5923.4727	0.00005029375
34568.6797	0.5101	23442.6836	5660.0195	0.00005357758
34667.8125	0.5156	23439.1484	5917.4409	0.00005561640
34766.9062	0.5213	23290.9766	5774.6953	0.00005715960
34865.9687	0.5271	23541.7187	5917.7656	0.00005877724
34965.3984	0.5330	23512.5547	5897.9102	0.00005977921
35064.4648	0.5388	23592.2891	5918.6133	0.00006168520
35163.5977	0.5450	23860.6094	6027.8047	0.00006349280
35262.8203	0.5513	23610.4687	6012.4883	0.00006700812
35361.4766	0.5582	23440.1289	6088.3516	0.00006944068
35460.8867	0.5653	23640.3672	6212.9570	0.00007149021
35559.9844	0.5726	23428.2344	6386.4297	0.00007345444
35659.0820	0.5797	23674.5508	6381.5703	0.00007666649
35758.3086	0.5872	21299.6172	6702.4844	0.00008231173
35857.4687	0.5953	21322.9687	6806.1328	0.00008870705
35957.0078	0.6046	21509.1016	7022.6016	0.00009783010
36056.1055	0.6146	21455.3945	6917.7344	0.00010989855
36155.2031	0.6257	21362.0898	7021.3164	0.00012544842
36254.3008	0.6378	21507.5234	7091.4922	0.00015053191
36353.3359	0.6269	20521.1016	6938.6875	0.00048219692

*A long dwell in the low cycle dominated regime for constant low-frequency ΔK shows a decreasing crack growth rate.

TABLE C.9

RESULTS OF TEST NO. 10

High Cycle Frequency: 248 Hz
Low Cycle Hold Time: 10 sec

Time (sec)	Crack Length (in.)	Max LF K (psi $\sqrt{in.}$)	HF K Range (psi $\sqrt{in.}$)	Growth Rate (in./sec)
10766.1172	0.2093	22325.0664	1580.7959	0.00000198970
11863.9023	0.2116	22226.8008	1839.7617	0.00000212665
13660.6797	0.2157	22393.7461	2033.7771	0.00000268970
15257.7422	0.2202	22254.2031	2331.8115	0.00000322044
17154.3750	0.2269	22475.9727	2470.9585	0.00000339681
17254.2305	0.2277	22912.5898	2435.9624	0.00000333224
18750.8086	0.2329	22799.3281	2710.3889	0.00000334025
20349.1367	0.2379	22537.5469	2763.6191	0.00000307281
21946.1992	0.2421	22395.0234	2874.8782	0.00000274948
23343.5508	0.2460	22283.1680	2880.5222	0.00000272386
24640.4161	0.2497	22619.8437	2926.6326	0.00000220554
26138.2539	0.2530	22193.0547	2991.0759	0.00000177671
27534.3437	0.2547	22843.3320	2938.9419	0.00000198376
28931.0625	0.2574	22723.1094	3171.9788	0.00000232992
30327.7852	0.2621	22766.3047	3205.4685	0.00000271645
30627.3516	0.2625	22859.0352	3230.3423	0.00000322488
32223.1523	0.2678	23159.9531	3509.7227	0.00000301020
34817.5117	0.2750	23335.3242	3610.4314	0.00000261505
36513.1680	0.2793	23077.0312	3689.4124	0.00000245161
39807.1523	0.2872	23458.0117	3729.5332	0.00000261812
40405.6562	0.2889	23501.5898	3903.8779	0.00000361425
40504.8789	0.2884	23655.9570	3922.0916	0.00000407825
41702.5195	0.2937	23746.0469	3943.3091	0.00000555115
42500.1055	0.2989	23632.6875	4032.5623	0.00000659695
43198.4648	0.3038	23770.7305	4121.0742	0.00000734338
43797.6016	0.3086	23790.0703	4281.8164	0.00000767354
44495.3281	0.3146	23574.8281	4334.0195	0.00000661424
45093.8320	0.3184	23668.3000	4293.9102	0.00000615232
46589.1445	0.3250	23698.8516	3708.1436	0.00000556470
47387.3594	0.3295	23873.2930	4064.7747	0.00000616498
47985.8633	0.3335	23863.7852	4122.4023	0.00000682494
48684.2227	0.3390	23835.9805	4293.1641	0.00000758923
49482.4414	0.3453	24098.0312	4242.8516	0.00000795503
50080.3125	0.3501	24080.2852	4256.4297	0.00000783179
50578.9609	0.3541	24080.1992	4341.4609	0.00000789639
51276.0547	0.3598	23872.3711	4361.6875	0.00000795780
52072.3750	0.3659	23832.6328	4519.0898	0.00000787275
52670.2500	0.3705	23861.8984	4585.0312	0.00000777698
53267.4883	0.3752	23770.6367	4707.4609	0.00000766006
53864.7305	0.3800	23536.5234	4694.4570	0.00000766449
54561.8242	0.3851	23808.5234	4710.8320	0.00000751789
55357.3117	0.3908	23586.0781	4760.2852	0.00000771607
56053.3437	0.3960	23435.2031	4976.1914	0.00000803499
56650.5859	0.4009	23687.6797	4935.0781	0.00000839662
57147.9687	0.4053	23672.8828	4945.6406	0.00000880012
57744.5781	0.4107	23853.4648	5023.7070	0.00000925156
58241.3281	0.4152	23951.8359	5181.6875	0.00000966686
58738.7109	0.4195	23955.2695	5103.7695	0.00001187917
59335.3203	0.4269	23724.5391	5232.0547	0.00002009184
59723.4805	0.4358	24160.9258	5346.4062	0.00003783348
60031.7852	0.4497	24571.6406	6414.6602	0.00007220265
60131.0078	0.4549	24401.7266	6349.0937	0.00010992614

TABLE C.9 (Cont'd)

Time (sec)	Crack Length (in.)	Max LF K (psi $\sqrt{in.}$)	HF K Range (psi $\sqrt{in.}$)	Growth Rate (in./sec)
60230.2344	0.4653	24383.7344	6596.3047	0.00013355352
60329.4570	0.4812	24322.9023	6752.2656	0.00015663158
60429.3125	0.4976	24210.8125	7052.8281	0.00017164793
60528.5352	0.5151	24282.8477	7312.5078	0.00018995855
60627.7617	0.5344	24301.9297	7680.3594	0.00021295148
60726.9844	0.5555	24235.3086	7944.0430	0.00024835579
60826.2070	0.5796	25286.7656	8857.4883	0.00030489918

TABLE C.10

RESULTS OF TEST NO. 11

High Cycle Frequency: 605 Hz
Low Cycle Hold Time: 10 sec

Time (sec)	Crack Length (in.)	Max LF K (psi $\sqrt{in.}$)	HF K Range (psi $\sqrt{in.}$)	Growth Rate (in./sec)
2290.0078	0.2079	22738.3437	227.7065	0.00000648826 *
2987.1924	0.2120	22518.0781	422.0615	0.00000580084
3786.7983	0.2163	22513.2461	232.8022	0.00000526712
4686.5117	0.2207	22305.4687	255.0401	0.00000481904
5586.0078	0.2247	22328.7305	317.1313	0.00000445204
6585.4375	0.2294	22395.8477	320.8130	0.00000376545
7485.0273	0.2308	22224.3359	583.5928	0.00000252213
7583.7852	0.2308	22627.6055	261.5728	0.00000148789
13575.6250	0.2376	22627.8125	204.6038	0.00000091406
18169.5586	0.2413	22965.0625	247.6978	0.00000095352
22164.6211	0.2453	22997.4453	229.2305	0.00000086142
24162.1797	0.2473	22766.8398	251.2065	0.00000087780
24261.8750	0.2471	22708.9492	606.9131	0.00000089227
31947.7891	0.2527	22872.7227	2311.0425	0.00000104874
37426.5352	0.2597	22761.3555	4308.6016	0.00000192064
38918.7500	0.2629	22848.7578	4317.6719	0.00000232386
40112.5977	0.2669	22801.5547	4335.1328	0.00000545417
41206.7148	0.2749	23005.9609	4456.3789	0.00001364187
41505.1797	0.2791	23114.5898	4519.4453	0.00002776025
41902.9023	0.2934	22878.8086	5679.0625	0.00006231878
42002.2461	0.2969	22419.9844	5883.8516	0.00009472504
42101.7461	0.3067	22292.9414	5980.3789	0.00010637489
42201.1680	0.3195	22294.5703	6259.7187	0.00011864821
42300.5117	0.3320	22342.4648	5488.4687	0.00011888782
42399.8516	0.3440	22473.9727	5951.2930	0.00011559056
42499.7891	0.3552	22096.6094	5949.0352	0.00011367828
42599.0117	0.3665	22115.8437	6290.7930	0.00011500654
42698.1562	0.3772	21816.7305	6472.8008	0.00011508747

TABLE C.11

RESULTS OF TEST NO. 12

High Cycle Frequency: 605 Hz
Low Cycle Hold Time: 10 sec

TIME (Sec)	CRACK LENGTH (inches)	MAX LF K (psi in)	HF K RANGE (psi in.)	GROWTH RATE (inches/sec)
499.2798	0 5449	41686.8047	443.1199	0.00003821819
599.7678	0 5489	41386.2500	1004.2280	0.00003664137
699.6240	0.552[illegible]	41204.4102	1010.5854	0.00003643995
799.4800	0.5560	41213.6523	1130.5286	0.00003625306
899.3359	0 5593	41035.8164	1440.7424	0.00003724804
999.1919	0 5632	40854.7461	1489.1851	0.00003754467
1099.6799	0 5671	40848.4180	1538.5725	0.00003780310
1198.9041	0.5712	40331.3750	1666.4360	0.00003706054
1298.7600	0 5747	40315.2617	1677.3757	0.00003474450
1398.6160	0.5780	40063.4336	1766.1792	0.00003480908
1498.4719	0.5810	39997.0625	2013.2786	0.00003430064
1598.3279	0.5846	39881.4805	1629.3350	0.00003630349
1697.5520	0.5884	39860.0508	2441.6672	0.00003620370
1796.7759	0.5924	39785.5820	2701.9609	0.00003557654
1897.2639	0.5960	39656.7812	2517.5942	0.00003306677
1996.4880	0.5989	39510.9844	2572.6995	0.00003011314
2096.3440	0.6016	39449.9141	2668.1091	0.00002864495
2196.2000	0.6041	39117.0273	2598.4189	0.00002909526
2296.0559	0.6071	39105.0781	2654.8840	0.00003068979
2395.2800	0.6096	38689.6602	2667.4263	0.00004080472
2495.1360	0.6150	38890.0586	2737.8218	0.00003817993
2594.3601	0.6193	38960.1797	3483.4497	0.00003600642
2694.2161	0.6201	36927.1016	3488.5422	0.00006604505
2793.4399	0.6274	38685.2578	3582.3401	0.00008235798
2893.2959	0.6382	38605.7812	3528.1506	0.00008789578
2992.5200	0.6491	35115.4180	3697.1140	0.00008254430
3091.7441	0.6609	39345.3672	3926.9143	0.00007832758
3191.6001	0.6670	39683.5195	3931.1694	0.00005444091
3291.4561	0.6658	39081.9141	4060.8308	0.00002569969
3390.6799	0.6686	39681.0586	4178.9961	0.00003155028
3490.5361	0.6721	39650.9883	4020.96[illegible]0	0.00003659808
3589.7600	0.6761	38875.9727	5725.7656	0.00004142890
3688.9841	0.6807	38664.5234	5638.9453	0.00004562846
3788.2[illegible]	0.6854	38612.3750	5647.0898	0.00005017189
3888.0640	0.6900	38171.4414	5803.3164	0.00005480160
396[illegible].2881	0.6955	37606.6875	5875.2578	0.00006465937
4085.8801	0.7021	37043.4531	6063.6680	0.00007712927
4185.7344	0.7102	36564.9180	6125.2266	0.00009316225
4284.9570	0.7202	35917.7031	6480.4766	0.00011187476

TABLE C.12

RESULTS OF TEST NO. 13

Constant load, no cycling

TIME (Sec)	CRACK LENGTH (inches)	MAX LF K (psi in)	HF K RANGE (psi in.)	GROWTH RATE (inches/sec)
11620.3008	0.2869	23961.6406		0.00000411751
12676.3984	0.2915	24174.6758		0.00000573215
13522.0000	0.2965	24442.5312		0.00000775572
13944.3984	0.2996	24753.0352		0.00000896139
14366.8008	0.3037	25381.7070		0.00000961069
14789.1992	0.3084	25693.0195		0.00001040402
15212.3008	0.3127	25964.2461		0.00001121570
15634.6992	0.3172	26117.9219		0.00001191794
16057.1992	0.3225	26356.3125		0.00001290539
16479.6016	0.3285	26861.6758		0.00001347179
16902.1016	0.3347	27032.3320		0.00001386898
17325.1016	0.3405	27329.1953		0.00001417301
17747.6016	0.3462	27339.4492		0.00001426718
18170.0000	0.3520	27724.2539		0.00001525549
18592.5000	0.3585	27902.6992		0.00001673370
19014.8984	0.3660	28219.9883		0.00001811901
19226.1992	0.3699	28531.8242		0.00001942298
19437.3984	0.3747	28767.6680		0.00001582147
19649.3008	0.3770	28978.1758		0.00001737023
19860.5000	0.3802	29255.1758		0.00001682866
20282.8984	0.3887	29572.7305		0.00001995124
20705.3008	0.3986	30180.0547		0.00002138640
21127.6992	0.4080	30800.1250		0.00002247342
21550.1992	0.4187	31212.8242		0.00002456056
21973.3008	0.4274	31410.1250		0.00002376697
22395.6992	0.4374	32171.3984		0.00002576357
22818.1016	0.4503	32966.9180		0.00002674197
23240.6016	0.4476	32808.2695		0.00005098156
23874.8984	0.4817	34921.5625		0.00010911345
24508.3984	0.5658	40816.2148		0.00018643984
24720.0000	0.6039	39784.8711		0.00018205498
24931.2500	0.6511	47027.1250		0.00016690358

TABLE C.13

RESULTS OF TEST NO. 20

High Cycle Frequency: 200 Hz
Low Cycle Hold Time: 10 sec

TIME SEC	CRACK LENGTH INCHES	LF K PSI √IN	HF K PSI √IN	GROWTH RATE INCHES/SEC
17954.7	.240163	15273.6	7164	1.46917E-05
18054	.242162	15372.9	5151.03	1.66078E-05
18551.1	.249403	15264.3	5348.05	1.50077E-05
18848.9	.25302	14908.5	5419.15	1.45979E-05
19246.4	.259096	14909.1	5467.51	1.70322E-05
19643.4	.264205	14717.2	5464.83	2.05388E-05
19841.9	.270317	14502.7	5676.84	2.24681E-05
20040.3	.275052	14225.7	5479.89	2.37580E-05
20239.2	.280027	14110.1	5611.23	2.64764E-05
20437.4	.285311	13845.3	5951.6	2.78892E-05
20635.5	.291132	13753.4	6069.58	2.96878E-05
20833.8	.297121	13696.8	6086.4	3.21142E-05
21032.1	.304989	13583.6	6125.34	2.96464E-05
21230.5	.31075	13364.6	6059.57	2.81352E-05
21330.2	.310891	13023.1	6291.51	1.78907E-05
23515.5	.318305	15120.1	4784.59	1.29412E-05
23614.7	.317878	14901.8	6349.48	2.29884E-05
23813.3	.322616	15354.3	6441.12	2.64979E-05
24011.8	.328782	15267.5	5979.44	2.97442E-05
24209.9	.334883	15114	6260.5	3.17100E-05
24408	.341087	14966.4	6092	3.35743E-05
24606.6	.348021	15152.5	6091.25	3.55871E-05
24804.6	.355339	14802.2	6628.76	3.80856E-05
24903.7	.359099	14999.3	6574.97	3.96216E-05
25101.9	.367231	14788.5	6522.24	4.28948E-05
25201.1	.371599	14591	6696.49	4.33230E-05
25300.2	.375907	14432.1	6854.77	4.45446E-05
25399	.38044	14389.9	6414.21	4.68675E-05
25597.4	.389736	14428	6831.84	5.13099E-05
25696.6	.394821	14343.9	7168.61	5.45249E-05
25795.8	.400364	14523.1	7017.95	5.79771E-05
25895	.406649	14283	6473.07	6.01029E-05
25994.1	.412764	13886.4	7108.94	6.12882E-05
26093.3	.418839	13769	7218.07	6.22954E-05
26193.4	.425618	13916.8	6776.31	5.60902E-05
26292.6	.431224	14177.9	7151.96	4.96666E-05
26392	.434714	13560.6	7006.57	3.97035E-05
26491.2	.436985	15041.1	5220.6	2.77574E-05
26887	.4446	15247	5292.08	1.69791E-05
27183.7	.448975	15366.4	5333.53	1.42793E-05
27481.3	.453807	15499.2	5379.63	1.32124E-05
27975.4	.457899	15612.6	5418.96	8.91923E-06
28073.7	.45764	15293.3	4706.38	5.58940E-06
30152.1	.465471	15141.6	4964.99	3.23035E-06
31340.4	.468748	15229.4	4775.05	2.96880E-06
32627	.472981	15284.1	4717.79	2.87439E-06
33616.5	.476378	15143.2	4980.29	2.99632E-06
34902.3	.479886	15400.4	4664.43	2.73551E-06
36781.7	.484786	15340.2	4739.94	2.38845E-06
38562.3	.488424	15314.4	4691.38	2.09577E-06
40244	.49173	15294.3	4482.22	1.90823E-06
43211.5	.497081	15480.7	4426.87	1.65563E-06
44695.7	.499353	15175.5	4220.74	1.46293E-06

TABLE C.14

RESULTS OF TEST NO. 21

High Cycle Frequency: 200 Hz
Low Cycle Hold Time: 5 sec

TIME SEC	CRACK LENGTH INCHES	LF K PSI √IN	HF K PSI √IN	GROWTH RATE INCHES/SEC
10150.7	.242761	14781.2	3763.4	[illegible]
11727.7	.247325	14776.2	3809.06	2.89537E-[illegible]
13303.9	.252022	14896.3	3879.15	3.1025[illegible]E-05
14755	.257116	14774.2	3930.39	3.44687E-05
17215	.265905	14802.6	3957.07	3.60695E-05
18793.4	.271698	14816.6	3997.14	3.34936E-06
19612.9	.274558	14787.6	3975.68	3.22298E-06
21000	.278799	14709.3	4030.09	3.75178E-06
21694.1	.279942	14925.8	4040.04	4.31119E-0[illegible]
22891.1	.285074	14699.7	4126.41	6.14916E-06
24215.1	.294109	14682.3	4133.04	8.82904E-06
25601.9	.308728	14602.3	4259.48	1.05878E-05
25980.1	.313666	14550.1	4346.51	9.32345E-06
26547.1	.319991	14678.1	4421.17	8.37080E-06
27115.1	.32363	14535.3	4459.72	7.07991E-06
27809.1	.326412	14318.1	4497.3	5.16632E-06
29638.1	.335239	14390.1	4538.23	6.90702E-06
30457.1	.340864	13990.1	4559.37	8.34519E-06
31088.1	.346346	14259.8	4506.71	9.30261E-06
32476.1	.362514	14242	4633.4	1.18272E-05
33106.1	.369923	14155.9	4712.29	1.34232E-05
33674.1	.377812	14030.6	4767.66	1.38347E-05
34242.1	.38604	13729.4	4775.33	1.44745E-05
34746.1	.393401	13783.7	4774.05	1.55901E-05
35313.1	.402634	13923.4	4892.49	1.70773E-05
35881.1	.412184	13858.2	5015.95	1.87174E-05
36259.1	.4189	13749.7	4984.63	2.07626E-05
36638.1	.427724	13631.4	5056.48	2.20227E-05
37016.1	.436387	13658.4	7568.14	2.43801E-05
37269.1	.44267	13306.1	5233.69	2.45049E-05
37647.1	.452515	13600.6	5334.54	2.48981E-05
37900.1	.459012	13475.8	5371.77	2.53211E-05
38278.1	.468341	13297.6	5485.23	2.52942E-05

TABLE C.15

RESULTS OF TEST NO. 23

High Cycle Frequency: 200 Hz
Low Cycle Hold Time: 5 sec

TIME SECONDS	CRACK LENGTH INCHES	LF K PSI-√IN	HF K PSI-√IN	GROWTH RATE INCHES/SEC
13973.6	.24845	15070.9	3419.12	2.71236E-06
15816.3	.254421	15099.7	3442.92	3.07845E-06
18007.3	.261231	14873.5	3355.35	3.45400E-06
19402.2	.2659	14783.9	3666.64	4.04708E-06
20896.7	.272048	14945.7	3720.24	5.23221E-06
21992.6	.277987	14825.9	3745.23	5.98945E-06
22690.5	.282363	14711.2	3756.07	6.09794E-06
23486.9	.287946	14573.8	3763.32	6.67876E-06
24432.9	.294741	14706.1	3821.41	6.76568E-06
25378.9	.300969	14699.9	3858.98	6.30215E-06
25976.5	.305065	14704	3915.98	5.85837E-06
26922.7	.310176	14645.6	3971.32	5.41620E-06
28018.3	.314487	14668	3925.81	4.26987E-06
34081.4	.332961	15232.6	4189	4.62325E-06
34673.7	.33532	15169.5	4297.49	9.28250E-06
35117.8	.339532	14931.6	4367.34	1.31958E-05
35463	.343865	15006.9	4416.23	1.47059E-05
35809	.349371	14829.6	4475.29	1.59329E-05
36105.8	.354304	14789.2	4524.63	1.73392E-05
36401.9	.359458	14828	4612.75	[illegible]
36698.3	.365063	14666.2	4690.06	2.04603E-05
36945.1	.370154	14534	4724.36	2.24713E-05
37192.4	.375874	14808.5	4853.29	2.56196E-05
37389.8	.381114	14747.4	5033.01	2.65292E-05
37587.8	.386873	14460.6	5085.29	3.08086E-05
37735.9	.391744	14622.7	5162.63	3.30694E-[illegible]
37933.3	398509	14419.3	5286.9	3.57566E-05
38081.9	.403913	14522.2	5295.75	3.89698E-05
38229.8	.409604	14273.1	5422.33	4.35185E-05
38378.1	.416234	14434.9	5555.52	4.91477E-05
38476.9	.421292	14478.5	5785.21	5.26470E-05
38575.9	.426942	14626.2	5873.24	5.41296E-05
38674.6	.43279	14825.5	6072.03	5.55864E-05
38773.4	.438208	14910.3	6214.54	5.47295E-05
38921.5	.446066	15071.1	5856.3	5.30147E-05
39070.1	.453645	15142.6	5840.14	5.46666E-03
39168.8	.459035	14841	5846.14	5.45398E-05
39267.5	.464295	14727.1	5883.31	5.80339E-05

TABLE C.16

RESULTS OF TEST NO. 24

High Cycle Frequency: 200 Hz
Low Cycle Hold Time: 2 sec

TIME SECONDS	CRACK LENGTH INCHES	LF K PSI-√IN	HF K PSI-√IN	GROWTH RATE INCHES/SEC
4606.84	.223925	15594.7	3179.65	5.05628E-06
5609.16	.229521	15641.2	3244.61	5.20793E-06
6411.5	.234768	15729.5	3296.21	5.20135E-06
7414.48	.239853	15763	3413.37	4.89075E-06
8816.3	.245684	15057.4	3682.07	4.14207E-06
11021.5	.253005	14865.3	3409.08	3.34664E-06
13029.8	.258689	14948.7	3418.56	3.28950E-06
14836.9	.26414	14853.5	3408.92	3.69339E-06
16241.8	.269325	14917	3761.31	4.24272E-06
17445.8	.27462	14676.8	3868.84	4.72856E-06
18649.4	.280763	14458.4	3850.18	5.27330E-06
19651.8	.286362	14493.5	3939.07	5.59561E-06
20654.4	.292063	14514.9	3946.46	5.96646E-06
21457.1	.297022	14548	3939	6.21908E-06
22460.4	.303414	14338.8	3982.93	6.53443E-06
23263.1	.308732	14465.2	4032.49	6.86742E-06
24265.7	.315691	14307.5	4077.22	7.33285E-06
25068.4	.321781	14406.5	4088.78	7.70411E-06
25869.9	.327979	14024.1	4166.57	8.17521E-06
26672.2	.33482	14311.8	4179	8.68808E-06
27474.8	.341937	14111.3	4264.76	9.43575E-06
28077.6	.347577	14217.6	4304.36	1.05102E-05
28680.6	.35399	14239.4	4379.00	1.18873E-05
29082.2	.358876	14156.5	4481.99	1.20302E-05
29483.3	.364469	14101.1	4576.48	1.28988E-05
29884.4	.369844	13986.7	4556.17	1.41380E-05
30285.5	.374763	14056.1	4540.04	1.61585E-05
30887.1	.384484	15062.1	4966.88	2.44796E-05
31288.2	.394678	14908.8	5371.99	3.71809E-05
31488.5	.401815	14949.7	5480.04	4.52557E-05
31688.9	.411762	15071.2	5628.37	5.08689E-05
31889.3	.423788	14960.5	5782.32	5.64521E-05
32089.8	.435124	15170	5918.37	5.98691E-05
32290.1	.447317	15193.8	6058.01	6.33767E-05
32490.8	.46023	15178.9	6250.05	6.77956E-05
32692	.474052	15336.2	6413.88	7.36265E-05
32892.4	.489203	15536.5	6621.06	8.15655E-05
33093	.506464	15222.5	6880.98	8.83606E-05
33293.7	.524824	15302.8	7195.33	9.54849E-05
33494.6	.544718	15342.5	7489.8	1.05131E-04
33695.5	.566616	15340.4	7823.79	1.14006E-04

TABLE C.17

RESULTS OF TEST NO. 25

High Cycle Frequency: 200 Hz
Low Cycle Hold Time: 2 sec

TIME SECONDS	CRACK LENGTH INCHES	LF K PSI $\sqrt{IN}$	HF K PSI $\sqrt{IN}$	GROWTH RATE INCHES/SEC
3610.3	.314565	15232.4	4183.33	9.66318E-06
4251.17	.32128	14956.2	4356.9	1.19874E-05
4731.53	.327102	15104	4479.3	1.44594E-05
5052	.331765	15076	4703.94	1.79219E-05
5372.7	.337393	14992	4754.94	2.20731E-05
5692.85	.344727	14754.2	4824	2.72575E-05
6013.3	.354088	14656.9	4959.78	3.33616E-05
6173.6	.359804	14789.1	5040.66	3.47997E-05
6333.65	.366015	14923	5122.27	3.66119E-05
6493.8	.371875	14611.7	5149.12	3.82572E-05
6653.9	.377934	14588.6	5224.06	3.94627E-05
6814.35	.384462	14841.9	5293.93	4.14606E-05
6974.95	.391241	14564.1	5364.33	4.38213E-05
7135.05	.398564	14551.3	5436.1	4.62507E-05
7295.3	.406035	14290.3	5499.68	4.84076E-05
7455.6	.413939	14338.3	5612.34	5.04204E-05
7615.85	.422356	14254	5716.72	5.26406E-05
7776.05	.430881	14145	5820.48	5.52307E-05
7936.25	.4397	13969.1	5891.86	5.83182E-05
8096.35	.449067	14082.9	5977.56	6.31815E-05
8256.35	.458976	14282.7	6406.62	7.12344E-05
8416.6	.470238	13962.8	6742.58	8.51581E-05
8576.85	.484288	14004.1	7157.55	1.03244E-04

TABLE C.18

RESULTS OF TEST NO. 26

High Cycle Frequency: 200 Hz
Low Cycle Hold Time: 10 sec

TIME SECONDS	CRACK LENGTH INCHES	LF K PSI $\sqrt{IN}$	HF K PSI $\sqrt{IN}$	GROWTH RATE INCHES/SEC
1387.89	.265289	20646.3	368.538	2.60107E-05
1684.83	.272813	20730.1	370.757	2.43103E-05
1981.78	.279544	20665.8	372.199	2.32146E-05
2279.08	.286124	20749.1	400.22	2.25147E-05
2575.89	.292666	20766.5	416.665	2.27702E-05
2872.87	.29948	20909.5	427.059	2.29000E-05
3170.42	.306379	20868.7	444.469	2.21918E-05
3368.47	.311033	20951.2	435.19	2.22762E-05
3669.29	.317605	21051	1025.44	2.09159E-05
3970.15	.323834	21135.3	1045.55	1.94536E-05
4271.24	.32927	21263	1054.79	1.75716E-05
4672.2	.335894	21337	1078.61	1.56418E-05
5073.03	.341657	21538.5	1094.12	1.39363E-05
5474.5	.34661	21475.1	1103.8	1.21865E-05
5975.8	.352082	21536.2	1120.6	1.07715E-05
6578.16	.357041	21685.7	1127.71	9.79167E-06
7280.9	.364605	21350.2	1167.49	9.58591E-06
8083.49	.37402	21726	1192.79	9.61611E-06
9889.53	.386309	21350.7	1180.33	6.58685E-06
21026.1	.414256	20889.9	1828.52	4.52905E-06
22129.9	.419472	20592.2	2052.56	6.73840E-06
23334	.429797	20497.5	4043.77	1.18570E-05
23735.3	.43503	20474.3	4287.65	2.27630E-05
23936	.438857	20348	4375.27	3.46956E-05
24137.2	.446038	19998.9	4487.82	4.09139E-05
24237.6	.45067	20268.7	4530.77	4.38715E-05
24438.4	.460062	20406.3	4660.48	4.96152E-05
24538.8	.464475	20460.6	4706.52	5.34657E-05
24739.5	.475906	20498.3	4831.52	6.34540E-05
24839.9	.482789	20644.6	4919.57	6.76531E-05
24940.1	.48982	20570.2	4990.77	7.17218E-05
25040.5	.497457	20661.2	5085.51	7.67511E-05
25141.4	.504959	20651.6	5152	8.33411E-05
25241.7	.513324	20474.1	5263.77	9.00567E-05
25342.2	.522867	20701.8	5364.22	1.00405E-04
25442.5	.533467	20440.6	5494.63	1.10882E-04
25542.8	.545155	20543.7	5614.01	1.21563E-04
25643.2	.557852	20857.3	5767.28	1.32535E-04
25743.6	.571526	20941.3	5937.38	1.42347E-04
25844	.586322	21080.6	6137	1.56928E-04
25944.3	.603259	21326.4	6339.12	[illegible]266E-04

TABLE C.20

RESULTS OF TEST NO. 27

High Cycle Frequency: 200 Hz
Low Cycle Hold Time: 10 sec

TIME SECONDS	CRACK LENGTH INCHES	LF K PSI-√IN	HF K PSI-√IN	GROWTH RATE INCHES/SEC
3705.31	.235605	20184.3	571.125	4.90554E-06
4606.97	.240756	20137.9	582.568	5.00307E-06
5908.89	.247186	20261.4	582.514	4.39706E-06
7010.94	.251669	20291.7	591.654	3.82553E-06
9518.75	.258409	20343.6	1768.82	2.77500E-06
12429.4	.265486	20550	2027.91	2.70623E-06
14236.6	.270472	20694.7	2077.96	2.93555E-06
15842.8	.275195	20730.7	2108.57	3.20174E-06
17548.9	.28121	20843.9	2159.4	3.56126E-06
19055.1	.286563	20597.9	2193.35	3.82398E-06
20360.3	.291671	20094	3157.88	4.05668E-06
21565.1	.296904	20081.5	3312.76	4.20887E-06
22769.9	.302229	20051.5	3379.22	4.31553E-06
24075.5	.307908	20233.8	3479.25	4.34907E-06
25380.6	.31366	20171	3556.58	4.25586E-06
26585.3	.318621	20350.4	3612.37	4.31478E-06
27890.8	.324578	20135.9	3666.41	4.12126E-06
29497.8	.331132	20288.3	3737.94	3.93100E-06
32307.1	.341365	20370.6	4552.75	4.31815E-06
33711.1	.34705	20259.5	4355.14	5.69834E-06
34614.2	.352225	20047.4	4413.06	7.45441E-06
35316.9	.35745	20211	4422.77	9.26753E-06
35918.6	.363327	20179.5	4494.42	1.07535E-05
36420.7	.36924	19924.9	4528.94	1.14498E-05
36922.3	.375385	20454.7	4598.05	1.26669E-05
37324.2	.380623	20275.1	4661.14	1.33550E-05
37825.7	.387334	20124.4	4618.51	1.52602E-05
38126.6	.391723	20132.4	4631.78	1.69568E-05
38528.4	.398941	20046.8	4764.84	1.89203E-05
38729	.403032	20071.4	4819.02	2.05254E-05
39029.9	.409307	20174.6	4871.8	2.20164E-05
39330.8	.416554	20227.9	4907.95	2.35808E-05
39531.7	.42122	20146.9	4937.88	2.36545E-05
39832.6	.42847	19904.3	5054.35	2.57998E-05
40133.6	.436162	19813.6	5115.13	2.87383E-05
40434.9	.444819	19657.4	5189.46	3.37808E-05
40635.5	.451647	19542.6	5265.78	3.76620E-05
40836	.459764	19579.2	5386.65	4.10950E-05
41036.7	.46888	19654.8	5545.32	4.50665E-05
41237.3	.478158	19548.9	5646.13	4.80814E-05
41438.	.488006	19434.7	5735.92	5.11966E-05
41538.7	.493115	19241.2	5792.14	5.26536E-05
41638.9	.498477	19285.6	5836.35	5.52501E-05
41739.1	.504159	19565.2	5888.69	5.86356E-05
41839.4	.509926	19381.5	5952.95	6.19948E-05
41939.8	.516162	19470.6	6117.85	6.75129E-05
42040.1	.523435	19485.9	6246.27	7.24997E-05
42140.3	.531042	19631	6387.59	7.80731E-05
42240.7	.538931	19556.7	6594.84	8.47517E-05
42340.9	.547512	19412.5	6790.22	9.31695E-05
42441.9	.557138	19684.1	7092.73	1.02856E-04
42542.2	.567876	19418.5	7339.22	1.13377E-04
42642.4	.579942	19307.8	7559.28	1.27458E-04

RESULTS OF TEST NO. 28

High Cycle Frequency: 200 Hz
Low Cycle Hold Time: 5 sec

TIME SECONDS	CRACK LENGTH INCHES	LF K PSI-√IN	HF K PSI-√IN	GROWTH RATE INCHES/SEC
2648.78	.240046	20179.4	749.787	7.74330E-06
3348.84	.245896	20176.1	766.559	8.19528E-06
3998.94	.251334	20137.5	772.358	8.55140E-06
4548.88	.256387	20267.3	782.697	8.49905E-06
5299.07	.262842	19997.3	789.463	8.61791E-06
5848.97	.267631	19922.4	803.888	8.50472E-06
6798.71	.275407	20245.4	810.225	8.39608E-06
7298.74	.278964	20260.1	811.107	9.96632E-06
8598.19	.295119	20533.7	843.442	9.98247E-06
9349.29	.300798	20024.9	2353.36	8.24692E-06
11204.7	.310807	20273.2	2634.49	4.54244E-06
13060.5	.31668	20428	2693.3	3.27657E-06
14766.3	.32178	20309.6	2761.4	3.25186E-06
16371.4	.327097	20190.7	2815.23	3.51192E-06
17926.6	.332811	19876.1	2974.32	3.71742E-06
19281.4	.337992	20045.7	3044.12	3.89707E-06
20636.7	.343595	19866.2	3158.71	3.95179E-06
21992	.348923	19799.5	3534.2	4.18675E-06
23146.8	.35355	19863.9	3568.99	4.70819E-06
24703.1	.361112	20004.1	4160.64	6.32707E-06
25356	.364951	19897.4	4297.7	8.12654E-06
26008.8	.370271	20096.6	4266.62	9.85634E-06
26460.6	.375188	19793.5	4279.03	1.11210E-05
26862.4	.379812	19831.4	4338.16	1.22304E-05
27364.6	.386365	19788.5	4370.34	1.35862E-05
27715.6	.391113	19926.3	4457.7	1.48092E-05
28117.3	.397384	19709.7	4482.02	1.57873E-05
28468.9	.404541	19872.4	4629.51	1.55083E-05
28769.9	.409051	19649.5	4669.59	1.52263E-05
29373.1	.417111	19593.2	4796.14	1.36610E-05
30526.1	.431645	20440.7	5414.36	1.66776E-05
30676.6	.434204	19859.2	6049.05	2.61597E-05
30826.8	.437143	20054.8	6021.97	4.13974E-05
31027.1	.446507	19620.6	6219.34	4.75576E-05
31077.1	.448787	19671.9	6266.59	4.79896E-05
31227.6	.456238	20144.8	6368.82	5.19722E-05
31377.8	.464868	19849.8	6495	5.76234E-05
31478	.470301	19589.5	6673.9	5.93147E-05
31578.1	.476389	19495	6737.04	6.35132E-05
31728.7	.486235	19259	6839.66	7.32649E-05
31828.8	.493762	19685.4	6930.1	8.30353E-05
31928.8	.502331	19576.1	7035.15	9.51575E-05
32029	.512143	19790.8	7142.33	1.30353E-04
32079	.518288	19545	7201.2	1.68188E-04
32129.6	.526682	19193.7	7295.67	2.09250E-04
32179.7	.537159	18970.8	7432.43	2.58190E-04
32229.9	.5506	19205	7622.74	3.41643E-04

TABLE C.21

RESULTS OF TEST NO. 30

High Cycle Frequency: 200 Hz
Low Cycle Hold Time: 5 sec

TIME SEC	CRACK LENGTH INCHES	LF K PSI $\sqrt{IN}$	HF K PSI $\sqrt{IN}$	GROWTH RATE INCHES/SEC
2536.11	.270249	21384.1	340.203	1.52431E-05
3531.94	.283215	21409.7	349.918	1.40442E-05
5125.69	.304068	21891.2	377.926	1.38879E-05
6022.22	.31663	22158.6	386.406	1.29077E-05
6919.44	.328192	22111.6	403.188	1.24193E-05
7666.46	.338991	20221.7	438.347	1.30675E-05
9058.19	.354705	19934.9	390.156	1.19024E-05
10103.3	.366602	20026.9	406.009	1.10187E-05
10899.9	.376936	19987.4	435.315	9.85667E-06
11845	.384753	19978.5	412.689	9.19678E-06
13262	.393241	19809.1	1522.25	6.31767E-06
16717.9	.408799	20180.4	1573.52	4.06503E-06
20327.1	.419784	20390.1	1651.33	3.25084E-06
24803.5	.43298	20437.8	1951.65	3.27670E-06
28005.6	.443593	21010.3	2673.5	3.48710E-06
31052.8	.454303	21001.6	2741.44	3.86281E-06
34254.2	.467388	21042.6	2780.82	4.32524E-06
37912.2	.483746	20146	752.491	4.97800E-06
39458.3	.491487	19936.3	517.393	5.20196E-06
41252.8	.501109	19470.5	535.271	5.75981E-06
42749.3	.51004	19906.3	552.954	6.82521E-06
44495.8	.522503	19747.7	565.465	9.98010E-06
45713.9	.534665	20310.7	4612.4	1.71221E-05
46070.1	.54262	19943.3	4633.72	2.55087E-05
46374.3	.549394	19989.7	4691.33	3.37897E-05
46628.5	.559197	19951.1	4776.45	3.72788E-05
46881.9	.569098	20256	4824.3	4.10796E-05
47085.4	.57746	19679.1	4848.79	4.43869E-05
47288.2	.586715	19723.8	4933.82	4.79476E-05
47491	.596852	20058.9	5061.52	5.16290E-05
47643.8	.604851	19756.5	5118.11	5.63949E-05
47796.5	.613595	19807.1	5183.5	6.19547E-05
47948.6	.622978	19962.9	5402.64	6.82441E-05
48100.7	.634079	20006.4	5660.25	7.22722E-05

TABLE C.22

RESULTS OF TEST NO. 31

High Cycle Frequency: 200 Hz
Low Cycle Hold Time: 5 sec

TIME SEC	CRACK LENGTH INCHES	LF K PSI $\sqrt{IN}$	HF K PSI $\sqrt{IN}$	GROWTH RATE INCHES/SEC
2081.88	.335799	29768	488.443	1.51308E-05
2676.39	.346381	30037.3	518.745	1.57077E-05
3221.53	.355087	30096.6	506.885	1.47550E-05
3776.39	.362973	30448.3	1327.95	1.37997E-05
4485.42	.372168	30372.2	1365.15	1.25640E-05
5295.14	.381229	30149	1395.49	1.09053E-05
6105.97	.389321	30963	2239.28	9.76339E-06
7018.19	.39768	30826.2	2327.9	8.93298E-06
8133.33	.406785	30716.6	2366.76	8.22917E-06
9248.61	.414905	31343.1	2409.42	8.33220E-06
10262.4	.422806	23008	2668.94	9.39563E-06
11327.6	.43293	30334	3444.71	1.16632E-05
11885.3	.439168	30034.3	4098.53	1.37667E-05
12545.5	.448843	29869.7	4267.44	1.61338E-05
13052.7	.457679	30083.3	4401.18	1.86552E-05
13459	.465095	29684.7	4451.28	2.13422E-05
13916.6	.475411	29820.1	4559.26	2.52906E-05
14220.8	.483282	29812.9	4658.13	2.79442E-05
14525.6	.492122	29922.5	4714.49	3.06652E-05
14779.8	.500603	29624.6	4750.7	3.35301E-05
15034	.509234	29303.2	4806.47	3.56431E-05
15288.1	.518525	29083.2	4914.85	3.78655E-05
15541.6	.528346	29155.3	4965.07	4.06528E-05
15795.8	.539072	29219.7	5024.22	4.41215E-05
15999.2	.548211	29334.2	5118.24	4.70995E-05
16202	.557866	29039.4	5229.38	5.02227E-05
16405.5	.568476	28879.1	5341.94	5.37809E-05
16608.3	.579901	28620.4	5427.09	5.66278E-05
16761	.588624	28378.3	5496.01	6.05860E-05
16913.1	.597864	28478.2	5582.71	6.52224E-05
17065.9	.607898	27996.2	5658.76	7.17634E-05
17167.6	.61383	28468.4	6020.88	9.21304E-05
17319.9	.630383	29053.5	6572.11	1.00003E-04
17421.9	.641767	28627.6	6840.15	1.09941E-04
17523.5	.653591	28513.9	7173.98	1.17643E-04
17726.6	.679745	27846.9	7694.4	1.25042E-04

TABLE C.23

RESULTS OF TEST NO. 32

High Cycle Frequency: 200 Hz
Low Cycle Hold Time: 5 sec

TIME SEC	CRACK LENGTH INCHES	LF K PSI √IN	HF K PSI √IN	GROWTH RATE INCHES/SEC
2797.2	.375859	30382.7	462.934	1.09281E-05
3546.9	.38417	30228.5	477.337	1.04080E-05
4354	.391748	30375	1771.11	9.48554E-06
5988.5	.404456	30735.7	1989	7.70614E-06
7571.9	.41495	30732.9	2156.41	6.77676E-06
9207.8	.425258	30691.1	2197.57	6.49242E-06
10383.8	.432886	30601.8	2204.13	6.56546E-06
12224.1	.444889	30720.4	2276.12	6.67801E-06
13655.6	.45466	30757.3	2316.1	6.71747E-06
15036	.463598	30537	2344.89	6.91846E-06
16569	.474159	30917	2397.86	7.81884E-06
18102.7	.486335	30577.5	2450.37	1.05522E-05
18615.9	.490387	31476.4	1846.72	1.28638E-05
20216.1	.51523	30418.6	3257.24	2.31793E-05
20666.1	.524255	30347	4575.21	3.61732E-05
20966.1	.535165	30558.4	4751.63	4.27819E-05
21216.2	.547083	30538.7	4904.18	4.64504E-05
21466.2	.558866	30581.4	5031.04	5.15841E-05
21716.9	.572423	30718.6	5128.4	5.67574E-05
21916.9	.583864	30832.5	5280.89	6.26409E-05
22116.9	.596646	30593.2	5389.04	6.84650E-05
22267.6	.607645	30845.2	5558.29	7.22772E-05
22417.7	.619586	30640.4	5700.08	7.13123E-05
22567.7	.630436	30670.8	5812.22	7.06642E-05

TABLE C.24

RESULTS OF TEST NO. 33

High Cycle Frequency: 200 Hz
Low Cycle Hold Time: 5 sec

TIME SEC	CRACK LENGTH INCHES	LF K PSI √IN	HF K PSI √IN	GROWTH RATE INCHES/SEC
891.597	.503505	40027.3	546.527	2.96116E-05
1190.28	.51164	40295.2	1672.72	2.72805E-05
1544.17	.521192	40209.7	1812.62	2.59391E-05
1898.44	.530049	40158.3	1847.43	2.49038E-05
2252.78	.538264	40121.4	1878.93	2.41725E-05
2657.64	.547535	40088.3	2357.11	2.50998E-05
3012.29	.556066	39628.8	2404.07	2.76526E-05
3367.01	.566087	40027.3	3065.15	3.12651E-05
3620.69	.574356	39635.2	3159.49	3.38052E-05
3873.61	.583292	38867.6	4207.73	3.71327E-05
4127.57	.593046	39106.2	4433.81	4.18041E-05
4380.56	.603656	39071.4	4812.26	4.75454E-05
4583.33	.613326	39020.5	5046.88	5.42475E-05
4786.11	.624892	38500.5	5187.29	6.18015E-05
4938.61	.634864	38404.9	5359.93	6.86088E-05
5090.63	.64558	38466.8	5547.41	7.85066E-05
5243.12	.657817	37978.2	5940.84	9.04089E-05
5344.44	.66712	37844.4	6278.03	1.00388E-04
5445.95	.677599	37584.6	6595.11	1.15192E-04
5547.35	.690031	37529.6	6892.07	1.32782E-04
5597.99	.696842	37003.8	7049.48	1.44110E-04
5648.68	.704119	37133.3	7232.64	1.53236E-04

TABLE C.25

RESULTS OF TEST NO. 34

High Cycle Frequency: 200 Hz
Low Cycle Hold Time: 5 sec

TIME SEC	CRACK LENGTH INCHES	LF K PSI $\sqrt{IN}$	HF K PSI $\sqrt{IN}$	GROWTH RATE INCHES/SEC
1199.83	.520776	39264.7	572.952	2.23906E-05
1499.44	.527852	39995.9	570.943	2.20114E-05
1799.47	.534848	40044.4	587.689	2.20336E-05
2156.28	.542783	39846.5	2288.7	2.13393E-05
2616.13	.551942	39444.6	2366.4	1.97302E-05
3024.81	.559348	39520.7	2378.97	1.87303E-05
3433.5	.566893	39414.9	2432.46	1.79203E-05
3842.18	.574184	39209.9	2730.55	1.76827E-05
4250.86	.581214	38734.7	2756.37	1.73420E-05
4711.42	.589244	38627.3	2892.72	1.67943E-05
5119.4	.595819	38310.2	3045.8	1.65568E-05
5528.79	.602398	37576.5	3095.11	1.65045E-05
6090.99	.61179	37811	3173.62	1.69469E-05
6449.2	.617424	37720.5	3396.75	1.89222E-05
6858.51	.625198	37977.7	3482.75	2.34761E-05
7216.02	.633943	38294	3543.84	3.25727E-05
7369.61	.638525	38897.1	4130.38	4.46391E-05
7574.3	.648211	39573.9	5165.45	6.44529E-05
7675.95	.65456	38967.3	6008.17	8.30216E-05
7778.3	.663386	38116.4	6479	1.09585E-04
7830.17	.669266	37972.4	6810.64	1.27637E-04
7881.34	.676018	37984.6	7009.25	1.47433E-04
7932.52	.683478	36834.4	7465.49	1.70636E-04

TABLE C.26

RESULTS OF TEST NO. 35

High Cycle Frequency: 200 Hz
Low Cycle Hold Time: 5 sec

TIME SEC	CRACK LENGTH INCHES	LF K PSI $\sqrt{IN}$	HF K PSI $\sqrt{IN}$	GROWTH RATE INCHES/SEC
2000.02	.220552	20267.9	313.35	1.46331E-05
2611.59	.229704	20240.8	297.527	1.48558E-05
3228.67	.238834	20314.3	326.257	1.48289E-05
3850.7	.248212	20189.5	314.477	1.43993E-05
4478.13	.257422	20152.7	339.132	1.40180E-05
5110.6	.266295	20139.7	335.925	1.34332E-05
5991.47	.277634	20758.4	1100.57	1.21808E-05
6886.41	.287598	20529.9	1120.84	1.09363E-05
7788.17	.296608	20468.7	1520.39	9.97757E-06
8924.91	.307081	20238.1	1545.55	9.18619E-06
10070.3	.316761	20079.2	1751.14	8.72959E-06
11224.6	.326537	20684.3	1771.08	8.57454E-06
12387.2	.336814	20706.5	1878.35	8.30781E-06
13558.9	.346413	20779.8	1967.86	8.10419E-06
14660.3	.355346	21317.8	1998.74	7.82721E-06
16097	.366256	21314.9	2034.97	7.36943E-06

TABLE C.27

RESULTS OF TEST NO. 36

High Cycle Frequency: 200 Hz
Low Cycle Hold Time: 2 sec

TIME SEC	CRACK LENGTH INCHES	LF K PSI $\sqrt{IN}$	HF K PSI $\sqrt{IN}$	GROWTH RATE INCHES/SEC
582.251	.52279	36239.4	794.299	6.24181E-05
975.532	.545328	40318.8	665.92	5.08084E-05
1173.72	.554126	40687.7	646.157	4.54792E-05
1373.04	.560293	40479.3	614.271	3.74973E-05
1787.29	.576002	41010.8	3818.71	3.75249E-05
2000.23	.583788	40642.2	4023.53	3.59086E-05
2429.35	.598895	40870.7	4199.52	3.46251E-05
2863.25	.599264	39471.7	4258.6	5.85767E-05
3301.49	.629442	41145.1	4559.42	9.51374E-05
3743.34	.676014	43895.2	5064.76	1.30634E-04

TABLE C.28

RESULTS OF TEST NO. [illegible]

High Cycle Frequency: [illegible] Hz
Low Cycle Hold Time: [illegible]

TIME SEC	CRACK LENGTH INCHES	LF K PSI $\sqrt{IN}$	HF K PSI $\sqrt{IN}$	GROWTH RATE INCHES/SEC
2406.93	.201142	20412.8	285.125	1.28245E-05
3017.27	.209973	20406.8	308.389	1.22103E-05
3835.74	.219856	20450.2	310.353	1.15944E-05
5423.18	.237148	20032.3	1280.97	9.77332E-06
6316.86	.244773	19948.2	1308.29	8.72546E-06
7442.93	.254139	20138.7	1003.53	8.21591E-06
8576.71	.263076	20392	1109.83	8.06245E-06
9716.42	.271473	20371.8	1307.28	8.15975E-06
10862.7	.280698	20517.5	1364.53	8.95050E-06
12016.7	.290896	20686.8	1396.94	1.04905E-05
12946.3	.300853	20782.2	3505.26	1.23492E-05
13649.2	.309817	20778.3	3714.31	1.40288E-05
14357.5	.320294	20792.9	3952.49	1.58348E-05
15070.7	.332323	20877.6	4106.95	1.74181E-05
15549.5	.340868	21036.8	4210.14	1.92647E-05
16031.5	.350345	20778.5	4321.05	2.07186E-05
16510.2	.360387	21047.5	4435.76	2.30221E-05
16936.1	.370187	20623.3	4285.71	2.60315E-05
17361.9	.381638	20727.8	4211.27	2.96901E-05
17787.7	.394916	20633	4918.64	3.46969E-05
18213	.410228	21452.1	5059.39	4.05215E-05
18426.5	.419416	21319.1	5156.63	4.33337E-05
18639.1	.42887	21356.7	5297.31	4.70418E-05
18852.6	.43908	21255.3	5388.45	5.09158E-05
19065.3	.450168	21601.1	5530.66	5.57455E-05
19278.8	.46262	21418.7	5739.16	5.94511E-05
19491.8	.475961	21362.9	5957.54	6.45650E-05
19704.7	.489891	21953	6148.06	7.07119E-05
19918.4	.504819	21590.2	6289.2	7.93374E-05
20130.7	.522147	21367.3	6684.8	8.92416E-05
20343.7	.541936	21432.5	7193.5	1.01465E-04

TABLE C.29

RESULTS OF TEST NO. 38

High Cycle Frequency: 200 Hz
Low Cycle Hold Time: 2 sec

TIME SEC	CRACK LENGTH INCHES	LF K PSI $\sqrt{IN}$	HF K PSI $\sqrt{IN}$	GROWTH RATE INCHES/SEC
850.736	.65165	39136.9	746.57	4.16333E-05
1068.82	.6611	38636	735.269	4.17149E-05
1289.97	.671393	37952.7	784.078	4.24626E-05
1523.46	.681145	37148.4	2261.8	4.15735E-05
1760.19	.690337	37049.2	2377.18	3.96830E-05
2000.68	.699051	36778.2	3930.93	3.83825E-05
2492.92	.717934	35904.7	6246.45	4.13657E-05

TABLE C.30

RESULTS OF TEST NO. 39

High Cycle Freuqency: 200 Hz
Low Cycle Hold Time: 180 sec

TIME SEC	CRACK LENGTH INCHES	LF K PSI $\sqrt{IN}$	HF K PSI $\sqrt{IN}$	GROWTH RATE INCHES/SEC
3061	.227391	20318.6	307.762	1.34865E-05
3601	.235284	20190.5	299.098	1.45503E-05
4321	.247346	20178.7	355.799	1.51738E-05
4861	.255971	20163.5	307.132	1.49006E-05
5401	.263852	20025	312.66	1.41691E-05
6121	.273637	20024.3	331.125	1.33242E-05
6841	.282697	19962.3	402.849	1.25362E-05
7562	.291224	19729.7	331.785	1.20062E-05
8282	.300104	19794.2	417.871	1.13862E-05
9002	.308193	19917.2	1143.38	1.07736E-05
9903	.317269	19930.5	1113.61	1.00390E-05
10984	.326865	19964.1	1128.57	9.67578E-06
12066	.337612	19941.2	1179.05	8.90287E-06
12967	.345934	19943.1	1211.61	8.07910E-06
13688	.351675	20402.2	2524.83	7.88914E-06
15310	.362065	19933.1	2595.84	6.26715E-06

TABLE C.31

RESULTS OF TEST NO. 40

High Cycle Frequency: 200 Hz
Low Cycle Hold Time: 180 sec

TIME SEC	CRACK LENGTH INCHES	LF K PSI $\sqrt{IN}$	HF K PSI $\sqrt{IN}$	GROWTH RATE INCHES/SEC
4862.16	.224916	20803	1988.55	5.60387E-06
6124	.232454	20791.8	2069.45	5.81127E-06
8466.53	.244775	20952.9	2217.8	5.32295E-06
10628.8	.254731	20856.5	2232.79	4.97156E-06
27383.6	.350457	19397.9	3247.91	4.46742E-06
33149.8	.368165	19536.1	3116.94	2.37025E-06
39456.4	.37881	19413.7	3456.37	1.95697E-06
45582.9	.392767	19[illegible]4	4356.08	3.14442E-06
48466.4	.405611	199[illegible]0.7	5008.89	5.89327E-06
49367.7	.415805	19820	5310.19	1.32590E-05
49728.1	.423876	20564.6	5500.3	3.73400E-05
49908.2	.428343	20175.4	5735.98	6.69787E-05

TABLE C.32

RESULTS OF TEST NO. 41

High Cycle Frequency: 200 Hz
Low Cycle Hold Time: 180 sec

TIME SEC	CRACK LENGTH INCHES	LF K PSI $\sqrt{IN}$	HF K PSI $\sqrt{IN}$	GROWTH RATE INCHES/SEC
12069.1	.456555	30475.6	510.935	1.69518E-05
12969.1	.472873	30953.3	551.435	2.01955E-05
13509.2	.485923	31156.8	529.656	1.90932E-05
14230.9	.506368	30271.8	2149.6	2.06432E-05
15131.4	.524105	30372.3	2500.81	1.85967E-05
16031.9	.534229	30745.2	2565.89	1.28805E-05
17612	.5438	30354.1	2867.2	7.95625E-06
18896	.553017	29900.3	2915.88	1.05250E-05
20180.8	.568245	30379.3	3772.74	1.68599E-05
20731.1	.577249	30861.4	4457.26	2.54616E-05
21098.5	.586283	29904.7	4832.91	3.65447E-05
21465.5	.600734	29781.4	5264.74	5.09255E-05
21649	.609319	30033.7	5614.28	6.41874E-05
21832.4	.620827	29872.8	5891.85	7.89586E-05

TABLE C.33

RESULTS OF TEST NO. 42

High Cycle Frequency: 200 Hz
Low Cycle Hold Time: 180 sec

TIME SEC	CRACK LENGTH INCHES	LF K PSI $\sqrt{IN}$	HF K PSI $\sqrt{IN}$	GROWTH RATE INCHES/SEC
56470.3	.346051	14928	4321.8	5.35195E-06
58448.9	.359031	15671.7	4429.95	6.89649E-06
60067.8	.370816	15591.1	4518.02	1.07271E-05
60787.1	.379115	15968.9	4607.83	1.69453E-05
61147	.384119	15923.2	4763.67	2.32200E-05
61506.7	.39279	15739.4	4831.52	2.67585E-05
61866.2	.403837	16227.6	4900.5	2.99493E-05
62225.9	.415136	16209.7	5080.98	3.23090E-05
62585.6	.427049	16402.7	4948.15	3.44885E-05
62945.9	.439987	16340.1	5251.68	3.64571E-05
63305.6	.453359	16680.5	5386.42	3.83925E-05
63665.1	.467475	16329	5551.35	4.07448E-05
64024.8	.48268	16708.3	5663.06	4.33959E-05

TABLE C.34

RESULTS OF TEST NO. 43

High Cycle Frequency: 200 Hz
Low Cycle Hold Time: 180 sec

TIME SEC	CRACK LENGTH INCHES	LF K PSI $\sqrt{IN}$	HF K PSI $\sqrt{IN}$	GROWTH RATE INCHES/SEC
6276.52	.270508	16069.6	4426.15	1.55146E-05
7352.14	.281753	15591.4	4637.38	1.47507E-05
8069.9	.29243	16166.7	4756.66	2.08054E-05
8428.43	.299514	16102.2	4853.77	2.54690E-05
8786.94	.309112	15640.6	4937.99	2.98083E-05
9145.48	.320845	16278.9	5088.47	3.40959E-05
9504.62	.334067	15890.2	5265.25	3.77073E-05
9863.11	.348344	16073	5479.9	4.09541E-05
10221.7	.363509	16682.7	5699.63	4.42677E-05
10938.8	.397238	16372.6	6098.45	4.87286E-05
11298	.415276	16533.5	6322.17	5.03253E-05
11477.3	.424225	16784.9	6485.63	5.11316E-05

TABLE C.35

RESULTS OF TEST NO. 44

High Cycle Frequency: 200 Hz
Low Cycle Hold Time: 180 sec

TIME SEC	CRACK LENGTH INCHES	LF K PSI IN	HF K PSI IN	GROWTH RATE INCHES/SEC
7165.76	.513595	41012.3	623.934	8.55542E-06
8241.41	.523347	41259.7	2606.96	1.35011E-05
8779.17	.529613	40159.8	2869.61	1.55682E-05
9137.64	.536767	40419.6	3027.82	1.53957E-05
9676.08	.547145	40346.1	3278.71	1.64974E-05
10393	.557079	40071.3	3362.06	1.39910E-05
11110.6	.565103	39968.2	3421.96	1.25462E-05
12186.2	.577035	39311.2	3630.83	1.48081E-05
12903.6	.587697	40630.4	4112.72	2.11307E-05
13620.6	.604154	40099.7	4439.72	1.86422E-05
16131.1	.646879	41929.3	4890.97	4.00056E-05
16310.4	.654503	41532.1	5138.16	5.53135E-05
16489.6	.662041	42630.2	5254.83	7.18609E-05
16668.8	.677036	40749.3	5351.43	8.90449E-05

TABLE C.36

RESULTS OF TEST NO. 46

High Cycle Frequency: 200 Hz
Low Cycle Hold Time: 2 sec

TIME SEC	CRACK LENGTH INCHES	LF K PSI IN	HF K PSI IN	GROWTH RATE INCHES/SEC
9631.25	.367864	30458.5	484.966	7.71886E-06
11242.7	.380835	30456.2	488.097	7.56679E-06
12264.1	.387836	30435.4	1849.62	7.22277E-06
13728.7	.397493	30209.2	1987.6	6.42116E-06
15193.9	.406909	30266.7	2164.03	6.38648E-06
16031.8	.411551	30124.3	2621.05	6.42596E-06
17916.3	.42375	29734.5	2685.74	7.16988E-06
19172	.432534	29567.9	3388.67	8.14466E-06
20010.8	.439094	29523.5	3607.5	9.36793E-06
21058.4	.449634	29443.3	3675.86	1.15481E-05
21897.6	.459458	29595	3840.79	1.37587E-05
22526.1	.468197	29333.7	4155.86	1.57161E-05
23155.1	.478836	29249.5	4280.29	1.77438E-05
23783.7	.490936	29235.4	4364.68	1.97976E-05
24203.5	.499381	29276.3	4508.81	2.11949E-05
24623.2	.508352	29213.1	4589.21	2.29015E-05
25042.2	.518167	29072.6	4637.84	2.49247E-05
25461.9	.529038	29849.4	4801.67	2.70057E-05
25881.6	.540925	28594.5	4946.53	2.92413E-05
26301.3	.553586	28806	5051.03	3.15794E-05
26720.7	.567326	28673.4	5151.52	3.41831E-05
27140.5	.582096	28551.5	5317.62	3.67852E-05
27350.3	.589866	28566.9	5415.38	3.85049E-05
27560.3	.598148	28556.5	5502.31	4.01892E-05
27770	.606729	28516.2	5614.7	4.21441E-05
27979.8	.615648	28403.2	5683.84	4.39207E-05
28189.6	.62505	28492.8	5761.75	4.62213E-05

TABLE C.37

RESULTS OF TEST NO. 47

High Cycle Frequency: 200 Hz
Low Cycle Hold Time: 10 sec

TIME SEC	CRACK LENGTH INCHES	LF K PSI IN	HF K PSI IN	GROWTH RATE INCHES/SEC
5461.17	.331421	29549.9	490.83	4.58923E-06
10114.9	.349872	29645.8	1151.54	3.65665E-06
12366.4	.357237	29927.9	1191.84	3.37474E-06
15232.3	.36623	29790.2	1184.59	3.23888E-06
18099.3	.37468	29804.5	1608.21	3.19975E-06
20863.6	.383359	29969.8	1596.01	3.25549E-06
23014.1	.390238	29730.6	2384.34	3.64731E-06
25370	.399037	29663.7	2461.62	4.66809E-06
27827.8	.412084	30160	2636.87	7.72139E-06
28749.8	.41973	29584.8	3008.95	1.26483E-05
29364.3	.427309	29254.6	4083.25	1.96343E-05
29774.4	.435027	28971.4	4161.16	2.56312E-05
30081.7	.443211	29231.8	4358.64	2.95346E-05
30388.9	.453052	29918.4	4422.33	3.35076E-05
30594.3	.460127	29014.1	4519.87	3.58748E-05
30901.5	.471618	29330.3	4669.44	4.00391E-05
31106.3	.480364	29208.1	4725.68	4.26667E-05
31311.2	.489113	29701.1	4819.65	4.50501E-05
31516.4	.498612	29954.6	4894.85	4.87157E-05
31721.3	.508798	28504.7	5029.51	5.23991E-05
31926	.519764	28770.8	5074.79	5.72547E-05
32130.9	.531742	29543.9	5316.53	6.28061E-05
32335.8	.545126	28954.1	5524.83	7.04291E-05
32541.1	.560165	29985.7	5636.9	7.84051E-05
32746.1	.576952	28480.3	5880.48	8.74923E-05
32848.6	.586211	28966	6056.09	9.20887E-05
32951	.595864	28805.6	6204.64	9.73516E-05
33053.5	.606048	29297.3	6315.1	1.03350E-04
33155.9	.616676	28853.7	6482.96	1.08853E-04
33258.3	.628268	28520.9	6596.82	1.16626E-04

END

DATE
FILMED

1-2-85

DTIC